



**Molecular and Functional Characterization of the Role of  
Foxp3+ Regulatory T (Treg) Cells in the Development of  
Intestinal Cancer**

**Ana Padilha**

Thesis submitted for the award of Ph.D.

The European Cancer Stem Cell Research Institute  
School of Biosciences  
Cardiff University

September 2018



## Declarations

This work has not been submitted in substance for any other degree or award at this or any other university or place of learning, nor is being submitted concurrently in candidature for any degree or other award.

Signed..... (candidate)                      Date .....

### **STATEMENT 1**

This thesis is being submitted in partial fulfilment of the requirements for the degree of Ph.D.

Signed..... (candidate)                      Date .....

### **STATEMENT 2**

This thesis is the result of my own independent work/investigation, except where otherwise stated, and the thesis has not been edited by a third party beyond what is permitted by Cardiff University's Policy on the Use of Third Party Editors by Research Degree Students. Other sources are acknowledged by explicit references. The views expressed are my own.

Signed..... (candidate)                      Date .....

### **STATEMENT 3**

I hereby give consent for my thesis, if accepted, to be available online in the University's Open Access repository and for inter-library loan, and for the title and summary to be made available to outside organisations.

Signed..... (candidate)                      Date .....

## Acknowledgements

Firstly, I would like to thank my supervisors Dr Lee Parry and Professor Awen Gallimore for the help and advice they offered throughout my PhD, and for the chance of working in such an exciting project.

I would like to thank all the members in of the Parry and Gallimore group for their contribution to my PhD project and help in the lab. I must also thank everyone in the ECSCRI. I feel really grateful to have had the chance to work for 4 years in such a friendly and supportive environment.

A special thanks to the members of the animal unit, particularly Mike Quirk, Elaine Taylor, Paul Chapman and Sarah Davies. Much of the work would not have been possible without your constant support!

I would like to thank my friends outside work, for their support during this journey and for always making me smile even in the most challenging moments.

Cancer Research UK have funded this work. I'm really proud to have been part of such an inspirational organization!

Por fim, gostaria de agradecer aos meus pais e irmã por sempre acreditarem em mim. A realização deste sonho seria impossível sem o seu constante suporte e motivação!



2.4.2	Depletion of Immune Cells or Neutralization of Cytokines .....	39
2.5	Tissue Harvesting and Processing .....	40
2.5.1	Dissection of Organs.....	40
2.5.2	Dissection of Intestines .....	40
2.5.3	Tissue Fixation.....	41
2.5.4	Paraffin Embedding .....	41
2.5.5	Sectioning of Paraffin Embedded Tissue .....	41
2.6	Histological Analysis .....	41
2.6.1	Preparation of Sections for H&E and IHC .....	41
2.6.2	Haematoxylin and Eosin (H&E) Staining.....	42
2.6.3	Immunohistochemistry (IHC).....	42
2.7	Cell Counting .....	45
2.7.1	Total Tumour Burden .....	45
2.7.2	Partial Tumour Burden.....	45
2.7.3	Apoptotic Index.....	45
2.7.4	Scoring of Immune Cell Types .....	45
2.8	Intestinal Epithelial Cells Extraction for Gene Expression Analysis .....	46
2.9	RNA extraction.....	46
2.10	Gene Expression Analysis: Quantitative Real-Time PCR (qRT-PCR) .....	46
2.11	Flow Cytometry .....	48
2.11.1	Preparation of Single Cells Suspensions from Tissues .....	48
2.11.2	Cell Surface Staining .....	50
2.11.3	Intracellular Antigen and Cytokine Staining.....	50
2.11.4	Flow Cytometry Analysis.....	52
2.12	Lgr5 RNAscope®.....	58
2.12.1	Preparation of Sections for RNAscope.....	58
2.12.2	Pre-treatment.....	58
2.12.3	Probe Hybridization.....	59
2.12.4	Probe Hybridization and Amplification.....	59
2.12.5	Signal Detection.....	59
2.12.6	Counterstain and Slides Mounting .....	60
2.12.7	RNAscope Analysis .....	60
2.13	Statistical Analysis .....	60
3	Investigating the immune effects of <i>Apc</i> deficiency in the early stages of CRC .....	61
3.1	Introduction .....	61
3.2	Results.....	63
3.2.1	Characterisation of Treg cells during tumourigenesis in the <i>Apc</i> <sup>min/+</sup> mouse ...	63

3.2.2	Characterising Treg cells during initiation of intestinal tumourigenesis by conditional deletion of the <i>Apc</i> gene in the intestinal stem cells (ISCs) .....	66
3.3	Discussion .....	81
4	Investigating the effects of Treg depletion after loss of <i>Apc</i> gene in the ISCs.....	85
4.1	Introduction .....	85
4.2	Results.....	86
4.2.1	Treg cell depletion reduces tumorigenic potential in the <i>Lgr5Cre<sup>ERT2</sup>Apc<sup>fl/fl</sup>Foxp3<sup>DTR</sup></i> mouse model .....	86
	.....	91
4.2.2	Examining the effects of Treg depletion on T-cell populations in the early stages of intestinal cancer.....	97
4.3	Discussion .....	112
5	Cellular subsets responsible for the anti-tumour immune response.....	116
5.1	Introduction .....	116
5.2	Results.....	117
5.2.1	Analysing the effect of CD4+ T-cells depletion in an <i>Apc</i> deleted mice .....	117
5.2.2	Analysing the effect of CD8+ T-cells depletion in an <i>Apc</i> deleted mice .....	129
5.2.3	Analysing the effect of IFN $\gamma$ neutralisation in an <i>Apc</i> deleted mice.....	141
5.3	Discussion .....	152
5.3.1	Evaluating the role of CD4+ cells in intestinal homeostasis.....	152
5.3.2	Evaluating the role CD8+ cells in the intestinal homeostasis.....	153
5.3.3	Evaluating the role of IFN $\gamma$ in the intestinal homeostasis .....	154
6	RNAscope analysis of <i>Lgr5</i> transcripts in the early stages of intestinal cancer.....	156
6.1	Introduction .....	156
6.2	Results.....	157
6.3	Discussion .....	172
7	General Discussion/Conclusion .....	174
8	References .....	179
9	Supplementary Material .....	204

## List of Figures

Figure 1.1 Histology of the murine small and large intestines.....	3
Figure 1.2 Organization of the intestinal epithelia and the markers for the different cell populations. ....	6
Figure 1.3 Schematic representation of the potential outcomes of ISC division.....	8
Figure 1.4 Schematic representation of the canonical Wnt signalling pathway in normal colonic and cancer cells. ....	10
Figure 1.5 Multi-step tumourigenesis of the intestinal epithelium.....	15
Figure 1.6 Schematic representation of the three different phases of the concept of cancer immunoediting.....	18
Figure 1.7 Differentiation of Naive CD4+ T-cells. ....	24
Figure 2.1 Representative flow cytometry plots showing gating strategy and examples of FMO's in the spleen. ....	53
Figure 2.2 Gating strategy for flow cytometry analysis of the indicated markers in each cell compartment analysed (spleen, MLN, SI IEL, SI LPL, LI IEL and LI LPL). ....	54
Figure 2.3 (Continuation) Gating strategy for flow cytometry analysis of the indicated markers in each cell compartment analysed (spleen, MLN, SI IEL, SI LPL, LI IEL and LI LPL). ....	55
Figure 2.4 (Continuation) Gating strategy for flow cytometry analysis of the indicated markers in each cell compartment analysed (spleen, MLN, SI IEL, SI LPL, LI IEL and LI LPL). ....	56
Figure 2.5 (Continuation) Gating strategy for flow cytometry analysis of the indicated markers in each cell compartment analysed (spleen, MLN, SI IEL, SI LPL, LI IEL and LI LPL). ....	57
Figure 3.1 Tregs quantification in the small intestine of an <i>Apc<sup>min/+</sup></i> mouse model. ....	64
Figure 3.2 Tregs quantification in the <i>Lgr5Cre<sup>ERT2</sup>Apc<sup>fl/fl</sup></i> mouse in small (SI) and large intestines (LI). ....	67
Figure 3.3 Relative gene expression of <i>Foxp3</i> in the small intestinal epithelium.....	68
Figure 3.4 Frequency of CD4+ cells expressing <i>Foxp3</i> in the specified compartments of the small and large intestines.....	70
Figure 3.5 Frequency of CD3+ T-cells in the specified compartments of the small and large intestines.....	72
Figure 3.6 Frequency of CD3+ T-cells expressing CD4 and CD8 in the specified compartments of the small and large intestines.....	74

Figure 3.7 Frequency of T-cells expressing Granzyme B in the specified compartments of the small and large intestines.....	76
Figure 3.8 Frequency of T-cells expressing IL-17A in the specified compartments of the small and large intestines.....	78
Figure 3.9 Frequency of T-cells expressing IFN $\gamma$ in the specified compartments small and large intestines.....	80
Figure 4.1 Tumour burden analysis in the SI and LI.....	87
Figure 4.2 Apoptotic index in the small intestinal crypts.....	91
Figure 4.3 Relative gene expression of the Wnt signalling markers Axin2 and c-Myc in the small intestinal epithelium.....	93
Figure 4.4 Relative gene expression of the ISCs markers Lgr5, Olfm4 and Ascl2 in the small intestinal epithelium.....	93
Figure 4.5 Relative gene expression of Foxp3 and IFN $\gamma$ in the small intestinal epithelium.....	96
Figure 4.6 Frequency of CD3+ T-cells in the specified compartments of SI and LI following Treg cells depletion.....	98
Figure 4.7 Frequency of CD3+ T-cells expressing CD4+ and CD8+ in the specified compartments of SI and LI following Treg cells depletion.....	100
Figure 4.8 Frequency of CD4+ cells expressing Foxp3 in the specified compartments of SI and LI following Treg cells depletion.....	102
Figure 4.9 Frequency of CD4+ and CD8+ cells expressing Granzyme B in the specified compartments of SI and LI following Treg cells depletion.....	104
Figure 4.10 Frequency of CD4+ and CD8+ cells expressing IL-17A in the specified compartments of SI and LI following Treg depletion.....	107
Figure 4.11 Frequency of CD4+ and CD8+ cells expressing IFN $\gamma$ in the specified compartments of SI and LI following Treg depletion.....	110
Figure 5.1 Tumour burden analysis in the small intestine of CD4+ cells depleted mice....	119
Figure 5.2 Relative gene expression of Wnt signalling markers in the small intestinal epithelium, following CD4+ cell depletion.....	121
Figure 5.3 Relative gene expression of ISC markers in the small intestinal epithelium, following CD4+ cells depletion.....	122
Figure 5.4 Relative gene expression of Foxp3 and IFN $\gamma$ in the small intestinal epithelium, following CD4+ cells depletion.....	123
Figure 5.5 Quantification of CD4+ cells in the small intestine following CD4+ cells depletion.....	126
Figure 5.6 Quantification of CD8+ T-cells in the small intestine following CD4+ cells depletion.....	128
Figure 5.7 Tumour burden analysis in the small intestine following CD8+ cells depletion..	131

Figure 5.8 Relative gene expression of Wnt signalling markers in the small intestinal epithelium, following CD8+ cells depletion. ....	133
Figure 5.9 Relative gene expression of ISC markers in the small intestinal epithelium, following CD8+ cells depletion. ....	134
Figure 5.10 Relative gene expression of Foxp3 and IFN $\gamma$ in the small intestinal epithelium, following CD8+ cells depletion .....	135
Figure 5.11 Quantification of CD4+ cells in the small intestine following CD8+ cells depletion. ....	138
Figure 5.12 Quantification of CD8+ cells in the small intestine following their depletion. ...	140
Figure 5.13 Tumour burden analysis in the small intestine following IFN $\gamma$ neutralisation..	143
Figure 5.14 Relative gene expression of Wnt signalling markers in the small intestinal epithelium, following IFN $\gamma$ neutralisation. ....	145
Figure 5.15 Relative gene expression of ISC markers in the small intestinal epithelium, following IFN $\gamma$ neutralisation. ....	146
Figure 5.16 Quantification of CD4+ cells in the small intestine following IFN $\gamma$ neutralisation. ....	149
Figure 5.17 Quantification of CD8+ cells in the small intestine following IFN $\gamma$ neutralisation. ....	151
Figure 6.1 <i>Lgr5</i> expression analysis in the small intestinal crypts following CD4+ T-cells depletion. ....	159
Figure 6.2 <i>Lgr5</i> expression analysis in the small intestinal crypts following CD8+ T-cells depletion. ....	161
Figure 6.3 <i>Lgr5</i> expression analysis in the small intestinal crypts following IFN $\gamma$ neutralisation. ....	163
Figure 6.4 <i>Lgr5</i> expression analysis in the small intestinal villi following CD4+ T-cells depletion. ....	167
Figure 6.5 <i>Lgr5</i> expression analysis in the small intestinal villi following CD8+ T-cells depletion. ....	169
Figure 6.6 <i>Lgr5</i> expression analysis in the small intestinal villi following IFN $\gamma$ neutralisation. ....	171
Figure 7.1 Representative model of the effects of Treg depletion in Apc deleted mice. ....	178
Figure S 9.1 Frequency of CD4+ cells expressing Foxp3 in the spleen and MLN.....	204
Figure S 9.2 Frequency of CD3+ T-cells in the spleen and MLN. ....	205
Figure S 9.3 Frequency of CD3+ cells expressing CD4 in the spleen and MLN. ....	206
Figure S 9.4 Frequency of CD3+ cells expressing CD8 in the spleen and MLN. ....	207
Figure S 9.5 Frequency of CD4+ expressing Granzyme B in the spleen and MLN.....	208
Figure S 9.6 Frequency of CD8+ cells expressing Granzyme B in the spleen and MLN....	209

Figure S 9.7 Frequency of CD4+ cells expressing IL-17A in the spleen and MLN.....	210
Figure S 9.8 Frequency of CD8+ cells expressing IL-17A in the spleen and MLN.....	211
Figure S 9.9 Frequency of CD4+ cells expressing IFN $\gamma$ in the spleen and MLN.....	212
Figure S 9.10 Frequency of CD8+ cells expressing IFN $\gamma$ in the spleen and MLN.....	213

## List of Tables

Table 2.1 Genotyping PCR reaction mixture and conditions.....	36
Table 2.2 Primer sequences and band sizes.....	38
Table 2.3 Antibody-specific conditions used for IHC .....	44
Table 2.4 TaqMan® qRT-PCR primers/probes .....	48
Table 2.5 SYBR® Green qRT-PCR primers.....	48
Table 2.6 Flow Cytometry Antibodies.....	51
Table 2.7 Amplification steps conditions .....	59

## Abbreviations and Definitions

### Symbols

°C= Degrees Celsius

µg = Micrograms

µl = Microlitre

µm = Micrometre

µM = Micromolar

fl/fl = Homozygously floxed allele

### A

APC = Adenomatous Polyposis Coli

Ascl2 = Achaete Scute like 2

AXIN2 = Axis Inhibitor Protein 2

### B

BMP = Bone Morphogenic Protein

bp = Base Pair

BSA = Bovine Serum Albumin

### C

CBC cells = Crypt Base Columnar cells

cDNA = Complementary DNA

CD3 = Cluster of Differentiation 3

CD4 = Cluster of differentiation 4

CD8 = Cluster of differentiation 8

CRC = Colorectal Cancer

Cre = Cre recombinase

CreERT2 = Cre recombinase-Estrogen receptor fusion transgene

CSC = Cancer Stem Cell

CT = Cycle threshold

### D

DAB= Diaminobenzidine

dH<sub>2</sub>O = Distilled H<sub>2</sub>O

DNA = Deoxyribonucleic Acid

DNase = Deoxyribonuclease

dNTP = Deoxynucleotide triphosphate

d.o. = days old

DVL = Dishevelled

DSS = Dextran Sodium Sulphate

### E

EDTA = Ethylenediaminetetraacetic acid

ER = Estrogen Receptor

EtOH = Ethanol

### F

FAP = Familial Adenomatous Polyposis

FMO = Fluorescence Minus One

Foxp3 = Forkhead box P3

Fzd = Frizzled

### G

g = Gram

GEMM = Genetically Engineered Mouse Model

gDNA = Genomic Deoxyribonucleic Acid

GSK-3 = Glycogen Synthase Kinase-3

### H

H&E = Haematoxylin and Eosin

HBSS = Hanks Balanced Salt Solution

hr = Hour

## **I**

IFN $\gamma$  = Interferon gamma

IHC = Immunohistochemistry

IL-17A = Interleukin 17A

IP = Intraperitoneal

ISC = Intestinal Stem Cell

## **K**

KRAS = Kirsten Rat Sarcoma viral oncogene homolog

## **L**

L = Litre

LOH = Loss of heterozygosity

LoxP = Locus of crossover of Bacteriophage P1

Lgr5 = Leucine-rich repeat containing G protein coupled receptor 5

## **M**

mg = Milligram

MHC I = major histocompatibility complex class I

MHC II = major histocompatibility complex class II

Min = Multiple Intestinal Neoplasia

mins = Minutes

ml = Millilitre

mM = Millimolar

mRNA = Messenger Ribonucleic Acid

## **N**

n = Number

## **O**

Olfm4 = Olfactomedin 4

O/N = Overnight

## **P**

PBS = Phosphate Buffered Saline

PCR = Polymerase Chain Reaction

PI = Post induction

PKA = Protein Kinase A

## **Q**

qRT-PCR = Quantitative Reverse Transcription Polymerase Chain Reaction

## **R**

RNA = Ribonucleic Acid

RNase = Ribonuclease

rpm = Revolutions per minute

RPMI = Roswell Park Memorial Institute

RT = Room Temperature

## **S**

SDS = Sodium Dodecyl Sulphate

secs = Seconds

## **T**

TA = Transit amplifying

Taq = DNA polymerase derived from *Thermus aquaticus*

TCF = T cell-specific transcription factor

## Abstract

Colorectal cancer (CRC) is one of the most common cancers in Europe and the fourth most common in the UK, being influenced by environmental factors, genetic mutations and interactions with the host immune system. The Wnt pathway plays a key role in maintaining intestinal homeostasis. Constitutive activation of Wnt occur in more than 80% of CRC, primarily due to the loss of the *Apc* gene. This mutation occurs in the intestinal stem cells (ISC), the cell of origin for CRC. ISCs are identified by *Lgr5* expression. The immune microenvironment of these tumours plays a key role in their progression. The local recruitment of immunosuppressive Foxp3<sup>+</sup> regulatory T-cells (Tregs) has been demonstrated in CRC patients, however it is unclear whether they limit or promote the anti-tumour immune responses. Importantly most of the studies were done in patients with advanced disease, highlighting the need to understand the role of these cells in the early stages of tumourigenesis.

To understand the influence of Tregs on an ISC following an oncogenic mutation, genetically modified mice were used. Using the *Lgr5* transgene, to conditionally delete *Apc* in the intestinal stem cell (ISC), it is possible to model the initial stages of CRC. This mouse was crossed with the *Foxp3*<sup>DTR</sup> mouse, which expresses the human diphtheria toxin receptor under the control of the *Foxp3* promoter (*Lgr5Cre*<sup>ERT2</sup>*Apc*<sup>f/f</sup>*Foxp3*<sup>DTR</sup>). Selective depletion of Tregs can be achieved by injection of diphtheria toxin, enabling the investigation of the role that Tregs and conventional T-cells play during malignant transformation. To identify the role of other immune cell populations in the anti-tumoral immune response, CD4<sup>+</sup> and CD8<sup>+</sup> cells were depleted and IFN $\gamma$  was neutralized in the *Lgr5Cre*<sup>ERT2</sup>*Apc*<sup>f/f</sup>*Foxp3*<sup>DTR</sup> mouse model.

Here, it was shown that 15 days following *Apc* deletion, the number of Tregs increased in the small and large intestines, spleen and mesenteric lymph nodes (MLN). Treg depletion, in *Apc* deleted mice, resulted in a reduction of the intestinal tumour burden. The same was observed in mice where CD4<sup>+</sup> and CD8<sup>+</sup> cells were depleted. IFN $\gamma$  neutralization had no effects.

In this mouse model, data suggest that CD4<sup>+</sup>, CD8<sup>+</sup> cells or IFN $\gamma$  do not play a role in the anti-tumour immune responses. Overall these data indicate that Tregs inhibit the immune recognition of newly transformed ISCs suggesting that Tregs play a key role in the early stages of intestinal cancer by promoting tumourigenesis. This is particularly important as Tregs can be a possible target in the early stages of CRC and their modulation might prevent tumour progression, improving the outcome of CRC patients.

# 1 General Introduction

## 1.1 Cancer

Cancer is responsible for about 8.2 million deaths worldwide and is the leading cause of human mortality (Cancer Research UK). There are various factors implicated in the development of cancer, such as genetic mutations and environmental factors (e.g. poor diet, smoking, exposure to sunlight, obesity and others) (Whiteman and Wilson 2016).

## 1.2 Colorectal Cancer

Colorectal cancer (CRC) is the second most common cancer diagnosed in Europe and the fourth most common cancer in the UK accounting for 12% of all new cancer cases (Cancer Research UK). Since the early 1970s the mortality rates of CRC have decreased by 44% in the UK, however the five-year survival rate of people diagnosed with CRC remains at 59% (Cancer Research UK).

The risk of developing CRC depends on several factors such as environmental (e.g. diet and microbiome), epigenetic, familiar history of CRC, inflammatory bowel disease (IBD) are also involved in the high incidence of CRC (Brenner *et al.* 2014). More than 90% of the CRC are adenocarcinomas that arise from adenomatous polyps, also known as adenomas (Giuliani *et al.* 2006). To understand the oncogenic process in the intestine it is needed to understand the basic biology that will be described in the next sections.

### 1.2.1 Intestinal anatomy and function

The intestine is part of the digestive system, where the food passes through and the nutrients are absorbed. It is formed by the small and the large intestines, approximately 7.5 metres long in humans (Drake *et al.* 2005) and 49 cm in mice (Fox *et al.* 2006).

The small intestine is divided into three parts: the duodenum, the jejunum and the ileum. The luminal surface of the small intestinal is formed by a single layer of epithelial cells. These cells are polarised and organized into finger-like projections called villi, responsible for increasing the surface area to optimize the absorption, and invaginations called the crypts of Lieberkühn, generally known as crypts. Beneath the villi and the crypts lies the lamina propria

which is composed of mesenchymal stromal fibroblasts which encase the blood supply of the small intestine. Underneath the epithelial and stromal compartment is located the smooth muscle layer which is responsible for the peristaltic movements of the food through the intestine (figure 1.1) (Williams *et al.* 1989).

The large intestine is divided into caecum, colon, rectum and anal canal. Most of the water that is ingested is absorbed in the large intestine. It is also where the faecal material is stored before it is egested (Williams *et al.* 1989). The large intestine is formed by a single layer of epithelial columnar cells, however only the crypts are present. Similar to the small intestine it also contains lamina propria, stromal fibroblasts and the sub and muscularis mucosae (figure 1.1). The majority of the cells that form the large intestine are mucus secreting cells (Barker *et al.* 2008).

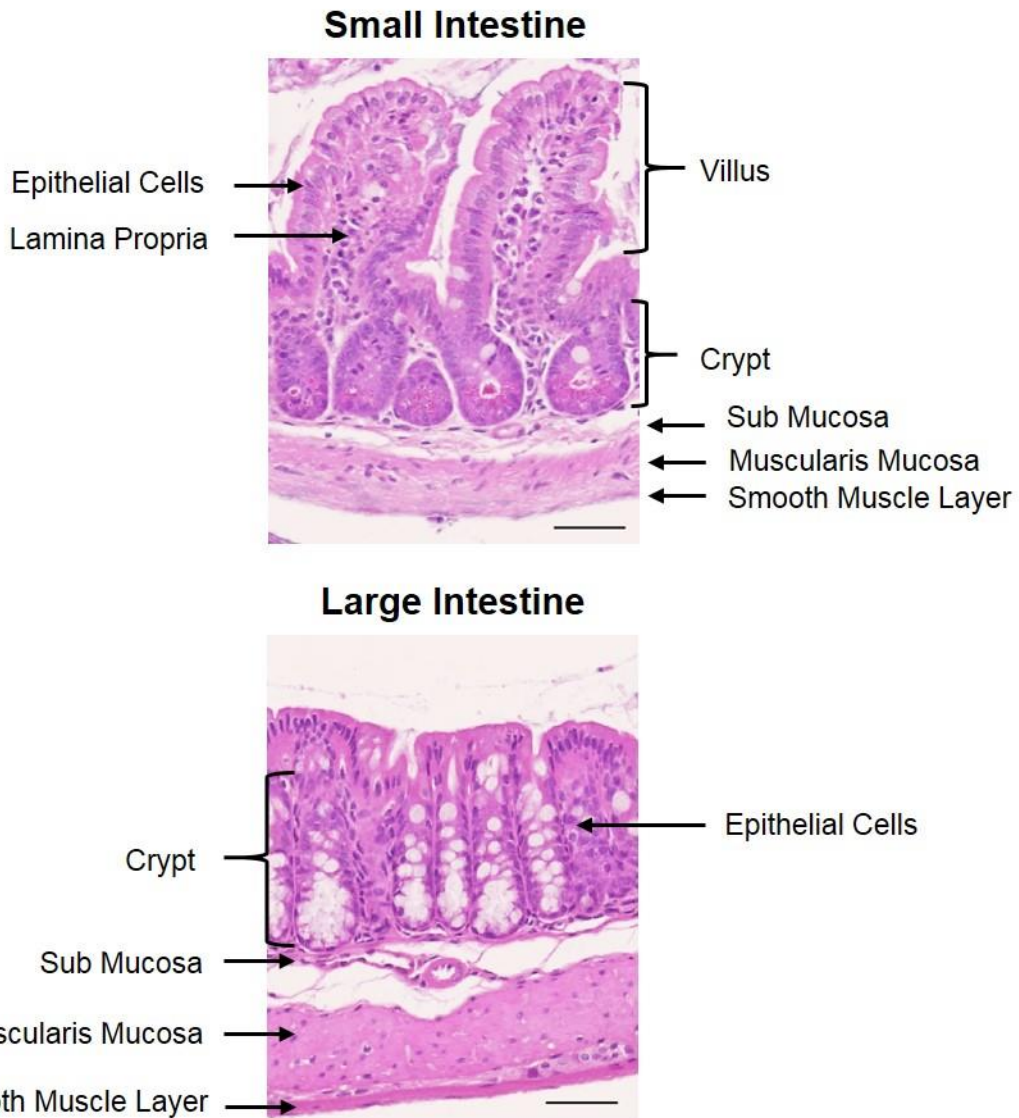


Figure 1.1 Histology of the murine small and large intestines.

The small intestine is formed by villi and crypts. Below the crypts there are the mucosae and the smooth muscle layer. The large intestine is formed by a single epithelial layer, forming the crypts and, below them, there are the mucosae layer. Scale bars represent 50  $\mu\text{m}$ .

### 1.2.2 Intestinal Epithelial Homeostasis

The small intestinal epithelium is a highly dynamic and regulated tissue with 6-9 crypts feeding cells into each villus. The stem cells, which are located in bottom of the crypts, continuously proliferate, migrate and differentiate. The intestinal epithelium is renewed every 5-6 days in humans and every 2-3 days in mice (Creamer 1967; Wright and Alison 1984) and there is a constant balance between proliferation and differentiation. There is a tight control of the genes that participate in these processes and this is done through various signalling pathways, such as Notch (Noah and Shroyer 2013; Kadur Lakshminarasimha Murthy *et al.* 2018), TGF- $\beta$ /BMP (Beck *et al.* 2003; Ihara *et al.* 2017), Hedgehog (Buller *et al.* 2012) and Wnt (Fevr *et al.* 2007; Krausova and Korinek 2014; Koch 2017). The Wnt signalling pathway will be discussed in more detail due to its relevance in this project.

The intestinal stem cells are generally known as Crypt Base Columnar cells (CBC). CBC cells, can be identified by the expression of markers such as the leucine-rich repeat-containing G-protein coupled receptor (*Lgr5*), olfactomedin 4 (*Olfm4*), achaete-scute family bHLH transcription factor 2 (*Ascl2*) and SRY-box 9 (*Sox9*) (figure 1.2). Due to the relevance in this project the *Lgr5* marker will be discussed in more detail. CBC cells proliferate and originate the cell progenitors, the transit amplifying (TA) cells that divide 4-5 times while they migrate along the crypt. Depending on the specific signals that are received, TA differentiate into the 4 different cell types that are found in the intestine, namely the enterocytes, goblet cells, enteroendocrine cells and Paneth cells (Gerbe *et al.* 2011). This process of migration and differentiation is controlled by conserved signalling pathways such as Wnt and Notch signalling pathways (Gregorieff *et al.* 2005), as well as Eph/ephrin signalling (Poliakov *et al.* 2004).

Most of the differentiated cells located in the villi are enterocytes. These cells are responsible for the absorption of the nutrients as well as secretion of hydrolytic enzymes that participate in the digestion of the food. The enterocytes are tightly pack together by cell-to-cell adhesions and form the barrier that prevents the movement of the microbes to the bloodstream avoiding, in this way, immune reactions against them (Barker 2014).

To assist the transit of luminal contents mucus is produced from the goblet cells, which produced a variety of mucin proteins. These mucins are responsible for the lubrication of the epithelium, protecting it from the mechanical stress caused by the food movement. In addition to mucins they produce trefoil proteins involved in tissue repair (Barker 2014). These cells are mainly located at the crypt-villus junction, particularly towards the distal end of the small intestine. Goblet cells are present in a higher frequency in the colon when compared to the small intestine (Mowat and Agace 2014)

Enteroendocrine cells, found throughout the crypt-villus axis, are present in a much lower number when compared to the other differentiated cell types. These cells secrete hormones, such as serotonin and secretin that control some of the intestinal functions including the regulation of glucose levels, modulation of food intake, gastrointestinal tract movement as well as mucosal immunity and repair (Schonhoff *et al.* 2004; Engelstoft *et al.* 2008; Moran *et al.* 2008).

Paneth cells, located exclusively in the bottom of the crypts (Barker *et al.* 2008), are long-lived (6-8 weeks) secretory cells that arise directly from the quiescent intestinal cells (Buczacki *et al.* 2013). In contrast to the other differentiated cells, Paneth cells migrate back down the crypt-villus axis, forming the intestinal stem cells (ISC) niche (Batlle *et al.* 2002). Paneth cells promote the immunity and protection of the ISC by secreting various antimicrobials such as cryptdins, lysozymes and other factors including TGF- $\alpha$  and Wnt3, being crucial in the intestinal homeostasis (Bevins and Salzman 2011).

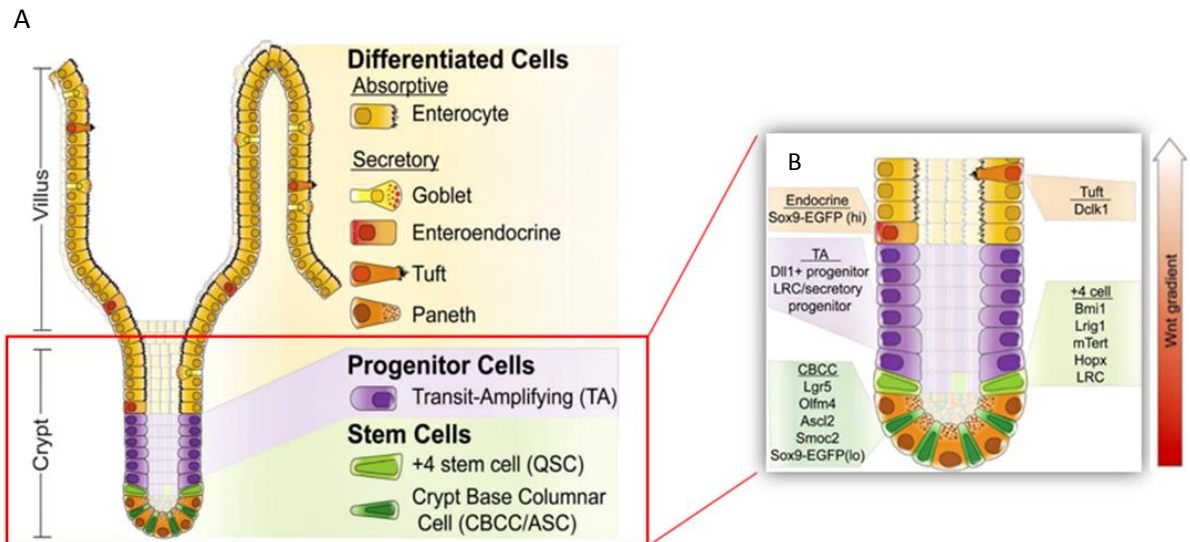


Figure 1.2 Organization of the intestinal epithelia and the markers for the different cell populations.

A) The stem cells are located in the bottom of the crypts. These cells proliferate and originate the progenitor cells that will then migrate along the villi and differentiate into either absorptive or secretory cells depending on the signals that they receive. B) The cell populations present in the intestinal epithelia can be identified by the expression of different markers. The Wnt signalling pathway has a very important role in the control of the intestinal homeostasis, being particularly active in the bottom of the crypts (Carulli *et al.* 2014).

### 1.2.2.1 Intestinal Stem Cell Competition

Intestinal stem cells (ISCs), located at the bottom of the crypts, are able to differentiate into all cell types within the intestine (Barker *et al.* 2007; Barker *et al.* 2008) during homeostasis or injury. This is a highly regulated mechanism that is coordinated with cell death that occurs in the villi, avoiding excessive loss of intestinal cells or, the opposite, abnormal accumulation of cells.

Stem cells can divide in three different ways. Under normal circumstances the cells divide asymmetrically which results in the formation of a daughter stem cell and a daughter TA cell, allowing self-renewal of the stem cell compartment as well as expansion of the TA compartment (Figure 1.3) (Potten and Loeffler 1990). Following injury, stem cells undergo symmetrical division originating either two daughter stem cells or two daughter TA cells, which contributes to the maintenance of intestinal homeostasis. On the other hand, in the absence of sufficient numbers of stem cells, TA cells are also able to de-differentiate back to true-stem cells, maintaining the intestinal homeostasis (Figure 1.3) (Shahriyari and Komarova 2013; Barker 2014).

During the differentiation process, cells move out of the crypt onto the villi, where they are shed. Contrary to the other differentiated lineages, Paneth cells move down to the crypt, where they assume position between the stem cells and form part of the stem cell niche (Sato *et al.* 2011). Buczacki and colleagues have demonstrated that in the mouse intestine, quiescent label retaining cells, the population that mature into enteroendocrine and Paneth cells during homeostasis can, in fact, upon injury, undergo rapid proliferation originating the main epithelial cell types. This research shows that established quiescent cells can function as a clonogenic reserve (Buczacki *et al.* 2013)

The ISC clones compete to occupy the stem cell niche, resulting in the ongoing monoclonal conversion in all crypts and leading to the elimination of mutant cells (Lopez-Garcia *et al.* 2010; Snippert *et al.* 2010; Ritsma *et al.* 2014). Snippert and colleagues generated a multi-colour Cre reporter and performed fate mapping of individual stem cells. The authors showed that Lgr5<sup>hi</sup> cells divide symmetrically giving rise to either two stem cells or two TA cells supporting the hypothesis that ISCs undergo neutral competition (Snippert *et al.* 2010), and contradicting the previously proposed model in which ISCs divide asymmetrically (Potten *et al.* 2002; Smith 2005). Further studies using computational and mouse models have confirmed the theory that stem cells located in the bottom of the crypts have a significant advantage to compete over the other cells located above (Mirams *et al.* 2012; Ritsma *et al.* 2014). More recently, with the use of a 3D individual cell-based model to study clonal competition in the intestine, Thalheim and colleagues have shown that not only cell distribution, but also niche composition, can impact on clonal competition (Thalheim *et al.*

2016). The authors have studied the impact of Wnt and Notch signalling pathways on clonal competition due to their importance for stem cell self-renewal and lineage specification, and have shown that mutations in these pathways result in phenotypic changes; this demonstrates that fixation probability of mutations is dependent on mutation acquisition (Thalheim *et al.* 2016). The model of ISC symmetric division predominates, however the mechanisms that drive fate choices regarding stem cell division are still unclear, being essential to test experimentally the mechanisms unveiled by multi-scale computational modelling.

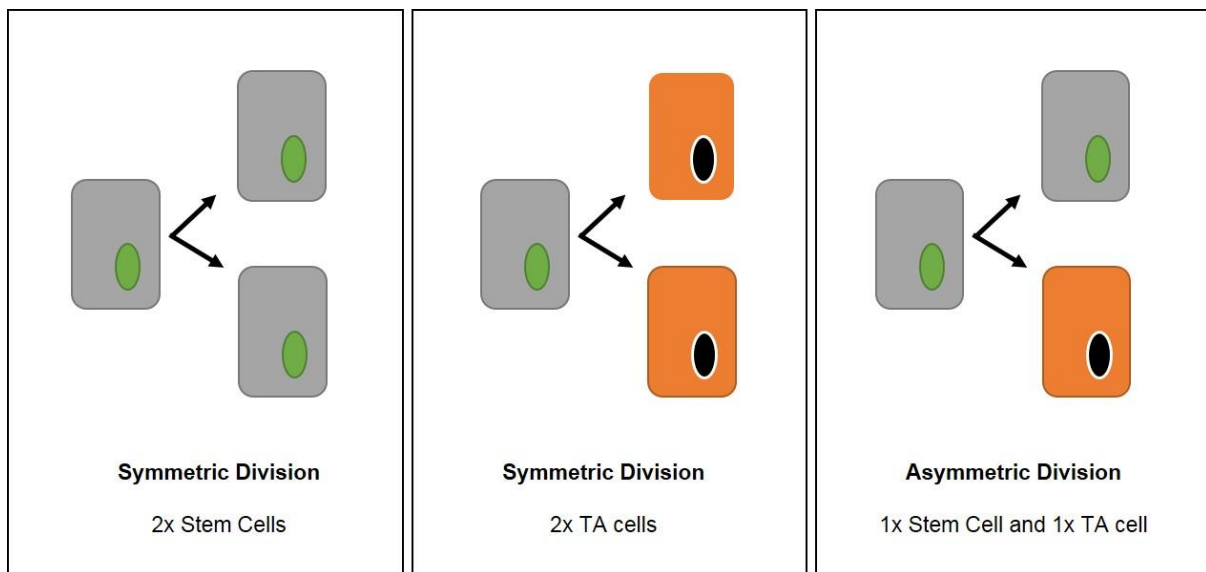


Figure 1.3 Schematic representation of the potential outcomes of ISC division.

ISCs – Grey cells; TA – Orange cells

### 1.2.3 Wnt Signalling Pathways

There are various signalling pathways involved in intestinal epithelial homeostasis that maintain the balance between cell proliferation, migration and apoptosis. One of the most important pathways is the Wnt signalling pathway due to its importance in morphogenesis during both embryogenesis and in the adult tissue self-renewal homeostasis (Clevers 2006). Three different Wnt pathways have been described: the canonical Wnt/ $\beta$ -catenin pathway, the non-canonical planar cell polarity pathway and the non-canonical Wnt/calcium pathway.

The canonical Wnt pathway is the major regulator of intestinal homeostasis and it will be described in more detail in the next section. The best characterized non-canonical pathway

is the planar cell polarity pathway. As the name suggests, this pathway controls cell polarity in morphogenetic mechanisms in vertebrates, including neural tube closure and gastrulation, through cytoskeletal changes (Zallen 2007). The Wnt/calcium pathway controls the calcium levels, regulating the transcription of genes important for cell fate and cell migration (Kohn and Moon 2005).

#### 1.2.3.1 Canonical Wnt Signalling Pathway

The canonical Wnt pathway, a conserved signalling pathway involved in development, regeneration, survival and cell proliferation, is crucial to the maintenance of homeostasis within the intestinal epithelia. Deregulation of this pathway occurs in 80% of human CRCs, leading to aberrant stem cell differentiation (Mazzoni and Fearon 2014).

In the absence of a Wnt ligand the pathway is in its “off state”.  $\beta$ -catenin is phosphorylated by the destruction complex formed by the scaffold protein Axin, Adenomatous Polyposis Coli (APC) tumour suppressor, glycogen synthase kinase-3 $\beta$  (GSK-3 $\beta$ ) and casein kinase 1  $\alpha$  (CK1-  $\alpha$ ). After phosphorylation,  $\beta$ -catenin is recognized by the  $\beta$ -transducin repeat-containing protein ( $\beta$ -TrCP) of the E3 ubiquitin ligase complex catalysing its ubiquitination. Following ubiquitination  $\beta$ -catenin is degraded in the proteasome. Low levels of free cytoplasmic  $\beta$ -catenin allow the interaction of Groucho-related gene (GRO) repressors with T-cell factor (TCF) proteins, leading to the recruitment of histone deacetylases (HDACs) resulting in the inhibition of Wnt target genes (figure 1.4) (Clevers 2006; Clevers *et al.* 2014).

Wnt activation occurs when the Wnt ligands bind to the Frizzled (FZD) and low-density lipoprotein-receptor related protein (LRP) co-receptor complex (Clevers 2006; Clevers *et al.* 2014), leading to the phosphorylation of LRP receptors by CK1-  $\alpha$  and GSK-3 $\beta$ . After this, DVL and Axin proteins are recruited to the plasma membrane where they become polymerized and activated. The destruction complex is inactivated by the DVL polymers, resulting in the accumulation of  $\beta$ -catenin in the cytoplasm, which translocates to the nucleus, binding to TCF proteins and activating the transcription of downstream target genes, including *c-Myc*, *Cyclin D1* and others (figure 1.4). Mutation of the *APC* gene leads to the activation of the Wnt signalling, even if Wnt ligands are not present, by promoting the dissociation of the destruction complex. Similar to what happens in the presence of Wnt ligands,  $\beta$ -catenin accumulates in the cytoplasm and translocates to the nucleus activating the transcription of Wnt target genes (figure 1.4) and promoting uncontrolled cell growth (Mazzoni and Fearon 2014). These transformed cells do not differentiate, remaining located at the crypt bottoms, leading to the initiation of CRC.

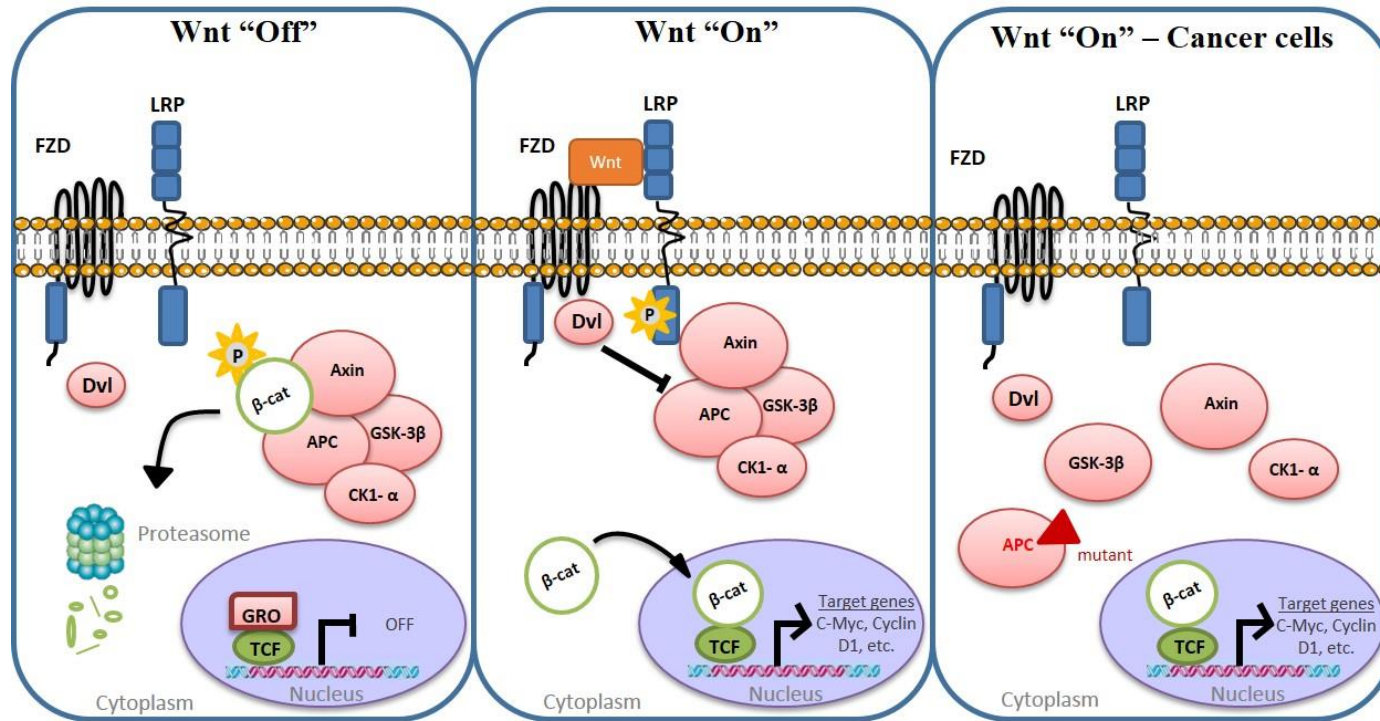


Figure 1.4 Schematic representation of the canonical Wnt signalling pathway in normal colonic and cancer cells.

In the absence of a Wnt ligand  $\beta$ -catenin binds to the destruction complex formed by APC, Axin, GSK-3 $\beta$  and CK1- $\alpha$  being phosphorylated and, after ubiquitination, degraded in the proteasome. In the presence of Wnt ligand, the destruction complex is inactivated and the  $\beta$ -catenin accumulate in the cytoplasm, translocate to the nucleus and promote the transcription of genes involved in proliferation and tumorigenesis. When the APC gene is mutated the destruction complex is not formed, leading to the translocation of  $\beta$ -catenin to the nucleus, promoting the transcription of Wnt target genes.

#### 1.2.4 Cancer Stem Cells

The concept of the existence of cancer stem cells (CSCs) was first proposed by Schofield a few decades ago (Schofield 1978) who suggested the tumour growth was sustained by a small population of cancer cells with the ability to self-renew. It has been shown that these cells reside in dedicated niches within the tumours, although their identification and elimination has been more challenging than what was expected (Batlle and Clevers 2017). The existence of this cell population explains the common recurrence of cancer in patients who have gone through initial successful chemotherapy and/or other treatments such as radiotherapy.

After Schofield, other researchers have shown evidence supporting the existence of CSC population. Bonnet and Dick showed that transplanting immune-deficient mice with a population of human acute myeloid leukemic cells characterized by the expression of a combination of the surface markers CD34<sup>+</sup>CD38<sup>-</sup> was sufficient for these mice to develop leukaemia (Bonnet and Dick 1997). Similar studies were performed to further analyse the presence of CSCs and their function in CRC initiation (Zhou *et al.* 2018). Dalerba and colleagues collected CRC solid tissues from surgical specimens and xenografts developed in nonobese diabetic/severe combined immunodeficient (NOD/SCID) mice, and performed flow cytometry to analyse surface markers (Dalerba *et al.* 2007); epithelial cancer cells expressing heterogeneous surface markers were cell sorted, and the capacity of different cell subsets to initiate tumours was tested by injecting them in NOD/SCID mice. The authors showed that the capacity to initiate tumours in the transplanted mice was restricted to a subpopulation of cells with enriched expression of epithelial cell adhesion molecule (EpCAM<sup>high</sup>) as well as expression of the surface marker CD44<sup>+</sup> (Dalerba *et al.* 2007).

Other studies have shown that a high density CD133<sup>+</sup> cell population could initiate tumour formation when injected in immunodeficient mice, whereas injection of CD133<sup>-</sup> cells failed to initiate tumourigenesis (O'Brien *et al.* 2007; Ricci-Vitiani *et al.* 2007). However, a year later, another study contradicted these results by showing that both CD133<sup>+</sup> and CD133<sup>-</sup> metastatic colon cells could initiate tumour formation (Shmelkov *et al.* 2008). More CSC markers have been identified in CRC such as aldehyde dehydrogenase 1 (ALDH1) (Hessman *et al.* 2012; Rassouli *et al.* 2016), octamer-binding transcription factor 4 (OCT 4) (Matsuoka *et al.* 2012; Wahab *et al.* 2017), SRY (sex determining region Y)-box 2 (SOX-2) (Neumann *et al.* 2011; Talebi *et al.* 2015), Nanog Homeobox (NANOG) (Hadjimichael *et al.* 2015; Wahab *et al.* 2017), *c-Myc* (Takahashi and Yamanaka 2006; Markowitz and Bertagnolli 2009) and the leucine rich repeat containing G protein-coupled receptor 5 (LGR5) which will be discussed in more detail in the following section (Barker *et al.* 2009; Ricci-Vitiani *et al.* 2009; Shimokawa *et al.* 2017; Leng *et al.* 2018).

Altogether, these studies agree with the cancer stem cell hypothesis, showing that this cell population can be identified by a variety of markers and can initiate tumourigenesis.

### 1.2.5 Lgr5 stem cells as the origin of CRC

The identification of a true stem cell population in the mouse intestine has been controversial. Several studies have suggested potential stem cell markers based on positional information of gene expression, which itself does not give enough evidence to define genes as ISCs markers (Barker et al. 2012). However, through lineage tracing (Barker and Clevers 2007) and in situ hybridization (Gregorieff et al. 2005) several markers have been identified. Barker and colleagues have identified the *Lgr5* as a marker of rapidly dividing stem cells in the small and large intestines (Barker et al. 2007). *Lgr5* was selected from a panel of genes due to its restricted crypt expression; it was shown by lineage tracing that *Lgr5*<sup>+</sup> CBC cells generated the epithelial lineages, suggesting that *Lgr5* represents the stem cell of both small and large intestines (Barker et al. 2007).

Lgr5 is a G-protein coupled receptor (GPCR) of the class A Rhodopsine-like family of GPCRs. These receptors control a variety of key functions by binding ligands such as hormones and neurotransmitters (Kumar et al. 2014). Leucine-rich repeat-containing GPCRs (LGRs) are distinct from the other GPCRs as they contain a large extracellular domain with, as the name suggests, multiple leucine-rich repeats. Apart from being a marker for intestinal stem cells, other studies have given insights into other functions of Lgr5, mainly from analysis of null or loss-of-function mutants. Disruption of Lgr5 resulted in total neonatal lethality, indicating the importance of Lgr5 in development. The Lgr5-null mice were characterized by gastrointestinal tract dilation and, interestingly, accelerated maturation of the Paneth cells, possibly indicating that during intestinal development Lgr5 negatively regulates Wnt signalling (Garcia et al. 2009). Lgr5 has been shown to modulate Wnt signalling pathway, upon binding to its ligand, R-spondin (RSPO). In the absence of RSPO, there is internalisation of two transmembrane E3 ligases (RNF43 and ZNRF3) and degradation of the Wnt receptors (FZD and LPR), keeping Wnt levels low. When RSPO binds to Lgr5, the E3 ligases are neutralised, and Wnt receptors are able to bind to the Wnt ligands as they are no longer degraded, leading to subsequent Wnt signalling activation (Carmon et al. 2011; de Lau et al. 2011; Glinka et al. 2011).

Following the confirmation that *Lgr5* is a marker for intestinal stem cells (Barker et al. 2007), Barker and colleagues demonstrated that loss of the *Apc* gene in Lgr5 stem cells led to their transformation within days, resulting in adenoma development (Barker et al. 2009). The transformed stem cells remained located in the bottom of the crypts giving origin to

microadenomas that developed into adenomas within 3-5 weeks. When the *Apc* gene was deleted in the non-stem cell compartment small lesions formed in the intestinal epithelium, although they did not form tumours even 200 days post induction (Barker et al. 2009), indicating that only the stem cells located in the bottom of the crypt were responsible for adenoma formation.

More recently, Shimokawa and colleagues have confirmed that human *LGR5*<sup>+</sup> cells act as cancer stem cells giving new insights into their plasticity (Shimokawa *et al.* 2017). The authors performed lineage tracing experiments with a tamoxifen-inducible Cre knock in allele of *LGR5* in patient-derived CRC organoids and showed the capacity of *Lgr5*<sup>+</sup> tumour cells to self-renew and differentiate (Shimokawa *et al.* 2017). Following ablation of the *Lgr5*<sup>+</sup> tumour cells in *LGR5*-iCaspase 9 knock in organoids, tumour regression was observed, however a few days later there was a re-emergence of the *LGR5*<sup>+</sup> CSCs. Further experiments showed that *LGR5*<sup>-</sup> cells dynamically replenished *LGR5*<sup>+</sup> after they were ablated and that the newly generated *LGR5*<sup>+</sup> cells would be killed following consecutive ablation, demonstrating why targeting CSCs can be so challenging, considering the robust plasticity of non-targeted cancer cells (Shimokawa *et al.* 2017).

### 1.2.6 Multi-step carcinogenesis of the intestine

In 1990 Fearon and Vogelstein described a multistep genetic model for the initiation and progression of CRC (Fearon and Vogelstein 1990). This model was formulated following a mutational profile study in CRC samples collected from different stages of the disease. Fearon and Vogelstein proposed that various mutations, from inactivation of tumour suppressor genes to activation of oncogenes, in a preferential sequence, were essential in the process of colorectal tumourigenesis (Figure 1.4) (Fearon and Vogelstein 1990). Since then, other studies have supported this model (Pino and Chung 2010).

The initiation of adenomas starts with intestinal crypt hyperplasia and the formation of aberrant crypts. A key and early event in intestinal tumourigenesis is the mutation of *APC*, a tumour suppressor gene (Kinzler and Vogelstein 1996). Dysfunction of the *APC* gene occurs in about 80% of CRCs (Rowan *et al.* 2000) leading to Wnt signalling activation and highlighting the importance of this gene in intestinal tumourigenesis (Morin *et al.* 1997; Zhang and Shay 2017). Mutations or deletion of the *APC* gene leads to the development of familial adenomatous polyposis (FAP), an autosomal dominant trait characterized by the development of colonic adenomatous polyps throughout life. These polyps are benign, however they can progress to adenocarcinomas if left untreated (Groden *et al.* 1991)

Following *APC* mutation, there is a hyper-proliferation of the abnormal cells giving origin to tumour mass growth and alteration of the normal tissue anatomy. The process of tumour progression encompasses activation of the *KRAS* or *BRAF* oncogenes (Fearon and Vogelstein 1990; Boutin *et al.* 2017) and loss of the tumour suppressor gene *TP53* (Li *et al.* 2015) leading to the formation of carcinoma and, ultimately, invasion and metastasis (Figure 1.5) (Fearon and Vogelstein 1990). Together with these changes there are other associated aberrations, including epigenetic changes such as DNA hypo-methylation and CpG island hyper-methylation. These changes in the DNA will directly influence the expression of oncogenes and silencing of tumour suppressor genes promoting tumour progression. Mismatch repair (MMR) gene mutations have also been implicated in CRC development (Li and Martin 2016)

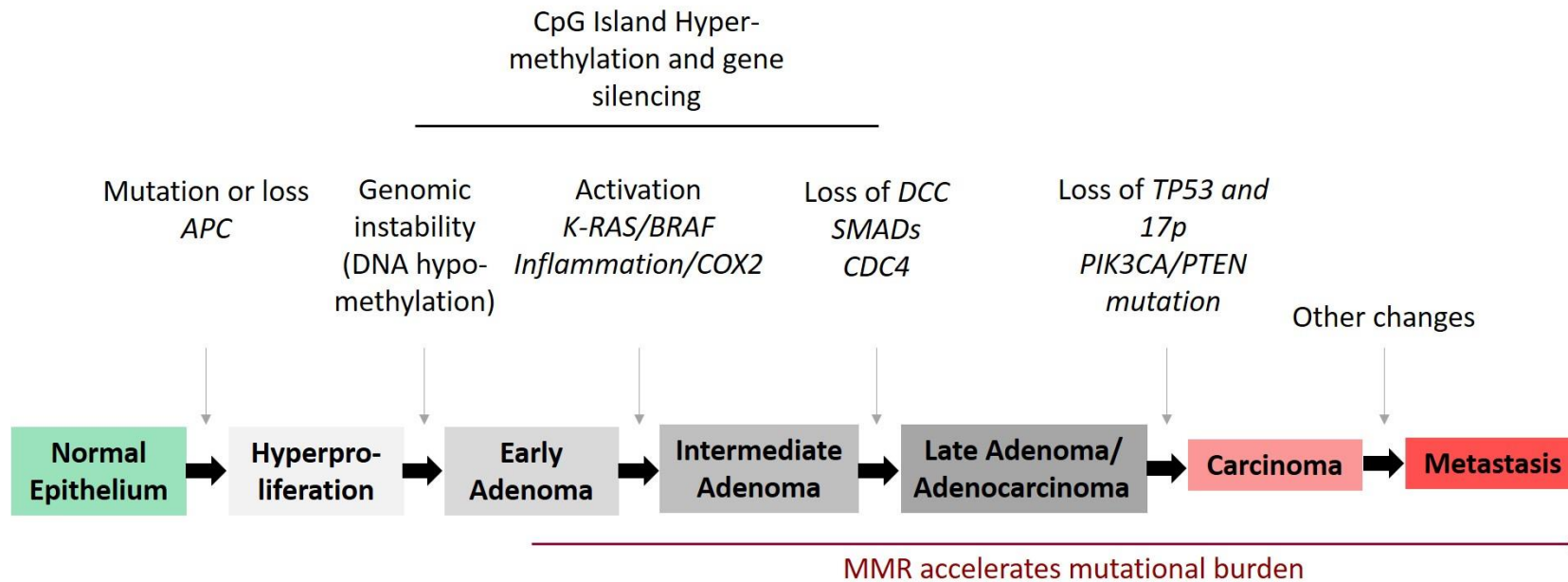


Figure 1.5 Multi-step tumourigenesis of the intestinal epithelium

Updated multi-step tumourigenesis model proposed by Fearon and Vogelstein (Fearon and Vogelstein 1990). Intestinal cancer initiation and progression occurs in a step-wise accumulation of mutations in various genes such as *APC*, *KRAS/BRAF*, *DCC*, *TP53*, *17p* and *PIK3CA/PTEN*. DNA hypomethylation, CpG island hyper-methylation and mutations in MMR genes can be present throughout tumour initiation and progression (adapted from (Hanahan and Weinberg 2011))

## 1.3 CRC and the Host Immune Environment

### 1.3.1 Cancer Immunosurveillance

In the early 1900's Paul Ehrlich proposed that the immune system could recognize, target and eliminate cancer cells. Around 50 years later, Burnet and Thomas proposed that the immune system has an important role in the control of cancer progression and created the hypothesis of the "Cancer Immunosurveillance". This hypothesis states that lymphocytes act as sentinels, recognizing and eliminating newly transformed cells (Burnet 1957). However, years later, this hypothesis was questioned by Stutman, who showed that there were no evidence that there was a difference in the number of tumours between immunodeficient and immunocompetent mice (Stutman 1974). Despite many studies performed in mice supporting this hypothesis of the transformed cells clearance, it is still difficult to show evidence in humans. People where immunosurveillance cleared any potential cancer, would not develop the disease and, as a consequence, would not be included in further studies. On the other hand, people diagnosed with cancer could be considered that their immune-mediated mechanisms of tumour control have failed (Gallimore and Godkin 2008).

### 1.3.2 Cancer Immunoediting

Immunosurveillance of the tumour cells is one part of the interaction between the immune system and the cancer. More recent studies have showed that the immune system, apart from eliminating cancer, is also able to initiate it, particularly during chronic inflammation (Grivennikov *et al.* 2010). The "Cancer Immunoediting" hypothesis, not only includes the capacity of the immune system to protect against cancer initiation, but also the fact that it can modify the immunogenicity of the developing tumour, allowing the escape of the tumour from the anti-tumour immune responses (Shankaran *et al.* 2001).

The "Cancer Immunoediting" hypothesis is described as consisting in three distinct phases: Elimination, Equilibrium and Escape. "Elimination" refers to the previously described immunosurveillance, when both innate and adaptive immune responses eliminate newly transformed cells (Figure 1.6 A) (Schreiber *et al.* 2011).

The "Equilibrium" phase occurs when not all the transformed cells are immediately destroyed by the immune system. Some of them are edited and sculpted by the adaptive immune system, leading to the dormancy of the tumour (Figure 1.6 B) (Schreiber *et al.* 2011).

Finally, “Escape” refers to the tumours that were previously edited by the immune system but escaped immune recognition. There are various mechanisms described by which escape can happen, such as loss of tumour antigen expression, an immunosuppressive microenvironment and resistance to cytotoxicity (Figure 1.6 C) (Schreiber *et al.* 2011).

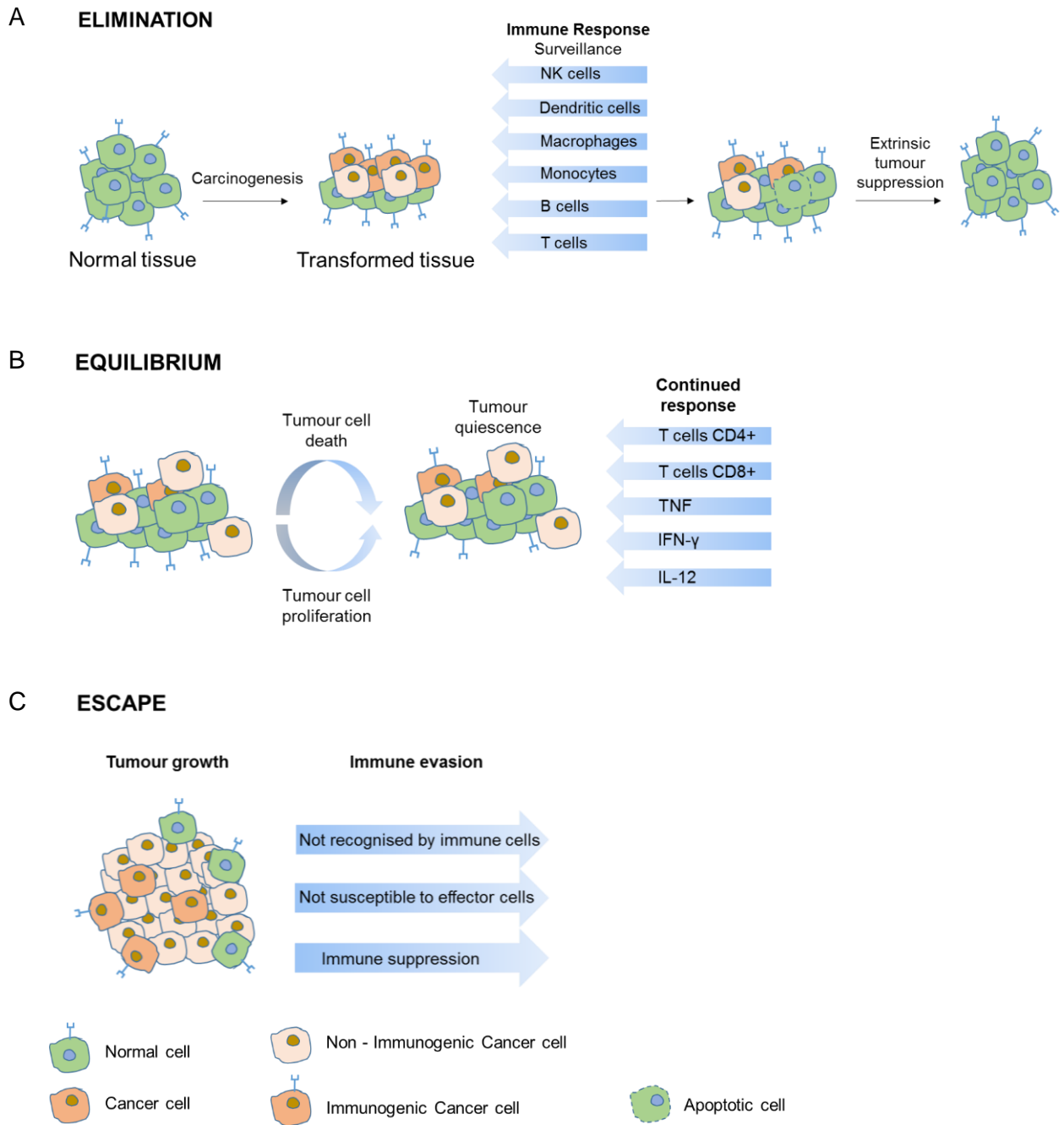


Figure 1.6 Schematic representation of the three different phases of the concept of cancer immunoediting.

A) “Elimination” involves both innate and adaptive immune responses to eliminate transformed cells. B) During “Equilibrium” the transformed cells that are not eliminated they can undergo immunogenicity editing and sculpting. C) During “Escape” the transformed cells lose their MHCs and/or antigen presentation capacity, they won’t be recognised by the immune system, escaping to the effector immune cells.

### 1.3.3 Immune response

In the presence of a foreign antigen the first response to its presence is given by the innate immune system, which recognize and destroys the antigen in a non-specific manner. There are various cell populations involved in this response, such as natural killer (NK) cells, macrophages, dendritic cells (DCs), neutrophils, eosinophils and basophils. These cells express pattern recognition receptors (PRRs) that recognize pathogen-associated molecular patterns (PAMPs) that usually are not present in the mammalian body, triggering an immune response to eliminate the foreign antigens (Parham 2015a).

On the other hand, when the innate immune system is not able to control an infection, another immune response is built by the adaptive immune system which has a more specialized and long-lasting response against the antigens. The adaptive immune response is performed by lymphocytes which recognize the pathogens by using cell-surface receptors that are specifically of just one molecular type. Each cell-surface receptor can have a very high number of different versions that bind to different ligands building a very specific response (Parham 2015b).

The adaptive immune response is mounted by B and T lymphocytes. B lymphocytes can act through two different ways: they can either recognize an antigen that binds to the B cell receptors promoting the proliferation of plasma cells and, as a consequence, there is the secretion of antibodies. The second mechanism relies on the fact that B cells can act like antigen-presenting cells (APCs), processing and presenting the antigens to the major histocompatibility complex (MHC) for recognition (Parham 2015c). T cells are distinguished from other lymphocytes by the expression on their surface of highly variable T cell receptors (TCRs) that recognize peptides presented by MHCs. The reactions that follow the binding of the peptides to the TCRs or MHCs depend on the T cell subpopulation that is participating. There are two different types of MHCs: MHC class I, which is responsible by presenting antigens from intracellular pathogens and MHC class II that presents antigens from extracellular pathogens (Parham 2015d).

#### 1.3.3.1 T-cells

T-cells are lymphocytes that are produced in the bone marrow and mature in the thymus. During development, they express cell-surface glycoproteins which determine their function and can be used to identify them. T-cells can give rise to two different lineages that arise from a common thymocyte progenitor:  $\alpha:\beta$  T-cells that are the majority of the T-cells and  $\gamma:\delta$  T-cells.  $\alpha:\beta$  T-cells share the expression of the surface marker CD3 and can be divided

into two different sub lineages depending on the expression of the co-receptors CD4 and CD8 that are part of the immunoglobulin superfamily of proteins. These co-receptors help the T-cell receptors recognize the antigens and MHC molecules. The CD4 co-receptors binds specifically to MHC class II molecules and CD8 co-receptors bind to MHC class I molecules. CD4 and CD8 are functionally similar but their structures are different. CD4 is a single polypeptide formed by four extracellular immunoglobulin-like domains. CD8 is a heterodimer formed by an  $\alpha$  and a  $\beta$  chain. Each of the chains are connected to the membrane-spanning region by immunoglobulin-like domains (Parham 2015d).

#### 1.3.3.1.1 CD8+ T-cells

CD8+ T-cells, also known as cytotoxic T-cells (CTLs), participate in the immune response against intracellular pathogens, such as bacteria and viruses, but also in anti-tumour immune responses (Harty and Bevan 1999; Radziewicz *et al.* 2007; Hadrup *et al.* 2013). CD8+ T-cells can exert their cytotoxic activity by three different mechanisms. Firstly, via the secretion of the cytokines IFN $\gamma$  and TNF $\alpha$ . These two cytokines have anti-viral and anti-tumour effects. Secondly CD8+ T-cells can release cytotoxic granules, such as perforin and granzymes, which are serine proteases. As the name suggests, perforins are proteins that able to form pores in the membrane of the targeted cell allowing the granzymes to enter the cell (Trapani and Smyth 2002). In the 1990's, an experiment showed that perforin-deficient mice developed more tumours, demonstrating the importance of CD8+ T-cells in cancer immunosurveillance (van den Broek *et al.* 1996). Granzymes will then cleave proteins inside the infected/malignant cell resulting in the apoptosis of the cell. Once this is done, CD8+ T-cells can then move to another infected cell, eliminating it.

Finally, CD8+ T-cells induce a cell to undergo apoptosis via Fas/Fas-ligand interactions. Fas-ligands (or CD95) are expressed by activated CD8+ T-cells on their surface. Fas-ligand will then bind to Fas that are located on the surface of the target cell. After the binding, Fas, through trimerization, will activate signalling molecules and, as a consequence, the caspase cascade, resulting in the apoptosis of the infected cell (Waring and Mullbacher 1999). Mice where Fas/Fas-ligand were mutated showed higher incidence of B-cell lymphomas. It has also been shown that cell death mediated by Fas/Fas-ligand interactions is fundamental for T-cell mediated immunosurveillance for B-cell lymphoma in mice (Davidson *et al.* 1998).

### 1.3.3.1.2 CD4+ T-cells

Naïve CD4+ T-cells differentiate into functionally effector cells upon T-cell receptor (TCR) stimulation by peptide-MHC present in APCs, usually DCs. CD4+ T-cells are part of a very heterogeneous population and can be divided into different subpopulations that secrete cytokines that will either activate or suppress other immune cells, promoting various types of immune responses. The CD4+ T-cell subpopulations can be distinguished by the cytokines and transcription factors that induce and determine, respectively, their differentiation, the cytokines that they produce and the cells that are helped by them (figure 1.7) (Tripathi and Lahesmaa 2014).

The first helper subsets that were described were the Th1 and Th2 (Mosmann *et al.* 1986). With subsequent research identifying Th9, Th17, Th22, follicular T cells (Tfh) and Treg.

The differentiation of Th1 cells is initiated by the cytokine IL-12 and their specific gene expression programme is regulated by the transcription factor T-bet (Szabo *et al.* 2000). Th 1 cells produce cytokines such as IL-12, IFN- $\gamma$ , TNF $\alpha$  and lymphotoxin (LT) that will help macrophages combat intracellular bacterial and viral infections (Szabo *et al.* 2003).

Th2 cells help B-cells, mast cells, basophils and eosinophils control parasite infections by producing IL-4, IL-5, IL-6 and IL-13 cytokines (Zhu and Paul 2010). The transcription factor that define Th2 differentiation is GATA3 (Zheng and Flavell 1997) and their differentiation is initiated by IL-4.

Th17 cells enhance neutrophils response against extracellular fungal and bacterial infections. The cytokines involve in their responses are IL-17, IL-22 and IL-23 (Zhu and Paul 2010). The transcription factor that determine Th17 differentiation is ROR $\gamma$ T but other transcription factors have been described as being part of the Th17 differentiation program. IL-6, IL-23 and TGF- $\beta$  can initiate the differentiation of Th17 cells (Chen *et al.* 2007).

Recently other T-cells were described, including Th9, Th22 and Tfh cells. Th9 development depends on the transcription factors PU.1 and IRF4 and their differentiation is initiated by IL-4 and TGF- $\beta$  (Tripathi and Lahesmaa 2014). These cells can have both beneficial and detrimental functions. Th9 cells promote immunity against helminth parasites and also participate in anti-tumour activity, particularly in melanoma by secreting IL-9 and IL-21. On the other hand, Th9 cells can exacerbate the immune response in the case of asthma; they also contribute to inflammatory bowel disease (IBD), impairing tissue repair processes and increasing intestinal permeability (Kaplan *et al.* 2015).

Th22 cells depend on the IL-6 and TNF to differentiate and aryl hydrocarbon receptor (AhR) for their transcriptional control (Duhon *et al.* 2009). These cells are characterized by a high production of IL-22, a cytokine that is secreted also by Th17 and NK cells. Although secretion of IL-22 is a common feature between these cell populations, Th22 cells are unique

in the secretion of IL-22 and absence of IL-17 and IFN- $\gamma$  production (Duhon *et al.* 2009). This cell population is believed to have an important role in tissue repair, particularly damaged epithelial barriers as well as promoting responses against some pathogens. Other functions of Th22 cells include skin homeostasis by inhibition of keratinocytes differentiation as well as gastrointestinal and respiratory tract cells. Protective effects in models of inflammatory bowel disease, pancreatitis and hepatitis have also been associated to Th22 cells (Trifari *et al.* 2009; Sabat *et al.* 2014).

Tfh cells participate in generation of B cell responses in germinal centres by secreting IL-21 and their differentiation depend on IL-6 and IL-21. Tfh cells are regulated by the transcription factor Bcl6 (Tripathi and Lahesmaa 2014).

Tregs lineage and function is defined by the expression of the transcription factor Foxp3 and these cells are responsible for the suppression of effector immune responses. Tregs secrete immunosuppressive molecules such as IL-10, TGF- $\beta$  and IL-35 (Corthay 2009). Tregs will be described in more detail in the following section due to their relevance to this project.

#### 1.3.3.1.3 Interferon-gamma (IFN- $\gamma$ )

IFN- $\gamma$  is produced by a variety of cells such as CD4+ T-cells, CD8+ T-cells, NK and NKT cells and it is a critical cytokine in the innate and adaptive immune system (Schoenborn and Wilson 2007). The receptor of IFN- $\gamma$  is formed by two subunits: IFN- $\gamma$ R1 and IFN- $\gamma$ R2 (Dunn *et al.* 2006). When IFN- $\gamma$  binds to its receptor there is the recruitment and activation of the Janus kinase (JAK1 and JAK2), leading to the activation of STAT1 and interferon regulatory factor 1 (IRF1). Following STAT1 and IRF1 phosphorylation, and translocation to the nucleus, IFN- $\gamma$ -regulated genes are transcribed (Horvath 2004).

Various studies have shown the importance of IFN- $\gamma$  in the anti-tumour immune responses in CRC (Wang *et al.* 2015a; Katlinski *et al.* 2017; Liu *et al.* 2017). Wang and colleagues have shown in a mouse model of *Apc*-mediated intestinal cancer (*Apc*<sup>Min/+</sup>), that mice deficient in IFN- $\gamma$  or IFN- $\gamma$  receptor subunit 1 (IFN- $\gamma$ R1) had an increased number and size of adenomas, with about 41% of the mice developing adenocarcinomas. The authors have also shown that heterozygous deletion of IFN- $\gamma$  promoted activation of the EGFR/Erk1/2 and Wnt signalling pathways (Wang *et al.* 2015a). More recent studies have shown that downregulation of IFN- $\gamma$ R1 occurs in human CRC as well as mouse models of CRC. Downregulation of IFN- $\gamma$ R1, apart from causing tumour development, promoted the formation of an immune-privileged niche and was associated with a poor prognosis. On the other side,

stabilization of IFN- $\gamma$ R1 improved response to anti-PDL1 therapy and survival, indicating the importance of IFN- $\gamma$ R1 in the efficacy of immunotherapies (Katlinski *et al.* 2017).

IFN- $\gamma$  has been shown to promote apoptosis in malignant cells (Liu *et al.* 2011; Kotredes and Gamero 2013; Ni and Lu 2018). Liu and colleagues have shown that metastatic colon carcinoma cell lines treated with TNF $\alpha$  and IFN- $\gamma$  reduced resistance to TNF-related apoptosis-inducing ligand (TRAIL), a protein that induces cell death by apoptosis, being very important in the anti-tumour responses. The authors treated a mouse model of metastatic CRC with TRAIL together with TNF $\alpha$  and IFN- $\gamma$ , and observed a reduced expression of the antiapoptotic protein Bcl-xL. This resulted in increased apoptosis through TRAIL-induced caspase 8 activation, leading to the suppression of the metastasis (Liu *et al.* 2011). Taken together, these studies and others show the importance of IFN- $\gamma$  in the anti-tumour immune responses.

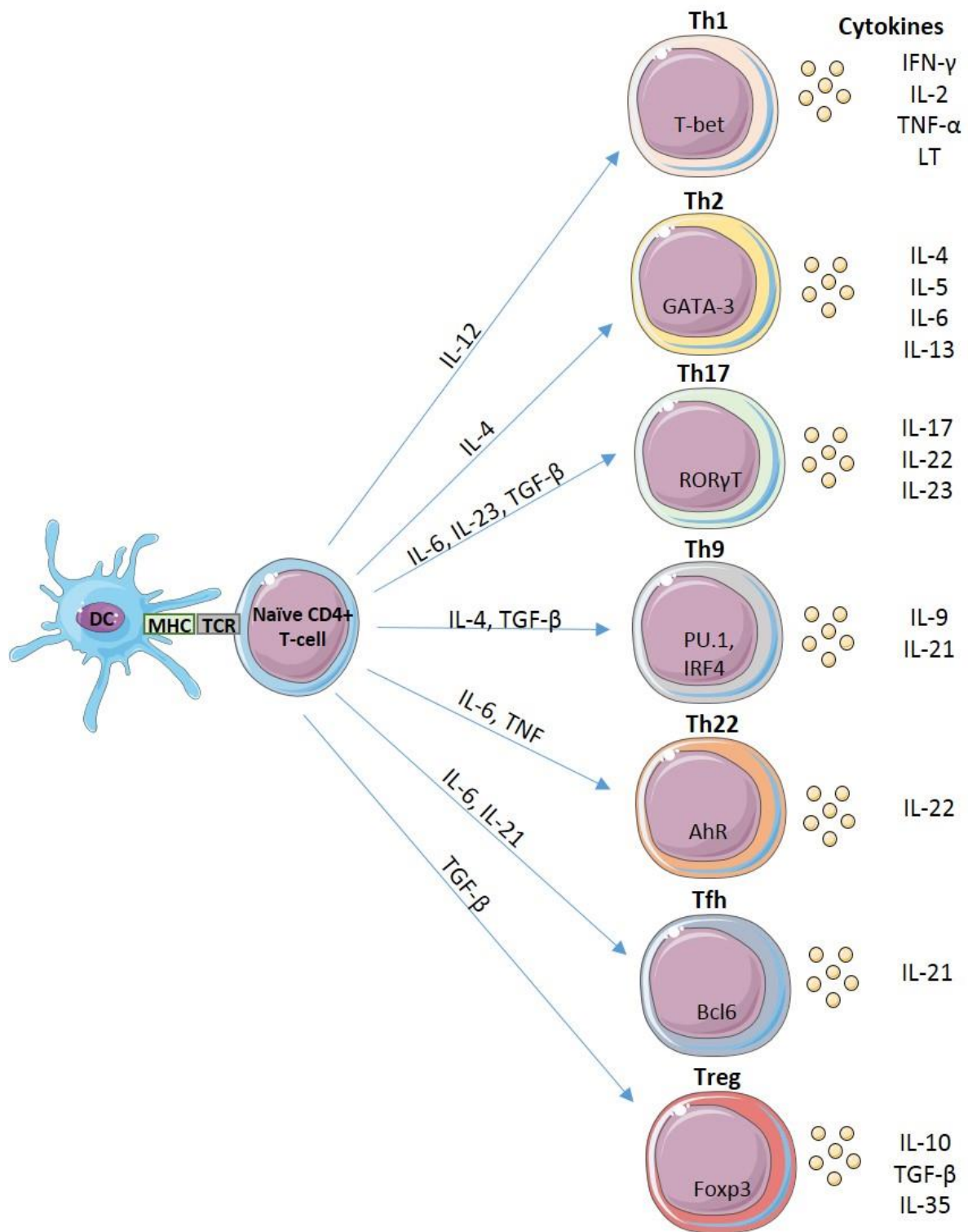


Figure 1.7 Differentiation of Naïve CD4+ T-cells.

Upon activation by DCs, and in the presence of specific cytokines, naïve CD4+ T-cells differentiate into different T helper (Th) or Foxp3+ regulatory T-cells (Treg) subsets. Each subset is defined by the expression of lineage specific transcription factors, and by the production of effector or immunosuppressive cytokines.

#### 1.3.3.1.4 Foxp3+ Regulatory T cells (Tregs)

##### 1.3.3.1.4.1 Tregs – an introduction to their discovery and function

Several studies showed evidence of the presence of a T-cell subpopulation responsible for suppression of active immune cells. The first marker identified for these cells was CD25 and its depletion would cause a series of autoimmune diseases. These mice could be rescued by reintroducing CD4+CD25+ but not CD4+CD25- cells (Sakaguchi *et al.* 1995). Subsequent studies identified a subpopulation of CD25+ cells which expressed the Forkhead box protein 3 (Foxp3). Foxp3 is a transcription factor encoded on the X chromosome which belongs to the member of the forkhead/winged-helix family. Studies performed in mice that had uncontrolled CD4+/CD8+ T-cell proliferation showed that *Foxp3* was not functional due to a mutation (Brunkow *et al.* 2001). It was demonstrated that CD4+CD25+ T-cells had higher expression levels of *Foxp3* when compared to CD4+CD25- T-cells. Further experiments demonstrated that CD4+CD25+Foxp3+ T-cells could suppress the proliferation of CD4+CD25- T-cells (Fontenot *et al.* 2003).

Bennett and colleagues demonstrated that, in humans, a mutation in the *Foxp3* gene affected Treg cells development and function. This was the cause of Immune dysregulation Polyendocrinopathy Enteropathy, X-linked (IPEX) syndrome, a fatal, early-onset, autoimmune disorder. The same was observed in the scurfy mice, where a spontaneous *Foxp3* mutation occurs, leading to the development of a lymphoproliferative disease with multiple organ inflammation (Godfrey *et al.* 1991; Bennett *et al.* 2001). All these evidences showed that Treg cells had a very important role in the regulation of the immune responses.

Further experiments were possible due to the creation of a mouse model that allowed the depletion of Foxp3+ cells after injection of the diphtheria toxin. These mice expressed the human diphtheria toxin receptor under the control of the Foxp3 promoter. Deletion of Foxp3+ cells caused a similar phenotype presented by the mice that were Foxp3 deficient, developing autoimmunity (Kim *et al.* 2007; Lahl *et al.* 2007).

Tregs can have different origins. Most of them derive from the thymus (tTregs), also known as natural Treg cells (nTregs), develop during the negative and positive selection. Tregs can also be induced in the periphery (pTregs) after antigen stimulation of the CD4+ T-cells.

One of the main functions of the Tregs is to maintain self-tolerance and the prevention of autoimmunity by controlling the expansion of T-lymphocytes that react against self-antigens. By promoting self-tolerance, Tregs prevent the occurrence of autoimmune diseases, promote foeto-maternal tolerance and suppress allergies. They are also important in the prevention of chronic inflammatory diseases (Maloy and Powrie 2001).

#### 1.3.3.1.4.2 Immunosuppressive mechanisms of Tregs

There are several mechanisms by which Tregs can exert their immunosuppressive activity have been demonstrated. Immunosuppression by Tregs can be achieved by the modulation of the APCs activity by contact-dependent interactions (Schmidt *et al.* 2012). It was shown that this activity was dependent on CTLA-4, a surface marker that is expressed on Tregs (Takahashi *et al.* 2000) and LAG-3 (lymphocyte-activation gene 3), a transmembrane protein. Gene expression studies performed by several groups allowed the identification of molecules with suppressive activity, such as: galectin-1 and galectin-10, TGF- $\beta$ , IL-10 and IL-35, a member of the IL-12 heterodimeric cytokine family (Shevach 2009). Tregs are also able to promote direct cytotoxicity as they express perforins and granzymes. This was observed in both humans and mice (Shevach 2009; Hoves *et al.* 2010).

#### 1.3.3.1.4.3 Tregs in Cancer

It is well known that Tregs are essential in maintaining peripheral tolerance and that they do it by preventing self-reactivity. In the 1970s and 1980s several studies started to establish a connection between a population of suppressive cells and anti-tumour immune responses (Zou 2006). After the identification of the CD25 as a Treg marker (Sakaguchi *et al.* 1995) other studies showed that the depletion of cells expressing this marker induced CD8+ T-cell responses and controlled the tumour growth (Onizuka *et al.* 1999; Shimizu *et al.* 1999). The opposite was observed after adoptive transfer of CD4+CD25+ T-cells to tumour-bearing mice, where the anti-tumour immunity was suppressed (Turk *et al.* 2004; Antony *et al.* 2005). Other experiments that were done after the discovery of the Foxp3 marker demonstrated that depletion of Foxp3+ cells would prevent the tumour initiation and development (Klages *et al.* 2010; Teng *et al.* 2010; Hindley *et al.* 2012).

Several studies showed increased numbers of Tregs in the tumour microenvironment in a variety of different cancers, such as: melanoma, lymphoma, pancreatic, breast, lung, gastric and others, when compared to tissue from healthy donors (Nishikawa and Sakaguchi 2010; Quezada *et al.* 2011; Scurr *et al.* 2012; Whiteside 2012). However, it is controversial whether this increased number of Tregs indicates a good or a bad prognosis, having different studies reporting opposite conclusions (Curiel *et al.* 2004; Alvaro *et al.* 2005; Sato *et al.* 2005; Bates *et al.* 2006; Mantovani *et al.* 2008; Perrone *et al.* 2008; Ladoire *et al.* 2011). This highlights the importance of studying the types of cancer and their origin, as Tregs may play different roles depending on that. In the case of inflammation-driven tumours, Tregs may have anti-

tumour effects by suppressing the inflammation that promoted the cancer initiation and development (Erdman *et al.* 2005; Grivennikov *et al.* 2010; Ruffell *et al.* 2010).

#### 1.3.4 T-cells and CRC

Cancer patients with increased tumour immune infiltrate correlates with an improved clinical outcome, when compared to patients with lower immune infiltrates in different types of cancers such as melanoma (Mihm and Mulé 2015), ovarian (James *et al.* 2017), head and neck (Schneider *et al.* 2018), breast (Ingold Heppner *et al.* 2016) and CRC (Braha *et al.* 2016).

An extensive study from Pagès and colleagues has shown that the absence of metastasis in human CRC samples was associated with increased infiltration of effector memory T-cells in the primary tumour (Pages *et al.* 2005). It was also reported that patients without metastasis and that remained disease-free had increased levels of granzyme B, T-bet, interferon regulatory factor 1 (IRF-1) and IFN $\gamma$  when compared with patients that relapsed (Pages *et al.* 2005). T-cell markers, such as CD3+, CD4+ and CD8+ were also significantly increased in patients with a better outcome (Pages *et al.* 2005). Following this study, the same group showed that, in three different cohorts of CRC patients, there was a high density of CD3+ and CD8+ T-cells, alongside with granzyme B and CD45RO, within the tumour centre and invasive margin (Galon *et al.* 2006). The high levels of these markers were associated with a longer disease-free survival for the three groups when compared to groups that showed a lower infiltration of these immune markers (Galon *et al.* 2006). A number of studies have associated lymphocytes infiltration in CRC with a better prognosis (Ropponen *et al.* 1997; Pages *et al.* 2005; Galon *et al.* 2006; Pages *et al.* 2009; Mei *et al.* 2014; Jakubowska *et al.* 2017), however it has becoming evident that disease outcome does not depend only in the quantity of the lymphocytes that are present, but also their type can have a distinct impact in the prognosis. A study by Tosolini and colleagues showed that CRC patients with increased expression of Th1 related-genes had a better survival when compared to patients with a lower gene expression. The opposite was observed with Th17 associated-genes. CRC patients with significantly higher expression of Th17 associated-genes had a earlier relapse, even in the presence of higher expression of Th1 associated-genes, indicating that Th17 responses were stronger in the tumour progression comparing to the anti-tumour responses by Th1 cells (Tosolini *et al.* 2011). Later, it was shown that CRC patients had increased levels of Th17 cells in their blood, particularly in more advanced stages of the disease, suggesting a key role of the Th17 cells in CRC progression (Wang *et al.* 2014).

#### 1.3.4.1 *Tregs and CRC development*

As previously described, there is a number of different malignancies where it is observed an increased frequency of Tregs, however it is still controversial whether this T-cell sub-population promotes or limits tumour progression. This is also applied in the case of CRC. Studies have demonstrated in the blood of CRC patients there was a higher frequency of Tregs (Wolf *et al.* 2003; Clarke *et al.* 2006). *In vitro* experiments showed that removal of these cells would increase T-cell responses against tumour antigens (Clarke *et al.* 2006). The increased frequency of Tregs in CRC patients was also observed in their intestines, when compared to healthy intestines (Ling *et al.* 2007). A study from our group analysed the CD4+ T-cells responses against the tumour antigens 5T4 and carcinoembryonic antigen (CEA) in CRC patients before and at multiple time-points following surgery (Betts *et al.* 2012). It was demonstrated that CRC patients had significantly increased levels of Foxp3+ when compared to healthy age-matched controls. The levels of Foxp3+ decreased to normal following the surgery, suggesting that CRC drives the activity of Tregs. Patients that relapsed had a significantly lower activity of 5T4 and CEA T-cell responses that was suppressed by Tregs, suggesting that Tregs contribute to tumour progression (Betts *et al.* 2012). A further study from our group supported this finding. It was shown that 5T4-specific T-cell responses were decreased in CRC patients, when compared to healthy controls, and they were further diminished with disease progression (Scurr 2013).

On the other side, several studies have associated increased frequencies of Tregs in CRC patients with a better outcome and improved survival. Both Salama *et al.* and Vlad *et al.* showed independently that a higher density of Tregs in the tumour was associated with a better outcome and improved survival (Salama *et al.* 2009; Vlad *et al.* 2015). In another study it was shown that lower frequencies of Tregs were associated with shorter CRC patient survival time (Sinicrope *et al.* 2009).

#### 1.3.4.2 *The intestinal immune system*

The intestine represents the biggest compartment of the immune system, containing many more immune cells than any other tissue in the body. The intestine is continually exposed to antigens and dietary immunomodulatory agents. The majority of the immune processes occurs in the mucosa, also referred as intestinal barrier. This barrier separates the inner and the outer environments blocking the passage of potentially harmful substances, but allowing the passage of nutrients and electrolytes, preserving the epithelial barrier, the immune responses, as well as allowing the tolerance against the intestinal microbiota. The

mucosal immune system is formed by three lymphoid areas: the lamina propria, the intraepithelial compartment and the Peyer's patches (PPs). The PPs are secondary lymphoid tissues, located in between the submucosa layer of the ileum and mucosa layer. They are covered by follicle-associated epithelium (FAE) that are formed by specialized microfold (M) epithelial cells that are responsible by the capture of the antigens that are in the intestinal lumen and their transport to the associated subepithelial dome (SED) (Reboldi and Cyster 2016).

In mice, both lamina propria and PPs contain a large number of B lymphocytes. The intraepithelial compartment contains more CD8+ T cells (Lefrancois and Lycke 2001; Jung et al. 2010). The PPs contain a higher number of CD4+ cells, (~45% of the CD3+ T-cells), when compared to CD8+ T-cells (~34%) and Tregs (~5%). They also contain other immune cell populations such as memory T-cells, naïve T-cells and dendritic cells (DCs) (Jung et al. 2010). All these lymphoid areas participate actively to respond to immunological insults in the intestine, as it is constantly exposed to various antigens from pathogens and the commensal bacteria.

## 1.4 Mouse Models of CRC

The use of mouse models has allowed many important breakthroughs in the understanding of tumorigenesis. Mice are relatively easy to genetically modify and this allows deeper studies from the early stages of cancer to long term studies. Here the *Apc*<sup>min</sup> mouse model and the *Lgr5Cre*<sup>ERT2</sup>*Apc*<sup>fl/fl</sup>*Foxp3*<sup>DTR</sup> will be described in more detail due to their relevance in this project.

### 1.4.1 *Apc*<sup>min</sup> mouse model

In the 1990's Moser and colleagues performed experiments where mice were treated with a germline mutagen called ethyl nitrosourea. Via the random mutagenesis approach, they identified predispose mice to develop spontaneous intestinal cancer, subsequent analysis demonstrated they carried a mutation in the *Apc* gene. The mutant gene was named Multiple Intestinal Neoplasia (*Min*) and the mouse model *Apc*<sup>min</sup>. This mouse model mimicked what happen in FAP patients, the development of multiple polyps in the intestine.(Moser *et al.* 1990), being very useful to study intestinal tumorigenesis.

It was well known that the loss of function of both *APC* alleles occurs in the earlier stages of about 80% of CRCs (Gryfe *et al.* 1997), however the requirement of a second “hit” to remove the WT allele limits the study of tumour initiation in this mouse model.

#### 1.4.2 Cre-lox technology

The Cre-lox system is a tool used for the deletion, insertion, translocation and inversion of DNA at specific sites. This system has been extensively used in the generation of mouse models for disease (Sauer 1998). This system consists of two major components: the Cre recombinase and its targets, known as *loxP* sites. The Cre recombinase is an enzyme derived from the Bacteriophage I and it has the ability, after activation, to recognise the *loxP* sites in the same orientation and excise the DNA sequence located between them. The Cre-expression can be linked to tissue-specific promoter allowing the control gene expression in specific tissues (Sauer 1998).

Using genetically modified mice with the Cre-lox technology it is possible to conditionally delete both *Apc* alleles within the intestinal epithelium. It was observed that, after *Apc* deletion, there was an activation of the Wnt signalling, with nuclear accumulation of  $\beta$ -catenin. *Apc* deletion also affected the dynamics of the intestinal epithelium by perturbing cell proliferation, migration, differentiation and apoptosis. The *Apc* mutant cells maintained what the authors called a “crypt progenitor-like phenotype” (Sansom *et al.* 2004).

#### 1.4.3 *Lgr5Cre<sup>ERT2</sup> Apc<sup>f/f</sup> Foxp3<sup>DTR</sup>* mouse model

The mouse model used in this project allows the deletion of the *Apc* gene specifically in the intestinal stem cells (ISC). The Cre-recombinase is linked to a modified estrogen receptor (ER), forming a transgene. This transgene remains inactive until an injection of tamoxifen. The tamoxifen will bind to the ER and the Cre-recombinase will be activated and able to recombine the *loxP* sites and delete the *Apc* gene. In this particular model, the Cre-recombinase is linked to the *Lgr5* promoter, meaning that the recombination will specifically occur in the cells that express *Lgr5* (Barker *et al.* 2007). Barker and colleagues have shown that activation of Cre was possible with a single IP injection of tamoxifen. The authors observed accumulation of nuclear  $\beta$ -catenin in the bottom of about 6% of the crypts within 3 days after Cre induction (Barker *et al.* 2009). Overtime the number of transformed stem cells increased and 8 days later it was possible to observe the presence of microadenomas within the associated villus stroma. At day 14 the authors observed a similar number of larger adenomas (around 8 %)

and the mice had to be sacrificed at day 36 (Barker *et al.* 2009). These lesions were observed in the mice small intestine, however *Lgr5* gene is also a marker of stem cells in the large intestine. Barker and colleagues detected the presence of transformed cells in the bottom of the colonic crypts within 8 days after Cre induction and the formation of microadenomas 3 weeks after induction. This showed that, in this model, the formation of microadenomas occur more frequently in the small intestine, however colonic stem cells are also transformed but in a lower frequency (Barker *et al.* 2009). *Lgr5* is not only expressed in the ISCs, but also foetal mammary stem cells (Trejo *et al.* 2017) and hair follicle stem cells (Jaks *et al.* 2008).

This mouse model was crossed with the *Foxp3*<sup>DTR</sup> mouse model that expresses the human diphtheria toxin receptor (DTR) under the control of the *Foxp3* promotor, allowing the depletion of the Tregs after diphtheria toxin injection (Kim *et al.* 2007).

## Hypothesis and Aims

Previous studies have demonstrated that CRC patients with an increase number of Tregs have a poorer prognosis. These studies were done mainly in patients with advanced disease, however it is still unclear the role of Tregs in the early stages of CRC. In this project I aimed to clarify the role of Tregs in the early stages of intestinal cancer. To do this, the following hypothesis were tested:

- **Hypothesis 1:** Treg numbers and frequency increase following deletion of the *Apc* gene in the ISCs.

Aim: To investigate the response of Tregs upon *Apc* deletion in the ISCs of the genetically modified *Lgr5Cre*<sup>ERT2</sup>*Apc*<sup>f/f</sup>*Foxp3*<sup>DTR</sup> mouse model.

- **Hypothesis 2:** Treg depletion in an *Apc* deleted mice reduce the intestinal tumour burden.

Aim: To assess tumour burden and immune changes following Treg depletion in *Lgr5Cre*<sup>ERT2</sup>*Apc*<sup>f/f</sup>*Foxp3*<sup>DTR</sup> mouse model.

- **Hypothesis 3:** Depletion of CD4+ and CD8+ T-cells, and IFN $\gamma$  neutralization increase the intestinal tumour burden.

Aim: Identification of immune cell populations and cytokines that participate in the anti-tumour immune response in the *Lgr5Cre<sup>ERT2</sup>Apc<sup>fl/fl</sup>Foxp3<sup>DTR</sup>* mouse model.

## 2 Material and Methods

### 2.1 Experimental Animals and Husbandry

All animal procedures were conducted according to the UK Animal (Scientific Procedures) Act 1986, under the authority of UK Home Office personal and project licences in accordance with the ARRIVE guidelines.

#### 2.1.1 Colony Maintenance and Breeding

All animals were maintained on an outbred background. Mice of known genotype and, at least, 6 weeks old were bred. The breeding was done in trios (one male and two females) and pups were weaned and ear clipped at approximately 4 weeks old for identification purposes and genotyping.

### 2.2 Transgenic Mouse Models

The mouse models used within this project were  $Apc^{min}$  (Moser *et al.* 1990) and  $Lgr5Cre^{ERT2}Apc^{fl/fl}Foxp3^{DTR}$  (Barker *et al.* 2007; Kim *et al.* 2007) (discussed in sections 1.4.1 and 1.4.3).

### 2.3 Experimental Procedures

All animal procedures were carried out in designated procedure rooms. The animals used in these procedures were at least 10 weeks old. Administration of the different treatments was done *via* intraperitoneal injection (IP).

#### 2.3.1 Animal Identification and Genotyping

The identification of the animals was done based on ear biopsies that were taken using a 2 mm ear punch (Harvard apparatus). The ear biopsies were kindly done by the staff in the animal unit (Elaine Taylor, Mike Quirk, Paul Chapman and Sarah Davies).

##### 2.3.1.1 Polymerase Chain Reaction (PCR)

Genotyping was performed by PCR using genomic DNA (gDNA) allowed the correct choice of the experimental cohorts. Part of the genotyping was kindly performed by Matthew Zverev.

#### 2.3.1.1.1 DNA Extraction

The ear biopsies were collected by the time the mice were weaned and stored at -20 °C in order to prevent degradation. Tissues were digested using 250 µl of lysis buffer (VWR) containing 0.4 mg/ml proteinase K (Sigma), overnight (O/N) at 42 °C with agitation. After the overnight incubation, 100 µl of protein precipitation solution (VWR) was added and mixed by inversion to the digested tissue. Following centrifugation at 13000 rpm for 10 min the protein and insoluble debris were pelleted. The supernatant was transferred to a 1.5 ml Eppendorf tube containing 250 µl of isopropanol (Thermo Fisher Scientific). The solution was mixed by inverting the tubes and centrifuged at 13000 rpm for 15 min to pellet the DNA. The supernatant was discarded, the pellet was left to dry for an hour at 32 °C and the DNA was resuspended in 250 µl Milli-Q water. The DNA was left at room temperature (RT) for short-term storage or at 4 °C for longer-term storage.

#### 2.3.1.1.2 Generic PCR Protocol

PCR reactions were done in 96 well semi skirted straight side plates (Alpha Laboratories). In each well, 3 µl of gDNA was mixed with 47 µl of PCR master-mix (see Table 2.1). A blank control was included, where the gDNA was replaced by dH<sub>2</sub>O. The 96 well-plates were covered with aluminium foil seals (StarLab) and air bubbles were removed by spinning the plates for 5 seconds in a PCR plate spinner (VWR). The reactions were run in a GS4 (G-Storm) thermocycler using the conditions shown in Table 2.1. Primer sequences are shown in Table 2.2.

#### 2.3.1.1.3 Visualization of the PCR Products

PCR products were separated by agarose gel electrophoresis. The agarose gel was prepared by mixing 2% of agarose (Eurogentech) in 1X Tris Borate EDTA (TBE) buffer (National Diagnostic). The mixture was heated in a microwave until boiling. After cooling the solution under running tap water, 14 µl of Safe View fluorescent nucleic acid stain (NBS biological) was added per 400 ml. The solution was poured into moulds (Bio-Rad) and combs were added to create the wells. Bubbles were removed using a tip. The gel was left to set for an hour and the combs were carefully removed. The gel was placed into an electrophoresis tank containing 1X TBE buffer with Safe View (10 µl Safe View per 100 ml 1X TBE). For the PCR products containing clear buffer, 5 µl of loading dye (50% glycerol (Sigma-Aldrich), 50% dH<sub>2</sub>O, 0.1% bromophenol blue (Sigma-Aldrich)) were added and gently mixed. 20 µl of the samples were loaded into the gel wells and

run at 120 V for approximately 30 min or until the loading dye had run more than half way across the gel. The gel was visualised under UV light using a GelDoc UV Transilluminator (Bio-Rad) and the images were captured using the GelDoc software (Bio-Rad).

Table 2.1 Genotyping PCR reaction mixture and conditions

	<i>Lgr5Cre</i> <sup>ERT2</sup>	<i>Apc</i> <sup>fl/fl</sup>	<i>Foxp3</i> <sup>DTR</sup>	<i>Cre</i>	<i>Apc</i> <sup>min</sup>
<b>PCR mix</b>					
DNA	3 µl	3 µl	3 µl	3 µl	3
Milli-Q water	31.1 µl	31.2 µl	31.2 µl	31.2 µl	31.1 µl
Taq PCR buffer	10 µl	10 µl	10 µl	10 µl	10 µl
PCR buffer (type)	Green	Green	Clear/Green (2:1)	Clear	Clear
MgCl <sub>2</sub> (5 mM)	5 µl	5 µl	5 µl	5 µl	5 µl
dNTPs (25 mM)	0.4 µl	0.4 µl	0.4 µl	0.4 µl	0.4 µl
Forward Primer (100 mM)	0.1 µl	0.1 µl	0.1 µl	0.1 µl	0.2 µl
Reverse Primer (100 mM)	0.1 µl	0.1 µl	0.1 µl	0.1 µl	0.2 µl
Taq Polymerase	0.2 µl	0.2 µl	0.2 µl	0.2 µl	0.2 µl
Taq Polymerase Brand	GoTaq	GoTaq	GoTaq	GoTaq	G2 Taq
<b>PCR thermal cycler conditions</b>					
Initial denaturation	3 min, 95 °C	3 min, 95 °C	3 min, 95 °C	3 min, 95 °C	2.5 min, 94°C
<b>Cycler number</b>	40	40	40	30	35

Step 1: denaturation	30 sec, 94 °C	30 sec, 95 °C	30 sec, 94 °C	30 sec, 94 °C	30 sec, 94 °C
Step 2: annealing	30 sec, 58°C	30 sec, 60°C	30 sec, 58°C	30 sec, 55°C	30 sec, 54°C
Step 3: extension	30 sec, 72°C	1 min, 72°C	30 sec, 72°C	1 min, 72°C	1 min, 72°C
Final extension	5 min, 72°C	5 min, 72°C	5 min, 72°C	5 min, 72°C	10 min, 72°C
	Hold at 10°C				

Table 2.2 Primer sequences and band sizes

Gene	Forward primer sequence	Reverse primer sequence	Product size
<i>Lgr5Cre<sup>ERT2</sup></i>	CTG CTC TCT GCT CCC AGT CT	Wildtype (WT): ATA CCC CAT CCC TTT TGA GC	WT=298 bp; Mutant=174 bp
		Mutant: GAA CTT CAG GGT CAG CTT GC	
<i>Apc<sup>fl/fl</sup></i>	GTT CTG TAT CAT GGA AAG ATA GGT GGT C	CAC TCA AAA CGC TTT TGA GGG TTG ATT C	WT=266 bp; Targeted=315 bp
<i>Foxp3<sup>DTR</sup></i>	WT: TGG ACC GTA GAT GAA TTT GAG TT	WT: CCA GAT GTT GTG GGT GAG TG	WT= 500 bp; HOM= 650 bp
	HOM: GGG ACC ATG AAG CTG CTG GCC G	HOM: TCA GTG GGA ATT AGT CAT GCC	
<i>Cre</i>	TGA CCG TAC ACC AAA ATT TG	ATT GCC CCT GTT TCA CTA TC	1000 bp
<i>Apc<sup>min</sup></i>	TTC TGA GAA AGA CAG AAG TTA	WT: GCC ATC CCT TCA CGT TAG	WT=450 bp Apc <sup>min</sup> = 200 bp
		Apc <sup>min</sup> : TTC CAC TTT GGC ATA AGG C	

## 2.4 Experimental Cohorts

After the genotyping was done and ascertained by PCR, mice of appropriate age were selected into control and experimental groups. Whenever possible, mice were housed in cages with other mice. Once animals were induced, they were monitored closely for signs of illness such as hunched body, pale feet, piloerection or any other signs of loss of condition.

### 2.4.1 Administration of Tamoxifen

Powdered tamoxifen (Sigma-Aldrich) was mixed in corn oil (Sigma-Aldrich) at a concentration of 10 mg/ml in a 70 °C water bath, while being stirred at intervals, until completely dissolved. Aliquots were stored at -20 °C, thawed before each procedure at 70 °C and kept warm until administration into the mice. Each aliquot was used only for 4 days. Mice were injected with 80 mg/Kg of tamoxifen *via* intraperitoneal (IP) injection for

4 consecutive days and sacrificed 15 days after the beginning of the treatment. Injections were done using a 1 ml syringe (BD Plastik) and a 25 G needle (BD Microlance3). Tamoxifen injection allowed the activation of the Cre-recombinase and deletion of the *Apc* gene in the ISCs.

## 2.4.2 Depletion of Immune Cells or Neutralization of Cytokines

### 2.4.2.1 Administration of Diphtheria Toxin (DT)

For *in vivo* depletion of Foxp3+ Treg cells 15 µg/Kg DT (Sigma), diluted in sterile phosphate buffered saline (PBS, ThermoFisher Scientific) was IP injected every other day for 15 days. Injections were done using a 1 ml syringe and a 26 ½ G needle (BD Microlance3).

### 2.4.2.2 Administration of CD4 Depleting Antibody

The CD4 depleting antibodies (clones YTS-191 & YTS-3) were gratefully received from Professor Awen Gallimore. These clones were grown and purified in Professor Awen Gallimore lab as previously described (Jones 2002). Mice were injected with 2 mg of each clone at day -1 and again one week later. Injections were done using a 1 ml syringe and a 26 ½ G needle (BD Microlance3).

### 2.4.2.3 Administration of CD8 Depleting Antibody

CD8+ depletion was achieved by IP injection of a depleting anti-CD8 monoclonal antibody (InVivoMab, clone YTS-169) (Bioxcell). The antibody was diluted in the InVivoPure pH 7.0 Dilution Buffer (Bioxcell) and 250 µg were injected at day -1 and 100 µg one week later. Injections were done using a 1 ml syringe and a 26 ½ G needle (BD Microlance3).

### 2.4.2.4 Administration of Interferon-gamma (IFN $\gamma$ ) Neutralising Antibody

IFN $\gamma$  neutralisation was achieved by injecting the mice with 2 mg of a neutralising IFN $\gamma$  antibody (clone XMG1.2) at day -1 and with 1mg one week later. Injections were done using a 1 ml syringe and a 26 ½ G needle (BD Microlance3). Similar to the CD4 depleting antibody, the XMG1.2 clone was grown and purified in Professor Awen Gallimore lab as previously described (Jones 2002).

## 2.5 Tissue Harvesting and Processing

All experimental animals were culled by cervical dislocation according to the Home Office Licence procedures (schedule 1 of Animals (Scientific Procedures) Act 1986). The tissues were dissected immediately after the animal sacrifice in order to avoid degradation of RNA (Ribonucleic Acid) and proteins.

### 2.5.1 Dissection of Organs

Mice were dissected in a designated area using a dissection kit. The abdomen was sprayed with 70% ethanol and it was opened longitudinally through the skin and smooth muscle wall. Spleen, a part of the liver and kidney were collected and fixed immediately as described in section 2.5.3. For flow cytometry experiments the whole spleen and mesenteric lymph nodes (MLN) were collected and placed in tubes containing RPMI 1649 medium supplemented with GlutaMAX (Life Technologies), penicillin/streptomycin (Thermo Fisher Scientific) and 5% Foetal Bovine Serum (FBS) (Thermo Fisher Scientific).

### 2.5.2 Dissection of Intestines

The stomach and caecum were dissected out and discarded. The small intestine and the large intestine were flushed with HBSS (phenol red, calcium and magnesium free (Thermo Fisher Scientific) containing HEPES buffer (Gibco) (1:100). Depending on the purpose, the intestines were processed in different ways that will be described below.

For tissue fixation, the small intestine was opened longitudinally and sections with different sizes were rolled into a “Swiss roll-like” structures using dissection tweezers, pinned with a needle and fixed in 10% formalin (Sigma-Aldrich) (section 2.5.3). The whole large intestine was rolled into “Swiss-like rolls” and fixed (section 2.5.3).

For gene expression analysis, a section of the small intestine (between the 5<sup>th</sup> cm of the small intestine and the 12<sup>th</sup> cm) was opened longitudinally and cut into small fragments. The intestinal fragments were brought to the main laboratory in a 50 ml tube with HBSS containing HEPES buffer.

For flow cytometry analysis the whole small and large intestines were open longitudinally and cut into small fragments that were placed into in a 50 ml tube with HBSS containing HEPES buffer.

### 2.5.3 Tissue Fixation

All tissues were quick-fixed in 10% neutral buffered formalin (Sigma-Aldrich) for 24 hours at 4 °C. After that, the formalin was replaced by 70% ethanol (EtOH) and kept at 4 °C until paraffin embedding.

### 2.5.4 Paraffin Embedding

After the fixation, the tissues were transferred to an embedding cassette (ThermoFisher Scientific) and processed using an automated processor (Leica TP1050). The tissues were dehydrated by immersion into increasing alcohol gradients (70% EtOH for 1 h, 95% EtOH for 1 h, 2x 100% EtOH for 1.5 h and 100% EtOH for 2 h) and 2x xylene for 2 h. Following the dehydration, the tissues were placed in liquid paraffin 3x for 1h each. The samples were then removed from the cassette and embedded in paraffin wax by hand and allowed to harden.

### 2.5.5 Sectioning of Paraffin Embedded Tissue

In order to prepare the tissue for Haematoxylin and Eosin staining (H&E, section 2.6.2) and immunohistochemistry (IHC, section 2.6.3), the paraffin embedded tissue was cut by a microtome (Leica RM2135) to 5 µm sections. The sections were placed on Poly-L-Lysine (PLL) coated slides and baked at 58 °C for 24 h.

Paraffin embedding, sectioning and H&E staining were performed by Derek Scarborough and Mark Isaac.

## 2.6 Histological Analysis

### 2.6.1 Preparation of Sections for H&E and IHC

Paraffin embedded tissue sections on PLL slides were dewaxed by immersion in xylene (Fisher Scientific) 2x for 5 min. The PLL slides were then rehydrated through incubations in a gradient of decreasing EtOH (VWR) (2x 3min in 100% EtOH, 1x 3min in 95% EtOH, 1x 3min 75% EtOH). The slides were removed and placed in dH<sub>2</sub>O in preparation for IHC staining.

## 2.6.2 Haematoxylin and Eosin (H&E) Staining

H&E was performed to allow the visualization of tissue morphology. Haematoxylin stains the cell nuclei, whereas Eosin marks the cytoplasm.

PLL slides were dewaxed and rehydrated as previously described (section 2.6.1) and immersed in Mayer's Haemalum (R.A. Lamb) for 45 secs, removed and briefly washed in running tap water. Slides were then stained with 1% Eosin (R.A. Lamb) solution for 5 min and washed again in running tap water to remove excess stain. Slides were dehydrated and mounted as described in section 2.6.3.7.

## 2.6.3 Immunohistochemistry (IHC)

IHC enabled the visualization of presence and location of specific proteins in the tissue PLL samples. The generic protocol will be described below, whereas the specific conditions for each target are described in Table 2.3.

### 2.6.3.1 *Blocking of Endogenous Peroxidase Activity*

The visualization of the antibodies involves an enzymatic reaction catalysed by horse radish peroxidase (HRP), so it is essential to block endogenous peroxidase activity. The slides were placed for 35 min in a peroxidase block solution (832 mg Citric Acid (Sigma-Aldrich), 2.2 g Sodium Dihydrogen Phosphate Dihydrate ( $\text{H}_2\text{NaO}_4\text{P} \cdot 2 \text{H}_2\text{O}$ , Fluka), 10 ml of 30% Hydrogen Peroxide ( $\text{H}_2\text{O}_2$ , Sigma-Aldrich) in 200 ml  $\text{dH}_2\text{O}$ ).

### 2.6.3.2 *Antigen Retrieval*

During fixation of the tissue it is possible that cross-linking bonds of amino-acids could form, altering the biochemistry of the proteins and masking the epitope of interest. When this happens, the epitope is no longer able to bind to the primary antibody having a negative impact on the IHC. Performing antigen retrieval allowed the unmasking of the antigen, restoring the epitope-antibody binding.

Slides were boiled in a pre-warmed solution of Tris Buffered EDTA (stock solution: 12.1 g of Tris Base (Fisher Scientific) and 0.93 g of EDTA (Sigma-Aldrich) in 50 ml  $\text{dH}_2\text{O}$ ; working solution: 20 ml of the stock solution in 1 L  $\text{dH}_2\text{O}$ , pH 8.0) for 50 min in a 1.5L beaker at approximately 225 °C. Following the antigen retrieval, the slides were left (in Tris EDTA buffer) at RT for 30 min to cool down. After that, they were washed 3x for 3 min in 1x PBS (Fisher Scientific).

A circle around each section was drawn using an ImmEdge PAP pen (Vector Labs), and slides were placed in a humidified chamber.

### *2.6.3.3 Blocking of Non-specific Antibody Binding*

Tissue sections were incubated for 30 min with normal serum that was derived from a different species than the primary antibody was raised in. Details of the serum for each antibody are indicated in Table 2.3.

### *2.6.3.4 Primary Antibody Treatment*

After blocking non-specific binding of the antibody, the serum was removed and the primary antibody, previously diluted in 1% Bovine Serum Albumin (BSA, Sigma-Aldrich), was applied and incubated. Slides were washed 3x 3 min in PBS. Slides were covered with parafilm (Sigma-Aldrich) in order to guarantee the hydration of the tissue and equal distribution of the antibody. Slides were washed 3x 3 min in PBS. The conditions for each antibody can be found in the Table 2.3.

### *2.6.3.5 Secondary Antibody Treatment*

The secondary antibody was chosen to recognise specifically the primary antibody species and isotype. The tissue sections were incubated with the secondary antibody for 30 min at RT. Slides were washed 3x 3 min in PBS. Details of the secondary antibodies are in Table 2.3.

### *2.6.3.6 Visualization of Antibody Binding*

To visualize the target protein antigen, its location and relative levels in the tissue sections an enzyme-specific, chromogenic colour development was used according to manufacturer's recommendations. Slides were incubated with the appropriate chromogen for 3 min at RT and washed 1x 3 min in dH<sub>2</sub>O and 3x 3 min in PBS. The chromogens utilised for each antibody are shown in Table 2.3.

### *2.6.3.7 Dehydration and Mounting of Slides*

Slides were placed for 50 secs in Mayer's medium for counterstain and briefly washed in running water until becoming clear. Sections were dehydrated in ascending alcohol concentrations (1x 2 min 70%, 1x 2 min 95%, and 2x 2min 100%) and 2x 5min in xylene. Slides were mounted using DPEX (ThermoFisher Scientific) and appropriate coverslips (ThermoFisher Scientific) and left to dry overnight.

Slides were scanned in the Axio Scan.Z1 Zeiss, using a 20x magnification.

Table 2.3 Antibody-specific conditions used for IHC

Primary antibody	Manufacturer	Serum Block	Primary antibody conditions	Secondary antibody	Chromogen
Anti-Mouse/Rat Foxp3	eBioscience	2.5% Normal goat serum (Vector Labs)	1:500, O/N at 4 °C	Anti-Rat (Mouse adsorbed) (ImmPRESS HPR, Vector Labs)	DAB (Peroxidase substrate kit, Vector Labs)
Rat Anti-Mouse CD8	eBioscience	2.5% Normal goat serum (Vector Labs)	1:200, O/N at 4 °C	Anti-Rat (Mouse adsorbed) (ImmPRESS HPR, Vector Labs)	DAB (Peroxidase substrate kit, Vector Labs)
Rat Anti-Mouse CD4	eBioscience	2.5% Normal goat serum (Vector Labs)	1:100, O/N at 4 °C	Anti-Rat (Mouse adsorbed) (ImmPRESS HPR, Vector Labs)	DAB (Peroxidase substrate kit, Vector Labs)
Rabbit Anti-Human CD3 (Polyclonal)	DAKO	2.5% Normal horse serum (Vector Labs)	1:300, O/N at 4 °C	Anti-Rabbit (ImmPRESS HPR, Vector Labs)	VIP (Peroxidase substrate kit, Vector Labs)
Anti-Mouse Beta-catenin	BD Biosciences	1% BSA	1:100, 1h30 at RT	Anti-Mouse (ImmPRESS HPR, Vector Labs)	SG (Peroxidase substrate kit, Vector Labs)

## 2.7 Cell Counting

To quantify histological sections the images that were acquired in the Zeiss Axio Scan.Z1 slide scanner were analysed using the ZEN image analysis software. Analysis was done from areas that were not crosscut and without staining artifacts. At least four biological replicates per cohort were analysed. Statistical analysis was conducted as explained in section 2.13.

### 2.7.1 Total Tumour Burden

To analyse the total tumour burden, the whole crypts touching the basement membrane with positive nuclear B-catenin staining (aberrant crypts), from both small and large intestines, were counted. The paraffin embedded tissues were cut into three serial sections separated by 120  $\mu\text{m}$  distance to avoid the quantification of the same aberrant crypts. Data was normalised by counting the total number of whole crypts touching the intestinal basement membrane.

### 2.7.2 Partial Tumour Burden

Partial tumour burden was analysed by assessing the number of whole crypts with positive nuclear B-catenin in 100 crypts of the first 5 cm of the small intestine. The average number of aberrant crypts was calculated and the mean across the cohorts was determined.

### 2.7.3 Apoptotic Index

Apoptotic index was determined from H&E sections. Apoptotic bodies were identified based on their appearance and their number was scored per crypt from 25 whole crypts. The average number of mitotic cells was calculated and the mean across the cohorts was determined.

### 2.7.4 Scoring of Immune Cell Types

The number of Tregs was determined by Foxp3 IHC staining. Cells were quantified in both small and large intestines in the *Lgr5Cre<sup>ERT2</sup> Apc<sup>fl/fl</sup>* mouse model in the surrounding tissue of normal and aberrant crypts of at a minimum number of 5 fields of view of at least 50 $\mu\text{m}^2$ . Foxp3 scoring was performed by Dr. Lee Parry prior the start of my project.

For the  $Apc^{min}$  mouse model, the number of Tregs was quantified in polyps and in a similar area of the surrounding normal tissue of the small intestine. The area was determined using the ZEN image analysis. Data were normalised by the number of Tregs per  $1000\mu m^2$ .

The number of CD4 and CD8+ T-cells was determined by CD4 and CD8 respectively IHC staining. Cells were counted from 25 normal and 25 aberrant whole crypts. The average number of positive cells was calculated and the mean across the cohorts was determined.

## 2.8 Intestinal Epithelial Cells Extraction for Gene Expression Analysis

After dissecting the tissue (section 2.5.2), the fragments were washed gently 3x with HBSS containing HEPES (1:100). The supernatant was discarded, 10ml 8mM EDTA (Sigma-Aldrich) were added to the intestinal fragments and left incubating on ice for 30 min. After that, falcon tubes containing the fragments were shaken vigorously, before being allowed to settle. Supernatant was collected into a fresh 50ml tube containing 10ml complete RPMI 1649 medium supplemented with GlutaMAX (Life Technologies), penicillin/streptomycin (Thermo Fisher Scientific) and 10% Foetal Bovine Serum (FBS) (Thermo Fisher Scientific). Further 10ml complete RPMI media were added to the fragments and re-shaken. Fragments were filtered through a  $70\mu m$  cell strainer (MACS) and supernatant collected. The 50ml tubes containing the supernatant were spun down at 1000rpm for 5 minutes. Supernatant was discarded and pellet was re-suspended in 1ml RNA later (Sigma-Aldrich).

## 2.9 RNA extraction

The intestinal epithelial cells extracted (section 2.7) were disrupted with 500  $\mu l$  RLT buffer (QIAGEN) and the RNA was purified with RNeasy mini kits (QIAGEN) according to manufacturer's recommendations. RNA was quantified using a NanoDrop 2000 spectrophotometer (ThermoFisher Scientific) and stored at  $-80\text{ }^{\circ}\text{C}$ .

## 2.10 Gene Expression Analysis: Quantitative Real-Time PCR (qRT-PCR)

RNA extracted (section 2.8) was reverse transcribed to generate complementary DNA (cDNA) using Superscript III Reverse Transcriptase (Invitrogen) according to the manufacturer's instructions. Quantitative real-time PCR was performed using either TaqMan® (table 2.4) or SYBR® Green (Table 2.5) assays.

For the TaqMan® assays the reaction was performed in a final volume of 10 µl containing 2 µl of diluted (1:5) cDNA sample (200ng), 5µl of 2x Gene Expression TaqMan® Master Mix (Applied Biosystems) and 0.5µl of 20x TaqMan® Gene Expression Assay probes (Applied Biosystems).

The SYBR® Green assays were performed in a final volume of 20 µl containing 1 µl of cDNA sample (1000 ng), 10 µl of Fast SYBR® Green Master Mix (Applied Biosystems) and 0.5 of 10µM forward and reverse primers (Applied Biosystems). All samples were prepared in triplicate, including a blank for each target gene.

Reactions were performed on an Applied Biosystems QuantStudio 7 Flex Real Time Machine. Relative expression of mRNA was calculated using the  $\Delta\Delta C_t$  method and ACT B was used as an internal control. Statistical analysis was conducted as explained in section 2.13.

Table 2.4 TaqMan® qRT-PCR primers/probes

Gene	Identification	Species	Source
ACTB	(DQ) Mix 20x	<i>Mus musculus</i>	Applied Biosystems
Lgr5	Mm00438890_m1	<i>Mus musculus</i>	Applied Biosystems
Olfm4	Mm01320260_m1	<i>Mus musculus</i>	Applied Biosystems
Ascl2	Mm01268891_g1	<i>Mus musculus</i>	Applied Biosystems
Ifng	Mm01168134_m1	<i>Mus musculus</i>	Applied Biosystems
Foxp3	Mm00475162_m1	<i>Mus musculus</i>	Applied Biosystems

Table 2.5 SYBR® Green qRT-PCR primers

Gene	Forward sequence	Reverse sequence	Species	Source
ACTB	TGT TAC CAA CTG GGA CGA CA	GGG GTG TTG AAG GTC TCA AA	<i>Mus musculus</i>	Applied Biosystems
Axin2	GCA GCT CAG CAA AAA GGG AAA T	TAC ATG GGG AGC ACT GTC TCG T	<i>Mus musculus</i>	Applied Biosystems
cMyc	CTA GTG CTG CAT GAG GAG ACA C	GTA GTT GTG CTG GTG AGT GGA G	<i>Mus musculus</i>	Applied Biosystems
CIITA	ACC CCC TAC ATC TCT ACC ACC T	TCG CAG TTG ATG GTA TCT GTG T	<i>Mus musculus</i>	Applied Biosystems

## 2.11 Flow Cytometry

### 2.11.1 Preparation of Single Cells Suspensions from Tissues

#### 2.11.1.1 Spleen and Mesenteric Lymph Node (MLN) Lymphocyte Extraction

Mice were harvested and spleen, MLN, small intestine (SI) and large intestine (LI) were collected as explained in section 1.5.1.

Spleen and MLN were homogenized using the back of a 1ml syringe plunger through a 70 µm cell strainer (MACS) and rinsed through with 4ml complete RPMI. The single cell suspensions were centrifuged at 1500 rpm for 5 minutes, supernatant was aspirated. MLN pellet was resuspend in 0.5 ml. Spleen pellet was resuspend with 2 ml red blood cells lysis buffer (Sigma) for 2 min at 37°C. 10 ml of complete RPMI was then added in order to stop the reaction and cells were centrifuged at 1500 rpm for 5 minutes. Supernatant was discarded and the pellet was resuspend in 5 ml complete RPMI media.

#### *2.11.1.2 Small and Large Intestine Lymphocyte Extraction*

Both SI and LI were dissected and collected as explained in section 2.5.2.

##### *2.11.1.2.1 Intra epithelial lymphocyte (IEL) fraction.*

15 ml of pre-warmed complete RPMI media with 5mM EDTA were added to the tubes containing the tissue and they were placed in a thermomixer (Eppendorf) at 300 rpm at 37°C for 20 minutes. Supernatant was collected, through a cell strainer, and placed to a fresh tube containing 5 ml complete RPMI media with 10 mM HEPES (Gibco). Another 15 ml of pre-warmed complete RPMI media with EDTA were added to the tissue and incubation was repeated in the thermomixer. Supernatant was collected and placed in the collection tube. 10 ml of complete RPMI media with HEPES were added to the tissue and incubation was repeated. Supernatant was collected and placed in the collection tube.

##### *2.11.1.2.2 Lamina propria lymphocyte (LPL) fraction*

In order to obtain the LPL fraction, the tissue was incubated in the thermomixer for 45 minutes with 10 ml complete RPMI media containing 1mg/ml collagenase VIII (Sigma) and 200U/ml DNase II (Sigma). Whilst tissue was digesting, Percoll (GE Health Life Sciences) density gradients were prepared. Percoll solutions were prepared the day before using sterile PBS or RPMI in the tissue culture hood and kept overnight at 4°C. 100% Percoll was prepared using 10X PBS (Fisher Scientific) (1:10), 75% and 30% Percoll were diluted in 1x PBS and the 40% Percoll in RPMI. A 15 ml tube was laid flat against the bench, with the head of the tube resting on its lid. Using a pipette pump, the 40% Percoll solution (pink) was slowly layered on top of the 70% Percoll solution (clear), then the tube was carefully turned upright. The tubes were stored at 4°C for later use. Following digestion, 200 µl EDTA was added to the LPL fraction to inhibit collagenase

activity and the tissue was further disrupted in a gentleMACS dissociator (MACS). Cells from the LPL fraction were collected through a cell strainer and placed into a fresh tube.

Tubes containing cells from SI (IEL & LPL) and LI (IEL & LPL) were centrifuged for 5 minutes at 1500 rpm. Supernatant was aspirated and resuspended in 3 ml 30% Percoll solution (clear). Carefully, it was added to the pre-prepared Percoll gradients as previously described. Tubes were centrifuged at 1800 rpm for 20 minutes with the brake off. Supernatant was aspirated until half of the 40% Percoll solution remained. Lymphocytes were collected and placed into a 15 ml tube containing 12 ml complete RPMI media, then centrifuged at 1500 rpm for 5 minutes.

### 2.11.2 Cell Surface Staining

0.2 – 1 x 10<sup>6</sup> lymphocytes from the different compartments (i.e. spleen, MLN, SI IEL, SI LPL, LI IEL and LI LPL) were plated out in a 96 round-bottomed well plate. Cells were washed twice in 200 µl PBS 1x. Dead cells were stained by adding and mixing well 3 µl of aqua amine-reactive viability dye (LIVE/DEAD Aqua, Invitrogen), previously diluted in PBS 1x (1:10), to the cell pellet and incubated for 15 minutes in the dark at room temperature. Cold FACS buffer (PBS containing 2% FBS and 5mM EDTA) was used to wash twice the cells prior the incubation with 50 µl per well of Fc Receptor block (eBioscience) diluted (1:200) in FACS buffer. Cells were incubated at 4°C in the dark for 10 minutes. After washing the cells twice with FACS buffer, they were stained with a surface stain panel (Table 2.3). A master mix of the antibodies, diluted in FACS buffer, was prepared and 25 µl of the mix was added to each well. Cells were incubated with the antibodies for 15 minutes at 4°C in the dark and washed twice in FACS buffer.

### 2.11.3 Intracellular Antigen and Cytokine Staining

To analyse intracellular cytokines, 0.2 – 1 x 10<sup>6</sup> cells were stimulated for 3 hours with complete RPMI media containing 50 ng/ml phorbol myristate acetate (PMA; Sigma – Aldrich), 1 µl/ml ionomycin (Sigma – Aldrich) and 5 µg/ml brefeldin A (Sigma – Aldrich).

After the stimulation was completed, cells were fixed and permeabilized with 200 µl of fixation / permeabilization solution (Foxp3 staining kit, eBioscience) overnight (maximum 16 hours) at 4°C in the dark. Cells were washed twice with 1x permeabilization buffer (eBioscience) and a master mix of the antibodies to stain intracellular markers/cytokines (Table 2.6) was prepared. The antibodies were diluted in 1x permeabilization buffer and 25 µl of the master mix was added to each well. Cells were incubated for 30 minutes at 4°C in the dark and washed twice in 1x permeabilization buffer. Finally, the pellets were resuspended in 200 µl FACS/fix buffer (FACS buffer with

2% formaldehyde (Fisher Scientific)). Single staining and Fluorescent Minus One (FMO) controls were included in the analysis. FMO's correspond to a sample that is incubated with the antibodies minus a specific one, helping in the choice of the correct position of gates during the analysis. Samples were run in a NovoCyte ® 3000 cytometer.

*Table 2.6 Flow Cytometry Antibodies*

<b>Antibody</b>	<b>Fluorochrome (Conjugate)</b>	<b>Clone</b>	<b>Isotype</b>	<b>Dilution</b>	<b>Company</b>
<i>Surface Antibodies</i>					
Anti-Mouse CD3	AF488	145-2C11	Armenian hamster IgG	1 in 50	eBioscience
Anti-Mouse CD4	BV421	GK1.5	Lewis IgG2b, κ	1 in 80	BD Biosciences
Rat Anti-Mouse CD8	APC-H7	53-6.7	LOU/M IgG2a, κ	1 in 100	BD Biosciences
<i>Intracellular Antibodies</i>					
Anti-Mouse/Rat Foxp3	PeCy7	FJK-16s	IgG2a, kappa	1 in 50	eBioscience
Anti-Human/Mouse Granzyme B	APC	QA16A02	Mouse IgG1, κ	1 in 50	Biolegend
Rat Anti-Mouse IL-17A	PE	TC11-18H10	Lewis IgG1, κ	1:100	BD Pharmingen
Rat Anti-Mouse IFN-	PerCP-Cy™5.5	XMG1.2	Rat IgG1, κ	1 in 50	BD Pharmingen

#### 2.11.4 Flow Cytometry Analysis

Flow cytometric data were analysed using the FlowJo version 10 and NovoExpress software. Gating strategy is represented in Figures 2.1 – 2.5.

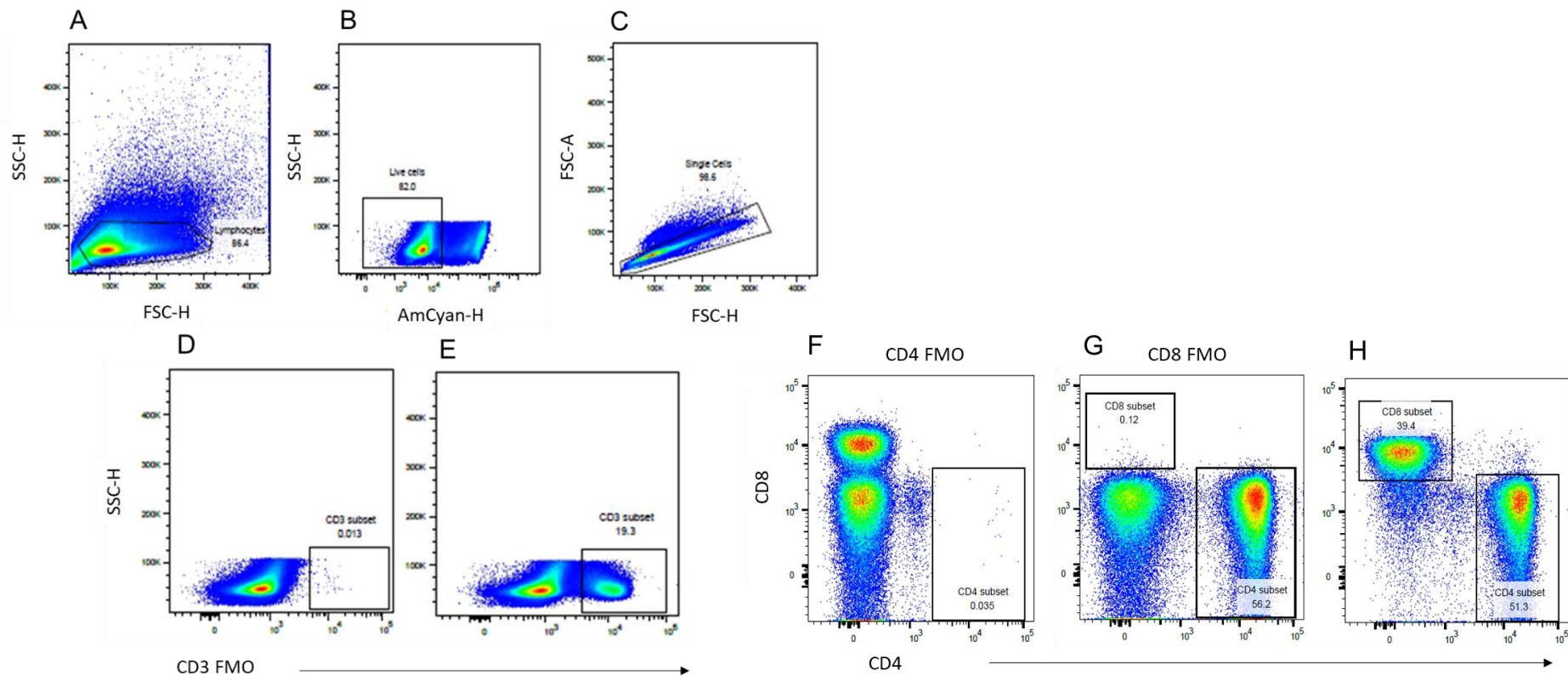


Figure 2.1 Representative flow cytometry plots showing gating strategy and examples of FMO's in the spleen.

Lymphocytes were identified based on forward (FSC) and side scatter (SSC) characteristics. Then, live cells were gated based on negative Amcyan staining. Single cells were gated based of forward scatter area (FSC-A) and height (FSC-H) characteristics. CD3+ cells were gated from singles cells and both CD4+ and CD8+ cells were gated from CD3+ cells. Fluorescence Minus One (FMO) controls were used to help the gating correctly the populations of interest. The same gating strategy was applied to all the markers analysed in each cell compartment.

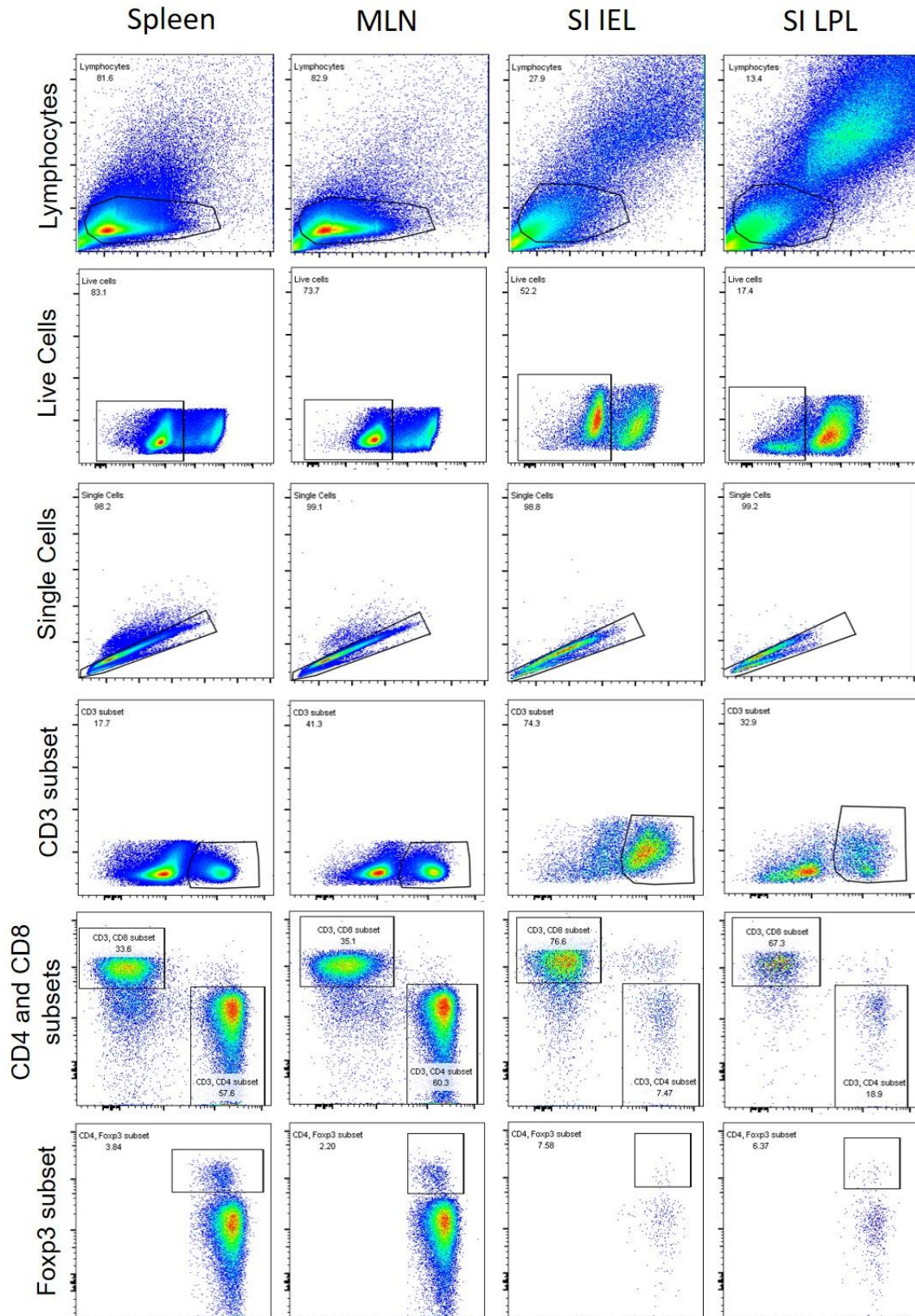


Figure 2.2 Gating strategy for flow cytometry analysis of the indicated markers in each cell compartment analysed (spleen, MLN, SI IEL, SI LPL, LI IEL and LI LPL).

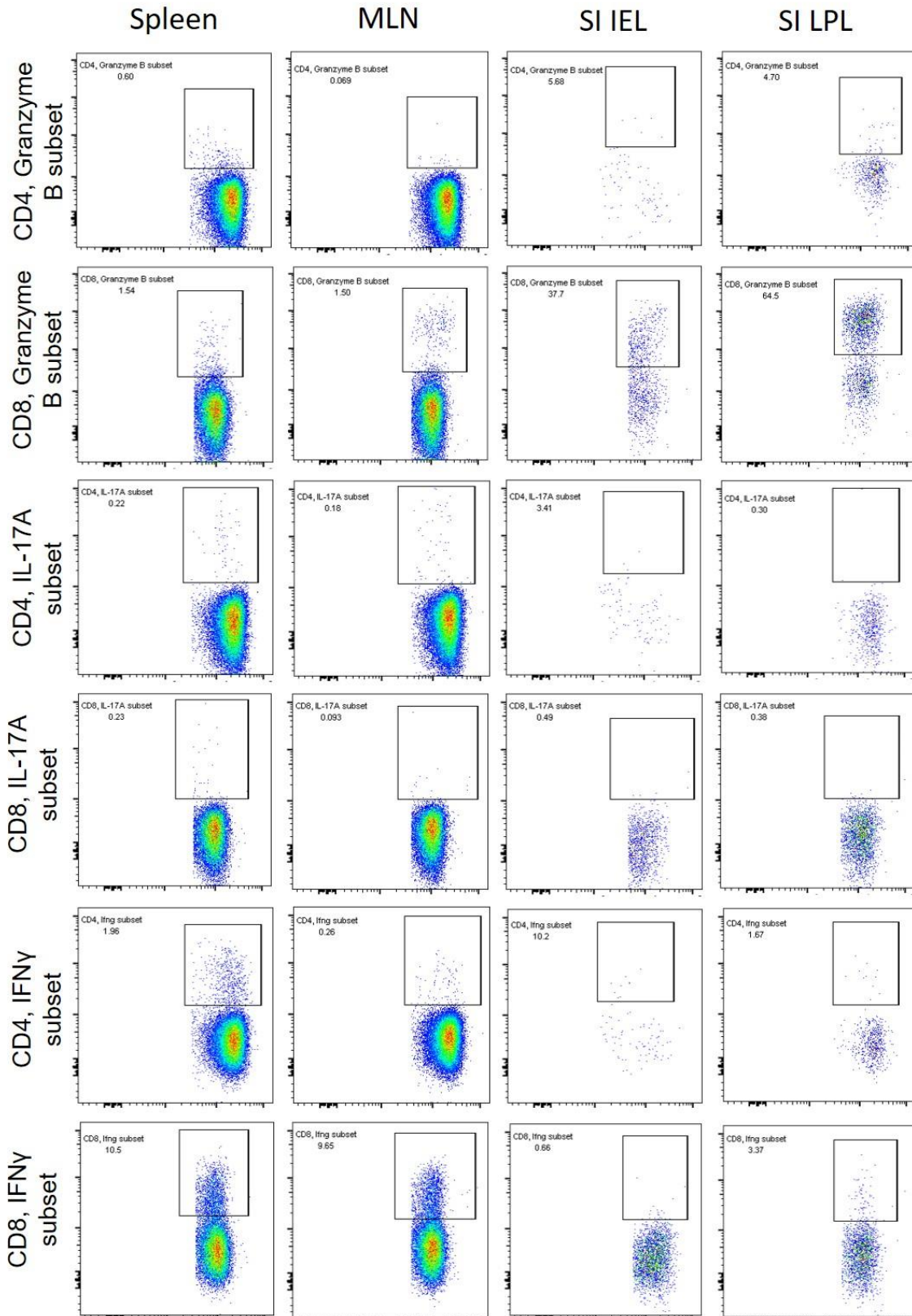


Figure 2.3 (Continuation) Gating strategy for flow cytometry analysis of the indicated markers in each cell compartment analysed (spleen, MLN, SI IEL, SI LPL, LI IEL and LI LPL).

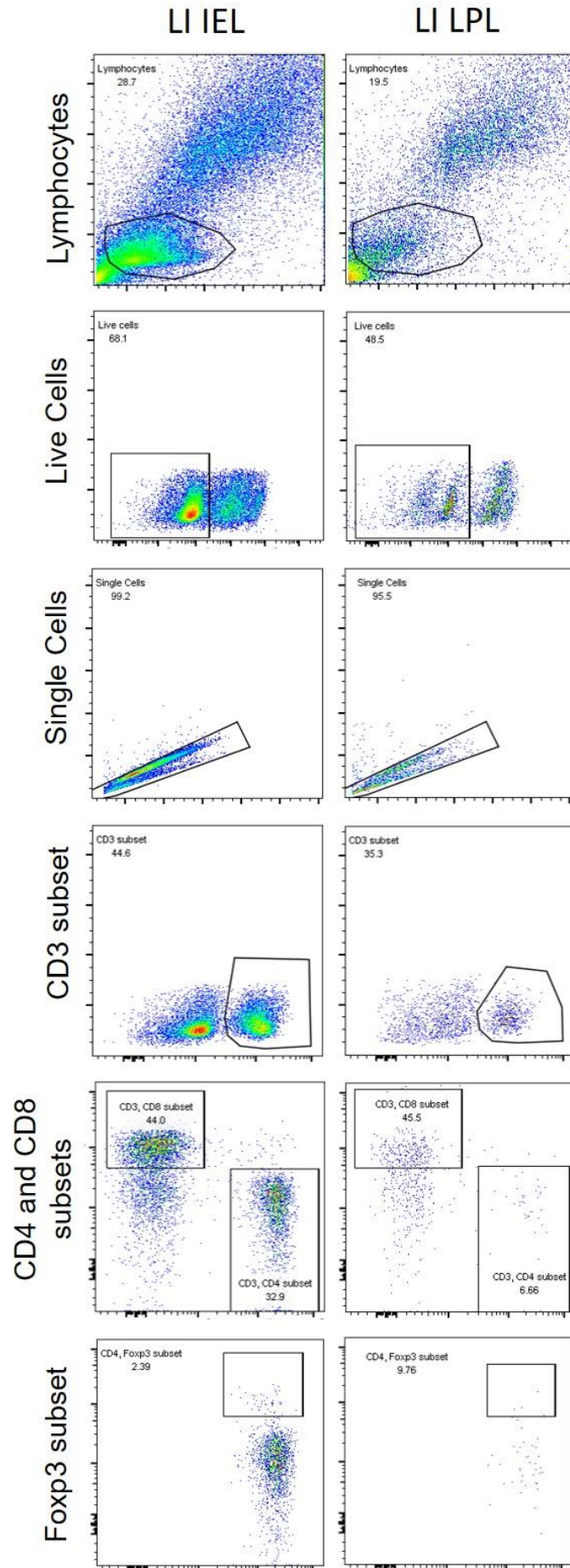


Figure 2.4 (Continuation) Gating strategy for flow cytometry analysis of the indicated markers in each cell compartment analysed (spleen, MLN, SI IEL, SI LPL, LI IEL and LI LPL).

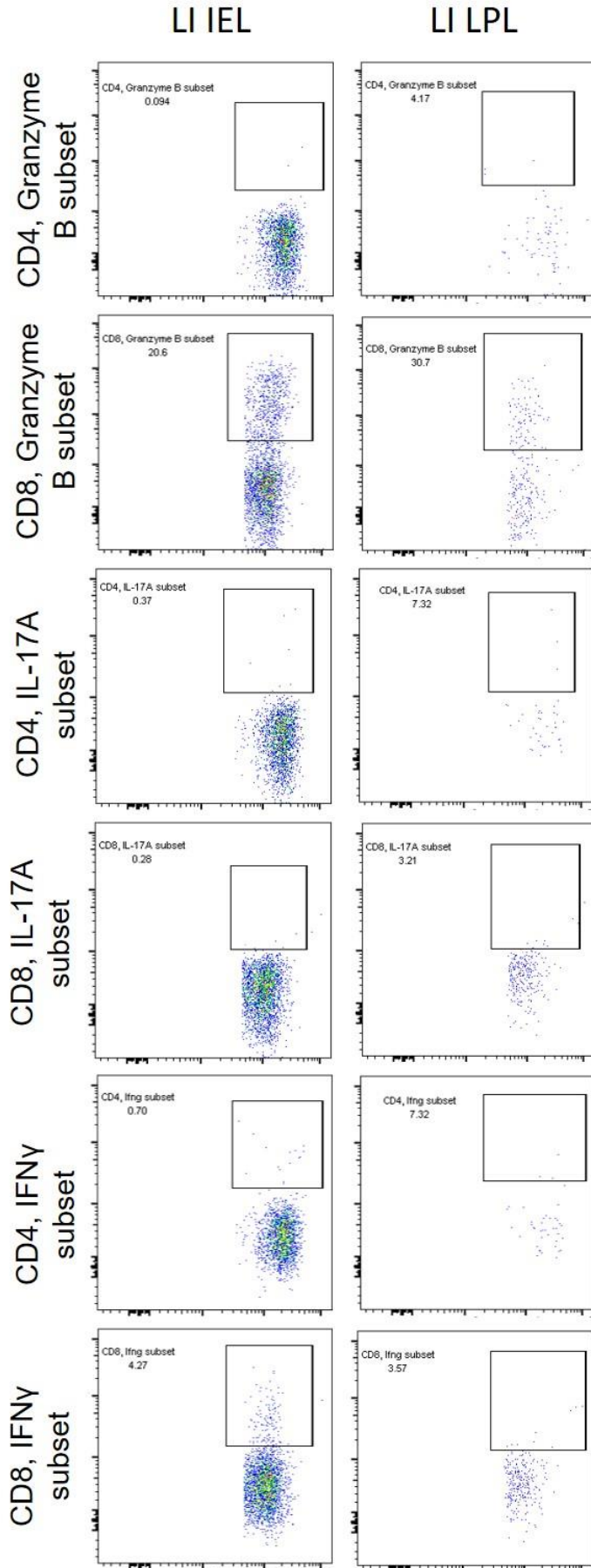


Figure 2.5 (Continuation) Gating strategy for flow cytometry analysis of the indicated markers in each cell compartment analysed (spleen, MLN, SI IEL, SI LPL, LI IEL and LI LPL).

## 2.12 Lgr5 RNAscope®

RNAscope allows the detection of RNA single molecules and their quantification in single cells.

### 2.12.1 Preparation of Sections for RNAscope

Prior to RNAscope, the PLL slides were baked in a dry oven for 1 h at 60°C. After that slides were dewaxed by immersion in fresh xylene 2x for 5 min and in 100% EtOH 2x for 1 min. The slides were left to air dry for 5 min at RT. A circle around the tissue section was drawn using an ImmEdge PAP pen.

### 2.12.2 Pre-treatment

The pre-treatment of the tissue allows an improved accessibility to the target RNA.

#### *2.12.2.1 Blocking of Endogenous Peroxide Activity*

To block the activity of endogenous peroxides, the tissue was covered with H<sub>2</sub>O<sub>2</sub> (ACD Bio, pre-treatment 1) for 10 min at RT. After that, the H<sub>2</sub>O<sub>2</sub> was removed and the slides were washed 2x for 5 min in dH<sub>2</sub>O.

#### *2.12.2.2 Antigen Retrieval*

Slides were boiled in a pre-warmed Target Retrieval (ACD Bio, pre-treatment 2) solution for 15 min in a 1.5 L beaker at approximately 100°C. Slides were carefully removed and washed 2x for 5 min in dH<sub>2</sub>O.

Slides were washed briefly with 5 dips in EtOH and left to dry at RT either for 5 min or overnight.

#### *2.12.2.3 Protease plus Treatment*

Together with the antigen retrieval, the protease plus treatment allow the RNAscope probes to access RNA by breaking cross links that could have occurred during the tissue fixation.

Slides were covered with protease plus (ACD Bio, pre-treatment 3) and incubated in a HybEZ oven at 40°C for 15 min. Slides were removed and washed 2x for 1 min in dH<sub>2</sub>O.

### 2.12.3 Probe Hybridization

The Lgr5 probe (mmLgr5, ACD Bio) was applied to the slides and placed in the HybEZ oven at 40°C for 2 h. A negative (dapB, ACD Bio) and a positive (mmPpib, ACD Bio) control were also included. Slides were removed and washed in 1x wash buffer (ACD Bio) 2x for 2 min.

### 2.12.4 Probe Hybridization and Amplification

The probe hybridization and amplification occur as a cascade of events. The probe amplification was done using the RNAscope® 2.5 HD Reagent Kit-BROWN (ACD Bio) kit. The conditions for the amplification steps are detailed in Table 2.7. Between each amplification step the slides were washed 2x for 2 min in wash buffer.

*Table 2.7 Amplification steps conditions*

<b>Amplification Step</b>	<b>Time (min)</b>	<b>Temperature (°C)</b>
#1	30	40
#2	15	40
#3	30	40
#4	15	40
#5	30	RT
#6	15	RT

### 2.12.5 Signal Detection

To detect the signal the RNAscope® 2.5 HD Reagent Kit-BROWN (ACD Bio) kit was used. Equal volumes of DAB-A and DAB-B were mixed into an appropriate sized tube, dispensed on the tissue samples and incubated for 10 min at RT. The excess was disposed and the slides were washed 2x for 2 min in dH<sub>2</sub>O.

### 2.12.6 Counterstain and Slides Mounting

Slides were placed in 50% haematoxylin diluted in Milli-Q H<sub>2</sub>O for 30 seconds at RT and briefly washed in running water until becoming clear. Slides were dehydrated in ascending alcohol concentrations (1x 2min 70% EtOH and 2x 2min 100% EtOH) and for 5 min in xylene. Slides were mounted using DPEX and appropriated coverslips and left to dry overnight.

### 2.12.7 RNAscope Analysis

To analyse the RNAscope data, the number of punctate dots from 25 crypts and 25 villi from the first 5 cm of the SI and LI were counted for each experimental group.

### 2.13 Statistical Analysis

Data presented were analysed using Graph Pad Prism 7 software. The Mann-Whitney U test, unpaired and two-tailed was used and p values less than 0.05 were accepted as statistically significant different. For analysis of qRT-PCR gene expression Whitney U test, unpaired and one-tailed was used due to a small n number (number of mice per cohort) of some groups.

## 3 Investigating the immune effects of *Apc* deficiency in the early stages of CRC

### 3.1 Introduction

The canonical Wnt pathway, a conserved signalling pathway involved in development, regeneration, survival and cell proliferation, is crucial to the maintenance of homeostasis within the intestinal epithelia. Deregulation of this pathway occurs in 80% of human CRCs, including the loss of function of the tumour suppressor gene *APC*, leading to aberrant stem cell differentiation (Mazzoni and Fearon 2014).

The intestinal epithelium is a dynamic tissue where stem cells continuously proliferate, migrate and differentiate. Intestinal stem cells are found in the crypts and are generally known as Crypt Base Columnar (CBC) cells (Gerbe *et al.* 2011). CBC cells proliferate and originate the cell progenitors that migrate along the villi. Depending on the specific signals that are received, cell progenitors differentiate into the different cell types that are found in the intestine (e.g. Goblet cells, Paneth cells, and others) (Gerbe *et al.* 2011). This process of migration and differentiation is controlled by conserved signalling pathways such as Wnt signalling and Notch pathways. CBC cells, which are maintained by the Paneth cells, can be identified by the expression of markers such as *Lgr5*, *Sox9* and *Olfm4*. It was demonstrated that, when the *Apc* gene is deleted, stem cells are transformed, do not differentiate and lead to the development of adenomas (Barker *et al.* 2009).

Previous studies have demonstrated that CRC progression depends on the interaction between the tumour and the host immune environment, comprising diverse cell types. Some of these cells include the CD4+ T cell population, which comprises regulatory T (Treg) cells and conventional T helper (Th) cells. Several CD4+T cell subsets are found within these two broad categories (Szabo *et al.* 2003; Corthay 2009; Zhu and Paul 2010; Tripathi and Lahesmaa 2014; Kaplan *et al.* 2015; Vlad *et al.* 2015).

Th cells activate other effector immune cells, controlling the adaptive immune response against foreign agents and cancer. On the other hand, Tregs are responsible for suppressing the activity of Th cells. Some of the specific functions of Tregs include: limiting inflammatory responses, the maintenance of tolerance to self-antigens tolerance thereby preventing the occurrence of autoimmune diseases, feto-maternal tolerance, suppression of allergy, and others (Corthay 2009). It is essential that a balance exist between the activities of these two cell populations.

The best Treg marker is Foxp3, a transcription factor that has an important role in the development, phenotype and functional maintenance of Tregs (Bennett *et al.* 2001; Fontenot *et al.* 2003).

It has been demonstrated that evaluating the density of CD3+ T-cells may have a higher prognostic value when compared to the routinely used TMN stage (Galon *et al.* 2006). While an increased tumour infiltration by some cell populations (e.g. CD8+ and CD45RO+) has been associated with favourable prognosis in CRC (Pages *et al.* 2005; Koch *et al.* 2006), the role of Tregs in this pathology is still unclear (Fontenot *et al.* 2003; Maeda *et al.* 2011).

Previous studies have shown that CRC patients have an increased number of Tregs (Betts *et al.* 2012; Syed Khaja *et al.* 2017). As Tregs suppress the activity of cytotoxic T cells, they are considered to have an inhibitory effect on the anti-tumour immune response being associated with disease progression, thus CRC patients with increased levels of Tregs have a poor prognosis (Betts *et al.* 2012; Liu *et al.* 2014), however there are some contradictory studies which suggest that Tregs may limit disease progression, possibly through suppressing the activity of tumour-promoting inflammatory cells (Erdman *et al.* 2005).

Considering that the majority of the previous studies were done in patients with advanced disease, I aimed to clarify the role of Tregs in the early stages of intestinal cancer, by analysing the immune changes in the murine intestines upon conditional *Apc* deletion in the intestinal stem cells (ISCs).

## 3.2 Results

### 3.2.1 Characterisation of Treg cells during tumourigenesis in the *Apc<sup>min/+</sup>* mouse

*Apc<sup>min/+</sup>* mice develop multiple polyps that can progress to adenocarcinoma, mimicking what happens to patients with FAP disease (see section 1.4.1). Previous studies have demonstrated that Tregs accumulate in intestinal adenomas of *Apc<sup>min/+</sup>* mice (Akeus *et al.* 2014; Chae and Bothwell 2015). Akeus and colleagues have shown, in mice between 70 and 154 days old (d.o.), increased frequencies of Tregs in adenomas of *Apc<sup>min/+</sup>* mice when compared to surrounding normal tissue.

Here the number of Tregs in polyps present in the small intestine of *Apc<sup>min/+</sup>* mice and normal adjacent tissue from mice at 60 d.o. and 180 d.o was quantified. Data were normalised by the number of Tregs per 1000 $\mu\text{m}^2$ . The minimum number of polyps present in a mouse was one and the maximum 13.

Intestinal sections were stained using IHC against B-catenin (grey) and Foxp3 (brown). The polyps were identified by their aberrant position in the tissue or by the positive B-catenin nuclear staining in the small intestinal crypts.

In accordance with previous reports (Akeus *et al.* 2014; Chae and Bothwell 2015) I found an increased number of Tregs in the polyps of 60 & 180 d.o. mice in comparison to normal surrounding tissue of the small intestine (Figure 3.1 Ai, Aii and 3.1 B). Despite comparable increases in total numbers of Tregs at both time points in polyps, when compared to normal adjacent tissue, the density and number of Tregs is reduced in the larger 180 d.o. polyps (Figure 3.1 B&C) when compared to 60 d.o. mice (Figure 3.1 B & C), indicating that Tregs accumulate in the polyps and may play a role in the early stages of the disease.

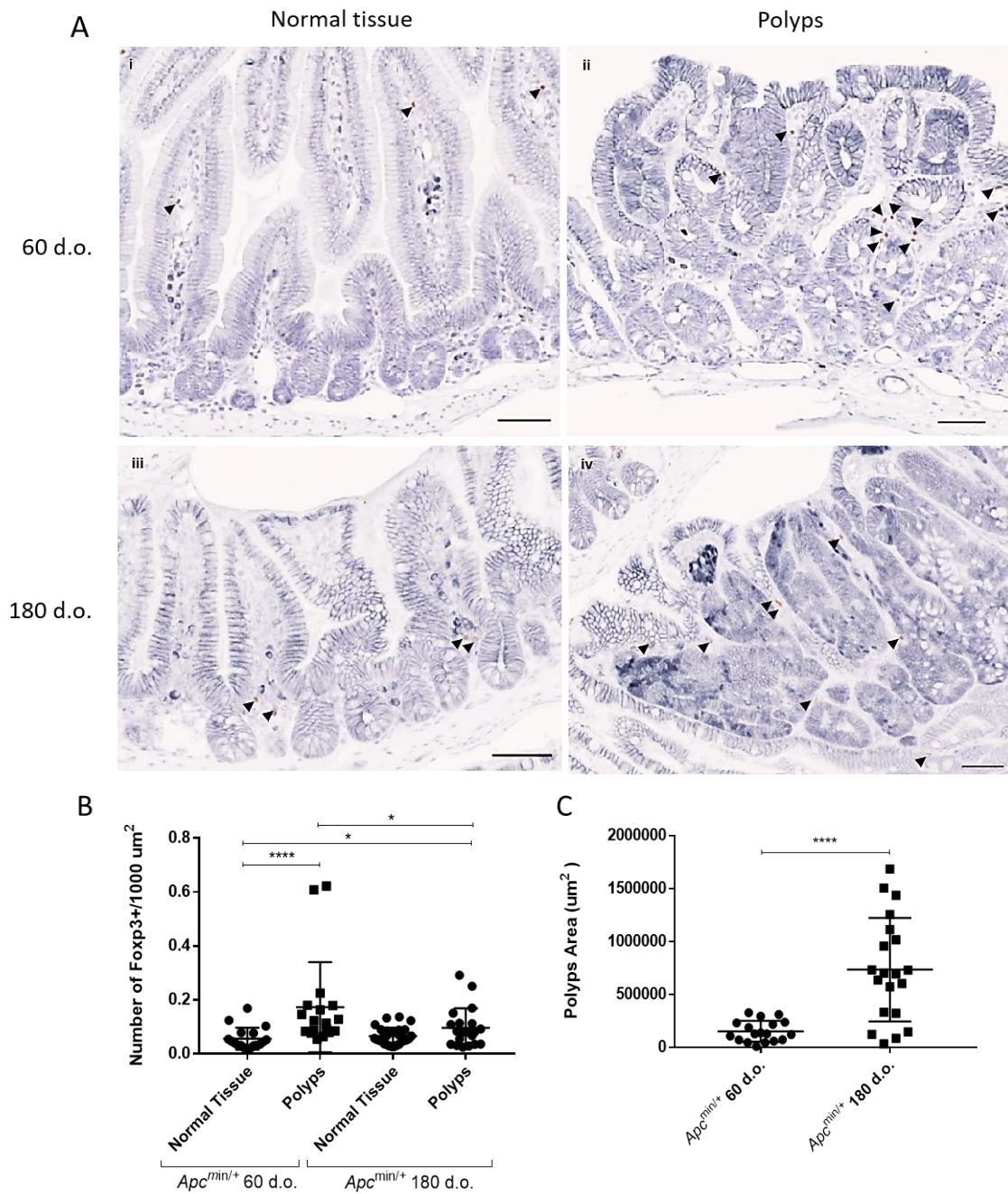


Figure 3.1 Tregs quantification in the small intestine of an  $Apc^{min/+}$  mouse model.

(A) Representative images of B-catenin (grey) and Fopx3 (brown) IHC staining of 60 d.o. and 180 d.o. age matched mice in normal tissue and polyps. Tregs are identified with black arrows. (B) Scoring of the Fopx3 IHC stained cells revealed an increased number of Tregs in polyps (A ii) compared to normal tissue in 60 d.o. mice (A i). There is no significant different in the number of Tregs between normal tissue (A iii) and polyps (A iv) in 180 d.o. mice. (C) Quantification of the polyps area in 60 and 180 d.o. mice. Polyps have an increased area in older mice. (\*) P value < 0.05, (\*\*\*\*) P value  $\leq$  0.0001. Data represent the quantification of at least one polyp and surrounding normal tissue. The maximum number of polyps identified in a mouse was 13,  $n \geq 4$

mice. Two-tailed Mann Whitney U test. Error bars represent Standard Deviation (SD). Scale bars represent 50  $\mu\text{m}$ .

### 3.2.2 Characterising Treg cells during initiation of intestinal tumourigenesis by conditional deletion of the *Apc* gene in the intestinal stem cells (ISCs)

The *Apc*<sup>min/+</sup> mouse model is an important model for the study of intestinal tumorigenesis, but the requirement for a “second hit” to remove the WT allele limits studies of tumour initiation.

To overcome the limitations of the *Apc*<sup>min/+</sup> model, we used the *Lgr5Cre*<sup>ERT2</sup>*Apc*<sup>fl/fl</sup> mouse model which allows temporal and conditional deletion of the tumour suppressor gene *Apc* and activation of the Wnt pathway in the *Lgr5* ISCs. Detailed description of the mouse model can be found in section 1.4.3. Here, Treg numbers were characterized in the intestines by IHC, gene expression of *Foxp3* in the small intestine and frequency of *Foxp3* by flow cytometry in mice 15 days after ISC deletion of *Apc*.

#### 3.2.2.1 *Apc* deletion in ISCs increases the number and frequency of Tregs

Paraffin sections of both non-induced and induced mice were stained with B-catenin (grey), *Foxp3* (brown) and CD3 (purple) antibodies. Tregs were quantified in both small (SI) and large (LI) intestines in at least 5 random fields of view of at least 50µm<sup>2</sup>. The IHC data demonstrates a significant increase in the number of Tregs, after *Apc* deletion, in both SI and LI when compared to non-induced mice (Figure 3.2).

Relative gene expression was performed in RNA extracted from epithelial cells from the small intestine. Relative expression of mRNA was calculated using the  $\Delta\Delta C_t$  method and ACT B was used as an internal control. Relative gene expression analysis confirmed an increased expression of *Foxp3* following *Apc* deletion (Figure 3.3).

Analysis by flow cytometry demonstrated the expansion of Tregs in the small intestine intraepithelial lymphocytes (SI IEL), small intestine lamina propria lymphocytes (SI LPL) and large intestine intraepithelial lymphocytes (LI IEL) (Figure 3.4). Expansion of Treg cells was also demonstrated in the spleen and mesenteric lymph nodes (MLN) (Figure S 9.1),

Taken together, these data show that Tregs start accumulating in the intestines and also other compartments (spleen and MLN), soon after the loss of function of the tumour suppressor *Apc* gene suggesting that Tregs play an important role from the early stages of intestinal cancer.

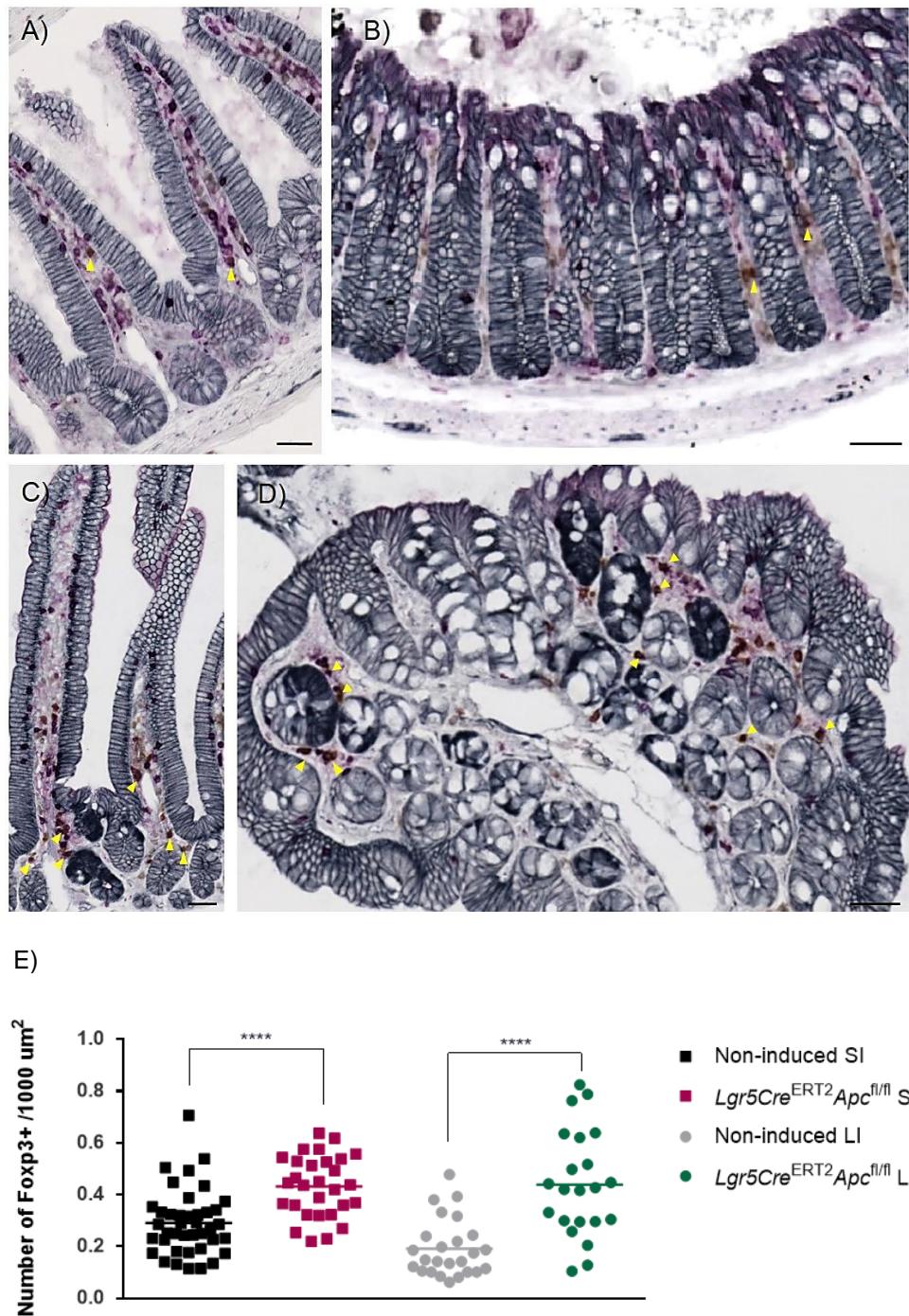


Figure 3.2 Tregs quantification in the *Lgr5Cre<sup>ERT2</sup>Apc<sup>fl/fl</sup>* mouse in small (SI) and large intestines (LI).

Representative images of  $\beta$ -catenin (grey) and Tregs (brown) IHC staining of SI (A) and LI (B) from non-induced mice; SI (C) and LI (D) from *Apc* deleted mice. Tregs are identified with yellow arrows. (E) Scoring of Tregs revealed an increased number of Treg. (\*\*\*\*) P value  $\leq$  0.0001. Data represents the quantification of Tregs in at least 5 random fields of view of at least  $50\mu\text{m}^2$ ,  $n \geq 3$  mice. Two-tailed Mann Whitney U test. Scale bars represent  $20 \mu\text{m}$ . This analysis was performed by Dr Lee Parry.

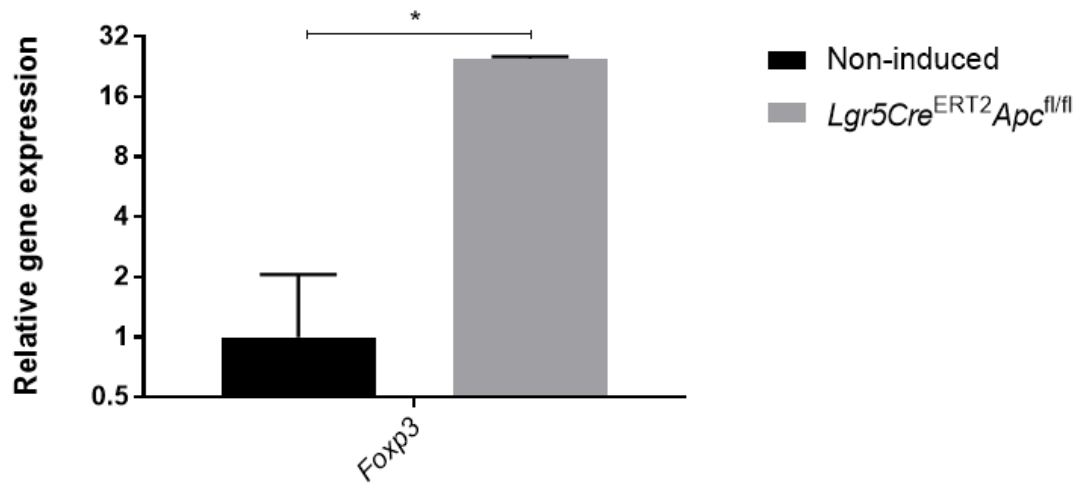
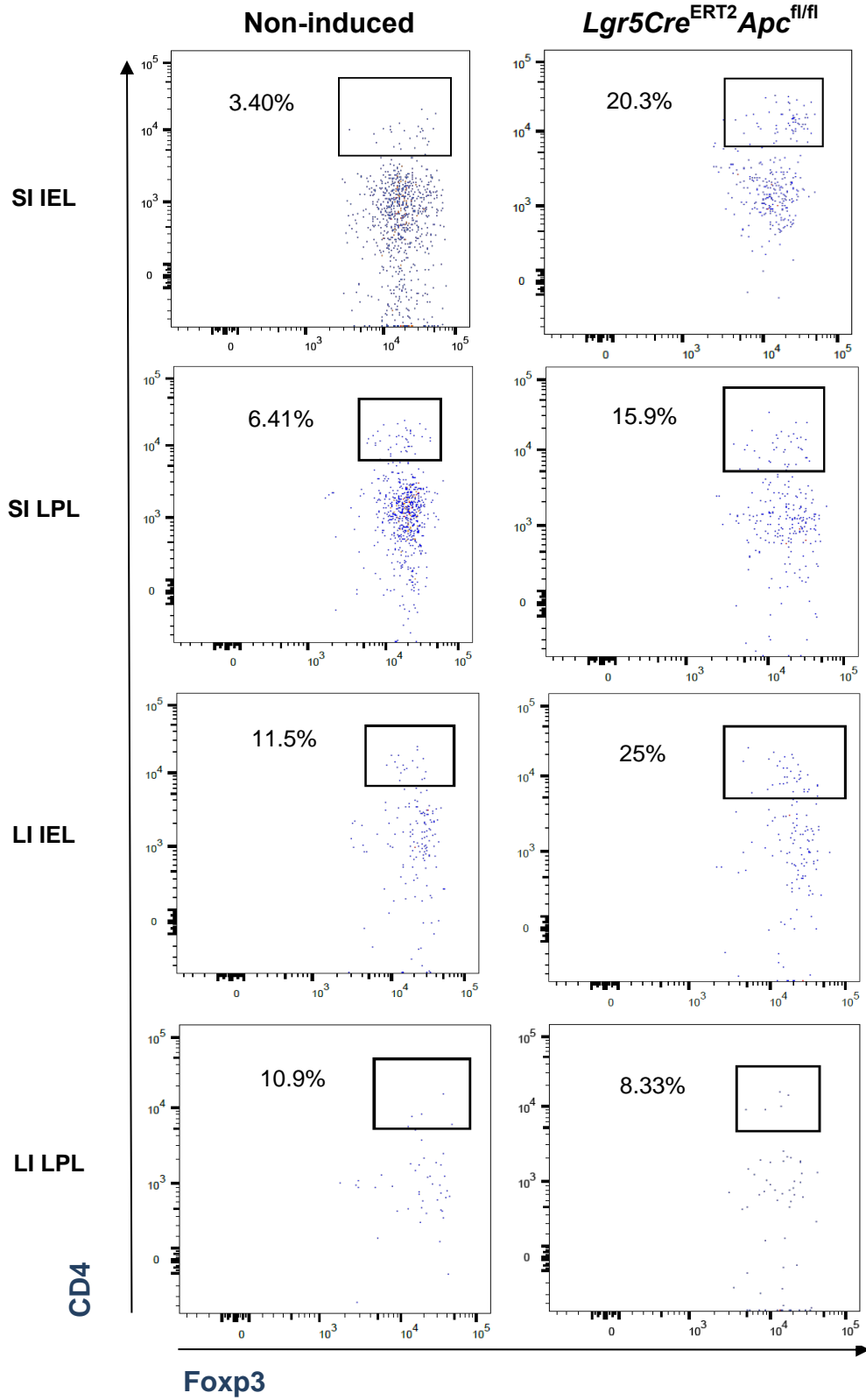


Figure 3.3 Relative gene expression of *Foxp3* in the small intestinal epithelium.

*Apc* deletion significantly upregulates the expression of *Foxp3*. Data represent a single experiment,  $n \geq 3$  mice per group. (\*) P value < 0.05, One-tailed Mann Whitney U test.

A



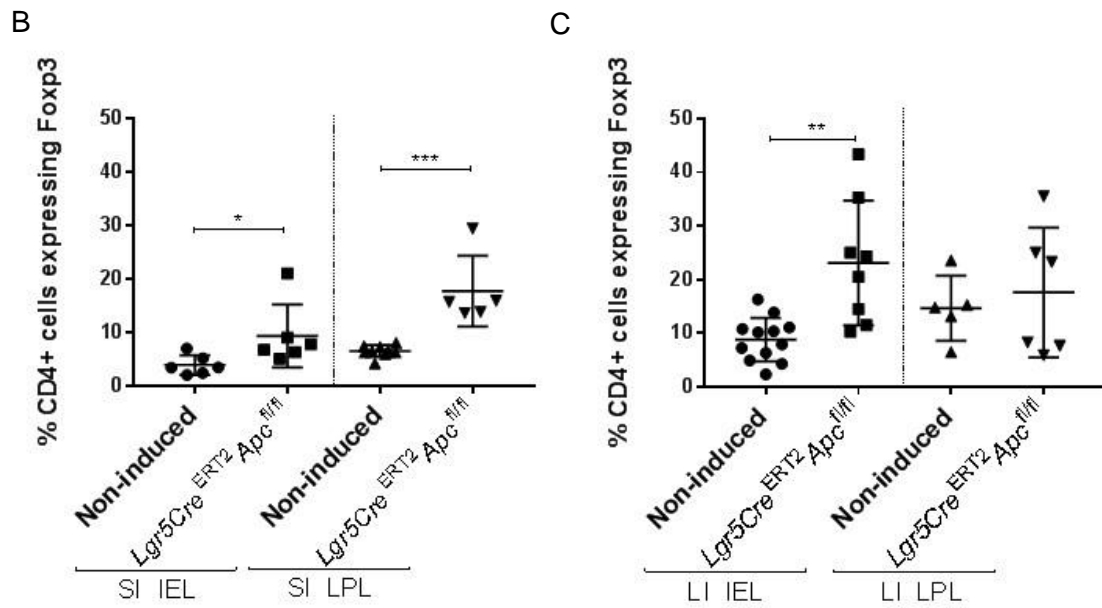


Figure 3.4 Frequency of CD4+ cells expressing Foxp3 in the specified compartments of the small and large intestines.

Representative flow cytometry plots of the frequency of Tregs in the small and large intestines of non-induced and *Lgr5Cre<sup>ERT2</sup>Apc<sup>fl/fl</sup>* mice (A). *Apc* deletion increases significantly the frequency of Foxp3+ cells in SI IEL, SI LPL (B) and LI IEL (C). Data represent a single experiment,  $n \geq 5$  mice per group. (\*) P value  $< 0.05$ , (\*\*) P value  $\leq 0.01$ , (\*\*\*) P value  $\leq 0.001$ , two-tailed Mann Whitney U test.

### 3.2.2.2 Examining the effects of *Apc* deletion in T-cell populations

Previous data showed for the first time that in the *Lgr5Cre<sup>ERT2</sup>Apc<sup>f/f</sup>* mouse model there is an increased number and frequency of Tregs following *Apc* deletion in the ISCs. To analyse further other immune changes caused by *Apc* deletion, it was performed flow cytometry for T-cell activation markers. Cells collected from the spleen, MLN, SI IEL, SI LPL, LI IEL and LI LPL were stained with CD3, CD4, CD8, Granzyme B, Foxp3, IL-17A and IFN $\gamma$  antibodies.

The gating strategy was based in the CD3, a T-cell marker, from which we further analysed the CD4+ and CD8+ T-cell sub-populations.

The frequency of CD3+ cells, was not altered in the compartment examined 15 days after ISC *Apc* deletion; SI (Figure 3.5 A), LI (Figure 3.5 B); spleen or MLN (Figure S 9.2), suggesting that *Apc* deletion does not impact in the total frequency of the T-cell population, however it might be different for each sub-population.

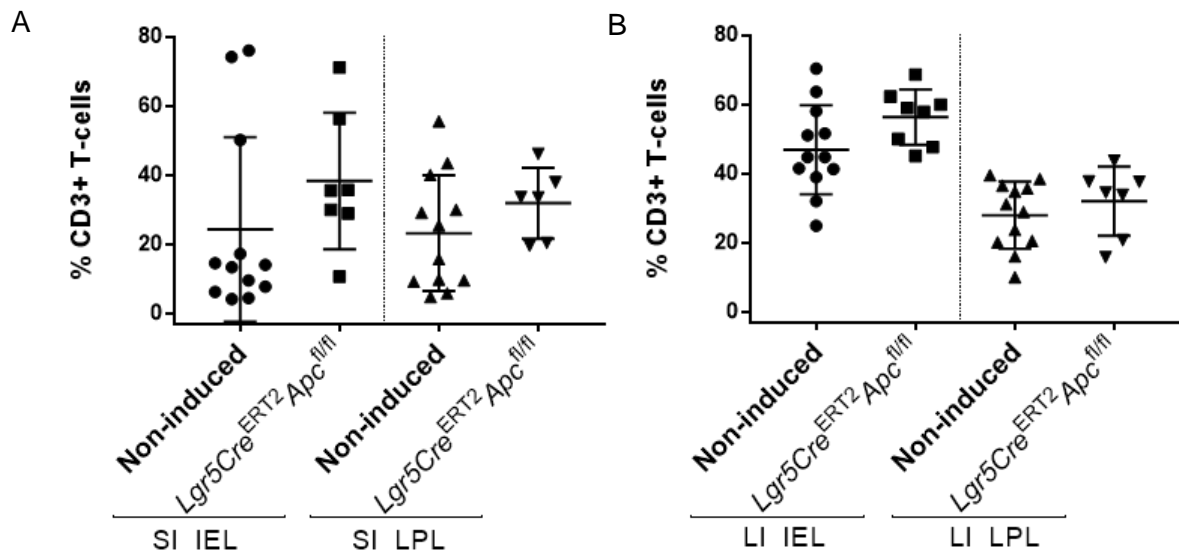


Figure 3.5 Frequency of CD3+ T-cells in the specified compartments of the small and large intestines.

*Apc* deletion does not alter the frequency of CD3+ cells in any of the intestinal compartments (A, B). Data represent a single experiment,  $n \geq 6$  mice per group. Two-tailed Mann Whitney U test.

I next analysed the frequency of CD4+ and CD8+ cells. CD3+CD4+ cells were significantly increased in the SI IEL (Figure 3.6 A) and with no alterations in the SI LPL (Figure 3.6 A) or LI (Figure 3.6 B). There were no significant changes in the spleen (Figure S 9.3), but a decreased CD3+CD4+ cell frequency was observed in the MLN (Figure S 9.3)

For the CD3+CD8+ cells, flow cytometry indicated no significant changes in this population in the SI (Figure 3.6 C), LI (Figure 3.6 D) or spleen (Figure S 9.4). However, in contrast to the CD3+CD4+ cells, they were significantly increased in the MLN (Figure S 9.4). These data imply that ISC *Apc* deletion resulted in induction of a CD4+ cells immune response in the small intestine within 15 days.

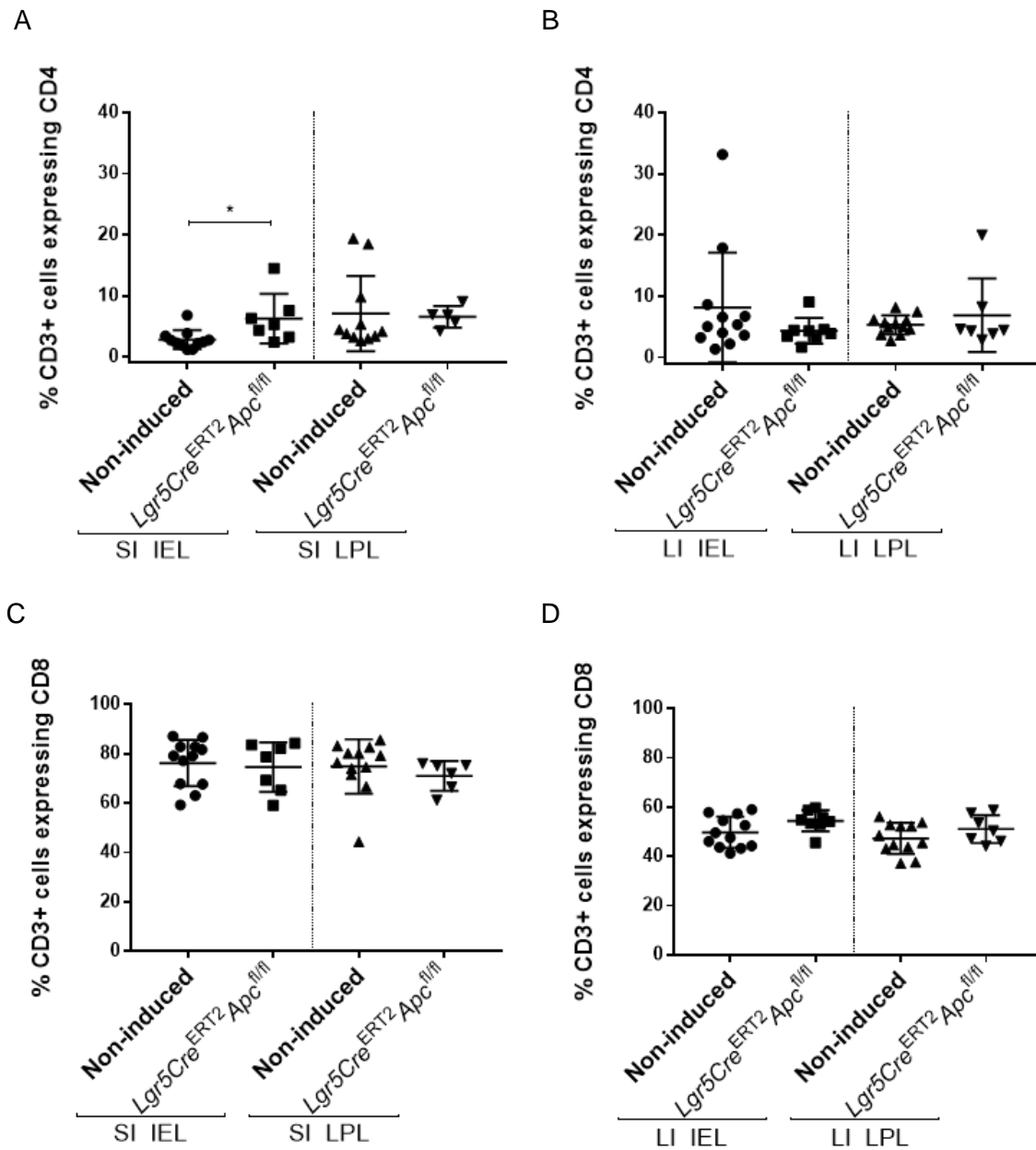


Figure 3.6 Frequency of CD3+ T-cells expressing CD4 and CD8 in the specified compartments of the small and large intestines.

*Apc* deletion resulted in a significantly increased frequency of CD4+ cells, but only in the SI IEL (A). There were no changes in the LI (B). *Apc* deletion didn't alter the frequency of CD8+ cells in both SI and LI (C, D). Data represent a single experiment,  $n \geq 5$  mice per group. (\*) P value < 0.05, two-tailed Mann Whitney U test.

To further characterise this response, I analysed the expression of effector molecules Granzyme B, IL-17A and IFN $\gamma$  which can be expressed by both CD3+CD4+ and CD3+CD8+ cell populations.

The percentage of CD4+ cells producing Granzyme B is not affected in SI (Figure 3.7 A), LI LPL (Figure 3.7 B) or spleen (Figure S 9.5) but significant increases are observed in LI IEL (Figure 3.7 B) and MLN (Figure S 9.5) as a result of *Apc* deletion.

The frequency of Granzyme B produced by CD8+ T-cells is not affected in any of the cell compartments analysed after *Apc* deletion (Figure 3.7 C, D; Figure S 9.6).

These data suggest that Granzyme B does not have an impact in the early stages of intestinal cancer.

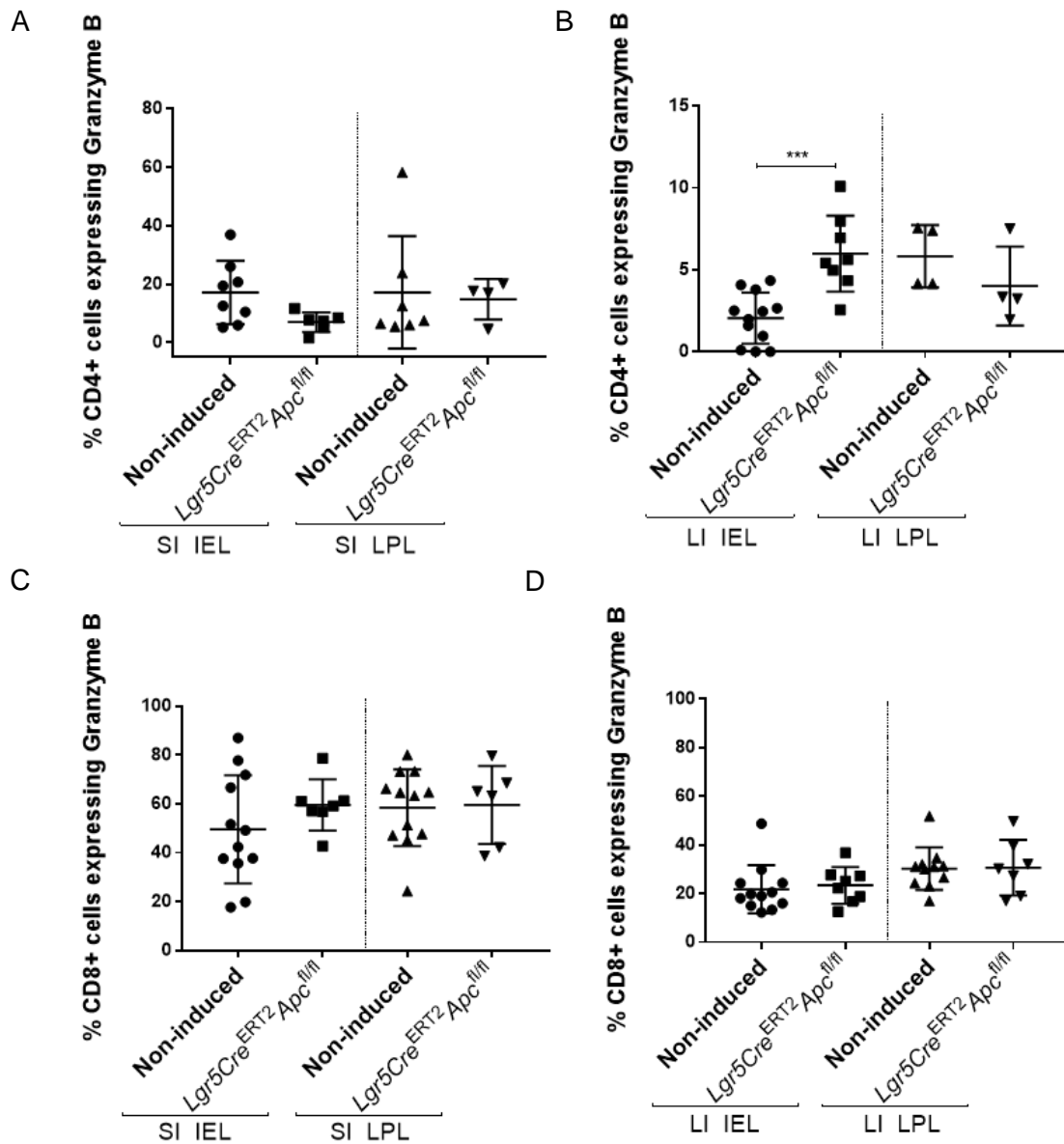


Figure 3.7 Frequency of T-cells expressing Granzyme B in the specified compartments of the small and large intestines.

*Apc* deletion did not alter the frequency of CD4+ cells expressing Granzyme B in the SI (A) but increases significantly in the LI IEL (B). There are no changes in the LI LPL compartment (B). The frequency of CD8+ cells expressing Granzyme B is not affected after *Apc* deletion in both SI (C) and LI (D). Data represent a single experiment,  $n \geq 4$  mice per group. (\*\*\*) P value < 0.001, two-tailed Mann Whitney U test.

IL-17A is an inflammatory cytokine that can be produced by either CD4+ or CD8+ cells, however the phenotype and function of CD8+ cells that are capable of producing IL-17A is poorly understood. There are studies showing that this cytokine plays a key role in the pathogenesis of autoimmune diseases and allergies, but it has been also demonstrated that it can have a protective role in the immunity against pathogens, indicating its controversial roles (Song and Qian 2013).

Here, I show that, following *Apc* deletion, there are no alterations in the frequency of CD4+IL-17A+ cells in SI (Figure 3.8 A), LI (Figure 3.8 B) and MLN (Figure S 9.7), being only increased in the spleen (Figure S 9.7). It is important to note that there is a high variability in the frequencies of IL-17A in both SI and LI.

The frequency of CD8+IL-17A+ cells is not altered in the SI following ISC *Apc* deletion (Figure 3.8 C), LI (Figure 3.8 D), spleen or MLN (Figure S 9.8). These data suggest that IL-17A does not participate the tumourigenesis in the early stages of intestinal cancer.

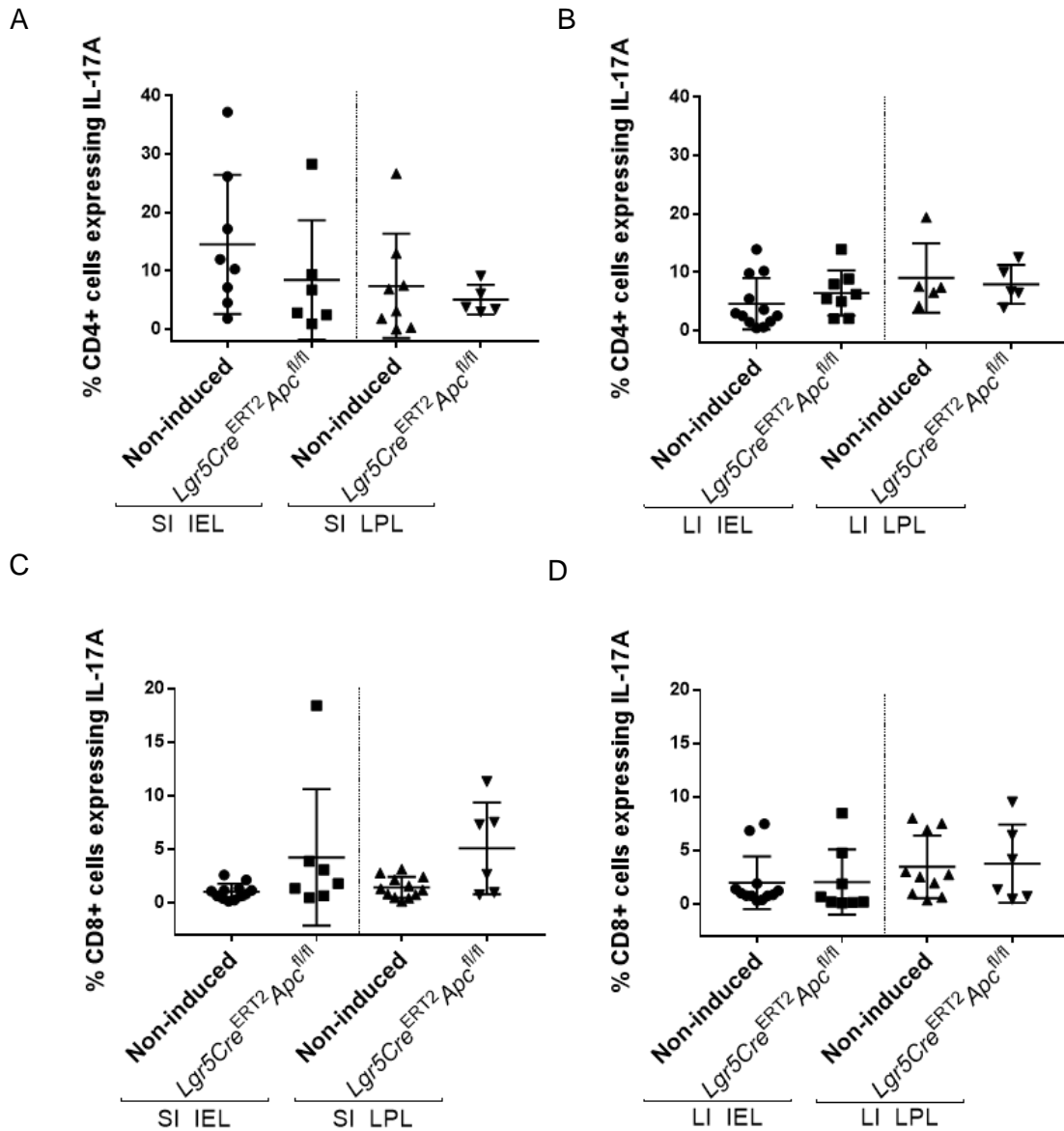


Figure 3.8 Frequency of T-cells expressing IL-17A in the specified compartments of the small and large intestines.

*Apc* deletion did not alter the frequency of CD4+ cells expressing IL-17A in the SI (A) and LI (B). The frequency of CD8+ cells expressing IL-17A is not affected in SI (C) or LI (D). Data represent a single experiment,  $n \geq 5$  mice per group. (\*\*) P value < 0.01, two-tailed Mann Whitney U test.

Interferon gamma (IFN $\gamma$ ) is produced by a variability of immune cells including CD4+ T-cells (Th1), CD8+ T-cells, NK and NKT cells (Schoenborn and Wilson 2007).

The frequency of CD4+IFN $\gamma$ + cells is not altered in SI (Figure 3.9 A), LI (Figure 3.9 B) and MLN (Figure S 9.9), being only increased in the spleen (Figure S 9.9) following *Apc* deletion. Again, it is observed a high variability in the frequencies of IFN $\gamma$  in both SI and LI.

Regarding to CD8+ IFN $\gamma$ + cells frequency, there are no significant changes in the SI (Figure 3.9 C), LI (3.9 D), spleen (Figure S 9.10) or MLN (Figure S 9.10).

Similar to IL-17A, these data suggest that there are no alterations in the secretion of IFN $\gamma$ + following *Apc* deletion, indicating that it does not participate in the early stages tumourigenesis.

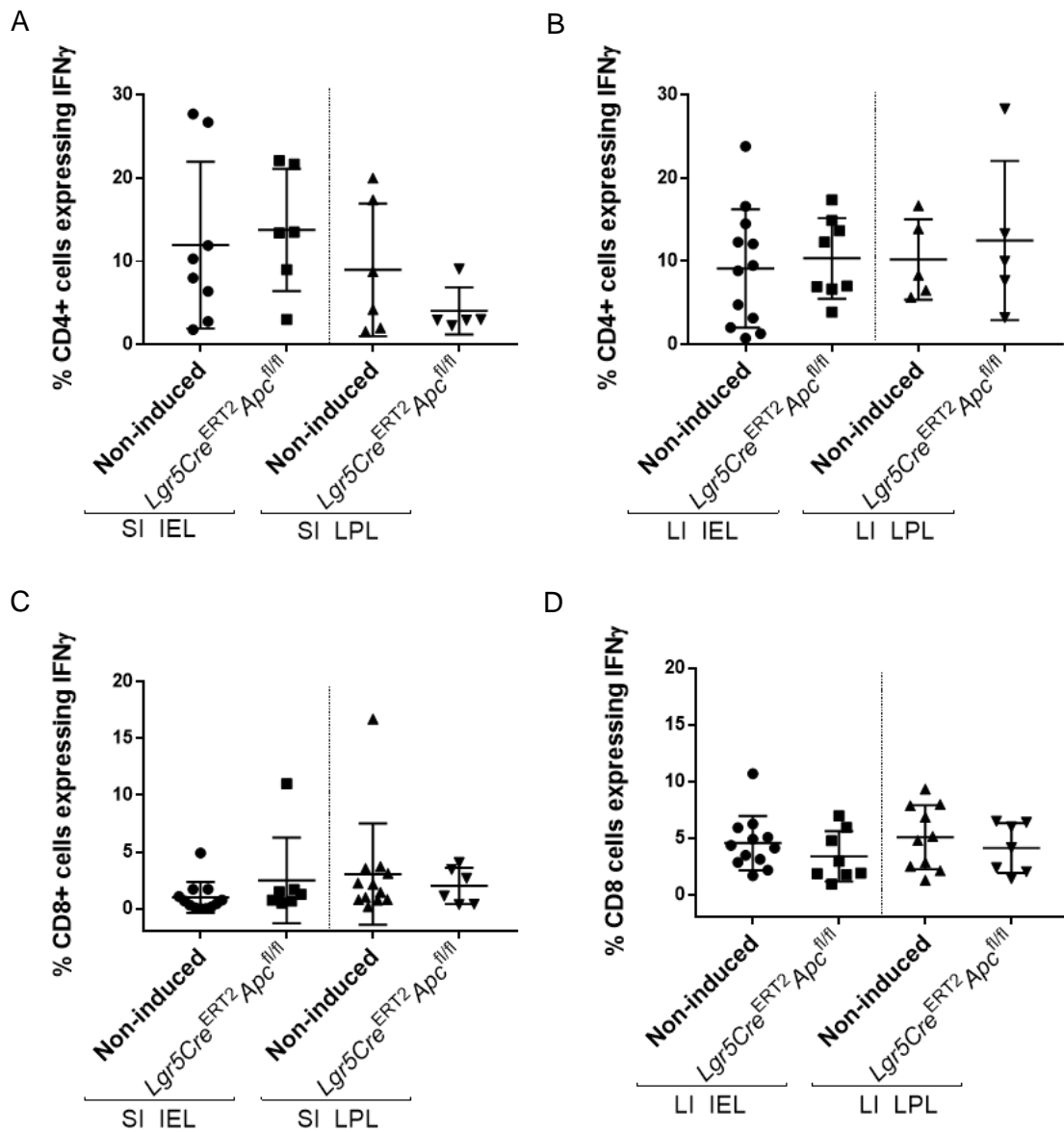


Figure 3.9 Frequency of T-cells expressing IFN $\gamma$  in the specified compartments small and large intestines.

*Apc* deletion did not alter the frequency of CD4+ IFN $\gamma$ + cells (A, B) as well as CD8+ IFN $\gamma$ + cells (C, D) in both SI and LI. Data represent a single experiment,  $n \geq 4$  mice per group. Two-tailed Mann Whitney U test.

### 3.3 Discussion

CRC can arise by various genetic alterations, including the deletion of the *Apc* gene, which is part of the Wnt signalling pathway (Barker et al. 2009). It has been demonstrated that CRC progression also depends on the interaction between the tumour and the immune system (Corthay 2009).

Previous studies have shown that CRC patients have an increased number of Treg cells (Syed Khaja et al. 2017). Some of these studies, including from our group (Clarke et al. 2006; Betts et al. 2012), indicate that an increased number of Tregs is associated with a bad prognosis. However, other studies have suggested the opposite; patients with increased levels of Tregs have a better prognosis (Sinicrope et al. 2009). Importantly, most of these studies were done in patients with advanced disease, however Rubinkiewicz and colleagues have demonstrated that Tregs increased in lymphocytic infiltrate of large intestinal polyps (Rubinkiewicz et al. 2016). Despite the fact that it is known that Tregs play a role in the pathology of intestinal cancer, there is still a need for clarification as to how Tregs actually promote malignant transformation.

In this chapter I aimed to further study how the Tregs were affected in the early stages of intestinal cancer. To do this I started by analysing the number of Tregs in the small intestine of *Apc<sup>min/+</sup>* mice in two groups of age matched mice (60 and 180 d.o.). The *Apc<sup>min/+</sup>* mouse model develop multiple polyps in the intestine that can progress to adenocarcinoma. Mice of different ages gave information about the numbers of Tregs in the early (60 d.o.) and later (180 d.o.) stages of disease progression. I hypothesized that the number of Tregs would be higher in polyps compared to the normal surrounding tissue in both groups of mice. Data showed that, as expected, the number of Tregs is increased in the polyps of 60 d.o. mice relatively to the normal adjacent tissue. Surprisingly, the older mice (180 d.o.) did not have a significant increased number of Tregs in the polyps when compared to the normal adjacent tissue, despite the fact that the area of the polyps in these mice was bigger than those from the 60 d.o. mice. It is possible that the recruitment of Tregs occur primarily in the early stages of the disease and that in later stages there is a stabilization in the number of Tregs recruited. The data obtained is similar to those previously published by other groups, where it was reported an increased number of Tregs in the polyps when compared to normal adjacent tissue (Akeus et al. 2014; Chae and Bothwell 2015); however the data described here show that the significant increase in the number of Tregs occurs only in younger mice, indicating that Tregs may play an important role in very early stages of the disease. As previously described, the *Apc<sup>min/+</sup>* mouse model is a very useful tool to study early stages of intestinal cancer, however the requirement of a second “hit” to remove the WT allele

limits the study of tumour initiation. To overcome this issue, I used a genetically modified mouse model, the *Lgr5Cre<sup>ERT2</sup>Apc<sup>fl/fl</sup>* mouse model, where it is possible to conditionally delete the *Apc* gene in the ISCs in a temporal manner.

It was demonstrated by IHC that, when the intestinal stem cell becomes malignant, there is an increased number of Tregs in both small and large intestines. This was also shown by an increase in the relative gene expression of *Foxp3*. The expression of Foxp3+ was examined by flow cytometry in different cell compartments including lymphocytes extracted from the spleen, MLN, epithelium and lamina propria from the whole small and large intestines (SI IEL, SI LPL, LI IEL and LI LPL respectively). Spleen and MLN were included in the flow cytometry analysis as they provide information about how the systemic response is affected in the different experimental groups. Apart from the LI LPL all the other cell compartments showed an increased frequency of CD4+ cells expressing Foxp3, confirming again the increased levels of Tregs following *Apc* deletion in the ISCs.

To better understand the immune changes following *Apc* deletion, flow cytometry was performed in the previously indicated cell compartments for a panel of T-cell activation markers such as CD3, CD4, CD8, Granzyme B, IL-17A and IFN $\gamma$ .

*Apc* deletion did not alter the frequency of CD3+ cells in any of the compartments studied, suggesting that the total frequency T-cells was not altered, however changes in the frequencies of the CD4+ and CD8+ cells might have occurred. To further analyse this, I then looked at specifically CD4+ and CD8+ cells. These cells are associated with a good prognosis in patients with CRC (Diederichsen *et al.* 2003; Galon *et al.* 2006; Deschoolmeester *et al.* 2011; Shibutani *et al.* 2017). CD4+ T-cells include a range of different sub-populations that participate in the adaptive immune response by enhancing or suppressing the immune response. There were no significant changes in the frequency of CD3+CD4+ cells after *Apc* deletion in the spleen, however there was a significant decrease of CD4+ cells frequency in MLN. In the small intestine there was an increased frequency of CD4+ cells but only in the IEL compartment. There were no significant changes in the frequency of CD4+ cells in the large intestine. The frequency of CD3+CD8+ cells was not altered in most of the cell compartments as a consequence of *Apc* deletion in the ISCs.

Salama and colleagues demonstrated that low expression of Granzyme B in CRC is associated with early metastatic invasion (Salama *et al.* 2011). Other studies have shown that high expression is associated with improved survival (Prizment *et al.* 2017) not only in CRC but other types of cancers such as lung and breast (Kontani *et al.* 2001). In this study, the frequency of CD4+ cells expressing Granzyme B was increased in the

MLN and LI IEL. There were no changes in the other cellular compartments. CD8+ cells expressing Granzyme B had no significant changes following *Apc* deletion.

The proinflammatory IL-17A cytokine has been associated with various immune responses, not only in the pathogenesis of autoimmune diseases, allergic responses, but also tumorigenesis (Song and Qian 2013). Several studies have shown that IL-17A can either promote cancer or have an antitumor role in different cancer models including CRC (Murugaiyan and Saha 2009; Yang *et al.* 2016). In general, data do not show significant changes in the frequency of IL-17A expressed by either CD4+ or CD8+ cells. The only alteration observed, after *Apc* deletion, is in the CD4+ cells expressing IL-17A in the spleen, showing an increased frequency of IL-17A. It was observed a big variability in the frequencies of the mice that were studied making difficult the interpretation of the data.

IFN $\gamma$  is a critical cytokine in innate and adaptive immunity. Various studies have demonstrated that IFN $\gamma$  plays an important antitumor role in CRC (Wang *et al.* 2015a; Katlinski *et al.* 2017; Liu *et al.* 2017). The frequency of CD4+ cells expressing IFN $\gamma$  is only increased in the spleen. It was not observed any alteration in the frequency of CD8+IFN $\gamma$ + cells in any of the cell compartments.

The numbers of Foxp3+ cells were significantly altered in the intestinal compartment 15 days after the initiation of tumorigenesis, implying an important role in the initiation of intestinal cancer. In general, however, our data show very little alterations in the expression of the T-cell activation markers analysed at the same time-point. It is possible that at this early time point, large scale changes in immune activation are not detectable. It is important to note that it was used the whole intestines in the flow cytometry analysis and thus alterations which may occur in distinct locations within the intestine may be missed. Performing other types of analyses, such as IHC and looking at the localization of the immune cells in normal tissue and lesions would most likely give more accurate information regarding the frequency and role of these cells in the early stages of intestinal cancer. The exact mechanism by which Tregs are attracted to the early lesions is still not clarified. Previous research showed that in the early stages of CRC there is the loss of the epithelial barrier, leading to the infiltration of bacteria and microbial products. This infiltration promotes the activation of immune cells that produce the cytokines IL-23 and IL-17, leading to tumour progression (Brenchley and Douek 2012; Goldszmid and Trinchieri 2012) (Yang and Karin 2014). The integrity of the epithelial barrier was not accessed, however future experiments should include this analysis as this could explain the accumulation of Tregs in the early lesions. More recently, Biton and colleagues have shown that ISCs enriched with MHC-II can act as non-conventional antigen-presenting cells. Upon stimulation of these cells with antigens,

they were able to interact with Th cells. Possibly *Apc* deletion in ISCs would promote their antigen-presenting function, being able to attract Tregs to the site of the early lesion (Biton *et al.* 2018). In the future, ISCs *Apc* deleted cells could be sorted by Fluorescent-activated cell sorting (FACS) and their MHC-II expression analysed. Next, the capacity of ISCs *Apc* deleted cells to activate Tregs could be tested *in vitro*.

In summary, in this chapter, it was shown that Tregs increase in number and frequency, following *Apc* deletion in the ISCs, in different cells compartments, particularly in the intestines, indicating a possible impact on cancer development in the intestine. To investigate whether Tregs play a pro- or anti-tumoral role in our mouse model, I considered it important to examine the consequences of their depletion on tumour development. This is detailed in the next chapter.

## 4 Investigating the effects of Treg depletion after loss of *Apc* gene in the ISCs

### 4.1 Introduction

Tregs have been associated with disease progression (Clarke *et al.* 2006; Betts *et al.* 2012; Syed Khaja *et al.* 2017). Previous studies have shown an increased frequency of Tregs in both CRC patients and mouse models of intestinal cancer (Akeus *et al.* 2014; Chae and Bothwell 2015), however the role of these immune cell population in the early stages of intestinal cancer remains unclear. In the previous chapter I showed that Tregs accumulate as soon as 15 days after *Apc* deletion. It was also showed increased frequency of Foxp3+ cells in the spleen, MLN, SI IEL, SI LPL and LI IEL. This correlated with a significant increase in the relative gene expression of *Foxp3* in the epithelial cell compartment of the small intestine.

Other studies have shown that depletion of Tregs in combination with other therapies improved the survival of patients with metastatic CRC (Scurr *et al.* 2017a; Scurr *et al.* 2017b). Studies performed in other mouse models have also shown reduction in the tumour progression by depleting Tregs (Akeus *et al.* 2015; Colbeck *et al.* 2017).

In this chapter I sought to establish the impact of Treg depletion on the pro-tumorigenic aberrant crypts produced by *Apc* deficient ISCs, by characterising the ISCs, target genes of the Wnt pathway and changes to the immune profiles in the early stages of intestinal cancer.

## 4.2 Results

### 4.2.1 Treg cell depletion reduces tumorigenic potential in the *Lgr5Cre<sup>ERT2</sup>Apc<sup>f/f</sup>Foxp3<sup>DTR</sup>* mouse model

#### 4.2.1.1 Total tumour burden

I started by quantifying the number of aberrant crypts in the whole small and large intestines of mice with ISC *Apc* deletion alone or with Treg depletion as well. Mice were either injected with tamoxifen to delete the *Apc* gene (*Lgr5Cre<sup>ERT2</sup>Apc<sup>f/f</sup>*) or with both tamoxifen and diphtheria toxin (DT) to achieve *Apc* deletion and Treg depletion respectively (*Lgr5Cre<sup>ERT2</sup>Apc<sup>f/f</sup>Foxp3<sup>DTR</sup>*). Based on previous experiments, the standard Cre induction regime of a single i.p. dose of tamoxifen for four consecutive days results in extensive *Apc* ISC deletion preventing analysis of single aberrant crypts. To overcome this, I reduced the induction regime to tamoxifen administration for two consecutive days. For experiments requiring concurrent depletion of Tregs, mice were administered DT the day before the first tamoxifen injection and then every other day for the duration of the experiment. Mice were dissected 15 days after the first treatment. For analysis, paraffin embedded tissues were cut into three serial sections of 5  $\mu\text{m}$  separated by 120  $\mu\text{m}$ . Slides were stained with a  $\beta$ -catenin antibody (section 2.6.3) and entire crypts from both small and large intestines which stained positive for nuclear  $\beta$ -catenin staining (aberrant crypts), were counted (section 2.7.1).

The number of aberrant crypts in the small intestine (SI) were reduced, although not significantly, in *Apc* deleted/Treg depleted mice (Figure 4.1 Aii; B) when compared to *Apc* deleted mice (Figure 4.1 Ai; B). In the large intestine (LI) the number of aberrant crypts were significantly reduced in *Apc* deleted/Treg depleted mice (Figure 4.1 Aiii, iv; C). Overall, these data suggest that Tregs may play a pro-tumoral role in the early stages of intestinal cancer, particularly in the LI.

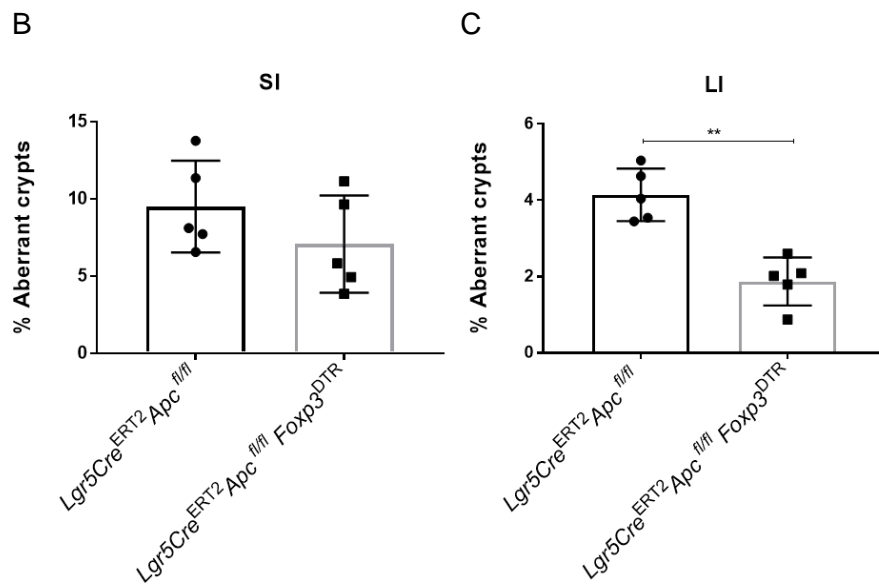
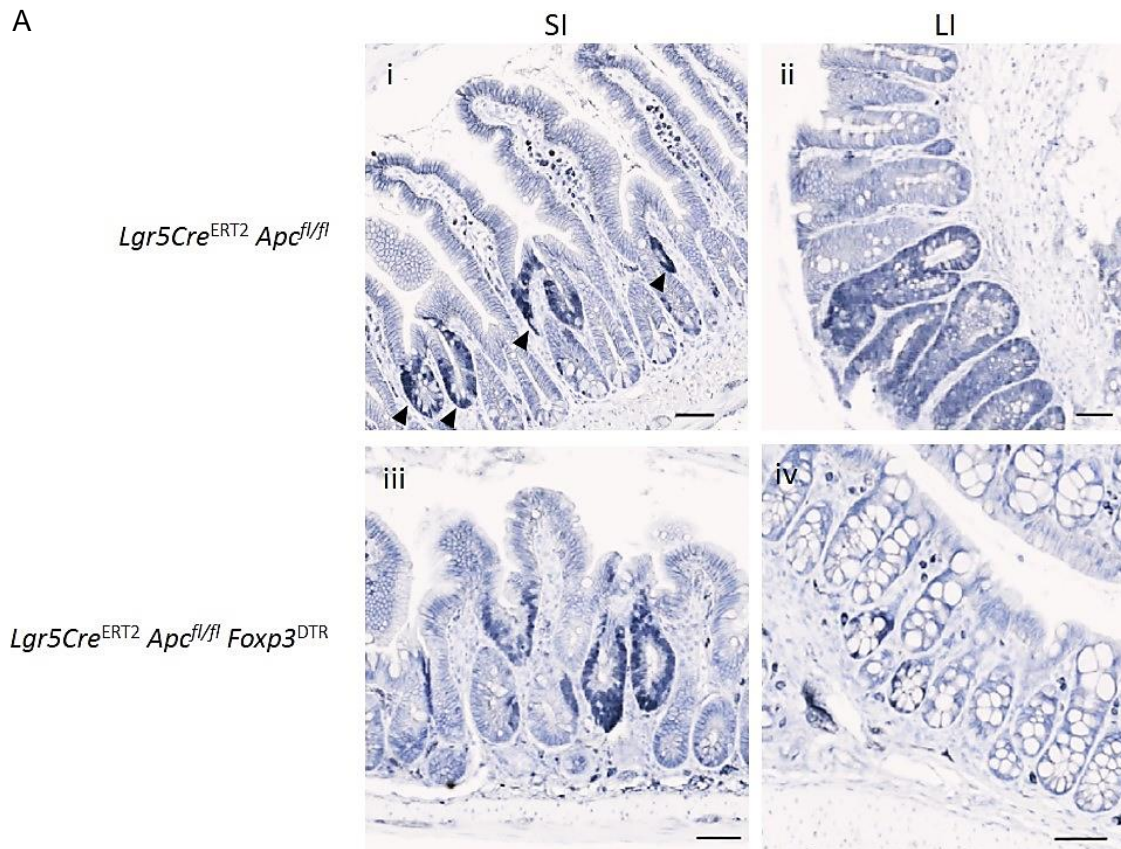


Figure 4.1 Tumour burden analysis in the SI and LI.

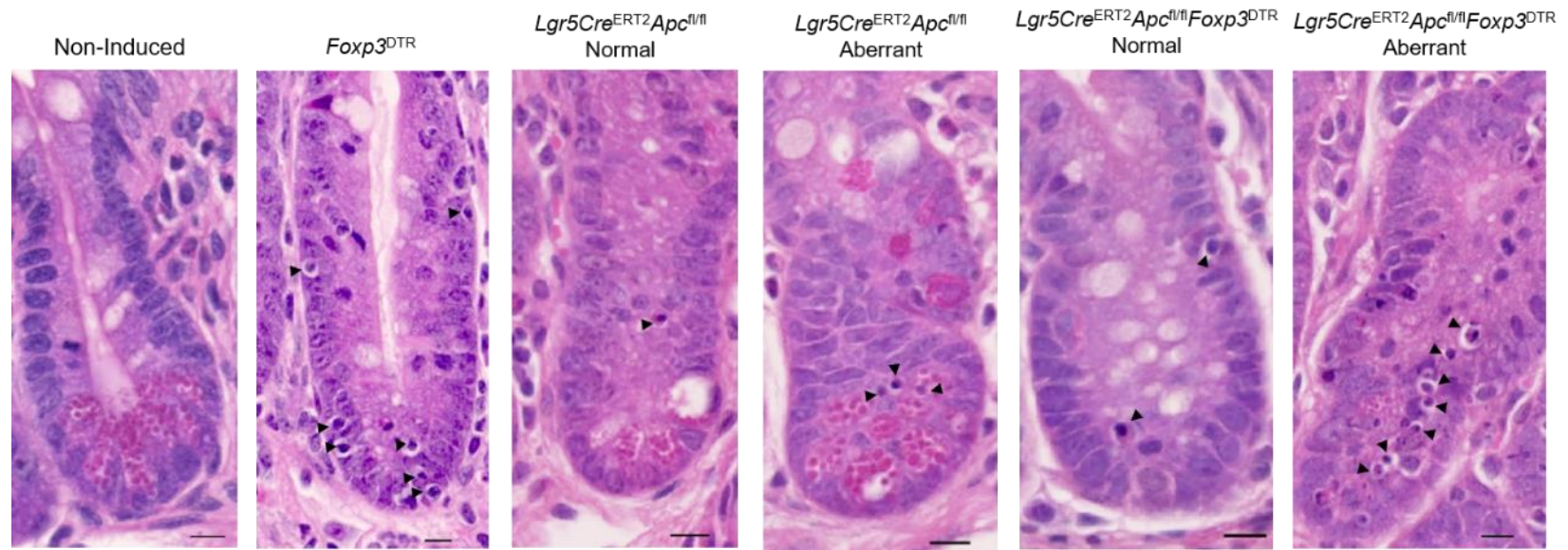
Representative images of B-catenin (grey) IHC staining of SI (i) and LI (ii) from *Apc* deleted mice (*Lgr5Cre<sup>ERT2</sup>Apc<sup>fl/fl</sup>*), SI (iii) and LI (iv) from *Apc* deleted/Treg depleted mice (*Lgr5Cre<sup>ERT2</sup>Apc<sup>fl/fl</sup>Foxp3<sup>DTR</sup>*). Black arrows indicate aberrant crypts. (B) There is a trend for a reduced number of aberrant crypts with *Apc* deletion/Treg cells depletion in the SI. (C) The

number of aberrant crypts is significantly reduced in the LI in *Apc* deleted/Treg depleted mice. Data represent a single experiment, n=5 mice per group. (\*\*) P value  $\leq 0.01$ , two-tailed Mann Whitney U test. Error bars represent Standard Deviation (SD). Scale bars represent 50  $\mu\text{m}$ .

#### 4.2.1.2 *Evaluating the apoptotic index following Apc deletion and Treg depletion*

To understand why Treg depletion in an *Apc* deleted mouse decreased the number of aberrant crypts, I analysed the apoptotic index within the crypts. Slides from the groups that were previously described in the tumour burden analysis were stained with H&E and apoptotic bodies were identified in small intestinal crypts by their morphology such as cell shrinkage, chromatin condensation and the presence of a border and their number was scored per crypt from 25 whole crypts. The average number of mitotic cells was calculated and the mean across the cohorts was determined. Mice with *Apc* deletion/Treg depletion had a significantly increased apoptotic index when compared to non-induced or *Apc* deleted mice. Treg depletion alone had a similar apoptotic index to *Apc* deleted/Treg depleted mice. Interestingly, *Apc* deleted/Treg depleted mice had an increased average number of apoptotic bodies in aberrant crypts when compared to normal crypts, indicating that Treg depletion affected aberrant but not normal crypts (Figure 4.2).

A)



B)

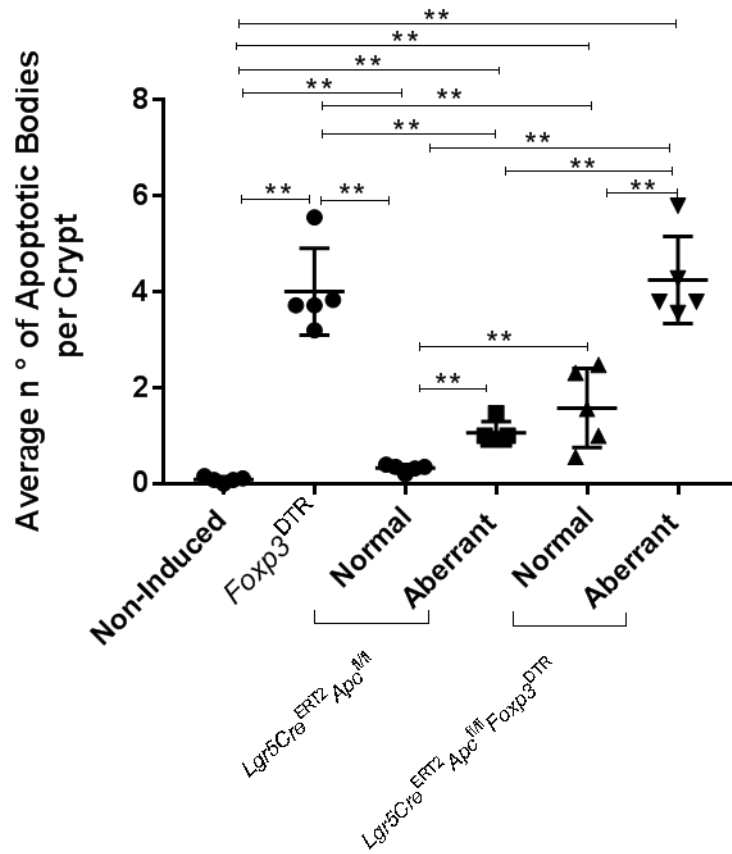


Figure 4.2 Apoptotic index in the small intestinal crypts.

(A) Representative images of H&E from crypts of non-induced, Treg depleted, *Apc* deleted and *Apc* deleted/Treg depleted mice. (B) The average number of apoptotic bodies is significantly increased with *Apc* deletion. As a result of Treg depletion there was an increased number of apoptotic bodies. Aberrant crypts in both *Apc* deleted and *Apc* deleted/Treg depleted mice had a significant higher number of apoptotic bodies when compared to normal adjacent crypts. Data represent a single experiment, n=5 mice per group. (\*\*) P value  $\leq 0.01$ , two-tailed Mann Whitney U test. Scale bars represent 10  $\mu\text{m}$ .

#### 4.2.1.3 Evaluating the gene expression of Wnt and ISC markers following *Apc* deletion and Treg depletion

Deletion of *Apc* leads to constitutive activation of the canonical Wnt signalling pathway perturbing homeostatic control of intestinal epithelia (Sansom *et al.* 2004). Previous data have shown that Treg depletion in *Apc* deleted mice significantly reduced the intestinal tumour burden. To verify whether this reduction was reflected in a reduced activation of the Wnt signalling, gene expression of Wnt markers was analysed in RNA extracted from small intestinal epithelial cells by qRT-PCR (see section 2.8). Relative expression of mRNA was calculated using the  $\Delta\Delta C_t$  method and ACT B was used as an internal control.

As expected, deletion of the *Apc* gene in the mouse ISCs (*Lgr5Cre<sup>ERT2</sup>Apc<sup>fl/fl</sup>*) caused a significant upregulation of the Wnt markers when compared to mice that were not induced with tamoxifen (non-induced) (Figure 4.3). I hypothesised that depleting Tregs in an *Apc* deleted mouse would decrease the expression of Wnt and ISC markers. In this analysis I have included, apart from the previously described groups (Non-induced and *Lgr5Cre<sup>ERT2</sup>Apc<sup>fl/fl</sup>*), two more experimental groups. *Foxp3<sup>DTR</sup>* corresponds to the group of mice that were injected only with DT, every other day for 15 days to deplete Tregs. Looking at the effects of Treg depletion alone would clarify what responses were mainly due to this immune alteration and independent of *Apc* deletion. The other experimental group was the *Lgr5Cre<sup>ERT2</sup>Apc<sup>fl/fl</sup> Foxp3<sup>DTR</sup>* mice that was injected for four consecutive days with tamoxifen, to delete the *Apc* gene as well as with DT every other day for 15 days to deplete Tregs, allowing the analysis of the effects of Treg depletion in the early stages of intestinal cancer. It was observed that Treg depletion alone (*Foxp3<sup>DTR</sup>*) did not alter the expression of Wnt target gene *Axin2* but significantly upregulated *c-Myc* (Figure 4.3). However, the increase in Wnt target gene expression associated with ISC deletion of *Apc* is attenuated, significantly for *Axin2*, in the absence of Treg cells (Figure 4.3). This finding is in keeping with the reduction in the number of aberrant crypts observed in this model.

The aberrant crypts are supported by ISCs. The expression of the ISCs markers *Lgr5*, *Olfm4* and *Ascl2* was analysed to verify whether the reduction of aberrant crypts in *Apc* deleted/Treg depleted mice was reflected in a downregulation of these markers. Both *Lgr5* and *Ascl2* have an increased gene expression after following *Apc* deletion (Figure 4.4). There is a trend for the upregulation of *Olfm4* although it is not significant (Figure 4.4). Treg depletion alone or in combination with ISC *Apc* loss significantly decreased the expression of *Lgr5*, itself a Wnt target, compared to non-induced and *Apc* deleted mice. (Figure 4.4). For the *Apc* deleted/Treg depleted group these changes were

mirrored by the other ISC markers *Olfm4* and *Ascl2* indicating that Tregs play a role in ISC numbers or activity (Figure 4.4).

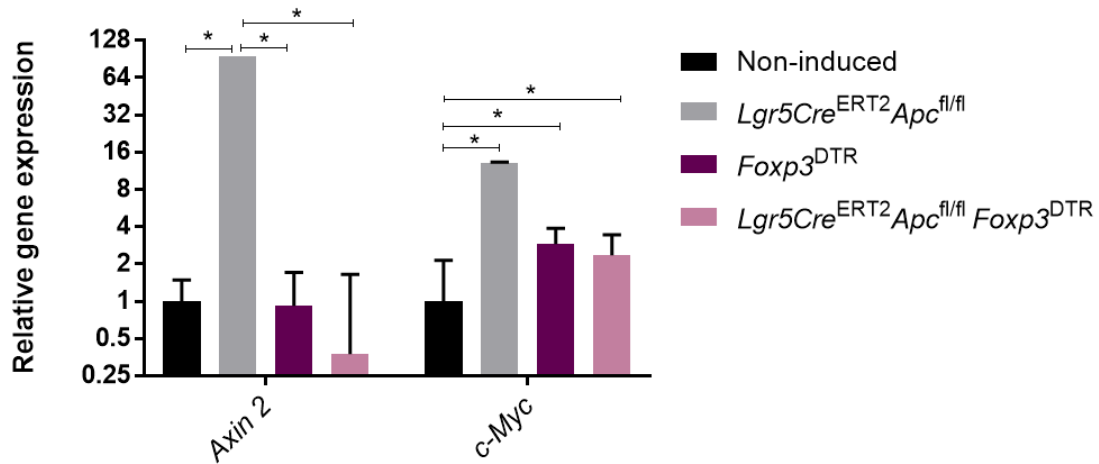


Figure 4.3 Relative gene expression of the Wnt signalling markers *Axin2* and *c-Myc* in the small intestinal epithelium.

*Apc* deletion significantly upregulates the expression of both *c-Myc* and *Axin2* genes. Treg depletion alone did not alter the expression of *Axin2*. The expression of *Axin2* has a trend to decrease, however not significant, with *Apc* deletion and Treg depletion. Treg depletion alone, and together with *Apc* deletion, significantly increases the expression of *c-Myc*. Data represent a single experiment,  $n \geq 3$  mice per group. (\*) P value < 0.05, one-tailed Mann Whitney U test.

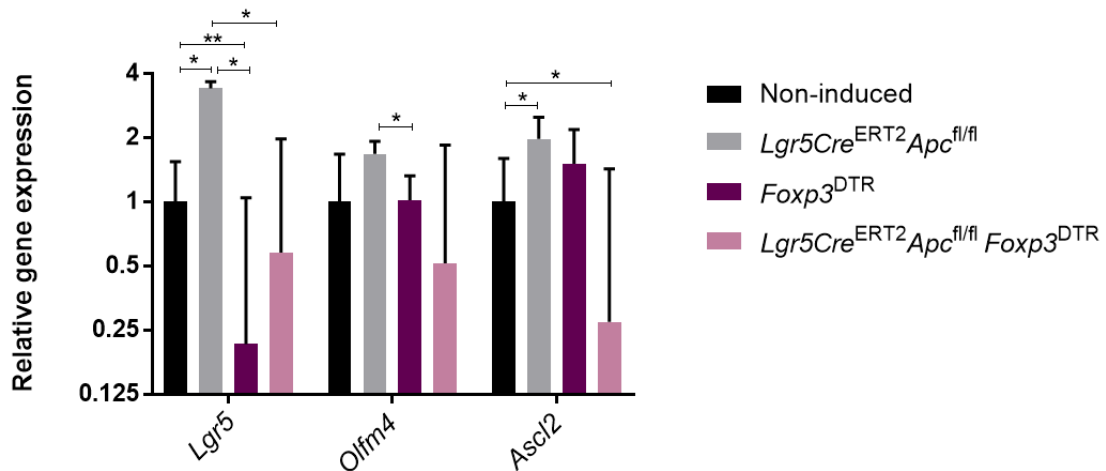


Figure 4.4 Relative gene expression of the ISCs markers *Lgr5*, *Olfm4* and *Ascl2* in the small intestinal epithelium.

*Apc* deletion significantly upregulates the expression of *Lgr5* and *Ascl2* genes. Treg depletion alone resulted in decreased the expression of *Lgr5* when compared to non-induced and *Apc*

deleted mice. The expression of *Olfm4* was decreased with Treg depletion, but not *Asc2*. *Apc* deletion and Treg depletion resulted in decreased the expression of the three ISC markers. Data represent a single experiment,  $n \geq 3$  mice per group. (\*) P value < 0.05, (\*\*) P value  $\leq 0.01$ , one-tailed Mann Whitney U test.

#### 4.2.1.4 Evaluating the gene expression of *Foxp3* and *IFN $\gamma$*

To begin to understand the role of the immune system cells in this phenotype I analysed the expression of *Foxp3*, a transcriptional factor expressed by Tregs, and *IFN $\gamma$*  by qRT-PCR as previously explained. It was shown in the previous chapter that *Apc* deletion resulted in a significant increased gene expression of *Foxp3*. Contrary to what was expected, Treg depletion alone did not result in a downregulation of *Foxp3* (Figure 4.5). Treg depletion in *Apc* deleted mice, as expected, resulted in a significant downregulation of *Foxp3* (Figure 4.5). In keeping with the ability of Tregs to prevent an anti-tumour immune response, the significant increase in expression *IFN $\gamma$*  observed in *Apc* deficient mice was further up regulated in the absence of Tregs, suggesting another beneficial effect of Treg depletion in the early stages of intestinal cancer (Figure 4.5).

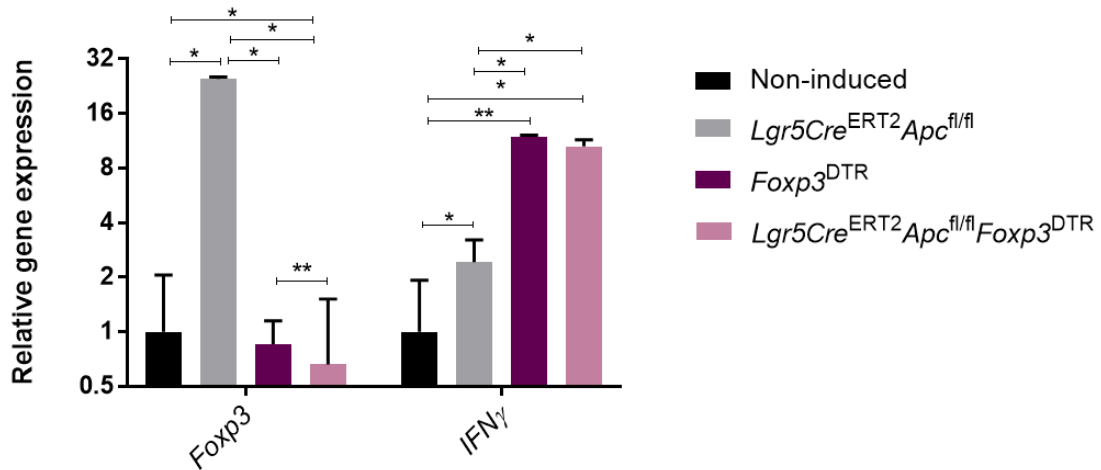


Figure 4.5 Relative gene expression of *Foxp3* and *IFN* $\gamma$  in the small intestinal epithelium.

*Apc* deletion significantly upregulates the expression of *Foxp3* and *IFN* $\gamma$ . Treatment with DT alone did not alter significantly the expression of *Foxp3*, however *Apc* deleted/Treg depleted mice had a significantly reduced expression of *Foxp3*. Relative gene expression of *IFN* $\gamma$  increased significantly after Treg depletion, alone and in combination with *Apc* deletion. *Foxp3* gene expression data for the non-induced and *Lgr5Cre*<sup>ERT2</sup>*Apc*<sup>fl/fl</sup> groups is repeated in figure 3.3. Data represent a single experiment, n  $\geq$  3 mice per group. (\*) P value < 0.05, (\*\*) P value  $\leq$  0.01, one-tailed Mann Whitney U test.

#### 4.2.2 Examining the effects of Treg depletion on T-cell populations in the early stages of intestinal cancer

In the previous chapter I have analysed the effects of ISCs *Apc* deletion in T-cell populations and cytokine markers. To understand whether the reduction in the intestinal tumour burden, following Treg depletion, was a result of an unleashed immune response, the previously described T-cell activation markers were analysed once again.

The frequency of CD3<sup>+</sup> cells was significantly increased in the SI IEL (Figure 4.6 A), LI IEL (Figure 4.6 B) and spleen (Figure S 9.2) following *Apc* deletion/Treg cells depletion. There were no significant changes in the LPL compartment of both SI (Figure 4.6 A) and LI (Figure 4.6 B) as well as MLN (Figure S 9.2).

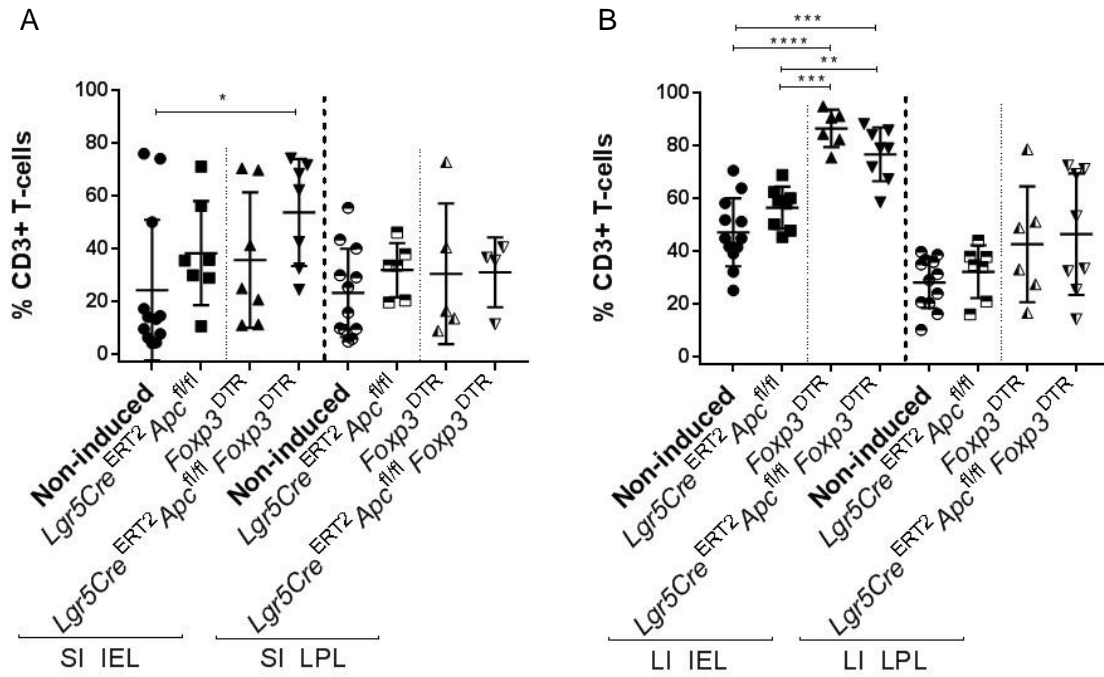


Figure 4.6 Frequency of CD3+ T-cells in the specified compartments of SI and LI following Treg cells depletion.

In the SI IEL only *Apc* deletion/Treg depletion increased the frequency of CD3+ cells. There were no significant changes in the SI LPL (A). In the LI IEL both Treg depletion and *Apc* deletion/Treg depletion resulted in an increased frequency of CD3+ cells. A trend for an increased frequency of CD3+ cells in the LI LPL was observed following Treg depletion and *Apc* deletion/Treg depletion (B). Data represent a single experiment,  $n \geq 4$  mice per group. Data for the non-induced and *Lgr5Cre*<sup>ERT2</sup>*Apc*<sup>fl/fl</sup> groups are repeated in figure 3.5. (\*) P value < 0.05, (\*\*) P value  $\leq 0.01$ , (\*\*\*) P value  $\leq 0.001$ , (\*\*\*\*) P value  $\leq 0.0001$ , two-tailed Mann Whitney U test.

Treg depletion alone or in combination with *Apc* deletion resulted in a significantly increased frequency of CD4+ cells in the SI IEL and LI (Figure 4.7). In the SI LPL, only Treg depletion resulted in a significantly increased frequency of CD4+ cells (Figure 4.7).

The effect of Treg depletion on the CD4+ T-cells is lost in the *Apc* deleted/Treg depleted mice, indicating that in the presence of *Apc* deleted intestinal cells activation of CD4+ naive cells, or their accumulation within the SI LPL, due to Treg depletion, is inhibited (Figure 4.7 A). Within the spleen and MLN there is a significant decreased in the frequency of CD4+ cells in the absence of Treg cells (Figure S 9.3). These data suggest that only in the intestines, Treg depletion allow the expansion of other sub-populations of CD4+ T-cells, such as Th1 cells, that may participate in the anti-tumour immune response.

The frequency of CD8+ cells is not altered in the SI IEL compartment; however, it is significantly decreased in the SI LPL, following Treg depletion (Figure 4.7 C). In contrast to SI, the frequency of CD3+CD8+ is significantly increased in the LI (Figure 4.7 D) and MLN (Figure S 9.4) in the absence of Treg cells as well as *Apc* deleted/Treg depleted mice. In the spleen the frequency of CD8+ cells is only significantly increased as a result of *Apc* deletion/Treg cells depletion (Figure S 9.4). These data suggest that Treg depletion unleashed an immune response by CD8+ cells, particularly in the LI compartment, possibly explaining the significantly reduced tumour burden observed in the LI.

Treg depletion was confirmed in SI (Figure 4.8 A), LI (Figure 4.8 B), spleen and MLN (Figure S 9.1) by the significant decreased frequency of CD4+ cells expressing Foxp3.

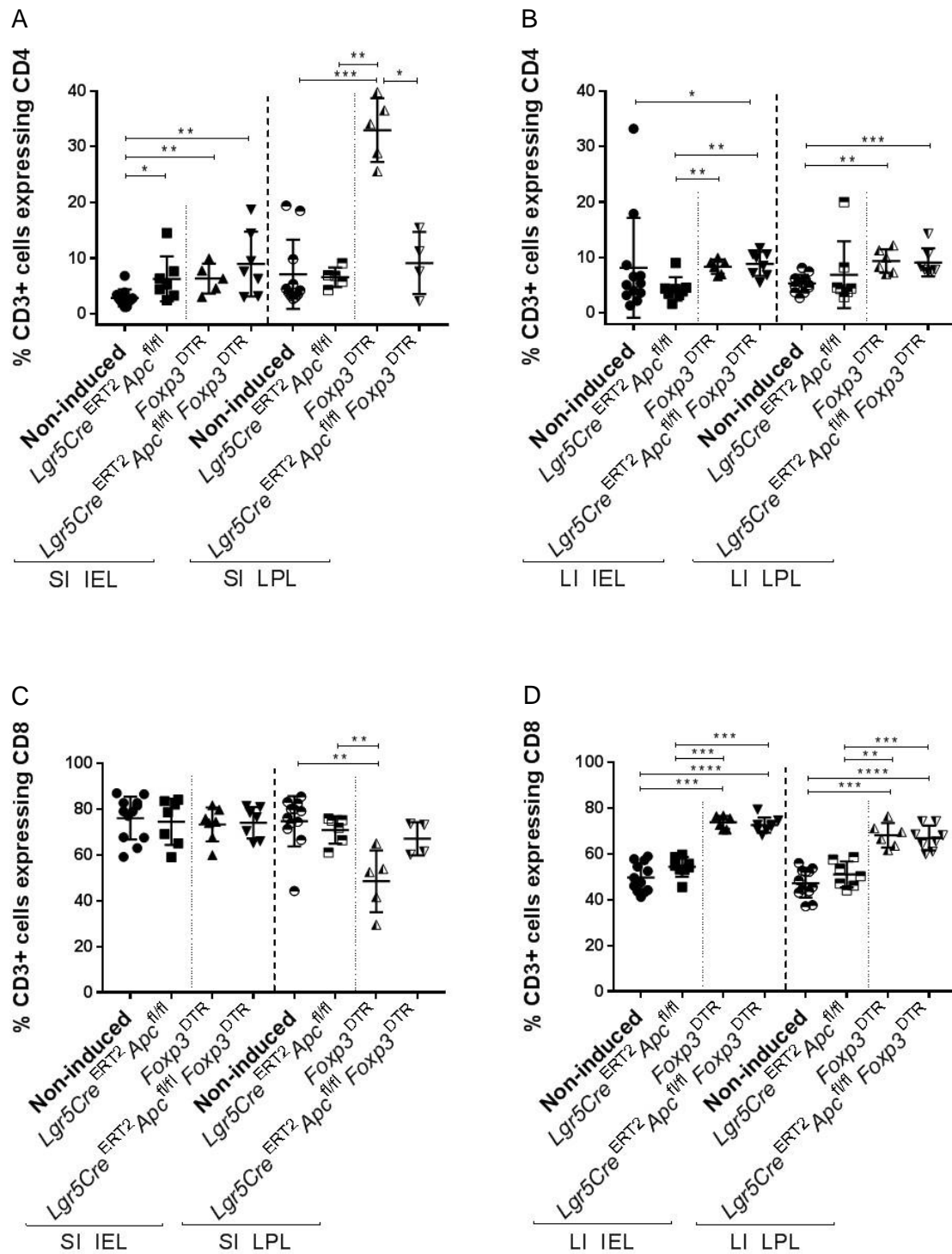


Figure 4.7 Frequency of CD3+ T-cells expressing CD4+ and CD8+ in the specified compartments of SI and LI following Treg cells depletion.

(A) The frequency of CD3 expressing CD4+ cells is significantly increased with both Treg depletion and *Apc* deletion/Treg depletion in the SI IEL. In the SI LPL only Treg depletion results in an increase in the frequency of CD4+ cells. (B) In the LI, both Treg depletion and *Apc* deletion/Treg

cells depletion results in an increase in the frequency of CD4+ cells. (C) The frequency of CD3+ cells expressing CD8 is only altered in the SI LPL where it is decreased following Treg depletion. (D) In the LI Treg depletion and *Apc* deletion/Treg depletion result in a significant increase in the frequency of CD8+ cells. Data represent a single experiment, n ≥ 4 mice per group. Data for the non-induced and *Lgr5Cre<sup>ERT2</sup>Apc<sup>fl/fl</sup>* groups are repeated in figure 3.6. (\*) P value < 0.05, (\*\*) P value ≤ 0.01, (\*\*\*) P value ≤ 0.001, (\*\*\*\*) P value ≤ 0.0001, two-tailed Mann Whitney U test.

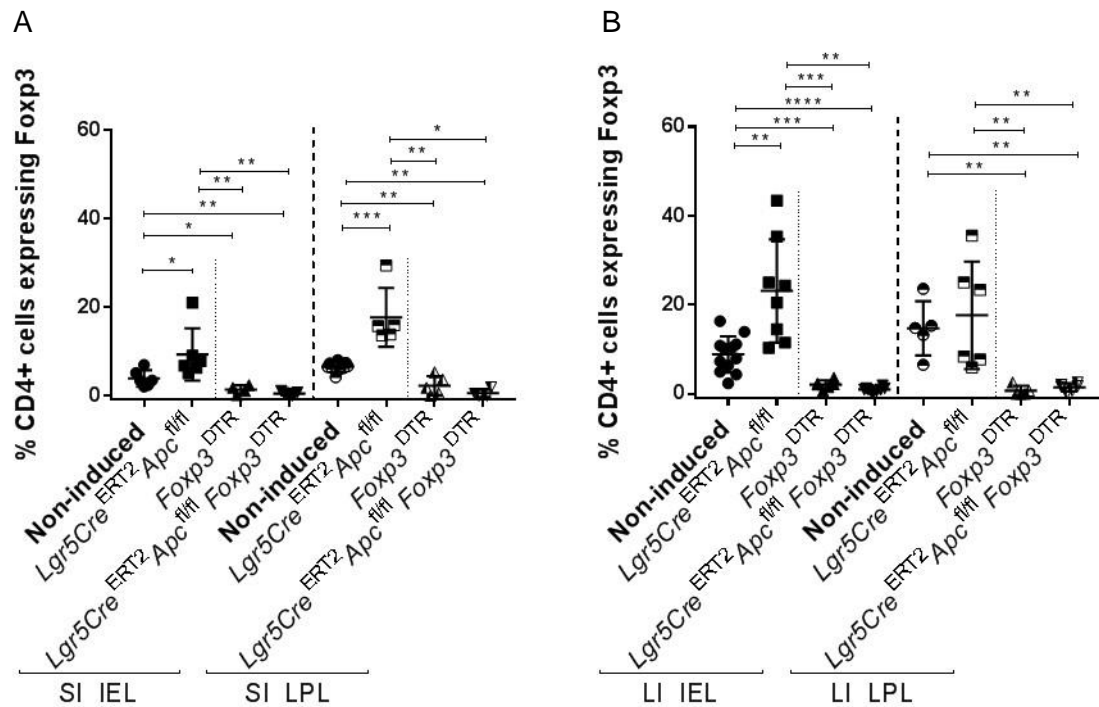


Figure 4.8 Frequency of CD4+ cells expressing Foxp3 in the specified compartments of SI and LI following Treg cells depletion.

(A) The frequency of CD4+ cells expressing Foxp3, as expected, is significantly reduced in the SI following DT treatment. (B) The same is observed in the LI where a reduced frequency of Foxp3+ cells is observed. Data represent a single experiment,  $n \geq 4$  mice per group. Data for the non-induced and *Lgr5Cre<sup>ERT2</sup>Apc<sup>fl/fl</sup>* groups are repeated in figure 3.4. (\*) P value  $< 0.05$ , (\*\*) P value  $\leq 0.01$ , (\*\*\*) P value  $\leq 0.001$ , (\*\*\*\*) P value  $\leq 0.0001$ , two-tailed Mann Whitney U test.

No differences were observed in the frequency of CD4+Granzyme B+ cells in the SI following Treg depletion or *Apc* deletion/Treg depletion when compared to non-induced mice (Figure 4.9 A). In the LI (Figure 4.9), spleen and MLN (Figure S 9.5) particularly Treg depletion alone resulted in a significantly increased frequency of CD4+Granzyme+ cells. This effect was significantly attenuated in *Apc* deleted/Treg depleted mice suggesting that these cells do not participate in the anti-tumour immune response in the early stages of intestinal cancer.

The frequency of CD8+Granzyme B+ cells is significantly increased in the SI IEL following *Apc* deletion/Treg depletion (Figure 4.9 C). There were no significant changes in the SI LPL, however the large spread in the data make a definitive conclusion difficult (Figure 4.9 C). In the LI (Figure 4.9 D), spleen and MLN (Figure S 9.6) an increased frequency of CD8+Granzyme B+ cells in both Treg depleted and *Apc*/Treg cells depleted group was observed, suggesting that Granzyme B secreted by CD8+ cells may have a role in the anti-tumour immune response.

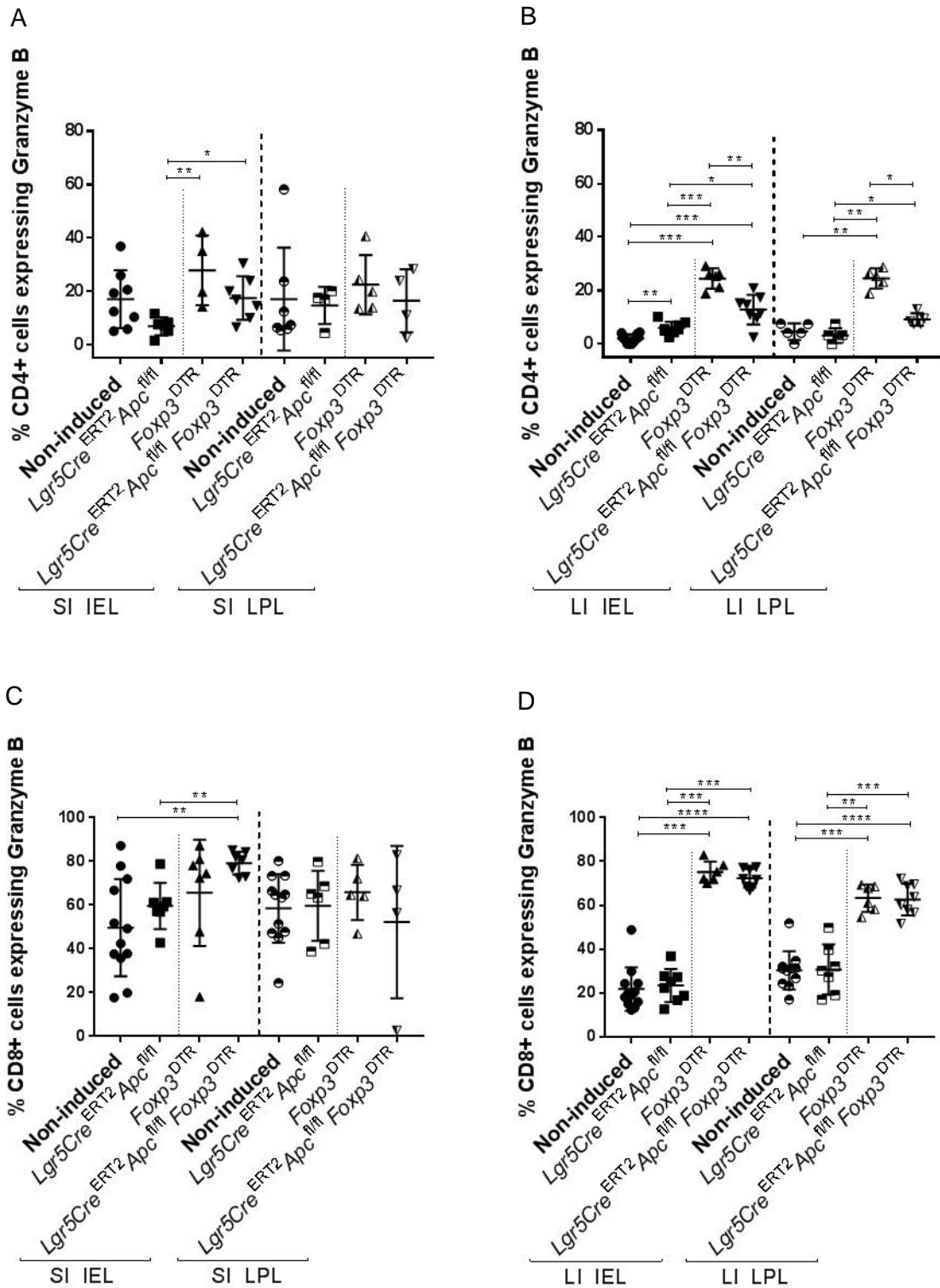


Figure 4.9 Frequency of CD4+ and CD8+ cells expressing Granzyme B in the specified compartments of SI and LI following Treg cells depletion.

(A) The frequency of CD4+ cells expressing Granzyme B was not altered in the SI following Treg depletion or Apc deletion/Treg depletion when compared to non-induced mice. (B) In the LI there

was an increased frequency of CD4+ cells expressing Granzyme B, especially following Treg depletion, as well as *Apc* deletion/Treg depletion. (C) The frequency of CD8+ cells expressing Granzyme B was increased following *Apc* deletion/Treg depletion in the SI IEL. There were no significant changes in the SI LPL. (D) In the LI both Treg depleted and *Apc* deleted/Treg depleted mice have an increased frequency of CD8+ cells expressing Granzyme B. Data represent a single experiment,  $n \geq 4$  mice per group. Data for the non-induced and *Lgr5Cre<sup>ERT2</sup>Apc<sup>fl/fl</sup>* groups are repeated in figure 3.7. (\*) P value  $< 0.05$ , (\*\*) P value  $\leq 0.01$ , (\*\*\*) P value  $\leq 0.001$ , (\*\*\*\*) P value  $\leq 0.0001$ , two-tailed Mann Whitney U test.

There were no significant alterations in the frequency of CD4+IL-17A+ cells in both SI (Figure 4.10 A) and LI (Figure 4.10 B) in any of the experimental groups. Contrary to the intestines, CD4+IL-17A cell frequency was significantly increased in both spleen and MLN (Figure S 9.7) particularly in Treg depleted and *Apc* deleted/Treg depleted mice, suggesting that a systemic immune response that is not mirrored in the intestine, thereby implying that this cytokine does not participate in initiation of intestinal cancer and/or in the anti-tumour immune response.

The frequency of CD8+IL-17A+ cells was significantly increased in the SI in *Apc* deleted/Treg depleted mice (Figure 4.10 C). In the LI IEL, only Treg depletion resulted in an increase in the frequency of IL-17A, with no alterations in the LPL compartment (Figure 4.10 D). Similar to CD4+IL-17A+ cells, the frequency of CD8+IL-17A+ cells was significantly increased in the spleen and MLN (Figure S 9.8) with both Treg depletion and *Apc* deletion/Treg depletion, however in both situations the frequency of IL-17A was very low, suggesting again that IL-17A does not have an important role in the early stages of intestinal cancer.

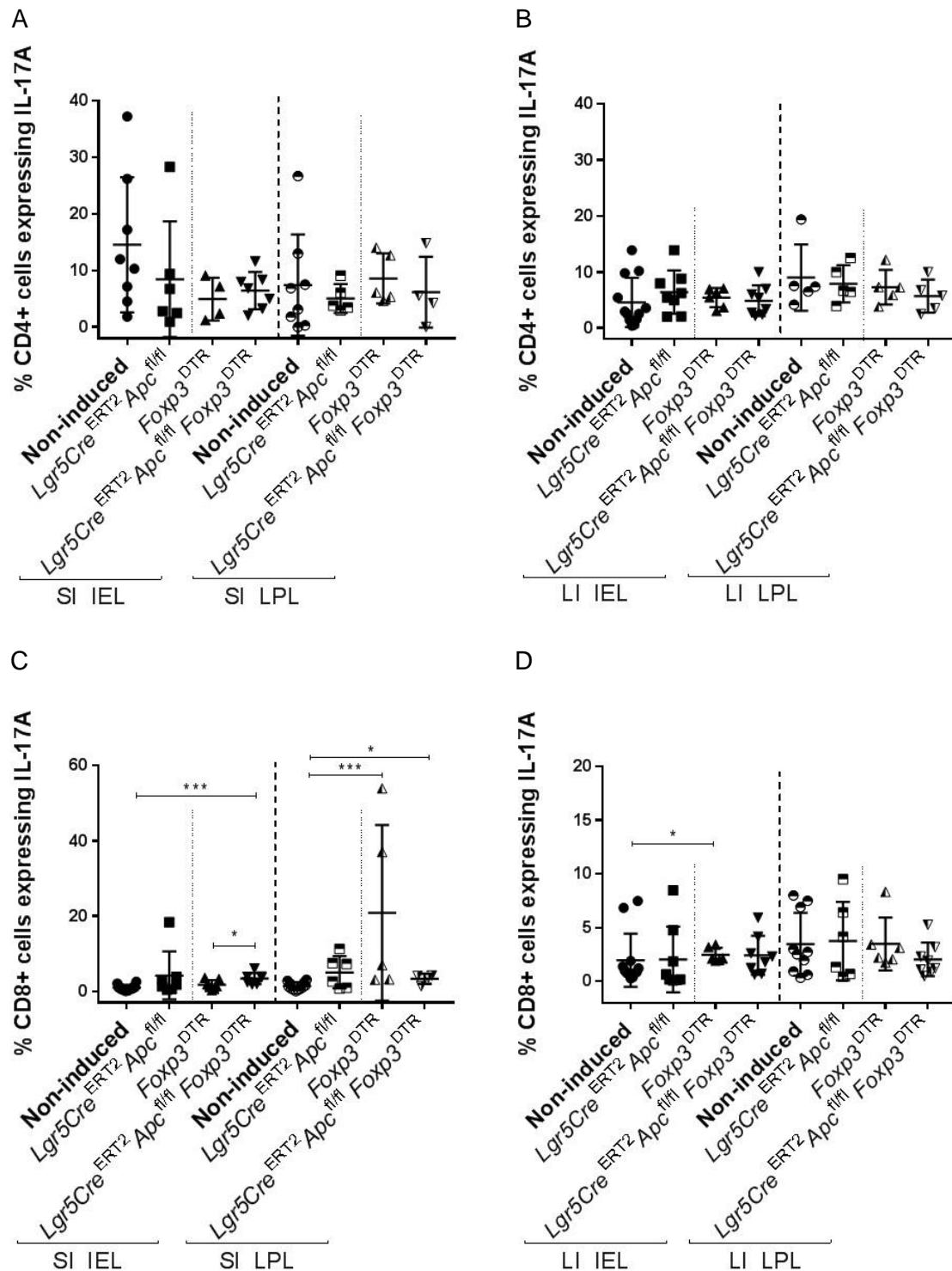


Figure 4.10 Frequency of CD4+ and CD8+ cells expressing IL-17A in the specified compartments of SI and LI following Treg depletion.

(A), (B) There were no significant changes in the frequency of CD4+ cells expressing IL-17A in both SI and LI. (C) The frequency of CD8+ cells expressing IL-17A was significantly increased in Apc deleted/Treg depleted mice. In the SI LPL, CD8+IL-17A+ cells frequency was significantly

increased in Treg depleted and *Apc* deleted/Treg depleted mice. (D) The frequency of CD8+ cells expressing IL-17A was significantly increased in *Apc* deleted/Treg depleted, but particularly in Treg depleted mice. Data represent a single experiment done,  $n \geq 4$  mice per group. Data for the non-induced and *Lgr5Cre<sup>ERT2</sup>Apc<sup>fl/fl</sup>* groups are repeated in figure 3.8. (\*) P value < 0.05, (\*\*\*) P value  $\leq 0.001$ , two-tailed Mann Whitney U test.

Finally, I analysed the frequency of IFN $\gamma$  in the different cell compartments. The frequency of CD4+IFN $\gamma$ + cells was significantly increased in the SI LPL (Figure 4.11 A), LI (4.11 B), spleen and MLN (Figure S 9.9) following Treg depletion. The effect of Treg depletion was attenuated in *Apc* deleted/Treg depleted mice, however it was still significantly increased in LI (4.11 B), spleen and MLN (Figure S 9.9) when compared to non-induced and *Apc* deleted mice.

Treg depletion significantly increased the frequency of CD8+IFN $\gamma$ + cells in SI (Figure 4.11 C), LI (Figure 4.11 D), spleen and MLN (Figure S 9.10). Again, we observed an attenuation of the effect of Treg depletion in *Apc* deleted mice, particularly in the SI LPL (Figure 4.11 C) and LI (Figure 4.11 D), suggesting that CD8+IFN $\gamma$ + cells may have an important role in the anti-tumour immune response in the early stages of intestinal cancer.

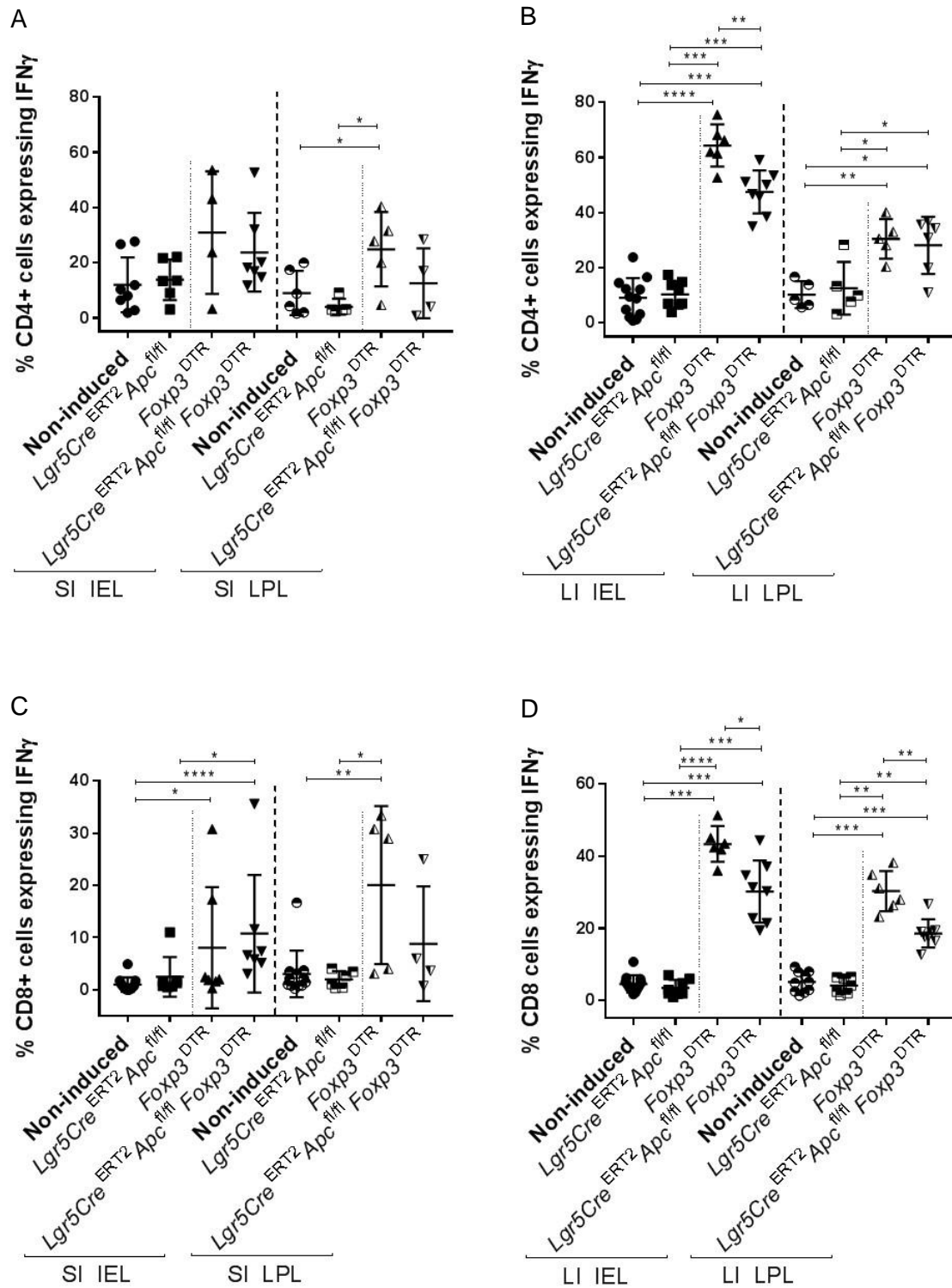


Figure 4.11 Frequency of CD4+ and CD8+ cells expressing IFN $\gamma$  in the specified compartments of SI and LI following Treg depletion.

(A) Treg depletion did not alter the frequency of CD4+ cells expressing IFN $\gamma$  in the SI IEL. There is an increased frequency of IFN $\gamma$  in the SI LPL in Treg depleted mice. (B) Both Treg depletion and *Apc* deletion/Treg cells depletion increased the frequency of CD4+ cells expressing IFN $\gamma$ . (C) The frequency of CD8+ cells expressing IFN $\gamma$  is increased particularly with *Apc* deletion/Treg

depletion in the SI IEL. In the SI LPL Treg depletion showed increased frequency of IFN $\gamma$ . (D) In the LI both Treg cells depleted and Apc deleted/Treg depleted mice had increased frequency of CD8+ cells expressing IFN $\gamma$ . Data represent a single experiment, n  $\geq$  4 mice per group. Data for the non-induced and *Lgr5Cre<sup>ERT2</sup>Apc<sup>fl/fl</sup>* groups are repeated in figure 3.9. (\*) P value < 0.05, (\*\*) P value  $\leq$  0.01, (\*\*\*) P value  $\leq$  0.001, (\*\*\*\*) P value  $\leq$  0.0001, two-tailed Mann Whitney U test.

### 4.3 Discussion

Treg cells play an important role in maintaining peripheral tolerance and preventing autoimmunity. Studies have shown that Tregs are increased in cancer patients, including in CRC. These studies led to divergent correlations between increased Tregs and disease outcome, which emphasized the interest of studying the role of these cells in tumour initiation and progression.

There is accumulating evidence that by depleting Tregs, an anti-tumour immune response is unleashed. In the recent years, studies performed in mouse models have shown that depletion of Tregs improved the anti-tumour immune response with a strong activation and amplification of CD4+ and CD8+ T-cells and the control of tumour growth (Chaput *et al.* 2007; Goudin *et al.* 2016).

A few clinical trials have tested the efficacy of depleting Tregs in cancer patients. Dannull and colleagues have shown that depletion of these cells in patients with metastatic renal cancer improved the stimulation of tumour-specific T-cell responses (Dannull *et al.* 2005). Another example is a randomized study from our group where patients with inoperable metastatic CRC were treated with a vaccine to improve serologic and T-cell responses against 5T4, an oncofoetal antigen expressed in more than 90% of CRCs, in combination with a low dose of cyclophosphamide, to deplete Tregs. Prior depletion of Tregs did not increase the immune responses generated by the vaccination, however each treatment, independently, improved the survival outcome of the patients without toxic effects (Scurr *et al.* 2017a; Scurr *et al.* 2017b).

The different approaches to deplete Tregs in clinical trials were mainly applied to patients with advanced disease and the studies in mouse models were done using a variety of cancer cell lines including ones derived from ovarian (Chen *et al.* 2012) and melanoma (Shabaneh *et al.* 2018). Fewer studies have been conducted, however it is essential in the context of colorectal cancer. There is a need to clarify the effects of Treg depletion in the initiation of intestinal cancer

By deleting the *Apc* gene in the ISCs, it is possible to mimic the early stages of intestinal cancer, with the formation of aberrant crypt foci and micro-adenomas. I also observed increased Treg cells numbers and frequencies in the intestines, spleen and MLN. The effects of Treg depletion were analysed for the first time in the genetically modified mouse model *Lgr5Cre<sup>ERT2</sup>Apc<sup>fl/fl</sup>Foxp3<sup>DTR</sup>*, giving new insights about what happens to the early stages of intestinal tumourigenesis in the absence of the immune suppressive Treg cell population. Here, it was hypothesized that by depleting the Treg cells the tumour burden would be reduced. Indeed, as expected, the number of aberrant

crypts was significantly reduced in the large intestine and there was a trend to be reduced in the small intestine, however not significant.

It was showed that in the Treg depleted mice there was an increased apoptotic index when compared to Treg replete mice indicating that Treg depletion affects directly the homeostasis of the intestinal crypts. However, when the number of apoptotic bodies was compared between normal and aberrant crypts of *Apc* deleted/Treg depleted mice, I observed that apoptosis was significantly increased in the aberrant crypts. These data suggest that by depleting Tregs, in the context of cancer, there is a specific effect in pro-tumorigenic but not in the normal tissue. A possible explanation by which Treg depletion increased apoptosis is that, as observed by flow cytometry analysis, Treg depletion led to increased secretion of IFN $\gamma$ . This cytokine is known to promote apoptosis in malignant cells, being this one of the mechanisms responsible for the anti-tumour responses promoted by IFN $\gamma$  (Liu *et al.* 2011; Kotredes and Gamero 2013; Ni and Lu 2018). The apoptotic index was calculated based on the identification of apoptotic bodies present in H&E stained sections. For this analysis other experiments were performed, such as IHC for cleaved caspase 3, a specific marker of apoptosis. However, because of unknown circumstances, the method did not work. In the future this experiment should be repeated and added to the analysis.

Accordingly, we demonstrated that Treg depletion, following *Apc* deletion, reduced the relative gene expression of the Wnt markers *Axin2* and *cMyc*, when compared to *Apc* deletion alone, indicative of reduced tumour burden. The same was observed with the ISCs markers *Lgr5*, *Olfm4* and *Ascl2*. Gene expression data confirmed that in Treg depleted mice there was a significant increased frequency of IFN $\gamma$ , a cytokine that, as previously described, participates in anti-tumour immune responses (Wang *et al.* 2015a; Katlinski *et al.* 2017; Liu *et al.* 2017). Although the gene expression of *Foxp3* was significantly reduced in the *Lgr5Cre<sup>ERT2</sup>Apc<sup>fl/fl</sup>Foxp3<sup>DTR</sup>* group, the same was not observed in the group treated with DT (*Foxp3<sup>DTR</sup>*) to achieve Treg depletion alone where the reduced gene expression of *Foxp3* was not significant. This could have happened because the depletion was not efficient in this particular group. Depletion efficiency should be tested by flow cytometry and/or ELISA. Altogether, these data indicate that, in this mouse model, Treg depletion, in the early stages of intestinal cancer, had a positive effect in promoting an anti-tumour immune response, particularly in the large intestine. Future experiments should include gene expression analysis in large intestine.

After analysing the effect of Treg depletion on tumour burden, we characterized the frequency of the previously described T-cell populations. In this analysis there was a high variability of some markers limiting the interpretation of the data. Intra-epithelial lymphocytes provide the first defence against infections, being essential in the regulation

of intestinal homeostasis (Sheridan and Lefrançois 2010). The frequency of CD3+ cells was significantly increased in the IEL compartment of both SI and LI, following Treg depletion in *Apc* deleted mice, with no significant alterations in the LPL compartment. This suggests that in the absence of Tregs, the inflammatory T-cell populations infiltrate particularly in the intra-epithelial compartment where they may exert an anti-tumour immune response.

As expected, we observed an increased frequency of CD4+ T-cells in the intestines, but decreased in the spleen and MLN of Treg depleted mice, providing evidence, again, that in the absence of the immune suppressive Treg cells, Foxp3- CD4+ T-cells can expand and exert their anti-tumour immune responses supporting the data from other groups in different mouse models (Wing *et al.* 2014; Goudin *et al.* 2016).

Infiltration of CD8+ T-cells has been associated with better survival in cancer patients, including the in early stages of CRC (Pages *et al.* 2009; Ziai *et al.* 2018). Our data shows that most significant changes in the frequency of CD8+ T-cells were observed in the LI where there was an increased frequency of this marker following Treg depletion and *Apc* deletion/Treg depletion. Surprisingly, no differences were observed in the SI. One possible explanation is that the whole SI and LI were analysed even though the highest recombination of the *Apc* gene and, as a consequence, the formation of micro-adenomas happens in the first 5 cm of the SI. It is possible that, by analysing only the first 5 cm of the SI, similar differences would have been observed.

The frequency of CD4+Granzyme B+ cells was increased in the intestines of Treg depleted mice, particularly in the LI. Treg depletion in *Apc* deleted mice attenuated the increased frequency of Granzyme B+ cells. Similar to CD4+Granzyme B+ cells, the frequency of CD8+Granzyme B+ cells was significantly increased in the LI following Treg depletion and, with equivalent frequency, in *Apc* deleted/Treg depleted mice. The fact that most significant changes occur in the LI may explain why, in this model, a significant decrease in the number of aberrant crypts observed in the LI, whereas only a trend is observed in the SI it is only observed a trend for a decreased number of aberrant crypts as the expression of Granzyme B has been associated to improved survival in CRC (Prizment *et al.* 2017).

As previously described, the role of IL-17A in tumorigenesis is controversial (Murugaiyan and Saha 2009; Yang *et al.* 2016). Our data does not show significant changes in both SI and LI following either Treg depletion or *Apc* deletion/Treg depletion for frequencies of CD4+IL-17A+ cells, indicating that these cells may not be relevant in the anti-tumour immune response in the early stages of intestinal cancer. On the other hand, CD8+IL-17A+ cells were significantly increase in the SI following *Apc* deletion/Treg depletion, suggesting a role of CD8+ cells. Further experiments, such as IL-17A

neutralization, should help understanding the role of IL-17A in the initiation of intestinal cancer in this mouse model.

The frequency of CD4+IFN $\gamma$ + cells in the SI was only increased in the LPL compartment following Treg depletion, indicating that in the early stages of intestinal cancer the secretion of IFN $\gamma$  by CD4+ T-cells does not play a relevant role in the anti-tumour immune responses in the SI. There was a significantly increased frequency of CD4+IFN $\gamma$ + cells in the LI, and CD8+IFN $\gamma$ + cells in both SI and LI following Treg depletion, however this was attenuated in *Apc* deleted/Treg depleted mice, with the exception of CD8+IFN $\gamma$ + cells in the SI IEL. Our data suggest that IFN $\gamma$  may play an important role in the anti-tumour immune responses in the early stages of intestinal cancer, similarly to what was previously published where it was demonstrated the anti-tumour role of IFN $\gamma$  in CRC (Wang *et al.* 2015a; Katlinski *et al.* 2017; Liu *et al.* 2017).

In the distant compartments, in both spleen and MLN, there was an increased frequency of Granzyme, IL-17A and IFN $\gamma$  – producing cells after Treg depletion demonstrating that depletion of these cells unleashes a peripheral immune response. The higher increased frequencies in the cytokine-producing cells were mainly observed in CD8+ T-cells, which indicates that, these cells may participate the anti-tumour immune responses in the initiation of intestinal cancer.

In summary, it was demonstrated that Treg depletion in an *Apc* deleted mouse decreases the tumour burden in the early stages of intestinal cancer, particularly in the large intestine. This may be explained by the increased apoptotic index in the intestine, particularly in the aberrant crypts, possibly caused by the increased secretion of IFN $\gamma$  by CD8+ cells; inactivation of Wnt signalling pathway and increased frequency of cells producing Granzyme B and IFN $\gamma$ , particularly CD8+ cells. Future experiments, to further understand the immune cell populations that participate in the anti-tumour immune responses, will include the depletion of CD4+ and CD8+ T-cells, and neutralisation of IFN $\gamma$ .

## 5 Cellular subsets responsible for the anti-tumour immune response

### 5.1 Introduction

The progression of tumourigenesis in CRC and other solid tumours involves interactions between the tumour and the host immune environment, that comprise a variety of cell types, including CD4+ and CD8+ cells (Szabo *et al.* 2003; Corthay 2009; Zhu and Paul 2010; Tripathi and Lahesmaa 2014; Kaplan *et al.* 2015; Vlad *et al.* 2015).

Previously I demonstrated, using the *Lgr5Cre<sup>ERT2</sup>Apc<sup>f/f</sup>Foxp3<sup>DTR</sup>* model, that 15 days following ISC *Apc* deletion there was an expansion of Tregs in the intestine, spleen and MLN. Depleting the Tregs in this model, led to a reduction in intestinal tumourigenesis. Treg depletion led to an expansion of CD8+ and CD4+ cells that expressed either granzyme B or IFN $\gamma$  in the intestine. This increase in CD8+ cells, while indicative of an anti-tumour response, was mainly due to the absence of Tregs.

The aim of this chapter was to identify whether the immune changes associated with Treg depletion play an anti-tumour role in the early stages of intestinal cancer.

I hypothesised that depletion of CD8+ cells and neutralisation of IFN $\gamma$  would increase the intestinal tumour burden in these mice as they have been considered responsible for the anti-tumour immune responses in a variety of cancers, including CRC (Pages *et al.* 2009; Ziai *et al.* 2018). CD4+ cells include in their population conventional T-cells that promote inflammation, but also Tregs, characterized by their immune-suppressor activity. By depleting CD4+ cells I sought to verify whether conventional T-cells play a key role in the early stages of intestinal tumourigenesis. I hypothesised that if CD4+ cell depletion increased the tumour burden, conventional T-cells play an important role in the anti-tumour immune responses. On the other side, if there was a decreased tumour burden with CD4+ cell depletion, this would suggest that Tregs are the sub-population of CD4+ cells with a more relevant role in the early stages of intestinal cancer.

To determine the importance of the CD4+, CD8+ cells and the cytokine IFN $\gamma$  in the reduction of tumour burden observed in the *Lgr5Cre<sup>ERT2</sup>Apc<sup>f/f</sup>Foxp3<sup>DTR</sup>* model, these mice were treated with antibodies to either deplete the immune cells or neutralise the cytokine. For each experimental group tumour burden was analysed in the first 5 cm of the small intestine, as well as the relative gene expression of Wnt signalling, ISCs and immune markers. Relative expression of mRNA was calculated using the  $\Delta\Delta C_t$  method and ACT B was used as an internal control. Finally, I quantified the number of CD4+ and CD8+ cells and analysed their localization in the small intestinal crypts.

## 5.2 Results

### 5.2.1 Analysing the effect of CD4+ T-cells depletion in an *Apc* deleted mice

#### 5.2.1.1 Examining the partial tumour burden following CD4+ cell depletion

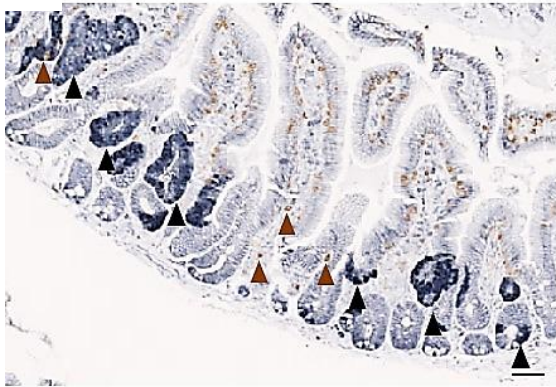
To analyse the role of CD4+ cells in the initiation of intestinal cancer, the *Lgr5Cre<sup>ERT2</sup>Apc<sup>f/f</sup>Foxp3<sup>DTR</sup>* mouse model was injected with two different depleting antibodies (clones YTS-191 & YTS-3) (section 2.4.2.2). Here, I compared four experimental groups: the previously described *Lgr5Cre<sup>ERT2</sup>Apc<sup>f/f</sup>* and *Lgr5Cre<sup>ERT2</sup>Apc<sup>f/f</sup>Foxp3<sup>DTR</sup>* groups, as well as following CD4+ cell depletion, (*Lgr5Cre<sup>ERT2</sup>Apc<sup>f/f</sup>*, Anti-CD4 and *Lgr5Cre<sup>ERT2</sup>Apc<sup>f/f</sup>Foxp3<sup>DTR</sup>*, Anti-CD4).

To determine the impact of CD4+ cell depletion on the intestine I analysed the tumour burden by quantifying number of *Apc* deficient aberrant crypts in the first 5 cm of the small intestine (section 2.7.2). Nuclear  $\beta$ -catenin was used as a surrogate marker of *Apc* loss to identify aberrant crypts (section 2.6.3). Depletion of CD4+ cells significantly reduced the tumour burden when compared to *Apc* deletion alone (Figure 5.1).

Fifteen days following *Apc* deletion in the ISCs there was a non-significant decrease in the number of aberrant crypts in the *Apc* deleted/Treg depleted mice, as shown previously. This reduction in aberrant crypts became significant in the *Apc* deleted/CD4+ cells depleted animals, in which all CD4+ cells, including Tregs, would be depleted. This indicates that, while Tregs play a role in the tumour burden, other CD4+ cells are also relevant. However, this effect was lost when CD4+ cells were depleted in combination with *Apc* deletion/Treg depletion, resulting in a non-significant decrease in aberrant crypts (Figure 5.1).

A

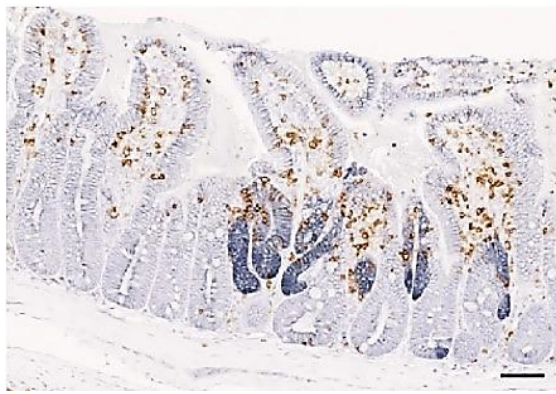
*Lgr5Cre<sup>ERT2</sup>Apc<sup>fl/fl</sup>*



*Lgr5Cre<sup>ERT2</sup>Apc<sup>fl/fl</sup>, Anti-CD4*



*Lgr5Cre<sup>ERT2</sup> Apc<sup>fl/fl</sup>Foxp3<sup>DTR</sup>*



*Lgr5Cre<sup>ERT2</sup>Apc<sup>fl/fl</sup>Foxp3<sup>DTR</sup>, Anti-CD4*



B

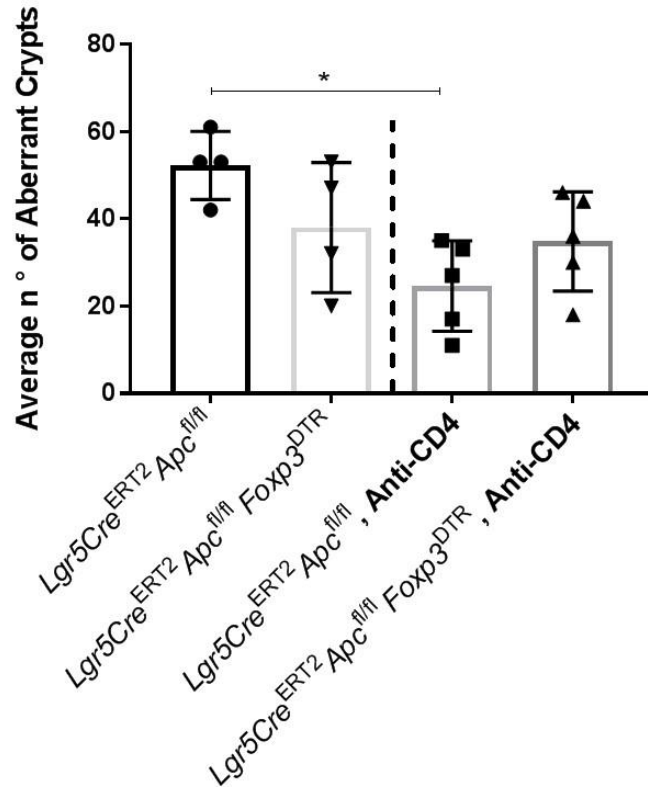


Figure 5.1 Tumour burden analysis in the small intestine of CD4+ cells depleted mice.

(A) Representative images of  $\beta$ -catenin (grey) and CD8+ cells (brown) IHC staining in the small intestine. Black arrows indicate aberrant crypts and brown arrows indicate CD8+ cells. (B) CD4+ cells depletion resulted in a significantly decreased the number of aberrant crypts in the small intestine of the *Apc* deleted mice. CD4+ cells depletion in *Apc* deleted/Treg depleted mice resulted in a trend for a decreased number of aberrant crypts. Data represent a single experiment,  $n \geq 4$  mice per group. (\*) P value < 0.05, two-tailed Mann Whitney U test. Error bars represent Standard Deviation (SD). Scale bars represent 50  $\mu$ m.

### 5.2.1.2 Evaluating the gene expression of Wnt, ISC and immune markers following CD4+ depletion

While CD4+ cells and Treg depletion reduced the number of aberrant crypts in the proximal 5cm of the *Lgr5Cre<sup>ERT2</sup>Apc<sup>fl/fl</sup>* small intestine (based on serial sections for the last group) it was only significant for CD4+ cells depletion. To identify whether this reduction was a significant feature for the whole intestine I examined Wnt signalling activation by analysing the relative gene expression of *Axin2* and *c-Myc*. A reduction in the expression level of these genes would support a reduction in the number of crypts with nuclear  $\beta$ -catenin. Relative gene expression was analysed in the intra-epithelial cells from the small intestine of *Apc* deleted/CD4+ cells depleted and *Apc* deleted/Treg and CD4+ cells depleted groups by qRT-PCR, and compared to the previously analysed experimental groups.

Depletion of CD4+ cells in *Apc* deleted mice resulted in a significantly reduced expression of the Wnt signalling markers *Axin2* and *cMyc* supporting the reduction in the number of aberrant crypts (Figure 5.2).

These aberrant crypts are supported by ISCs, so I looked at the expression of ISCs markers in mice where CD4+ cells were depleted. Depletion of CD4+ cells and Tregs in *Apc* deleted mice resulted in a significantly decreased relative gene expression of *Lgr5*, when compared to *Apc* deleted mice (Figure 5.3). There were no significant changes in the gene expression of *Olfm4* and *Ascl2* following CD4+ cell depletion (Figure 5.3), indicating that CD4+ cell depletion affects particularly *Lgr5*, also a Wnt target, suggesting again that the reduction of the number of crypts is supported by a reduction in the Wnt activation.

Depletion of CD4+ cells resulted in a significantly reduced relative gene expression of *Foxp3*. As previously explained, *Foxp3* is a transcription factor expressed by Tregs, and these cells also express the CD4 marker (Figure 5.4). *IFN $\gamma$*  gene expression was significantly decreased following *Apc* deletion/CD4+ cells depletion when compared to *Apc* deletion and the other groups where Tregs were depleted (Figure 5.4). *IFN $\gamma$*  can be secreted by a variety of immune cells, including CD4+ cells, which explains its reduction when these cells are depleted.

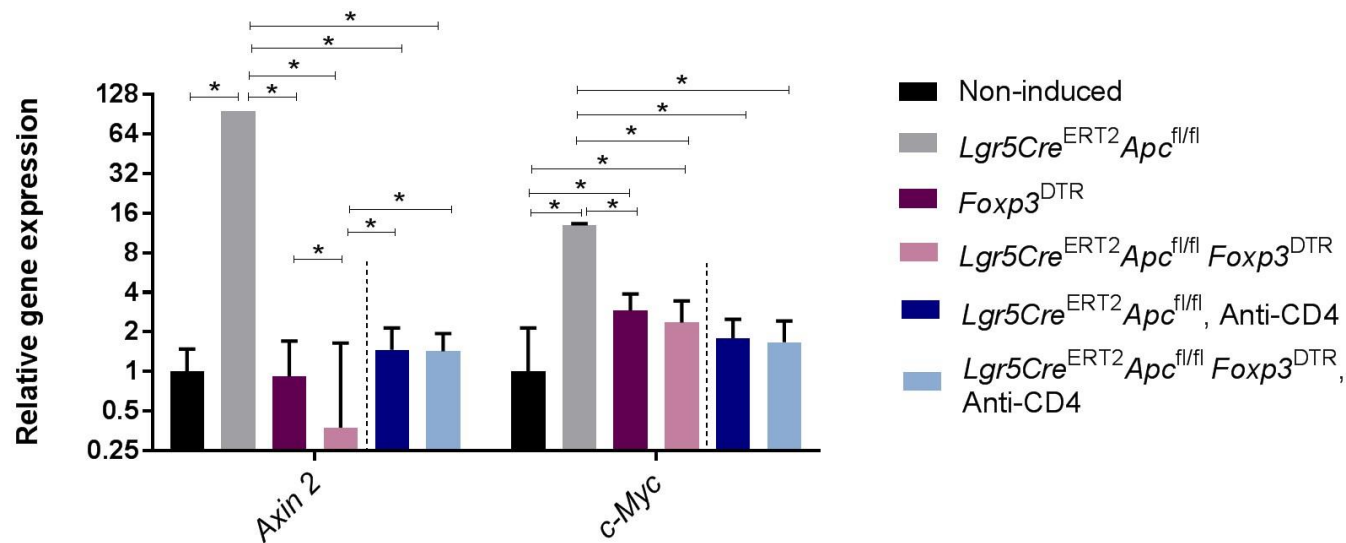


Figure 5.2 Relative gene expression of Wnt signalling markers in the small intestinal epithelium, following CD4+ cell depletion.

Depletion of CD4+ cells, in both *Apc* deleted and *Apc* deleted/Treg cells depleted mice resulted in a decreased relative gene expression of *Axin2* and *cMyc* when compared to *Apc* deletion alone. Data represent a single experiment, n ≥ 3 mice per group. Data for the non-induced, *Lgr5Cre*<sup>ERT2</sup>*Apc*<sup>fl/fl</sup>, *Foxp3*<sup>DTR</sup>, *Lgr5Cre*<sup>ERT2</sup>*Apc*<sup>fl/fl</sup>*Foxp3*<sup>DTR</sup> groups are repeated in figure 4.3. (\*) P value < 0.05, one-tailed Mann Whitney U test

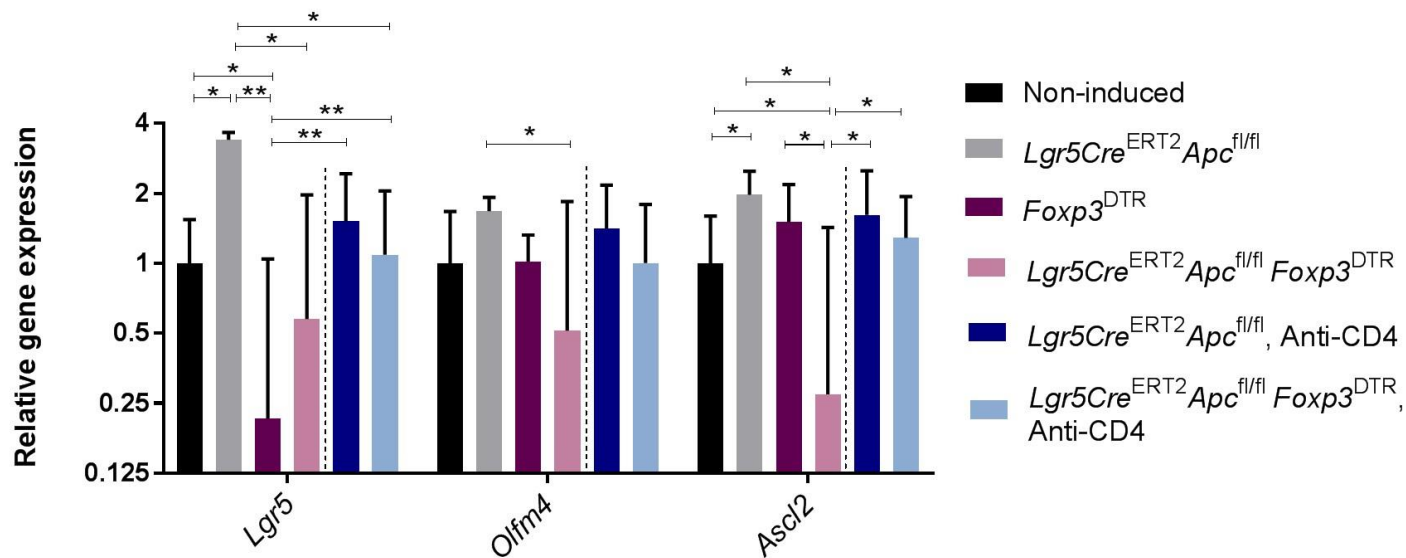


Figure 5.3 Relative gene expression of ISC markers in the small intestinal epithelium, following CD4+ cells depletion.

Depletion of CD4+ cells in both *Apc* deleted and *Apc* deleted/Treg depleted mice resulted in a decreased relative gene expression of *Lgr5* when compared to *Apc* deleted mice. There were no significant changes in the relative gene expressions of *Olfm4* and *Ascl2* following CD4+ cells depletion. Data represent a single experiment, n ≥ 3 mice per group. Data for the non-induced, *Lgr5Cre*<sup>ERT2</sup>*Apc*<sup>fl/fl</sup>, *Foxp3*<sup>DTR</sup>, *Lgr5Cre*<sup>ERT2</sup>*Apc*<sup>fl/fl</sup>*Foxp3*<sup>DTR</sup> groups are repeated in figure 4.4. (\*) P value < 0.05, (\*\*) P value ≤ 0.01, one-tailed Mann Whitney U test.

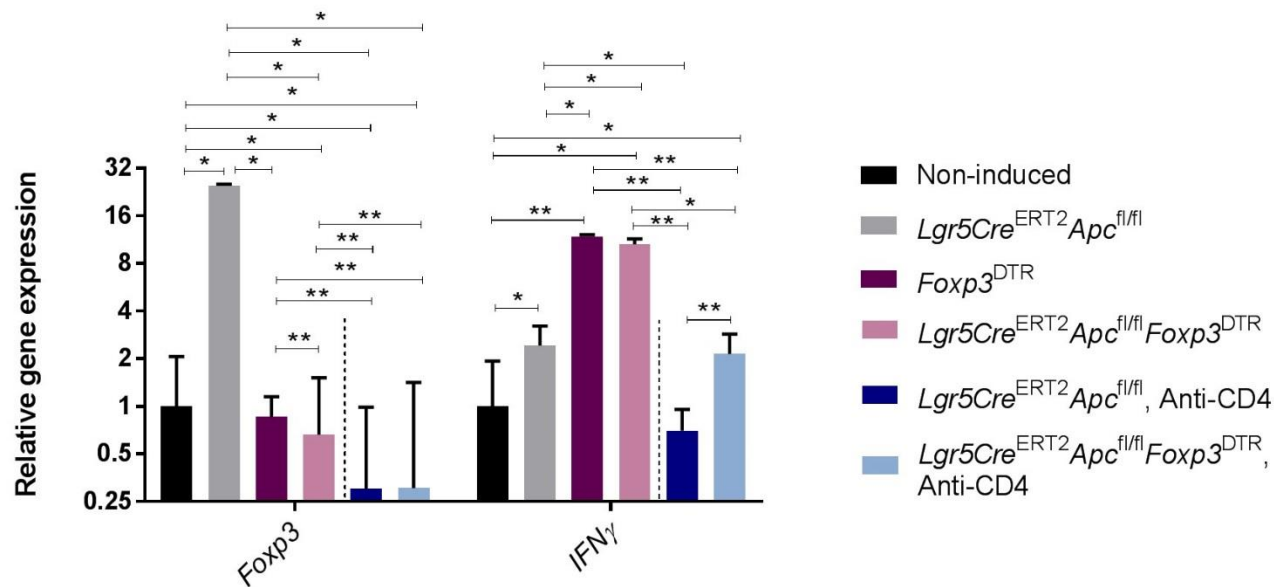


Figure 5.4 Relative gene expression of *Foxp3* and *IFN* $\gamma$  in the small intestinal epithelium, following CD4+ cells depletion.

Relative gene expression of *Foxp3* was significantly reduced following CD4+ cells depletion in *Apc* deleted and *Apc* deleted/Treg depleted mice. CD4+ cells depletion significantly decreased the gene expression of *IFN* $\gamma$  particularly in *Apc* deleted mice when compared to *Apc* deleted, Treg depleted and *Apc* deleted/Treg depleted mice. Data represent a single experiment, n  $\geq$  3 mice per group. Data for the non-induced, *Lgr5Cre*<sup>ERT2</sup>*Apc*<sup>fl/fl</sup>, *Foxp3*<sup>DTR</sup>, *Lgr5Cre*<sup>ERT2</sup>*Apc*<sup>fl/fl</sup>*Foxp3*<sup>DTR</sup> groups are repeated in figure 4.5. (\*) P value < 0.05, (\*\*) P value  $\leq$  0.01, one-tailed Mann Whitney U test

### 5.2.1.3 Evaluating the number of T-cells following CD4+ depletion

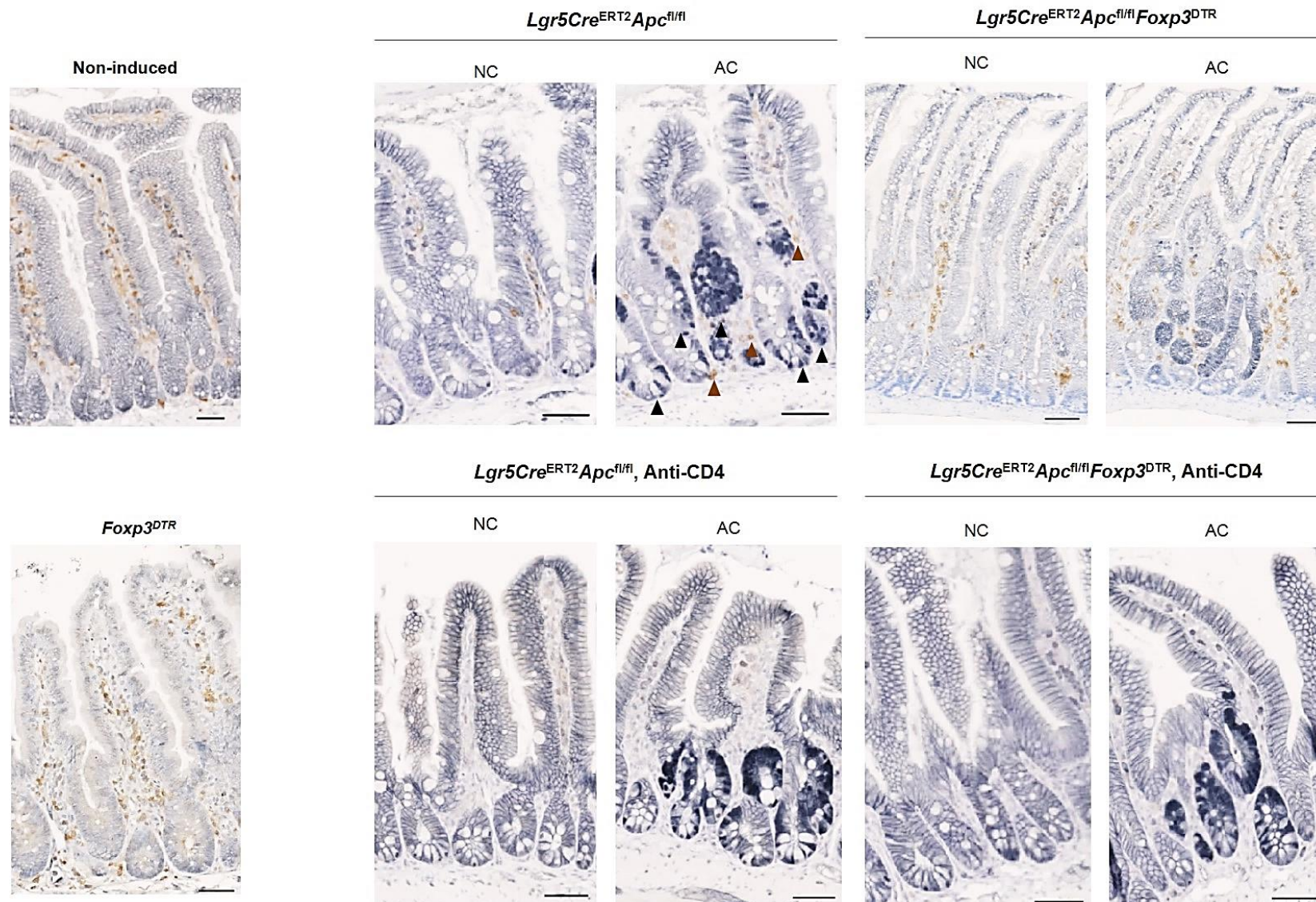
The number of CD4+ and CD8+ cells was quantified in slides stained with the respective antibodies. The experimental groups analysed were the previously described *Lgr5Cre<sup>ERT2</sup>Apc<sup>fl/fl</sup>* and *Lgr5Cre<sup>ERT2</sup>Apc<sup>fl/fl</sup>Foxp3<sup>DTR</sup>* groups, as well as following CD4+ cell depletion, (*Lgr5Cre<sup>ERT2</sup>Apc<sup>fl/fl</sup>*, Anti-CD4 and *Lgr5Cre<sup>ERT2</sup>Apc<sup>fl/fl</sup>Foxp3<sup>DTR</sup>*, Anti-CD4). A group of non-induced mice and another with Tregs depletion alone (*Foxp3<sup>DTR</sup>*) were also included in the analysis. For each experimental group, the number of either CD4+ or CD8+ cells were quantified in both normal crypts (NC) and aberrant crypts (AC). Here, I wanted to analyse whether these immune cells would have a different localization between normal and aberrant tissue that is characterized by the positive  $\beta$ -catenin nuclear staining.

Injection with the Anti-CD4 antibody nearly depleted completely the CD4+ cells in the mice small intestine (Figure 5.5).

As expected, Treg depletion alone significantly increased the number of CD4+ cells when compared to crypts from non-induced mice (Figure 5.5), suggesting that without the immunosuppressive activity of Tregs the other conventional T-cells could expand. In both *Apc* deleted and *Apc* deleted/Treg depleted mice CD4+ cells cluster around the newly formed lesions, where there is a significantly higher number of CD4+ cells when compared to normal adjacent tissue (Figure 5.5), suggesting a role of these cells in the initiation of intestinal cancer, supported by the reduction in the tumour burden upon their depletion (Figure 5.1).

Similar to CD4+ cells, CD8+ cells are significantly increased when Tregs are absent, suggesting again that upon Treg depletion the immune response is unleashed. Apart from *Apc* deleted/Treg depleted mice, that show a high number of CD8+ cells in both normal and aberrant crypts, in all the other experimental groups there is a significantly increased number of CD8+ cells in aberrant crypts (Figure 5.6). CD4+ cell depletion in *Apc* deleted mice significantly increased the number of CD8+ cells in the aberrant crypts. This effect might be explained by the fact that Tregs are a sub-population of the CD4+ cells and, as a consequence of CD4+ cell depletion, Tregs will be also depleted and will not exert their immune suppressive activity, explaining the increased number of CD8+ cells (Figure 5.6).

A



B

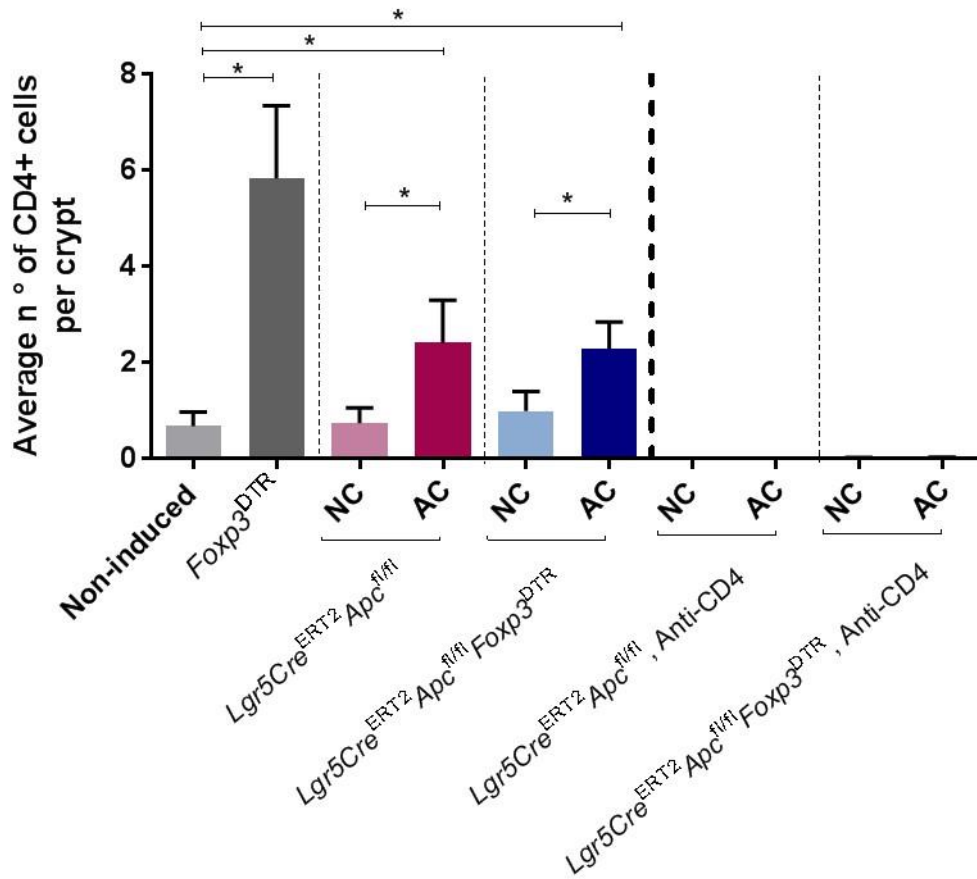
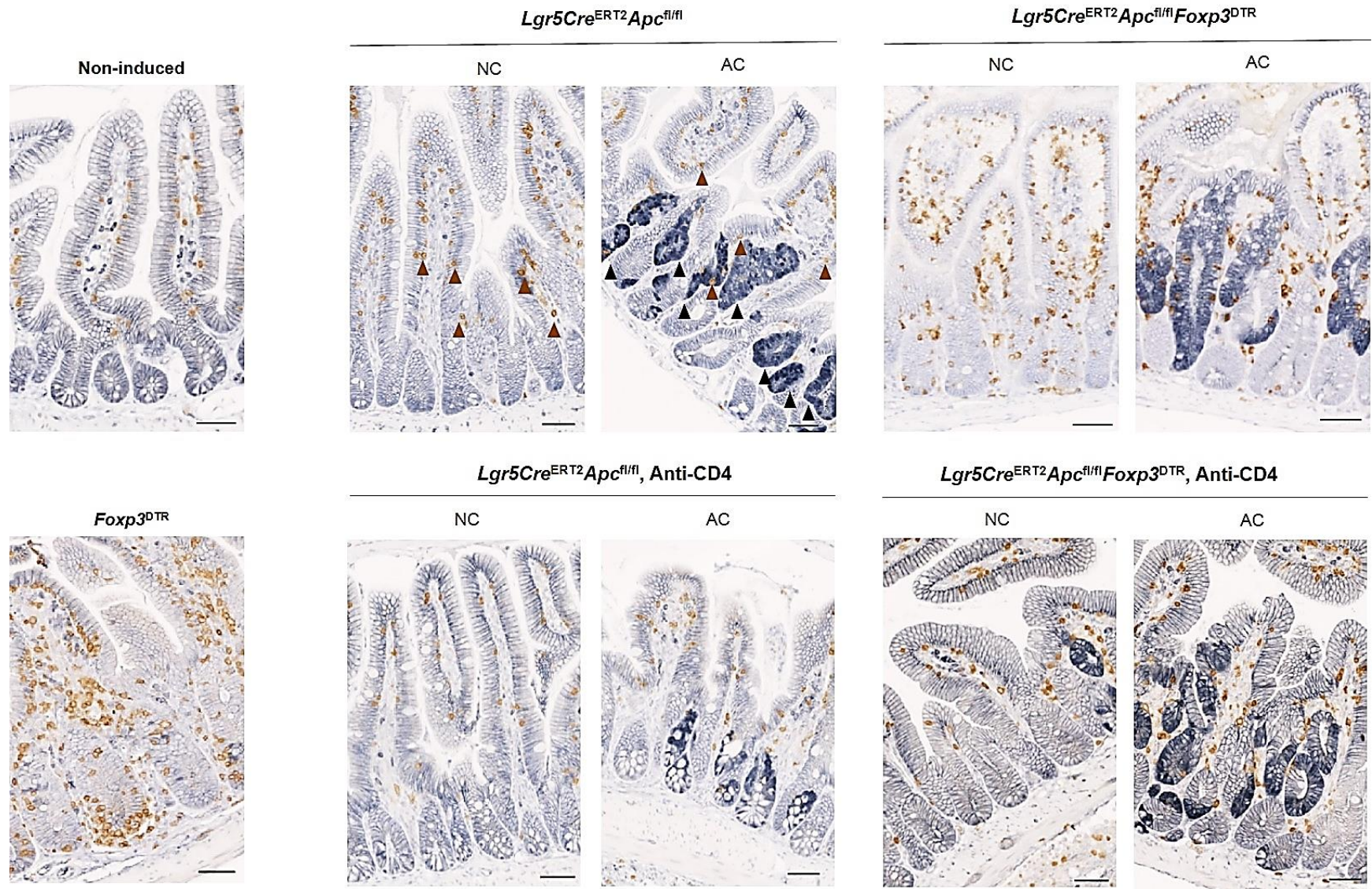


Figure 5.5 Quantification of CD4+ cells in the small intestine following CD4+ cells depletion.

(A) Representative images of  $\beta$ -catenin (grey) and CD4+ cells (brown) IHC staining in the small intestine. Black arrows indicate aberrant crypts (AC) and brown arrows indicate CD4+ cells. (B) CD4+ cells were significantly increased in Treg depleted mice. In both *Apc* deleted and *Apc* deleted/Treg depleted mice CD4+ cells were increased in the aberrant crypts when compared to normal crypts (NC). Data represent a single experiment,  $n \geq 4$  mice per group. (\*) P value < 0.05, two-tailed Mann Whitney U test. Error bars represent Standard Deviation (SD). Scale bars represent 50  $\mu$ m.

A



B

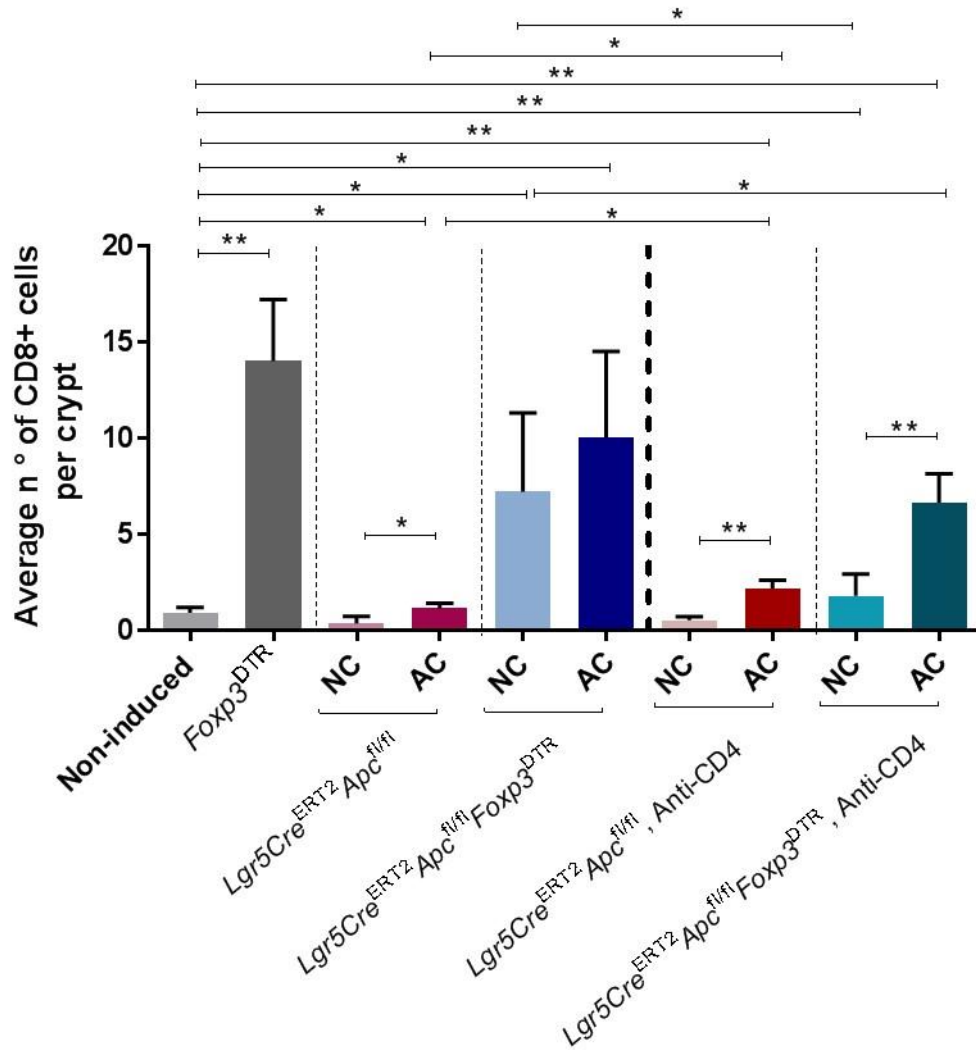


Figure 5.6 Quantification of CD8+ T-cells in the small intestine following CD4+ cells depletion.

(A) Representative images of  $\beta$ -catenin (grey) and CD8+ cells (brown) IHC staining in the small intestine. Black arrows indicate aberrant crypts and brown arrows indicate CD8+ cells. (B) CD8+ cells numbers were significantly increased in Treg depleted mice. Apart from *Apc* deleted/Treg depleted mice, there was a significantly increased number of CD8+ cells in aberrant crypts (AC), when comparing to normal crypts (NC). Data represent a single experiment,  $n \geq 4$  mice per group. (\*) P value < 0.05, (\*\*) P value  $\leq 0.01$ . Two-tailed Mann Whitney U test. Error bars represent Standard Deviation (SD). Scale bars represent 50  $\mu$ m.

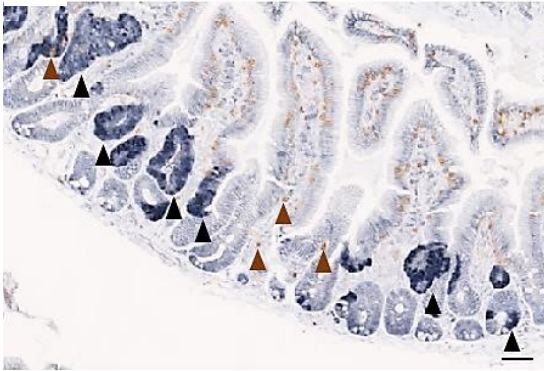
## 5.2.2 Analysing the effect of CD8+ T-cells depletion in an *Apc* deleted mice

### 5.2.2.1 Examining the partial tumour burden following CD8+ depletion

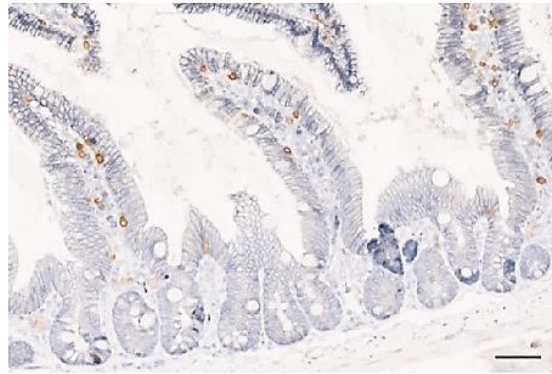
To analyse the role of CD8+ cells in the initiation of intestinal cancer, mice were injected with a monoclonal antibody (clone YTS 169) to selectively deplete CD8+ cells (see section 2.4.2.3). Four experimental groups were compared: the previously described *Lgr5Cre<sup>ERT2</sup>Apc<sup>f/f</sup>* and *Lgr5Cre<sup>ERT2</sup>Apc<sup>f/f</sup>Foxp3<sup>DTR</sup>* groups, as well as following CD8+ cell depletion, (*Lgr5Cre<sup>ERT2</sup>Apc<sup>f/f</sup>*, Anti-CD8 and *Lgr5Cre<sup>ERT2</sup>Apc<sup>f/f</sup>Foxp3<sup>DTR</sup>*, Anti-CD8). The tumour burden was analysed as previously described in the first 5 cm of the small intestine. Contradicting the proposed hypothesis, that CD8+ cell depletion would increase the number of aberrant crypts, it was observed that CD8+ cell depletion in *Apc* deleted mice significantly decreased the tumour burden in the small intestine (Figure 5.7). There is a trend for a decreased tumour burden in *Apc* deleted mice were both CD8+ T-cells and Tregs were depleted (Figure 5.8), suggesting that in the early stages of intestinal cancer CD8+ cells play a pro-tumoral role.

A

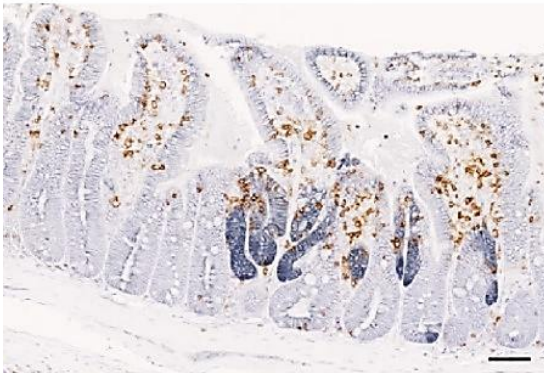
*Lgr5Cre<sup>ERT2</sup>Apc<sup>fl/fl</sup>*



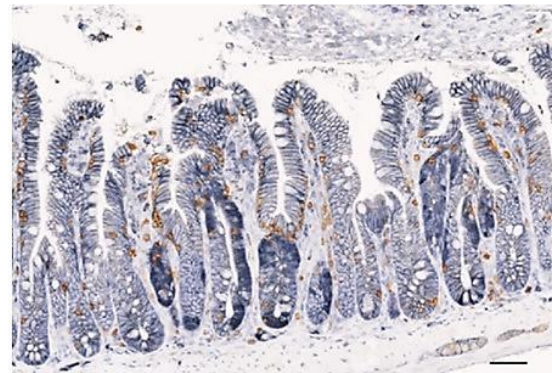
*Lgr5Cre<sup>ERT2</sup>Apc<sup>fl/fl</sup>, Anti-CD8*



*Lgr5Cre<sup>ERT2</sup>Apc<sup>fl/fl</sup>Foxp3<sup>DTR</sup>*



*Lgr5Cre<sup>ERT2</sup>Apc<sup>fl/fl</sup>Foxp3<sup>DTR</sup>, Anti-CD8*



B

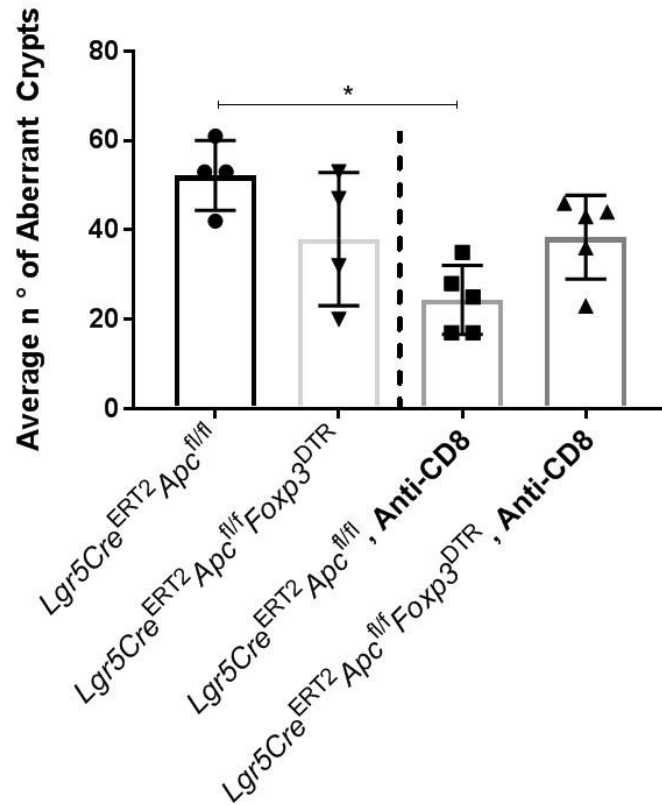


Figure 5.7 Tumour burden analysis in the small intestine following CD8+ cells depletion.

A) Representative images of  $\beta$ -catenin (grey) and CD8+ cells (brown) IHC staining in the small intestine. Black arrows indicate aberrant crypts and brown arrows indicate CD8+ cells. (B) CD8+ cells depletion resulted in a significantly decreased number of aberrant crypts in the small intestine of the *Apc* deleted mice. *Apc* deleted/Treg and CD8+ cells depleted mice had a trend for a decreased number of aberrant crypts. Data for the *Lgr5Cre<sup>ERT2</sup>Apc<sup>fl/fl</sup>* and *Lgr5Cre<sup>ERT2</sup>Apc<sup>fl/fl</sup>Foxp3<sup>DTR</sup>* groups are repeated in figure 5.1. Data represent a single experiment,  $n \geq 4$  mice. (\*) P value < 0.05, two-tailed Mann Whitney U test. Error bars represent Standard Deviation (SD). Scale bars represent 50  $\mu$ m.

### 5.2.2.2 Evaluating the gene expression of Wnt, ISC and immune markers following CD8+ depletion

To analyse whether the effects of CD8+ depletion were a feature of the whole intestine, the expression of Wnt markers were analysed. It was hypothesised that the observed reduction in the tumour burden would be reflected in the non-activation of the Wnt pathway. As expected, the decreased tumour burden observed in *Apc* deleted/CD8+ cell depleted mice were reflected in the reduction of the relative gene expression of the Wnt signalling markers, *Axin2* and *c-Myc*, when compared to *Apc* deletion alone (Figure 5.8). Interestingly, CD8+ cell depletion alone resulted in a significantly reduced relative gene expression of Wnt targets (Figure 5.8), suggesting that these immune cells play a role in the Wnt signalling activation.

As the aberrant crypts are supported by ISCs, next I analysed the gene expression of ISCs markers. CD8+ cell depletion significantly reduced the relative gene expression of *Lgr5* in *Apc* deleted and *Apc* deleted/Treg depleted mice when compared to *Apc* deletion alone (Figure 5.9). There were no significant changes, following CD8+ cell depletion, in *Olfm4* and *Ascl2* was significantly decreased in *Apc* deleted mice (Figure 5.9). Taken together, these data show that, depletion of CD8+ cells resulted in a reduced gene expression of the Wnt markers *Axin2* and *c-Myc*, as well as the ISC marker *Lgr5*, itself a Wnt marker, suggesting that the reduction in the number of aberrant crypts is supported by the reduced Wnt signalling,

To verify whether depletion of CD8+ cells had an impact in the gene expression of Tregs and the cytokine IFN $\gamma$ , the relative gene expression of *Foxp3* and IFN $\gamma$  were analysed. CD8+ cell depletion alone significantly reduced the relative gene expression of *Foxp3*, however this effect was rescued when CD8+ cells were depleted in *Apc* deleted mice (Figure 5.10). This might be a consequence of *Apc* deletion that, as previously shown, significantly increases the expression of *Foxp3*. As previously explained, IFN $\gamma$  can be secreted by a variety of immune cell populations, including CD8+ cells. As expected, CD8+ cell depletion, alone or in *Apc* deleted mice, significantly decreased the gene expression of IFN $\gamma$ . However, this effect was rescued in *Apc* deleted/Treg depleted mice in the absence of CD8+ cells, where a significantly increased gene expression of IFN $\gamma$  was observed that might be explained by Treg depletion (Figure 5.10).

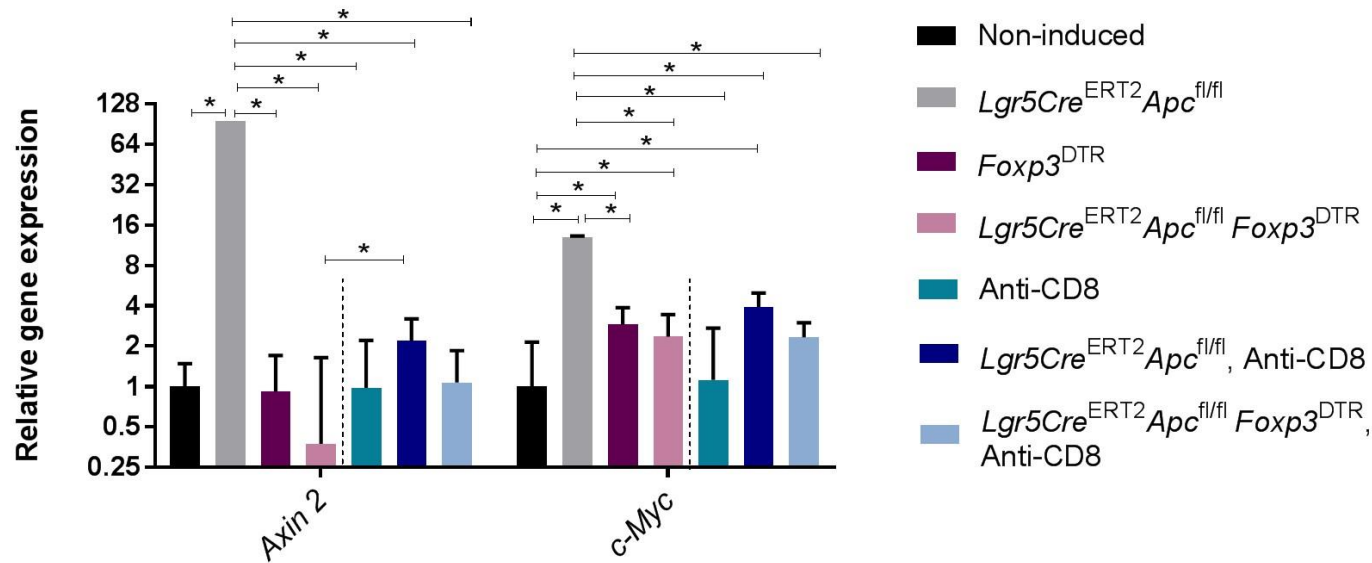


Figure 5.8 Relative gene expression of Wnt signalling markers in the small intestinal epithelium, following CD8+ cells depletion.

CD8+ cells depletion alone and in combination with *Apc* deletion and *Apc* deletion/Treg depletion resulted in a significantly decreased relative gene expression of *Axin2* and *c-Myc* when compared to *Apc* deleted mice. Data represent a single experiment,  $n \geq 3$  mice per group. Data for the non-induced, *Lgr5Cre*<sup>ERT2</sup>*Apc*<sup>fl/fl</sup>, *Foxp3*<sup>DTR</sup>, *Lgr5Cre*<sup>ERT2</sup>*Apc*<sup>fl/fl</sup>*Foxp3*<sup>DTR</sup> groups are repeated in figures 4.3 and 5.2. (\*) P value < 0.05, one-tailed Mann Whitney U test.

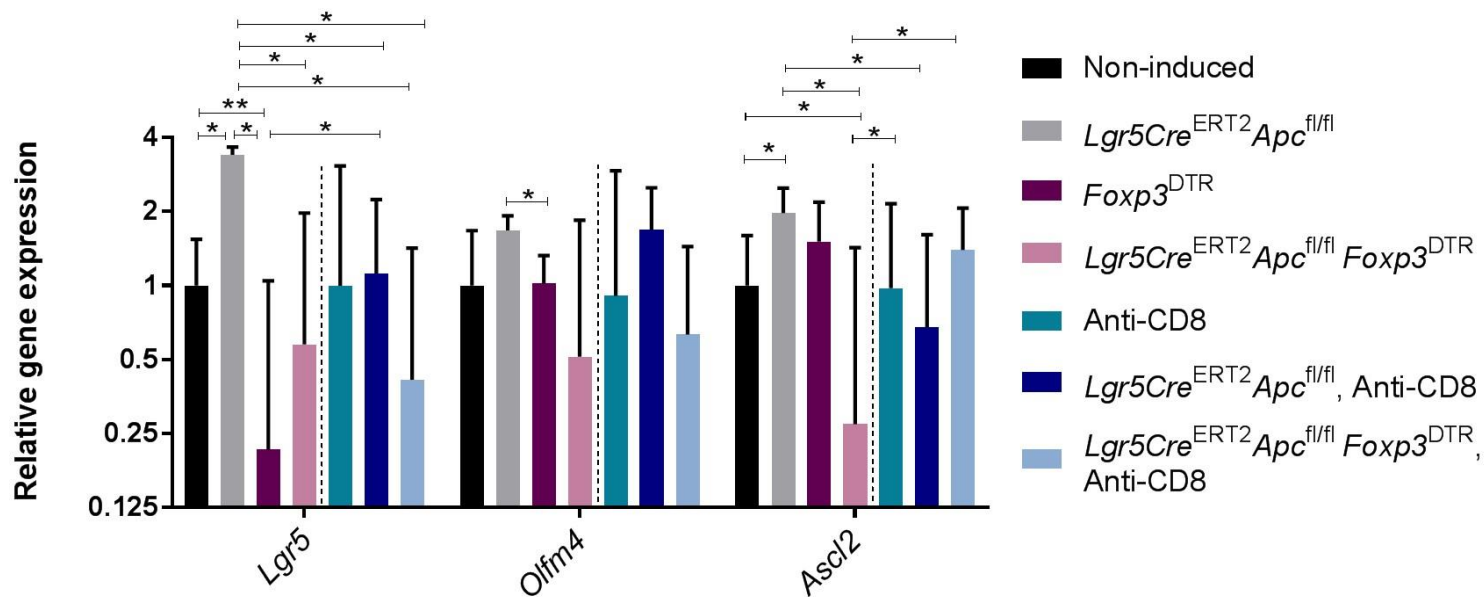


Figure 5.9 Relative gene expression of ISC markers in the small intestinal epithelium, following CD8+ cells depletion.

CD8+ cells depletion resulted in a decreased the relative gene expression of *Lgr5*, particularly in *Apc* deleted/Treg depleted mice. There were no changes in the *Olfm4*. *Ascl2* was significantly decreased in *Apc* deleted/CD8+ cells depleted mice when compared to *Apc* deletion alone. Data represent a single experiment,  $n \geq 3$  mice per group. Data for the non-induced, *Lgr5Cre*<sup>ERT2</sup>*Apc*<sup>fl/fl</sup>, *Foxp3*<sup>DTR</sup>, *Lgr5Cre*<sup>ERT2</sup>*Apc*<sup>fl/fl</sup>*Foxp3*<sup>DTR</sup> groups are repeated in figures 4.4 and 5.3. (\*) P value < 0.05, (\*\*) P value  $\leq 0.01$ , one-tailed Mann Whitney U test.

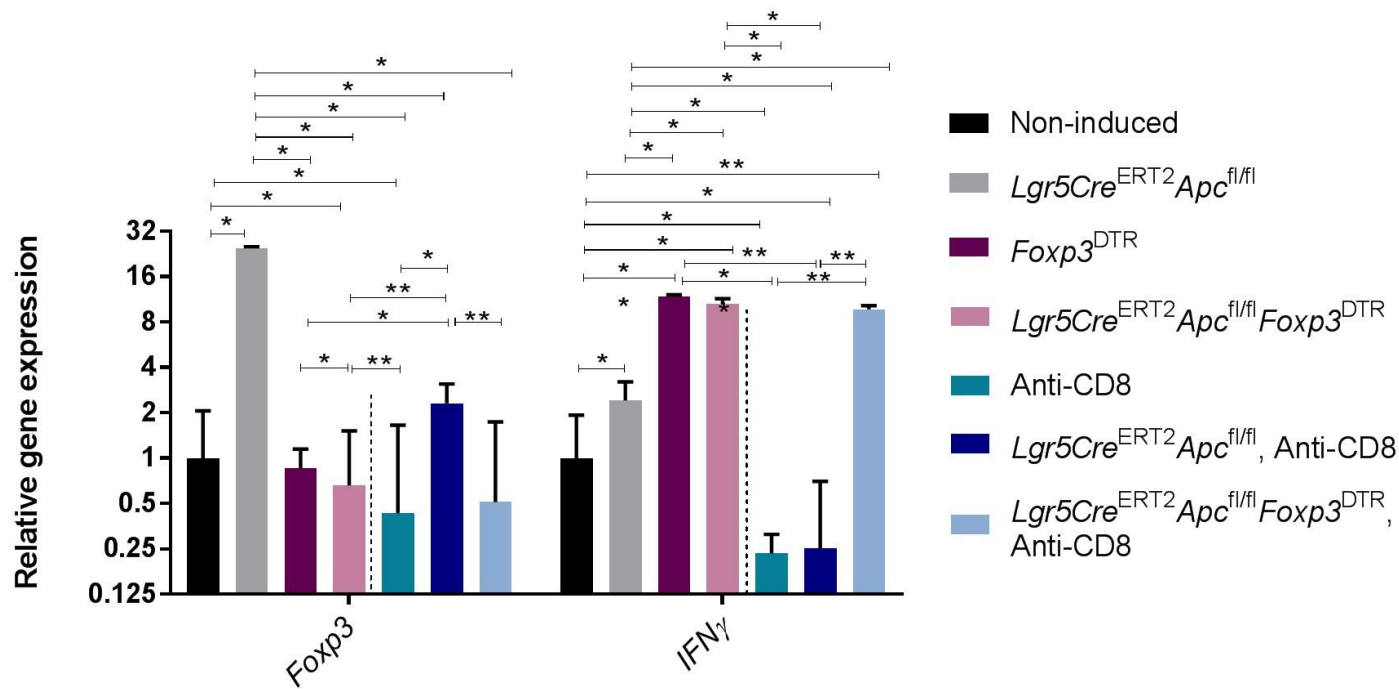


Figure 5.10 Relative gene expression of *Foxp3* and *IFN $\gamma$*  in the small intestinal epithelium, following CD8+ cells depletion

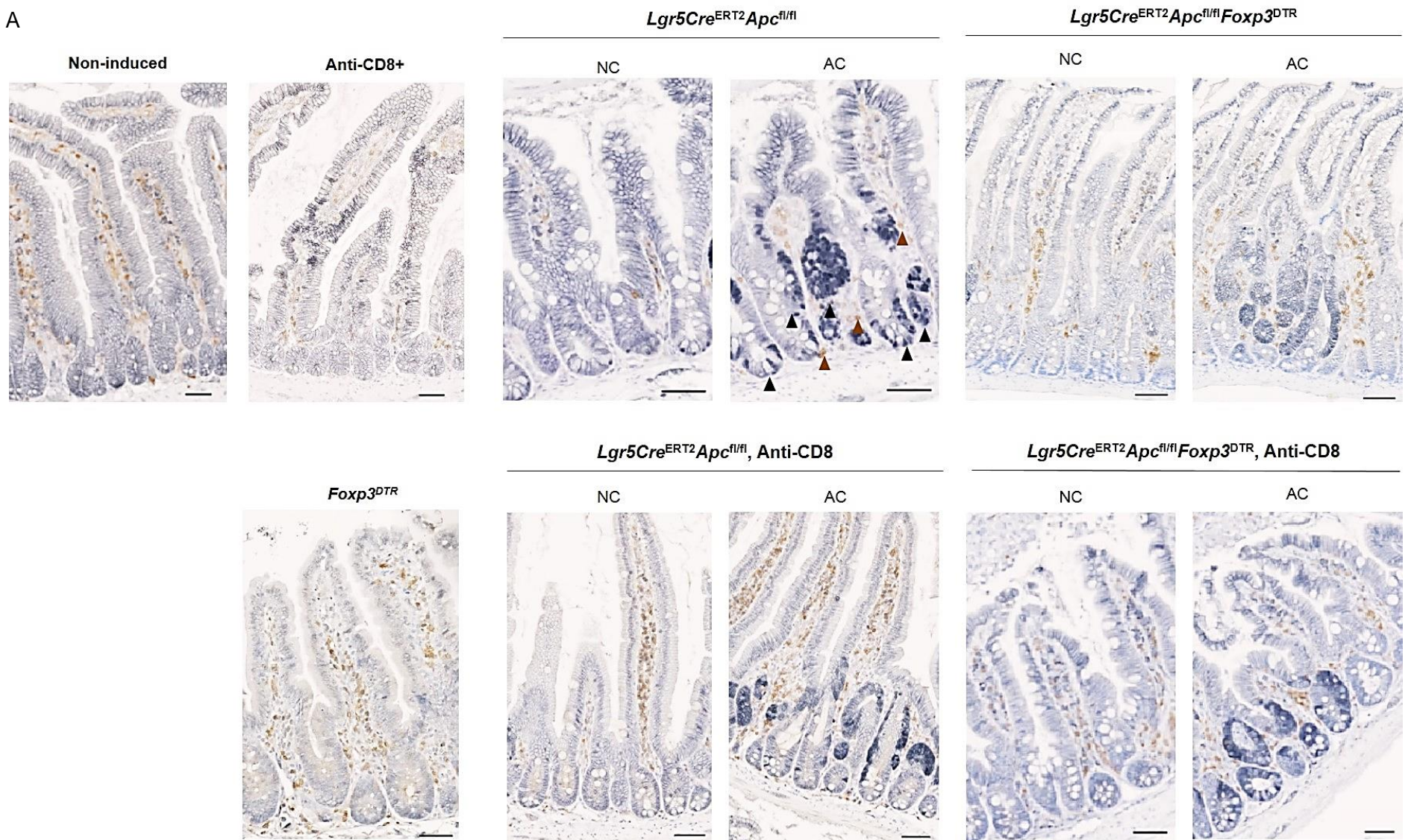
CD8+ cells depletion resulted in a significantly reduced expression of *Foxp3* and *IFN $\gamma$* , however in the last one the relative gene expression was rescued in *Apc* deleted/Treg depleted mice. Data represent a single experiment,  $n \geq 3$  mice per group. Data for the non-induced,  $Lgr5Cre^{ERT2}Apc^{fl/fl}$ ,  $Foxp3^{DTR}$ ,  $Lgr5Cre^{ERT2}Apc^{fl/fl}Foxp3^{DTR}$  groups are repeated in figures 4.5 and 5.4. (\*) P value < 0.05, (\*\*) P value  $\leq$  0.01, one-tailed Mann Whitney U test.

### 5.2.2.3 Evaluating the number of T-cells following CD8+ cell depletion

The number of CD4+ and CD8+ cells was quantified in CD8+ cell depleted mice, as previously described, in both normal (NC) and aberrant crypts (AC). Similar to the analysis performed for the T-cell quantification in the CD4+ cell depleted mice, here I included the following groups: non-induced, *Foxp3<sup>DTR</sup>*, *Lgr5Cre<sup>ERT2</sup>Apc<sup>fl/fl</sup>* and *Lgr5Cre<sup>ERT2</sup>Apc<sup>fl/fl</sup>Foxp3<sup>DTR</sup>* groups. The groups where CD8+ cells were depleted were: *Lgr5Cre<sup>ERT2</sup>Apc<sup>fl/fl</sup>*, Anti-CD8; *Lgr5Cre<sup>ERT2</sup>Apc<sup>fl/fl</sup>Foxp3<sup>DTR</sup>*, Anti-CD8; and CD8 depletion alone (Anti-CD8). CD8+ cell depletion alone did not alter significantly the number of CD4+ cells in the small intestinal crypts, suggesting that in the absence of CD8+ cells there are no alterations in the infiltration of CD4+ cells (Figure 5.11). However, CD4+ cells were significantly increased following CD8+ cells depletion in *Apc* deleted and *Apc* deleted/Treg depleted mice, particularly in the aberrant crypts (Figure 5.11). There were no differences in the number of CD4+ cells between *Apc* deleted and *Apc* deleted/CD8+ cell depleted mice (Figure 5.11), suggesting that CD8+ cell depletion does not have an impact in the infiltration of CD4+ cells in the intestine in the early stages of intestinal cancer.

As expected, mice injected with the antibody to achieve CD8+ cell depletion, had a significantly decreased number of CD8+ cells in the small intestinal crypts, when compared to non-induced mice (Figure 5.12). In *Apc* deleted/CD8+ cell depleted mice significant increase in the number of CD8+ cells around the newly formed lesions was observed, suggesting that in the context of *Apc* deletion there is a recruitment of these cells to the pro-tumoral tissue even when mice are injected with a depleting antibody to eliminate CD8+ cells. These data suggest a role of these cells in the initiation of intestinal cancer. CD8+ cell depletion in *Apc* deleted/Treg depleted mice had a significantly increased number of CD8+ cells, possibly due to Tregs depletion that, itself, resulted in a significantly increased number of CD8+ cells (Figure 5.12)

A



B

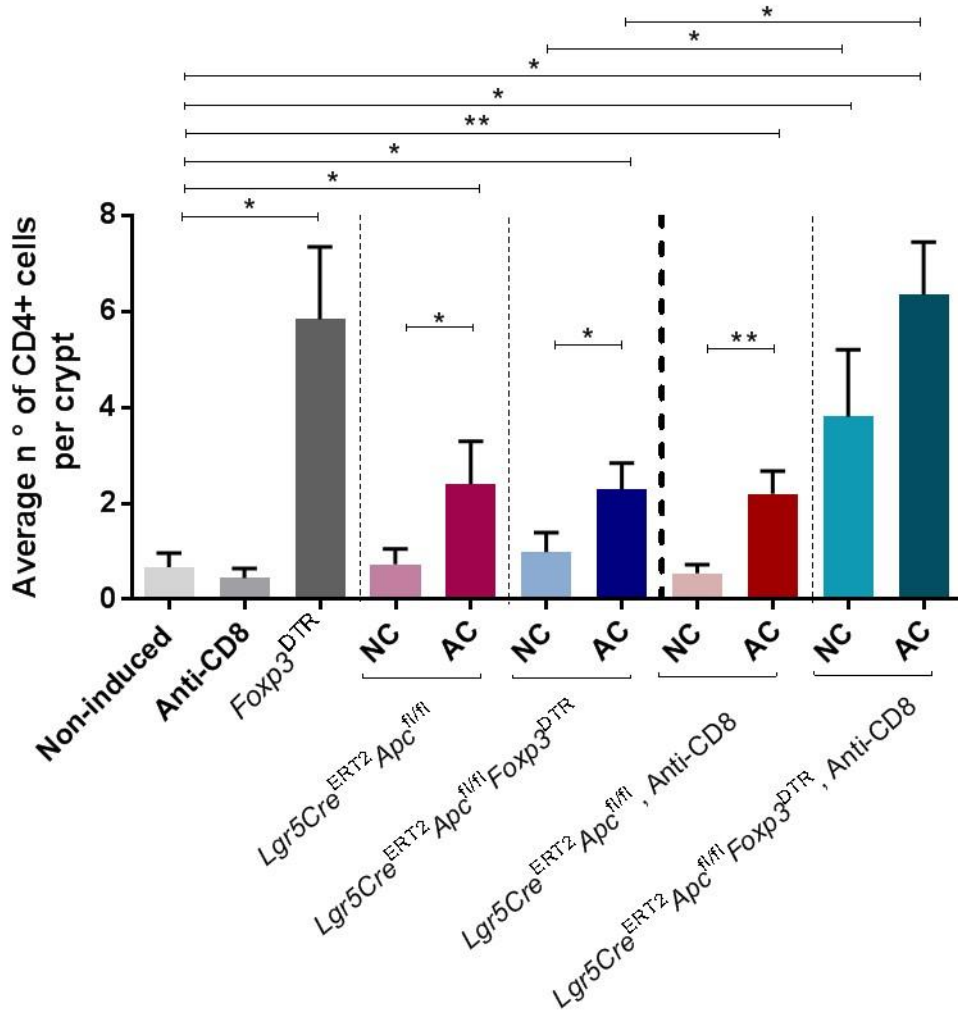
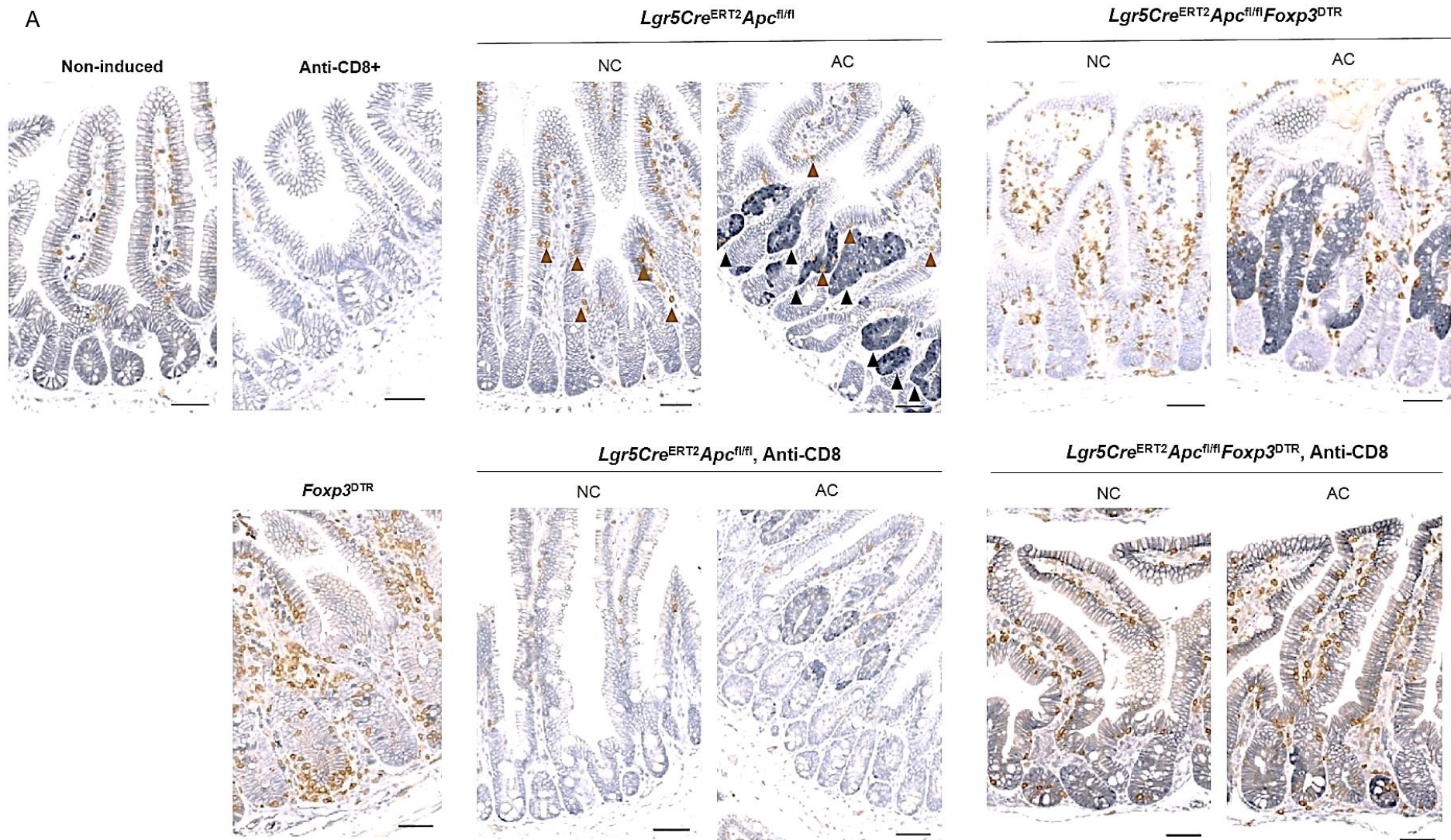


Figure 5.11 Quantification of CD4+ cells in the small intestine following CD8+ cells depletion.

(A) Representative images of  $\beta$ -catenin (grey) and CD4+ cells (brown) IHC staining in the small intestine. Black arrows indicate aberrant crypts and brown arrows indicate CD4+ cells. (B) CD4+ cells were significantly increased in the aberrant crypts (AC) of *Apc* deleted/CD8+ cells depleted mice when compared to normal crypts (NC). CD8+ cells depletion in *Apc* deleted/Treg depleted mice significantly increased the number of CD4+ cells, but with no differences between normal and aberrant crypts. Data represent a single experiment,  $n \geq 4$  mice per group. Data for the non-induced, *Foxp3<sup>DTR</sup>*, *Lgr5Cre<sup>ERT2</sup>Apc<sup>fl/fl</sup>* and *Lgr5Cre<sup>ERT2</sup>Apc<sup>fl/fl</sup>Foxp3<sup>DTR</sup>* groups are repeated in figure 5.5. (\*) P value < 0.05, (\*\*) P value  $\leq$  0.01. Two-tailed Mann Whitney U test. Error bars represent Standard Deviation (SD). Scale bars represent 50  $\mu$ m.



B

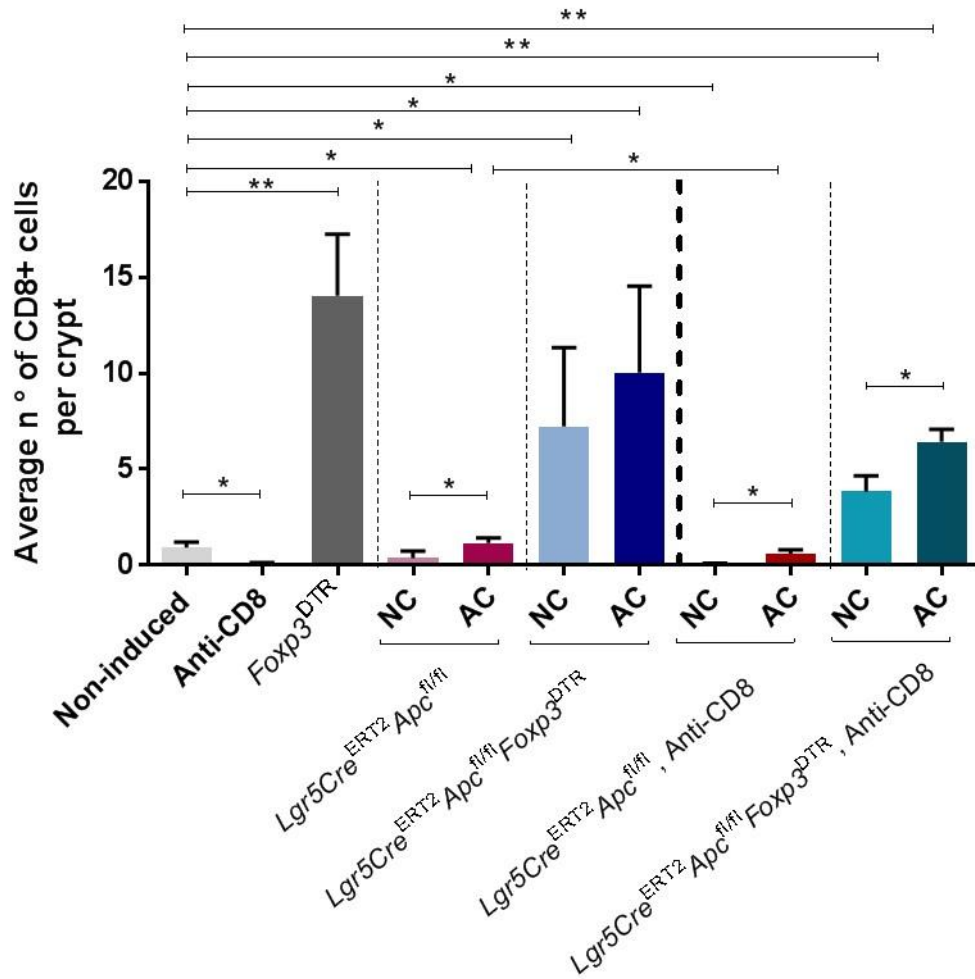


Figure 5.12 Quantification of CD8+ cells in the small intestine following their depletion.

(A) Representative images of  $\beta$ -catenin (grey) and CD8+ cells (brown) IHC staining in the small intestine. Black arrows indicate aberrant crypts and brown arrows indicate CD8+ cells. (B) CD8+ cells depletion resulted in a significantly decreased number of CD8+ cells in the crypts when compared to non-induced mice. *Apc* deleted and *Apc* deleted/Treg depleted mice, even following CD8+ cells depletion, had a significant increased number of CD8+ cells in the aberrant crypts. Data represent a single experiment,  $n \geq 4$  mice per group. Data for the non-induced, *Foxp3*<sup>DTR</sup>, *Lgr5Cre*<sup>ERT2</sup>*Apc*<sup>fl/fl</sup> and *Lgr5Cre*<sup>ERT2</sup>*Apc*<sup>fl/fl</sup>*Foxp3*<sup>DTR</sup> groups are repeated in figure 5.6. (\*) P value < 0.05, (\*\*) P value  $\leq$  0.01, two-tailed Mann Whitney U test. Error bars represent Standard Deviation (SD). Scale bars represent 50  $\mu$ m.

### 5.2.3 Analysing the effect of IFN $\gamma$ neutralisation in an *Apc* deleted mice

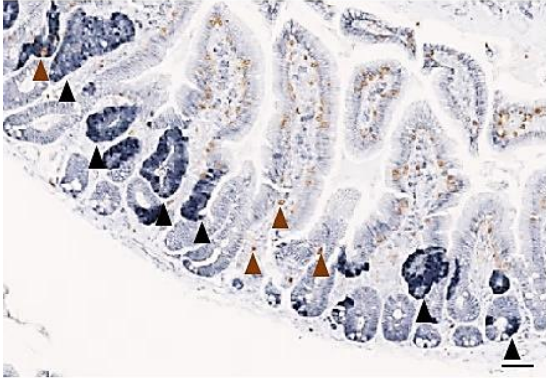
#### 5.2.3.1 Examining the partial tumour burden following IFN $\gamma$ neutralisation

Finally, I analysed the effects of IFN $\gamma$  in the early stages of intestinal tumourigenesis. Mice were injected with an antibody to specifically neutralise IFN $\gamma$  (clone XMG 1.2) (section 2.4.2.4).

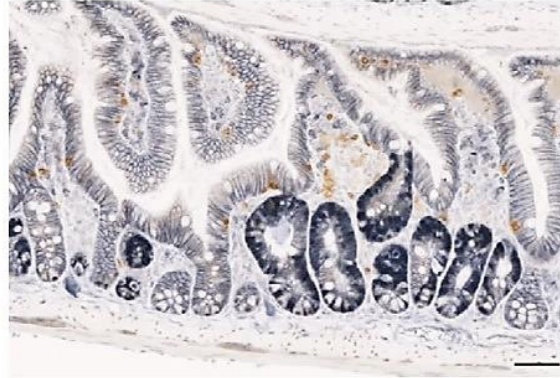
As previously, I started by quantifying the tumour burden in the first 5 cm of the small intestine of mice following IFN $\gamma$  neutralisation. Similar to the analysis performed for the CD4+ and CD8+ cell depletion experiments, I included the *Lgr5Cre<sup>ERT2</sup>Apc<sup>fl/fl</sup>* and *Lgr5Cre<sup>ERT2</sup>Apc<sup>fl/fl</sup>Foxp3<sup>DTR</sup>* groups. The groups where IFN $\gamma$  was neutralised were: *Lgr5Cre<sup>ERT2</sup>Apc<sup>fl/fl</sup>*, Anti-IFN $\gamma$  and *Lgr5Cre<sup>ERT2</sup>Apc<sup>fl/fl</sup>Foxp3<sup>DTR</sup>*, Anti-IFN $\gamma$ . Considering that IFN $\gamma$  has been associated to play a role in the anti-tumour immune responses, I hypothesised that the neutralisation of this cytokine would significantly increase the tumour burden. Contrary to what it was expected, IFN $\gamma$  neutralisation did not have a significant effect in the tumour burden of *Apc* deleted and *Apc* deleted/Treg depleted mice (Figure 5.13), suggesting that it does not play a key role in the early stages of intestinal cancer.

A

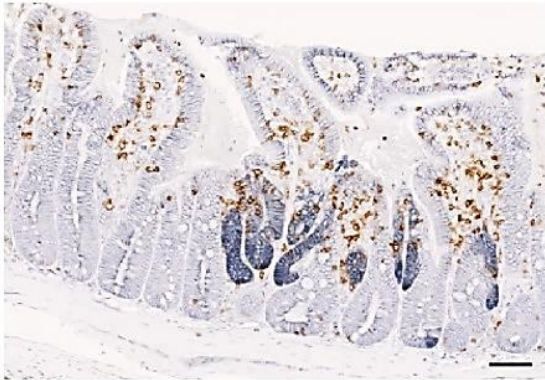
*Lgr5Cre<sup>ERT2</sup>Apc<sup>fl/fl</sup>*



*Lgr5Cre<sup>ERT2</sup>Apc<sup>fl/fl</sup>, Anti-IFN $\gamma$*



*Lgr5Cre<sup>ERT2</sup>Apc<sup>fl/fl</sup>Foxp3<sup>DTR</sup>*



*Lgr5Cre<sup>ERT2</sup>Apc<sup>fl/fl</sup>Foxp3<sup>DTR</sup>, Anti-IFN $\gamma$*



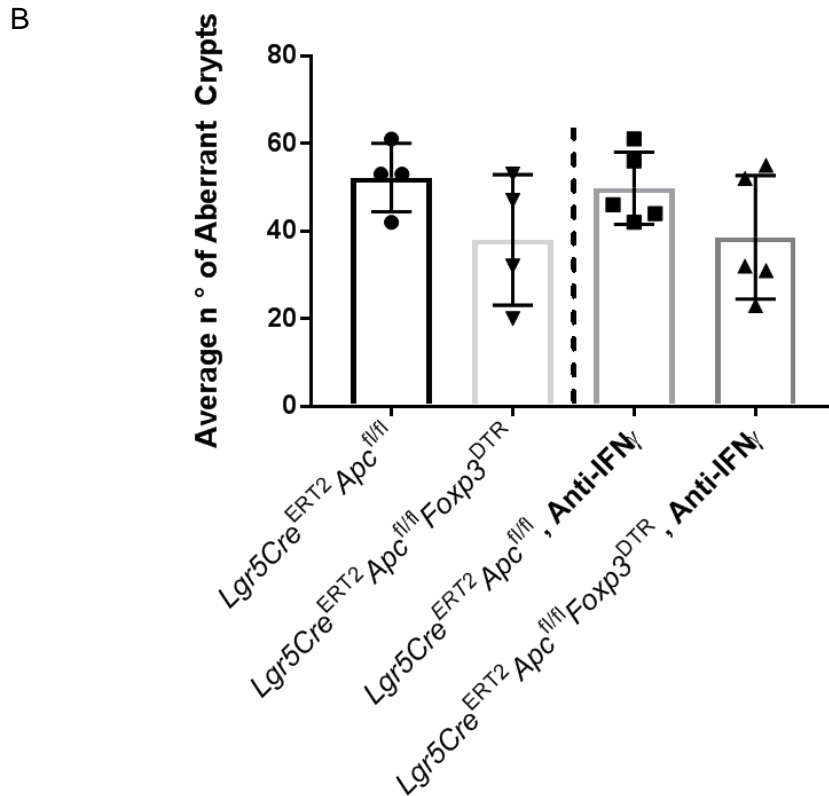


Figure 5.13 Tumour burden analysis in the small intestine following IFN $\gamma$  neutralisation.

(A) Representative images of  $\beta$ -catenin (grey) and CD8+ cells (brown) IHC staining in the small intestine. Black arrows indicate aberrant crypts and brown arrows indicate CD8+ cells. (B) IFN $\gamma$  neutralisation did not alter the tumour burden in *Apc* deleted and *Apc* deleted/Treg depleted mice. Data for the *Lgr5Cre*<sup>ERT2</sup>*Apc*<sup>fl/fl</sup> and *Lgr5Cre*<sup>ERT2</sup>*Apc*<sup>fl/fl</sup>*Foxp3*<sup>DTR</sup> groups are repeated in figures 5.1 and 5.7. Data represent a single experiment, n  $\geq$  4 mice per group. Two-tailed Mann Whitney U test. Error bars represent Standard Deviation (SD). Scale bars represent 50  $\mu$ m.

### 5.2.3.2 Evaluating the gene expression of Wnt and ISC markers following IFN $\gamma$ neutralisation

Considering that IFN $\gamma$  did not alter the tumour burden in the small intestine when compared to *Apc* deleted mice, I hypothesised that relative gene expression of Wnt signalling markers would be similar to the one observed in *Apc* deletion alone. Interestingly, IFN $\gamma$  neutralisation attenuated the effect of Wnt targets upregulation when compared to *Apc* deletion alone or *Apc* deletion /Treg depletion, suggesting that there was less Wnt signalling in these mice (Figure 5.14).

Next, I looked at the expression of ISCs, responsible for the support of aberrant crypts, and observed that *Lgr5* gene expression, also known as a Wnt marker, was significantly reduced following IFN $\gamma$  neutralisation, when compared to *Apc* deleted or *Apc* deleted/Treg depleted mice (Figure 5.14), suggesting again that there was a lower activation of the Wnt signalling pathway. Both *Ascl2* and *Olfm4* had a significantly reduced gene expression following IFN $\gamma$  neutralisation in *Apc* deleted/Treg depleted mice, when compared to *Apc* deletion alone, suggesting a possible reduction in the malignant ISC population (Figure 5.15).

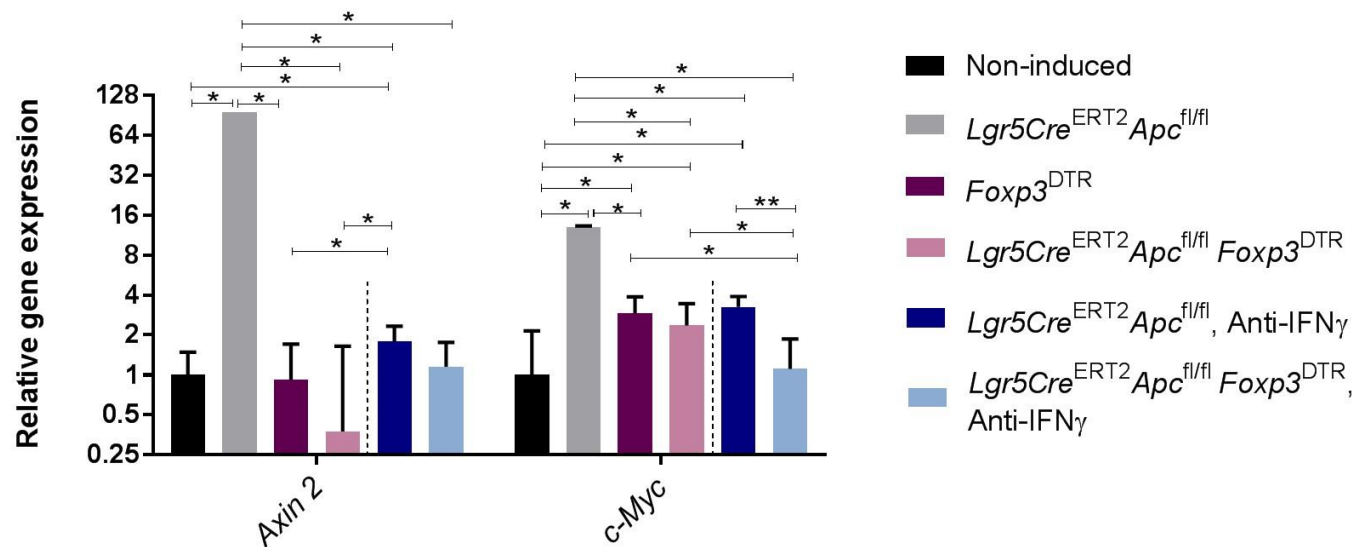


Figure 5.14 Relative gene expression of Wnt signalling markers in the small intestinal epithelium, following IFN $\gamma$  neutralisation.

IFN $\gamma$  neutralisation resulted significantly increased relative gene expression of the Wnt markers *Axin2* and *c-Myc* when compared to non-induced mice, but it was significantly decreased in comparison to *Apc* deleted mice. IFN $\gamma$  neutralisation in *Apc* deleted/Treg depleted mice resulted in a significantly decreased expression of *c-Myc* when compared to *Apc* deleted/IFN $\gamma$  neutralised mice. Data represent a single experiment,  $n \geq 3$  mice per group. Data for the non-induced, *Lgr5Cre*<sup>ERT2</sup> *Apc*<sup>fl/fl</sup>, *Foxp3*<sup>DTR</sup>, *Lgr5Cre*<sup>ERT2</sup> *Apc*<sup>fl/fl</sup> *Foxp3*<sup>DTR</sup> groups are repeated in figures 4.3, 5.2 and 5.8. (\*) P value < 0.05, (\*\*) P value  $\leq$  0.01, one-tailed Mann Whitney U test.

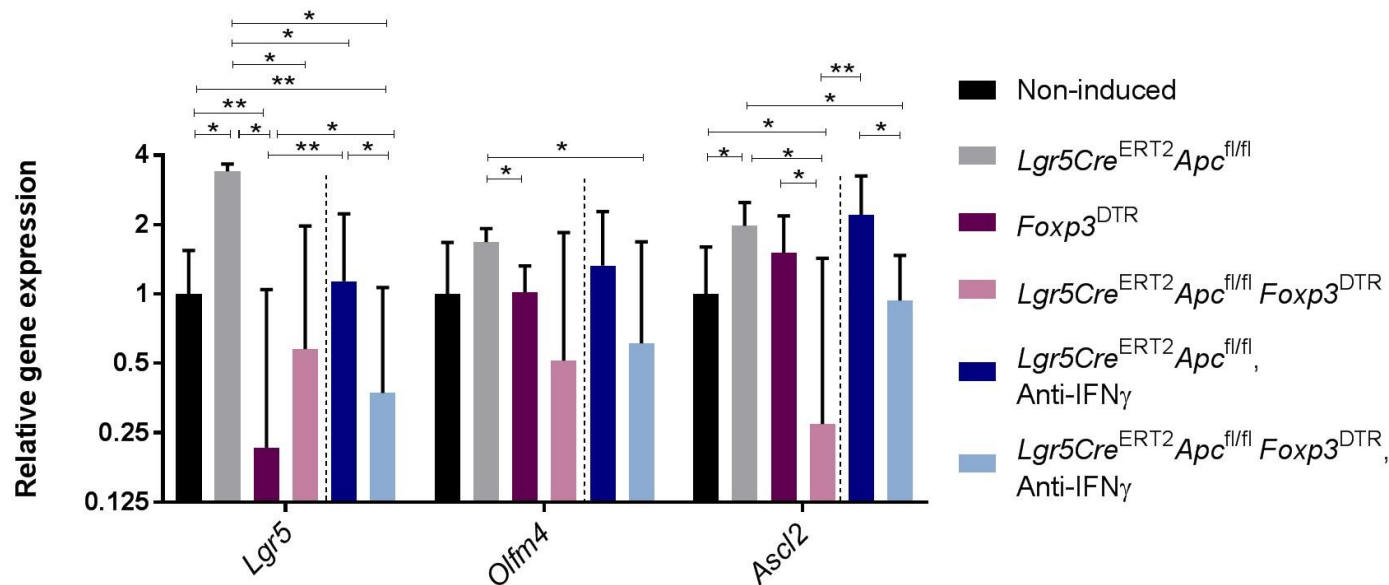


Figure 5.15 Relative gene expression of ISC markers in the small intestinal epithelium, following IFN $\gamma$  neutralisation.

Relative gene expression of the ISC markers, following IFN $\gamma$  neutralisation, was not altered when compared to non-induced mice. *Lgr5* was significantly downregulated when compared to *Apc* deleted mice. Treg depletion in *Apc* deleted/IFN $\gamma$  neutralised mice resulted in a significantly reduced relative gene expression of *Lgr5* and *Ascl2* when compared to *Apc* deleted/IFN $\gamma$  neutralised mice. Data represent a single experiment,  $n \geq 3$  mice per group. Data for the non-induced, *Lgr5Cre*<sup>ERT2</sup>*Apc*<sup>fl/fl</sup>, *Foxp3*<sup>DTR</sup>, *Lgr5Cre*<sup>ERT2</sup>*Apc*<sup>fl/fl</sup>*Foxp3*<sup>DTR</sup> groups are repeated in figures 4.4, 5.3 and 5.9. (\*) P value < 0.05, (\*\*) P value  $\leq$  0.01, one-tailed Mann Whitney U test

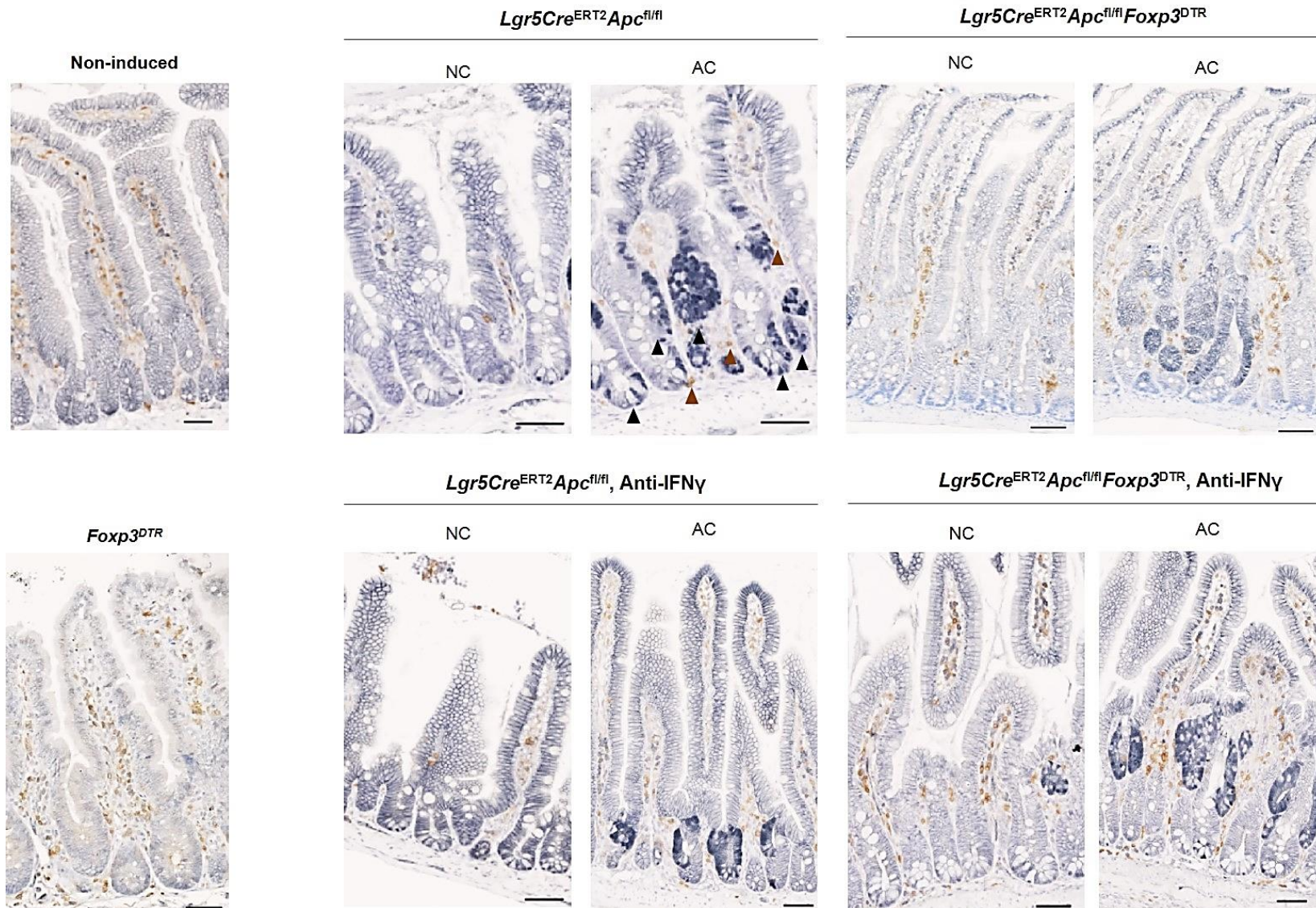
### 5.2.3.3 Evaluating the number of T-cells following IFN $\gamma$ neutralisation

The number of T-cells was quantified as previously described for the other groups. Similar to the analysis performed for the T-cell quantification in the CD4+ and CD8+ cell depleted mice, the following groups were included: non-induced, *Foxp3<sup>DTR</sup>*, *Lgr5Cre<sup>ERT2</sup>Apc<sup>fl/fl</sup>* and *Lgr5Cre<sup>ERT2</sup>Apc<sup>fl/fl</sup>Foxp3<sup>DTR</sup>* groups. The groups where IFN $\gamma$  was neutralised were: *Lgr5Cre<sup>ERT2</sup>Apc<sup>fl/fl</sup>*, Anti-IFN $\gamma$  and *Lgr5Cre<sup>ERT2</sup>Apc<sup>fl/fl</sup>Foxp3<sup>DTR</sup>*, Anti-IFN $\gamma$ .

IFN $\gamma$  neutralisation resulted in a significantly increased number of CD4+ cells in the aberrant crypts of *Apc* deleted and *Apc* deleted/Treg depleted mice, when compared to normal crypts (Figure 5.17). Interestingly, IFN $\gamma$  neutralisation in *Apc* deleted and *Apc* deleted/Treg depleted mice significantly increased the number of CD4+ cells in both normal and aberrant crypts when compared to same group, but without neutralisation of this cytokine, possibly suggesting that a higher infiltration of CD4+ cells was happening so the secretion of IFN $\gamma$  could be increased back to normal and that this process was facilitated by the absence of Tregs.

IFN $\gamma$  neutralisation significantly increased the number of CD8+ cells in the aberrant crypts of *Apc* deleted, but particularly in *Apc* deleted/Treg depleted mice (Figure 5.18). There were no differences in the numbers of CD8+ cells between *Apc* deleted or *Apc* deleted/Treg depleted and the same groups but following IFN $\gamma$  neutralisation (Figure 5.18), suggesting that IFN $\gamma$  neutralisation did not have an impact in the infiltration of CD8+ cells and that, possibly, CD4+ cells are the main responsible cell population for the secretion of IFN $\gamma$  in the intestine.

A



B

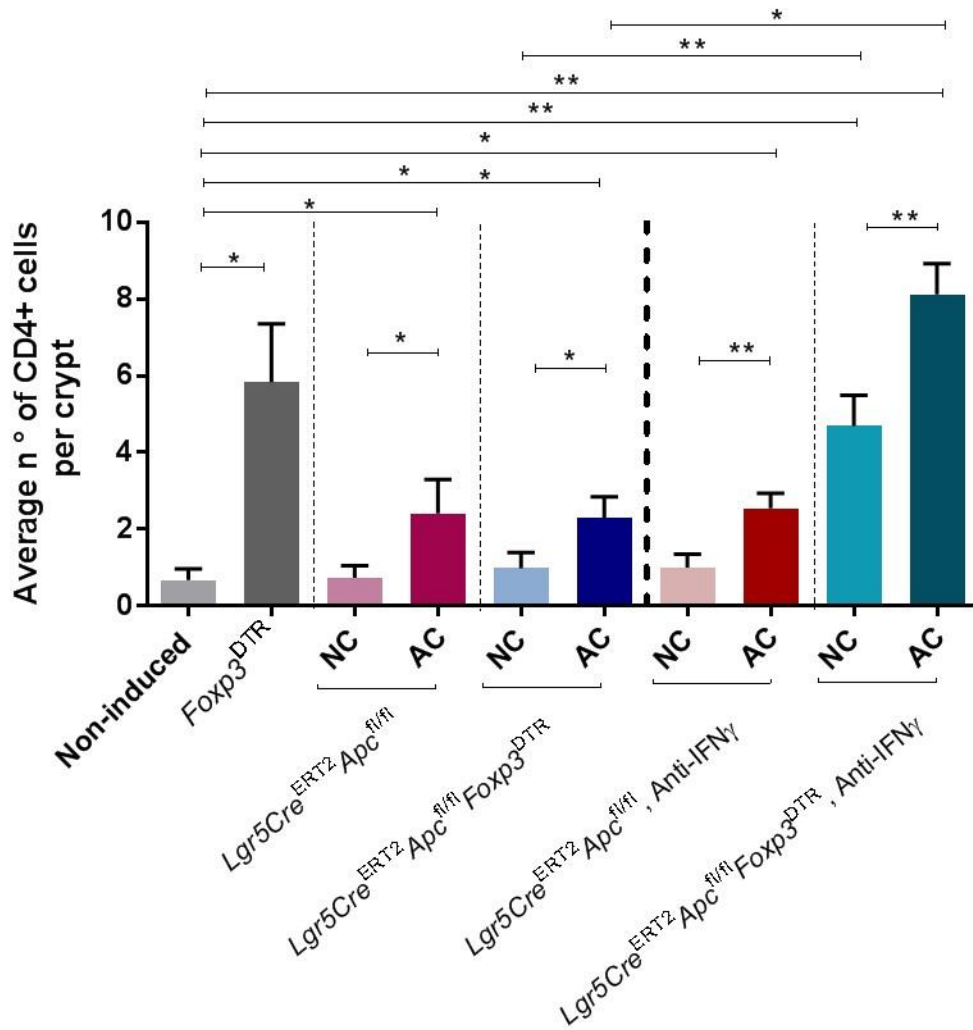
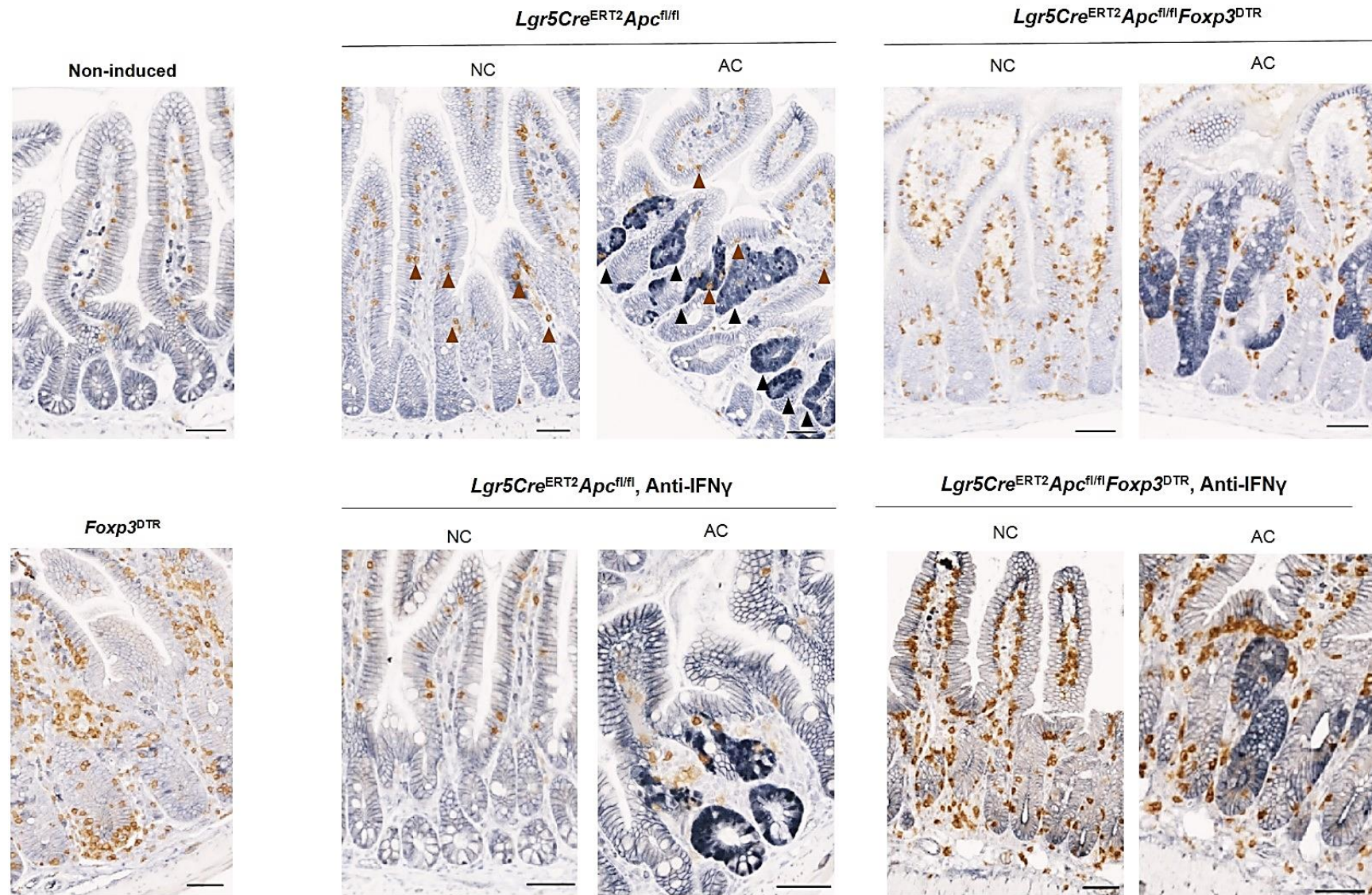


Figure 5.16 Quantification of CD4+ cells in the small intestine following IFN $\gamma$  neutralisation.

(A) Representative images of  $\beta$ -catenin (grey) and CD4+ cells (brown) IHC staining in the small intestine. Black arrows indicate aberrant crypts and brown arrows indicate CD4+ cells. (B) IFN $\gamma$  neutralisation resulted in a significantly increased number of CD4+ cells in the aberrant crypts in both *Apc* deleted, but particularly *Apc* deleted/Treg depleted mice, when compared to normal surrounding tissue. Data represent a single experiment,  $n \geq 4$  mice per group. Data for the non-induced, *Foxp3<sup>DTR</sup>*, *Lgr5Cre<sup>ERT2</sup>Apc<sup>fl/fl</sup>* and *Lgr5Cre<sup>ERT2</sup>Apc<sup>fl/fl</sup>Foxp3<sup>DTR</sup>* groups are repeated in figures 5.5 and 5.11. (\*) P value < 0.05, (\*\*) P value  $\leq$  0.01, two-tailed Mann Whitney U test. Error bars represent Standard Deviation (SD). Scale bars represent 50  $\mu$ m.

A



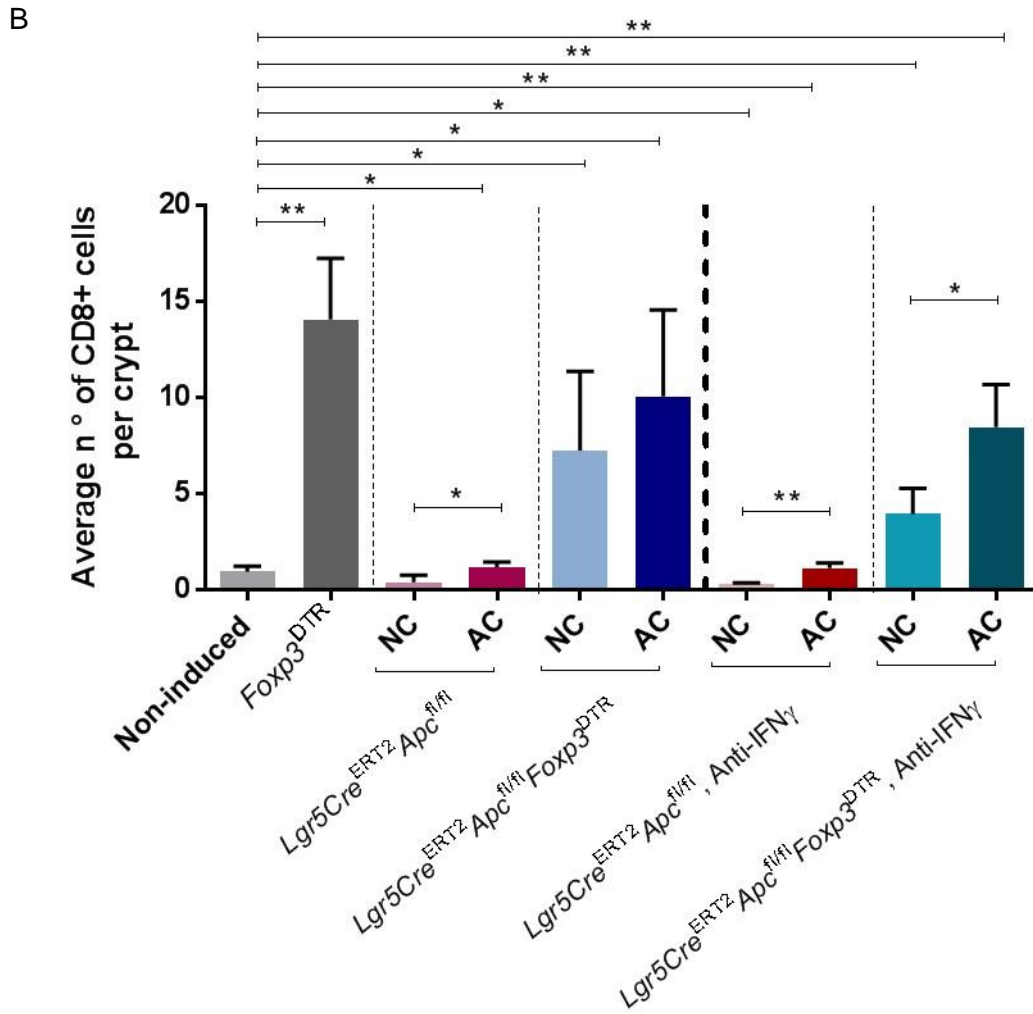


Figure 5.17 Quantification of CD8+ cells in the small intestine following IFN $\gamma$  neutralisation.

(A) Representative images of  $\beta$ -catenin (grey) and CD8+ cells (brown) IHC staining in the small intestine. Black arrows indicate aberrant crypts and brown arrows indicate CD8+ cells. (B) IFN $\gamma$  neutralisation resulted in a significantly increased number of CD8+ cells in the aberrant crypts of *Apc* deleted and *Apc* deleted/Treg depleted mice when compared to normal crypts. Data represent a single experiment,  $n \geq 4$  mice per group. Data for the non-induced, *Foxp3*<sup>DTR</sup>, *Lgr5Cre*<sup>ERT2</sup>*Apc*<sup>fl/fl</sup> and *Lgr5Cre*<sup>ERT2</sup>*Apc*<sup>fl/fl</sup>*Foxp3*<sup>DTR</sup> groups are repeated in figures 5.6 and 5.12. (\*) P value < 0.05, (\*\*) P value  $\leq$  0.01, two-tailed Mann Whitney U test. Error bars represent Standard Deviation (SD). Scale bars represent 50  $\mu$ m.

## 5.3 Discussion

The immune system has a complex role in cancer as immune cells can act both as suppressors of tumour initiation and progression (Dunn *et al.* 2004), but also as promoters of the disease (Balkwill and Coussens 2004). Recently, infiltration of tumours with high numbers of lymphocytes has been associated with a better prognosis and improved survival of cancer patients, not only in CRC (Galon *et al.* 2006; Mei *et al.* 2014; Braha *et al.* 2016), but also other tumour types such as breast (Menegaz *et al.* 2008) and lung cancer (Al-Shibli *et al.* 2008; Dieu-Nosjean *et al.* 2008). Previously, I have shown that Treg depletion increased both frequency and number of CD4+ and CD8+ cells regardless whether *Apc* is deleted. The frequency of IFN $\gamma$  was also increased upon Tregs depletion. In this chapter, I wanted to evaluate whether these alterations in the T-cells and IFN $\gamma$  play a role in reducing the number of aberrant crypts in the small intestine.

### 5.3.1 Evaluating the role of CD4+ cells in intestinal homeostasis

CD4+ cells are a very heterogeneous population that includes a variety of sub-populations that have been described as pro- and anti-tumoral. These sub-populations comprise, for example Tregs, Th1 and Th17 cells. Tosolini and colleagues have analysed, in CRC patients, the balance between different populations of T-lymphocytes and how they correlate with disease-free survival. They have shown that increased frequencies of Th17 cells were associated with a poor prognosis, whereas increased numbers of Th1 cells was linked to a prolonged disease-free survival (Tosolini *et al.* 2011). I have previously shown that Treg depletion results in a decreased tumour burden in the intestine. In this chapter, I demonstrated that depletion of CD4+ cells significantly reduced the small intestinal tumour burden. Taken together, these data indicate that in the early stages of tumour initiation, CD4+ T cells are more likely to promote than prevent tumour growth. A more in-depth analysis of the T cell subsets involved is now needed.

Interestingly, CD4+ cell depletion in *Apc* deleted and *Apc* deleted/Treg cells depleted mice resulted in a significantly reduced gene expression of the Wnt markers *Axin2* and *c-Myc*, when compared to *Apc* deletion alone, suggesting again that depletion of CD4+ cells was beneficial in the early stages of intestinal cancer. CD4+ cell depletion was associated with reduced the gene expression of the ISC and Wnt marker *Lgr5*, in *Apc* deleted mice, but had no effects in the other ISC markers *Olfm4* and *Ascl2*, suggesting that the ISC population was not altered.

In a recently published study, it was demonstrated that CRC suppress CD4+ T-cells immunity through canonical Wnt signalling (Sun *et al.* 2017). Sun and colleagues

demonstrated that  $\beta$ -catenin was elevated in intra-tumoral T-cells, which correlated with decreased IFN $\gamma$  expression and increased IL-17A expression in activated CD4 $^{+}$  cells (Sun *et al.* 2017). Here, CD4 $^{+}$  cells depletion, in *Apc* deleted mice, significantly reduced the relative gene expression of IFN $\gamma$  when compared to *Apc* deleted mice.

Analysis of CD8 $^{+}$  cells number, in CD4 $^{+}$  cells depleted mice, showed an accumulation of these cells around the newly formed lesions compared to normal surrounding tissue. The same was observed in *Apc* deleted mice, suggesting that CD8 $^{+}$  T-cells play a key role in the anti-tumour immune responses in the early stages of intestinal cancer.

### 5.3.2 Evaluating the role CD8 $^{+}$ cells in the intestinal homeostasis

CD8 $^{+}$  cells have long been considered a key population in anti-tumour immunity and infiltration by these cells has been associated to a better prognosis in a number of malignancies such as breast (Liu *et al.* 2012; Ziai *et al.* 2018), melanoma (van Oijen *et al.* 2004), ovarian (Hamanishi *et al.* 2007), pancreatic (Fukunaga *et al.* 2004) as well as CRC (Galon *et al.* 2006; Pages *et al.* 2009; Mlecnik *et al.* 2011; Ziai *et al.* 2018).

It is therefore surprising that the data herein demonstrate that CD8 $^{+}$  cells depletion in *Apc* deleted mice significantly reduces the tumour burden in the small intestine. In accordance with this, Wnt signalling markers were significantly reduced in CD8 $^{+}$  cell depleted mice when comparing to *Apc* deleted mice, indicating a reduction in Wnt activation and supporting the decreased number of aberrant crypts. The same was observed for the ISC markers *Lgr5* and *Ascl2*, possibly indicating a reduction in the ISC pool and, as a consequence, a reduction in the number of *Apc* deficient ISC, resulting in a decreased number of aberrant crypts. The increased gene expression of *Foxp3* was attenuated following CD8 $^{+}$  cell depletion in *Apc* deleted mice, when compared to *Apc* deletion alone, suggesting again a beneficial effect of CD8 $^{+}$  cell depletion in this model. CD8 $^{+}$  cell depletion significantly reduced the gene expression of IFN $\gamma$ . CD8 $^{+}$  cell depletion alone did not alter the number of CD4 $^{+}$  cells in the small intestinal crypts, however CD8 $^{+}$  cell depletion in *Apc* deleted mice significantly increased the number of CD4 $^{+}$  cells in the aberrant crypts, possibly suggesting that CD4 $^{+}$  cells may be having a beneficial effect in controlling tumour growth.

Treatment with the depleting antibody, as expected, significantly reduced the number of CD8 $^{+}$  cells, however not completely. Interestingly, CD8 $^{+}$  T-cells accumulated in the aberrant crypts of *Apc* deleted, but particularly *Apc* deleted/Treg depleted mice, suggesting that these cells are attracted to the pro-tumorigenic tissue in the absence of Tregs even when a depleting antibody is applied. Another possible explanation is that is

this experimental group (*Lgr5Cre<sup>ERT2</sup>Apc<sup>fl/fl</sup>Foxp3<sup>DTR</sup>*, Anti-CD8) CD8+ cell depletion was not efficient. In the future, a higher dose of depleting antibody or injection with another clone (YTS-156) together with YTS-169 could be tested in order to improve CD8+ depletion (Jones *et al.* 2002). To further understand the effects of T-cell depletion in the reduction of the number of aberrant crypts, other experiments should be included, such as cleaved caspase 3 IHC to analyse the intestinal apoptotic index, as this may be a possible mechanism by which there is a reduction in the tumour burden.

Taken together, these data suggest that CD8+ cell depletion had a beneficial effect in the early stages of intestinal cancer, contradicting the initial hypothesis that CD8+ cells depletion would promote tumourigenesis.

### 5.3.3 Evaluating the role of IFN $\gamma$ in the intestinal homeostasis

Finally, I analysed the effect of IFN $\gamma$  neutralisation in the initiation of intestinal cancer. The interaction between the tumour and the immune cells is a controlled process in all stages of tumour progression, in which IFN $\gamma$  plays a key role. Studies have shown that genetic variations in IFN $\gamma$  are associated with a lower survival following CRC diagnosis (Slattery *et al.* 2011; Bondurant *et al.* 2013; Di Franco *et al.* 2017; Kosmidis *et al.* 2018). Wang and colleagues investigated the role of IFN $\gamma$  deficiency in *Apc<sup>min</sup>* mice. IFN $\gamma$  deficient mice had an increased number and size of adenomas with increased Wnt signalling (Wang *et al.* 2015a). Moreover, administration of IFN $\gamma$  inhibited the proliferation of *Apc* mutated colon cancer cell line but not wild-type cell lines *in vitro*. *In vitro* knockdown of IFN $\gamma$  increased cell proliferation and colony formation, suggesting that IFN $\gamma$  participates in the anti-tumour immune responses (Wang *et al.* 2015a).

Surprisingly, IFN $\gamma$  neutralisation did not increase the tumour burden in the small intestine of the treated mice. IFN $\gamma$  neutralisation significantly increased the expression of the Wnt markers *Axin2* and *c-Myc*, however this effect was attenuated when compared to *Apc* deletion alone, suggesting a beneficial effect of IFN $\gamma$  neutralisation in this mouse model. Relative gene expression of the ISC markers were only significantly reduced following IFN $\gamma$  neutralisation in *Apc* deleted/Treg depleted mice when compared to *Apc* deleted mice. This was similar to what was observed in *Apc* deleted/Treg depleted mice, possibly indicating that this effect is mainly due to Treg depletion and not IFN $\gamma$  neutralisation. IFN $\gamma$  neutralised mice had an increased number of both CD4+ and CD8+ cells around the newly formed lesions. A limitation in this study was the fact that IFN $\gamma$  neutralization was not confirmed by IHC and/or flow cytometry. This is clearly necessary before any firm conclusions can be drawn. Importantly, for the immune cell depletion and cytokine neutralisation, the tumour burden was only quantified in the first 5 cm of the

small intestine due to experimental limitations, particularly the concentration of antibodies available for the injections. Further experiments should include the quantification of the total tumour burden in serial sections of the whole small and large intestines in order to confirm these findings. Considering that it was not possible to include a group with CD4+ depletion and IFN $\gamma$  neutralisation alone, in the next experiments these should be included. Future experiments should also include confirmation of T-cell depletion and IFN $\gamma$  neutralisation by IHC, flow cytometry and/or ELISA.

In summary, in this chapter it was shown that both CD4+ and CD8+ cell depletion significantly decreased the small intestinal tumour burden. IFN $\gamma$  neutralisation had no effect on the number of aberrant crypts. The changes in the intestine, as a consequence of the altered immune system in the *Lgr5Cre<sup>ERT2</sup>Apc<sup>fl/fl</sup>Foxp3<sup>DTR</sup>* following T-cell depletion and IFN $\gamma$  neutralisation, gave unexpected results, such as the decreased tumour burden following CD8+ cell depletion.

One possible explanation is that CD8-depleting antibodies might impact on the ISC pool thereby reducing the targets for *Apc* deletion and, as a consequence, reducing the intestinal tumour burden. Further experiments should include CD8+ cell depletion following *Apc* deletion in the ISCs in order to clarify whether the reduced tumour burden observed is a consequence of eliminating CD8+ cells and not because ISCs number was altered by the antibody treatment. In addition, changes in the *Lgr5* ISC stem cells could be analysed *in situ* by RNAscope. This will provide information about the changes in *Lgr5* transcripts, not only their number, but also localization in the intestine, possibly giving new insights into how the immune system impacts intestinal homeostasis. Part of this analysis will be presented in the following chapter.

## 6 RNAscope analysis of *Lgr5* transcripts in the early stages of intestinal cancer

### 6.1 Introduction

In the previous chapter it was demonstrated that depletion of CD4+ and CD8+ T-cells significantly reduced the tumour burden in the mice small intestine. This was particularly surprising with CD8+ T-cells depletion, where it was expected an increased number of aberrant crypts, as these cells have been considered responsible for the anti-tumour immune response in a variability of cancers (van Oijen *et al.* 2004; Liu *et al.* 2012; Ziai *et al.* 2018), including CRC, but the opposite was observed.

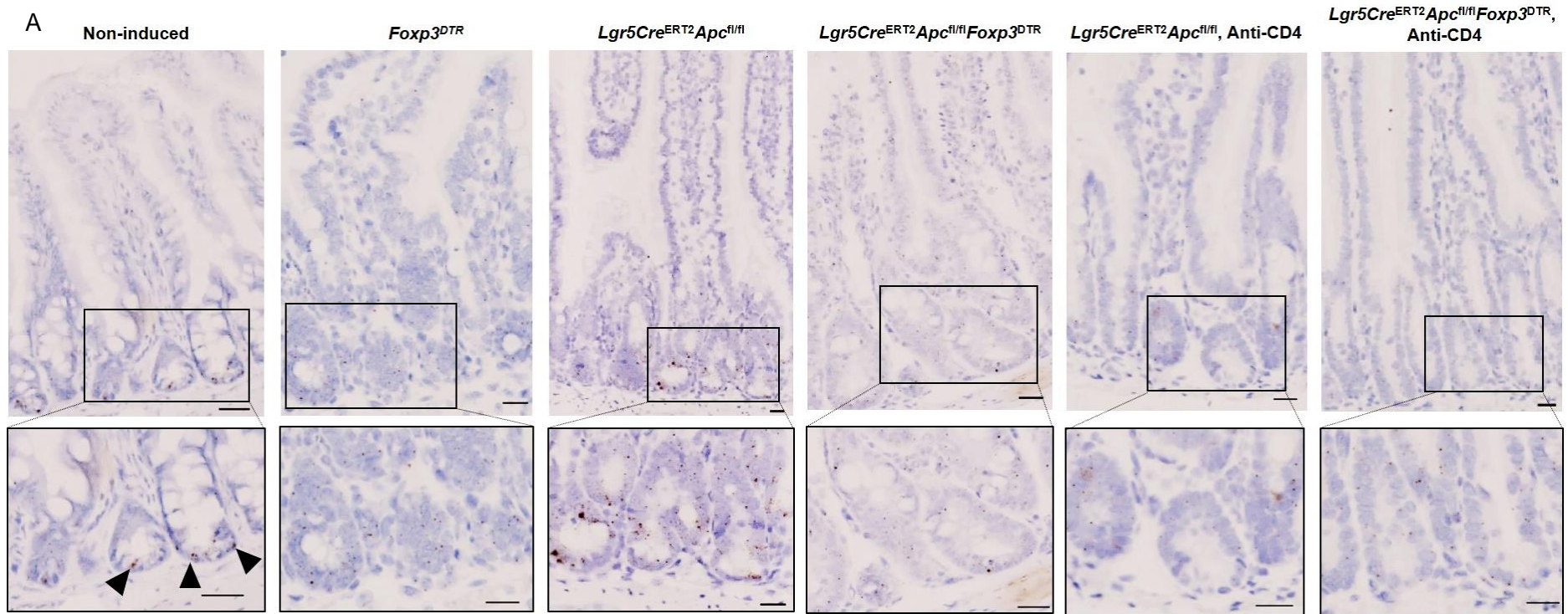
Depletion of CD8+ cells was done prior to *Apc* deletion in the ISCs. It is possible that this altered the stem cell pool. If that was the case, a lower number of ISCs would be transformed explaining the reduced number of aberrant crypts. It was, then, hypothesised that depletion of T-cells would impact in the homeostasis of the ISCs and that it would have a direct effect in the initiation of intestinal cancer. To start testing it, the number of *Lgr5* transcripts was analysed by RNAscope in the small intestine of the previously described groups. This method allows the visualization of the transcripts in the tissue providing quantitative data on expression of *Lgr5*, the number of cells which express it and their localisation.

## 6.2 Results

The previously described groups were used in the analysis of *Lgr5* transcripts by RNAscope staining. *Lgr5* transcripts were identified by the brown stained dots, independently of the intensity of the staining. As expected, the number of *Lgr5* transcripts was significantly increased in the crypts of *Apc* deleted mice (Figure 6.1), when compared to non-induced mice, reflecting the increase that was previously observed in the gene expression analysis by qRT-PCR (Figure 4.4). Interestingly, Treg depletion in *Apc* deleted mice resulted in a reduced number of *Lgr5* transcripts when compared to *Apc* deletion alone (Figure 6.1), suggesting that the reduced tumour burden in *Apc* deleted/Treg depleted mice (Figure 4.1) can be explained by a reduced number of transformed ISC. The same is observed in mice where CD4<sup>+</sup> cells were depleted (Figure 6.1), possibly explaining again the reduced tumour burden observed (Figure 5.1). Interestingly, Treg depletion alone did not alter significantly the number of *Lgr5* transcripts, however altered the re-distribution of the transcripts, possibly suggesting that Tregs play a role in the homeostasis of ISCs (Figure 6.1).

Depletion of CD8<sup>+</sup> T-cells did not alter the number of *Lgr5* transcripts when compared to non-induced mice, however there was a re-distribution of the transcripts from the bottom to other parts of the crypts (Figure 6.2). The same was observed in *Apc* deleted/CD8<sup>+</sup> cell depleted mice (Figure 6.2). Taken together these data suggest that depletion of CD8<sup>+</sup> cells alter the homeostasis of the ISCs and that is might be the reason why CD8<sup>+</sup> cell depletion in *Apc* deleted mice resulted in a reduced tumour burden (Figure 5.7).

IFN $\gamma$  neutralisation resulted in a significantly decreased the number of *Lgr5* transcripts in *Apc* deleted mice and altered their re-distribution in the crypts (Figure 6.3), however, in this case, the reduced number of *Lgr5* transcripts was not reflected in a reduced tumour burden (Figure 5.13).



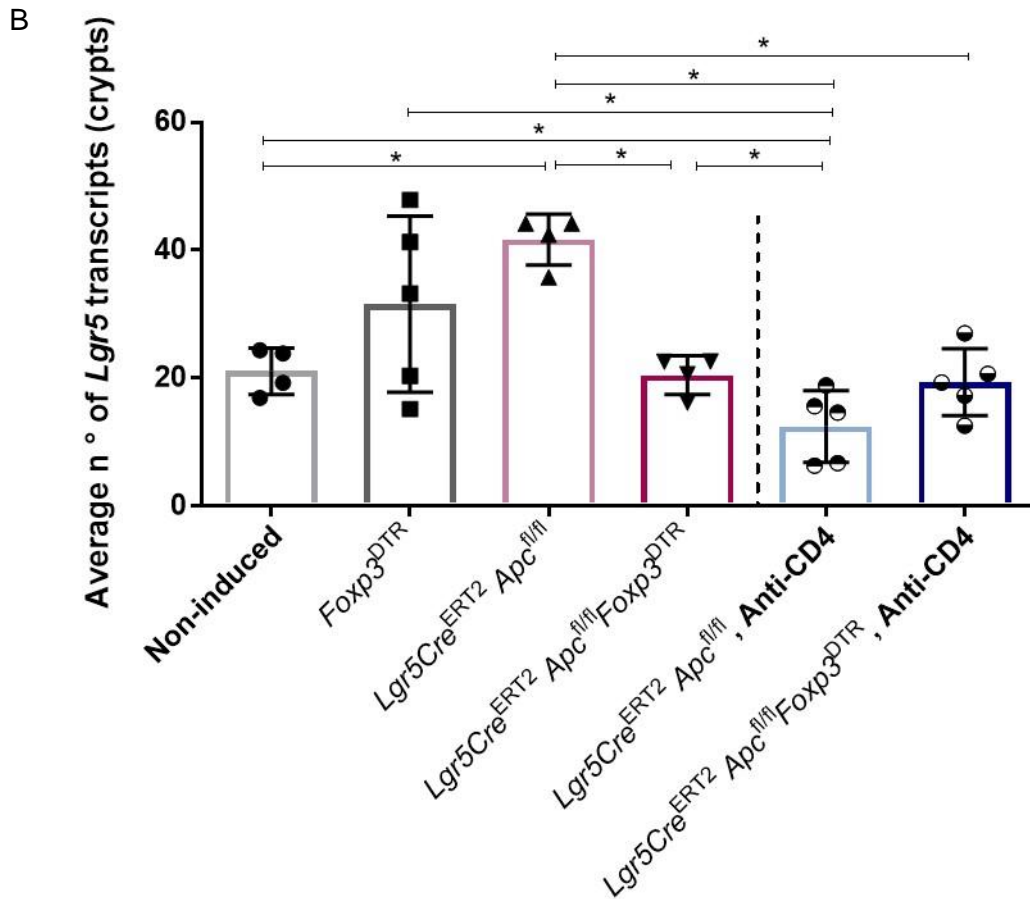
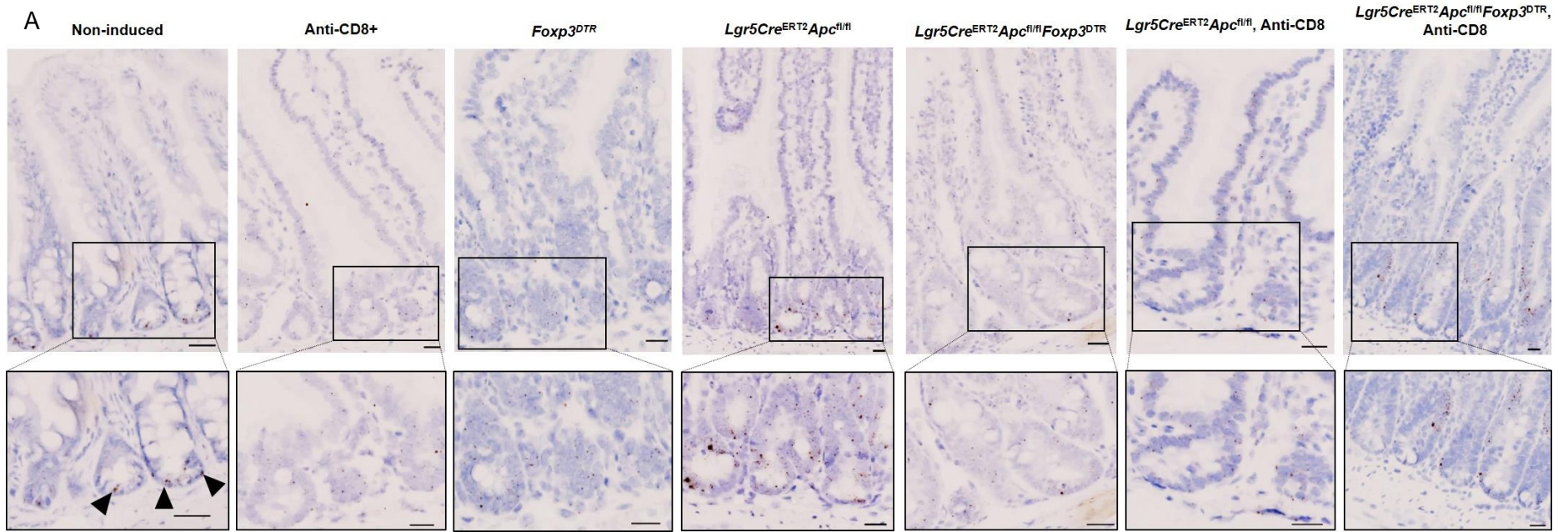
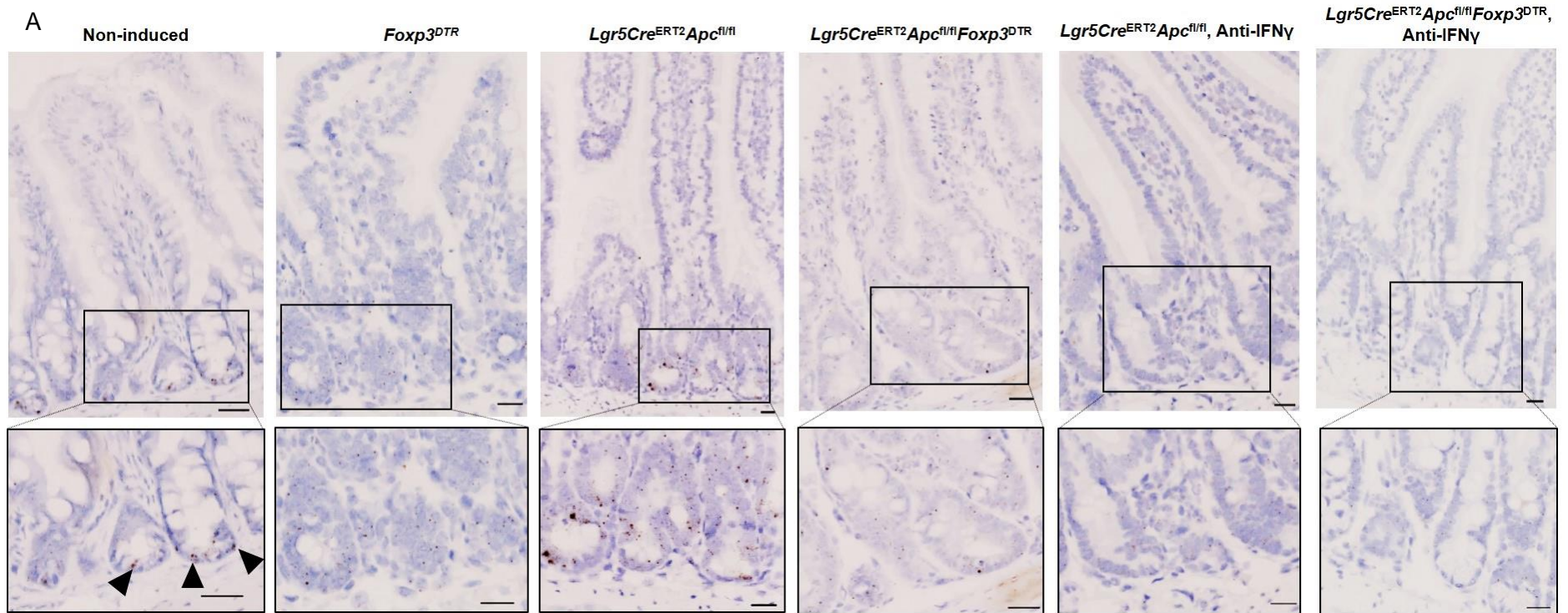


Figure 6.1 *Lgr5* expression analysis in the small intestinal crypts following CD4+ T-cells depletion.

(A) Representative images of *Lgr5* (brown) RNAscope staining in the small intestine. Black arrow indicated an example of a brown dot representing an *Lgr5* transcript. (B) *Apc* deletion significantly increased the number of *Lgr5* transcripts in the crypts. Depletion of CD4+ T-cells in *Apc* deleted mice significantly reduced the number of *Lgr5* transcripts. Data represent a single experiment,  $n \geq 4$  mice per group. (\*) P value < 0.05, two-tailed Mann Whitney U test. Error bars represent Standard Deviation (SD). Scale bars represent 20  $\mu$ m.







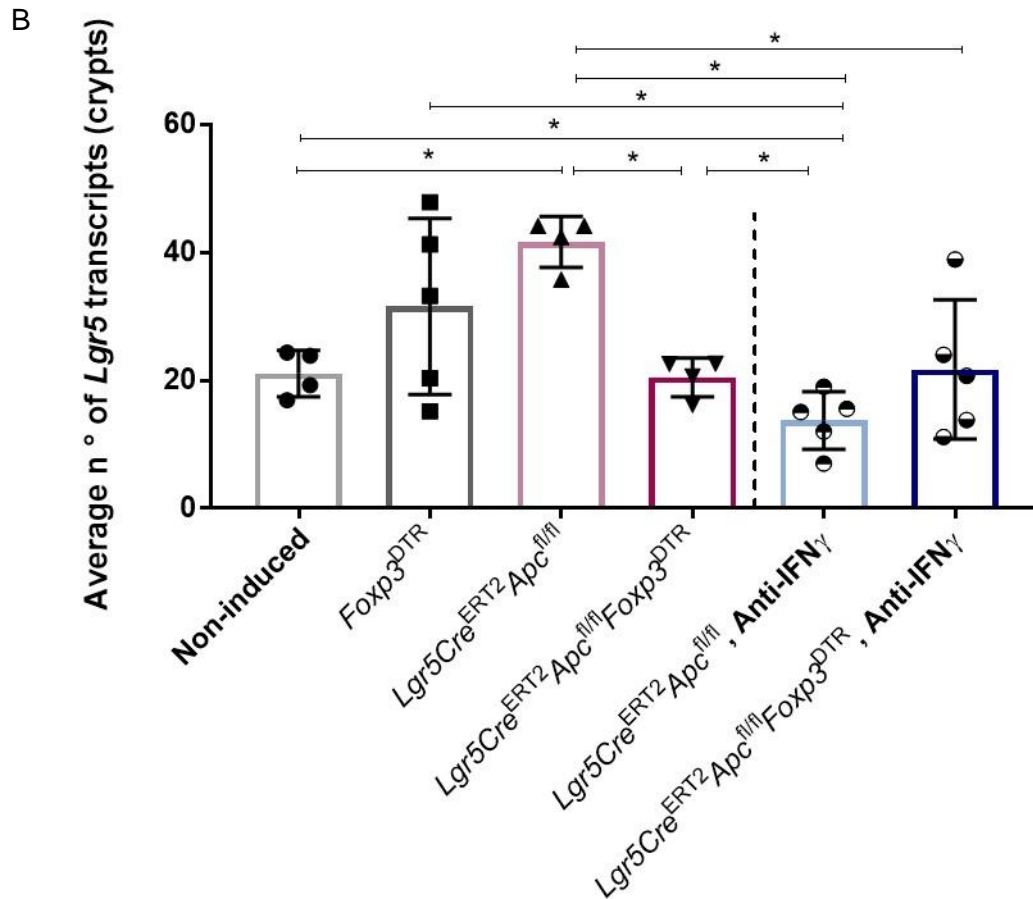


Figure 6.3 *Lgr5* expression analysis in the small intestinal crypts following IFN $\gamma$  neutralisation.

(A) Representative images of *Lgr5* (brown) RNAscope staining in the small intestine. (B) IFN $\gamma$  neutralisation in *Apc* deleted mice significantly reduced the number of *Lgr5* transcripts in the crypts. There were no significant changes following IFN $\gamma$  neutralisation in *Apc* deleted/Treg cells depleted mice. Data represent a single experiment,  $n \geq 4$  mice per group. Data for the non-induced, *Foxp3*<sup>DTR</sup>, *Lgr5Cre*<sup>ERT2</sup>*Apc*<sup>fl/fl</sup> and *Lgr5Cre*<sup>ERT2</sup>*Apc*<sup>fl/fl</sup>*Foxp3*<sup>DTR</sup> groups are repeated in figures 6.1 and 6.2. (\*) P value < 0.05, two-tailed Mann Whitney U test. Error bars represent Standard Deviation (SD). Scale bars represent 20  $\mu$ m.

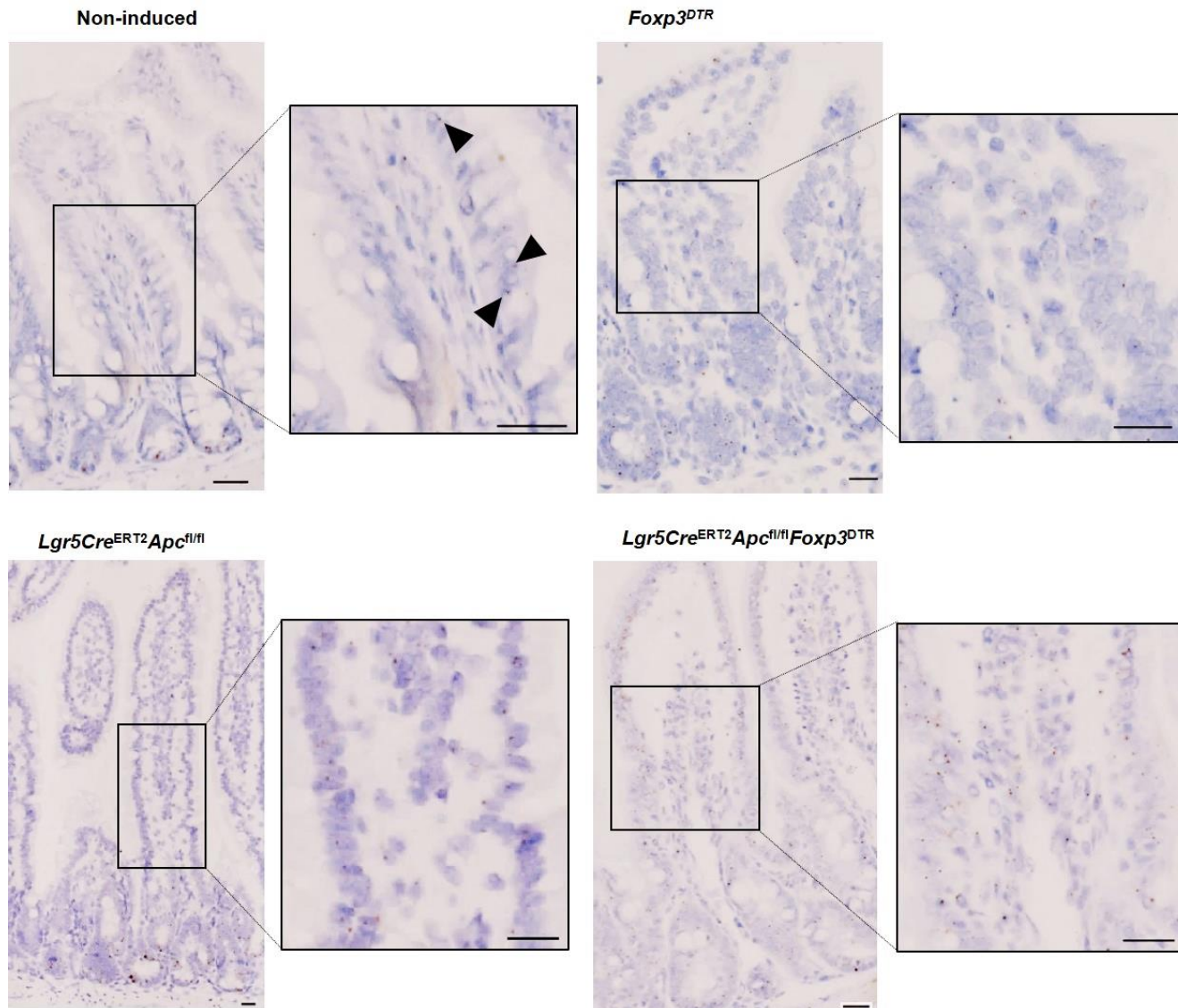
To further evaluate the how the immune changes affected the homeostasis of the ISCs, the number of *Lgr5* transcripts was quantified in the villi of the previously analysed mice. As expected, the number of *Lgr5* transcripts was significantly increased in the villi of *Apc* deleted mice (Figure 6.4). Depletion of CD4+ cells in *Apc* deleted mice had no effect in the number of *Lgr5* transcripts in the villi, however increased in *Apc* deleted/Treg depleted mice, suggesting again that the immune cell populations may play a role in the homeostasis of ISCs (Figure 6.4).

Interestingly, CD8+ T-cells depletion, alone and in combination with *Apc* deletion, significantly increased the number of *Lgr5* transcripts in the villi, however this effect was significantly attenuated in *Apc* deleted/Treg cells depleted mice (Figure 6.5), suggesting once again a role of the immune system in the regulation of ISCs homeostasis.

The number of *Lgr5* transcripts was not altered following IFN $\gamma$  neutralisation in *Apc* deleted mice, however it was significantly increased in *Apc* deleted/Treg cells depleted mice (Figure 6.6).

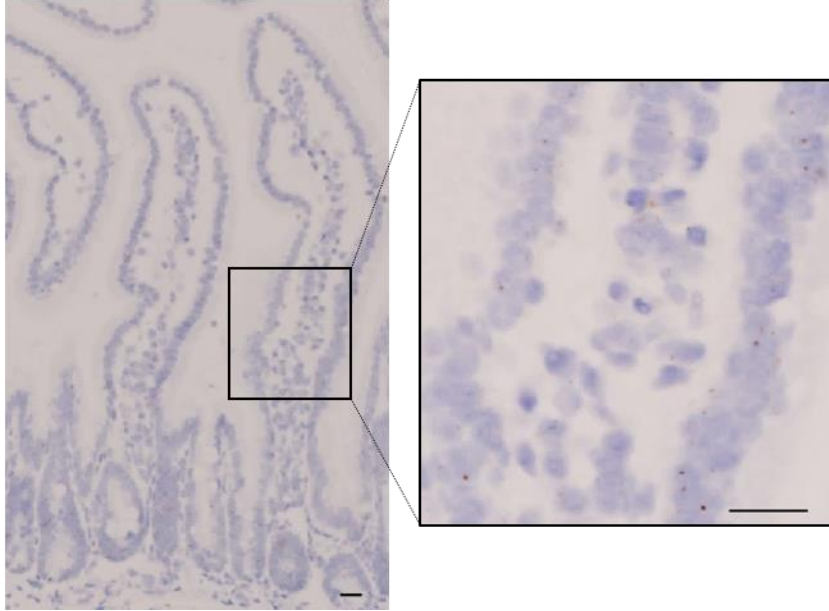
Taken together, these data show that either depletion of T-cells or neutralization of IFN $\gamma$  result in an altered distribution of *Lgr5* transcripts from the bottom of the crypts to other parts, including the villi, suggesting a role of these cells in the ISCs homeostasis.

A

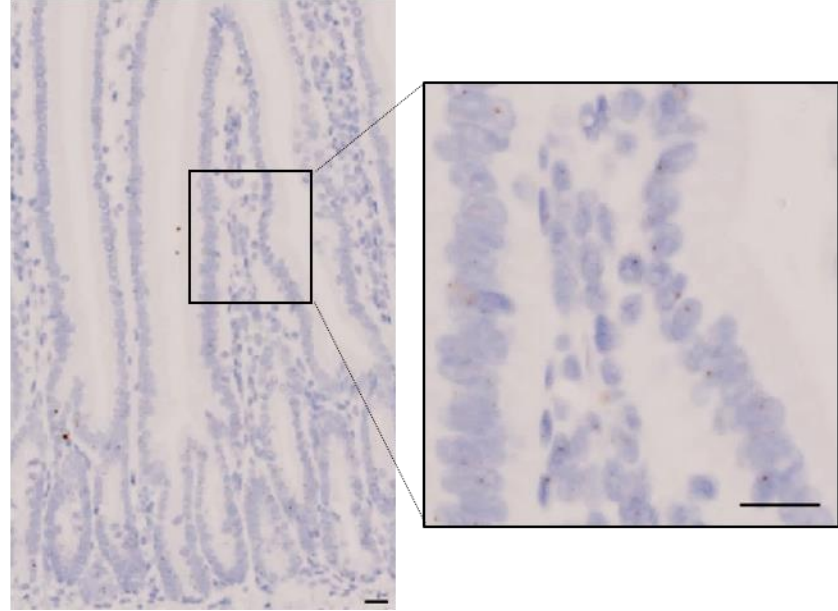


B

*Lgr5Cre<sup>ERT2</sup>Apc<sup>fl/fl</sup>*, Anti-CD4



*Lgr5Cre<sup>ERT2</sup>Apc<sup>fl/fl</sup>Foxp3<sup>DTR</sup>*,  
Anti-CD4



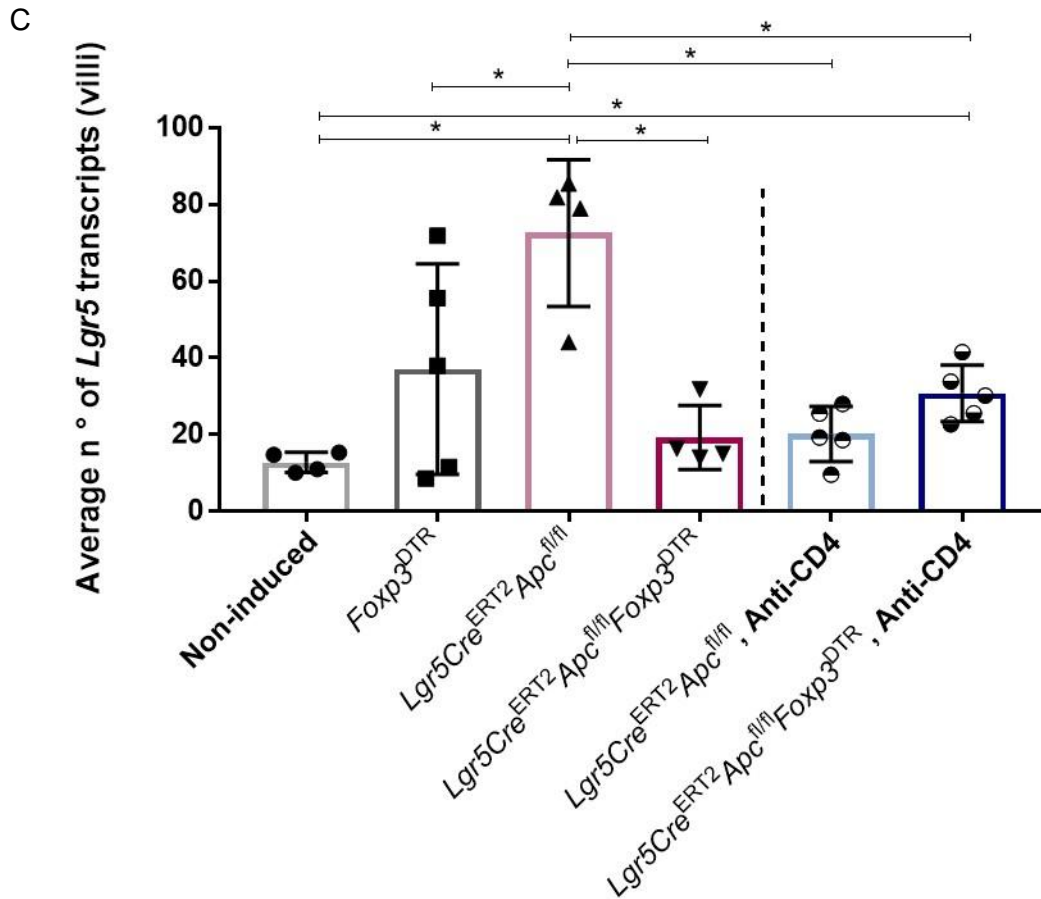
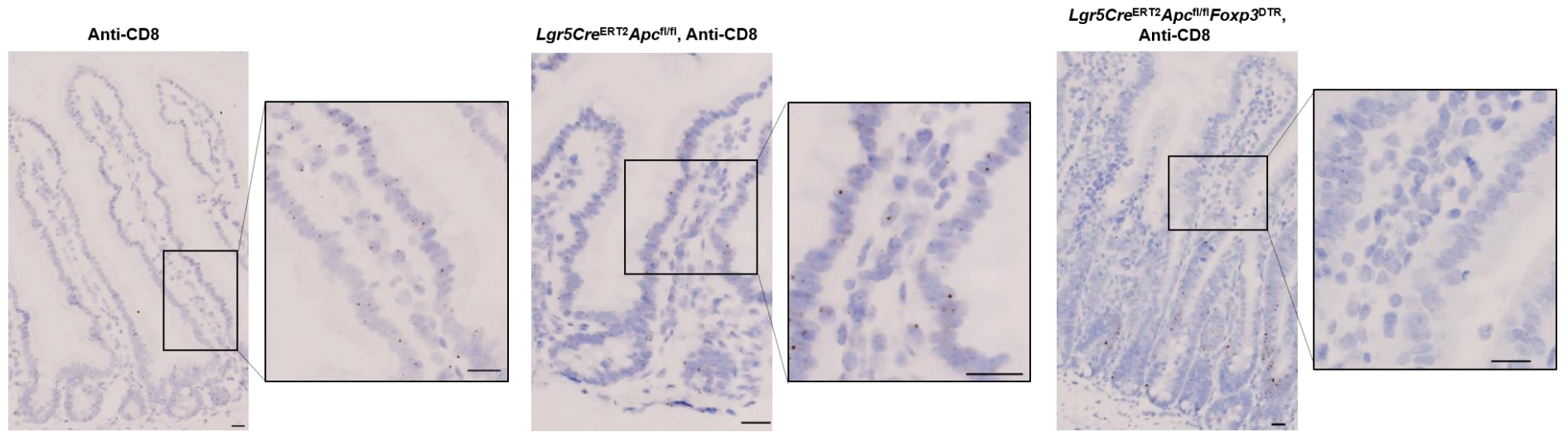


Figure 6.4 *Lgr5* expression analysis in the small intestinal villi following CD4+ T-cells depletion.

(A) & (B) Representative images of *Lgr5* (brown) RNAscope staining in the small intestine. (C) *Apc* deletion significantly increased the number of *Lgr5* transcripts in the villi. Depletion of CD4+ T-cells in *Apc* deleted did not alter the number of *Lgr5* transcripts, however increased in the villi of *Apc* deleted/Treg cells depleted mice. Data represent a single experiment,  $n \geq 4$  mice per group. (\*) P value < 0.05, two-tailed Mann Whitney U test. Error bars represent Standard Deviation (SD). Scale bars represent 20  $\mu\text{m}$ .

A



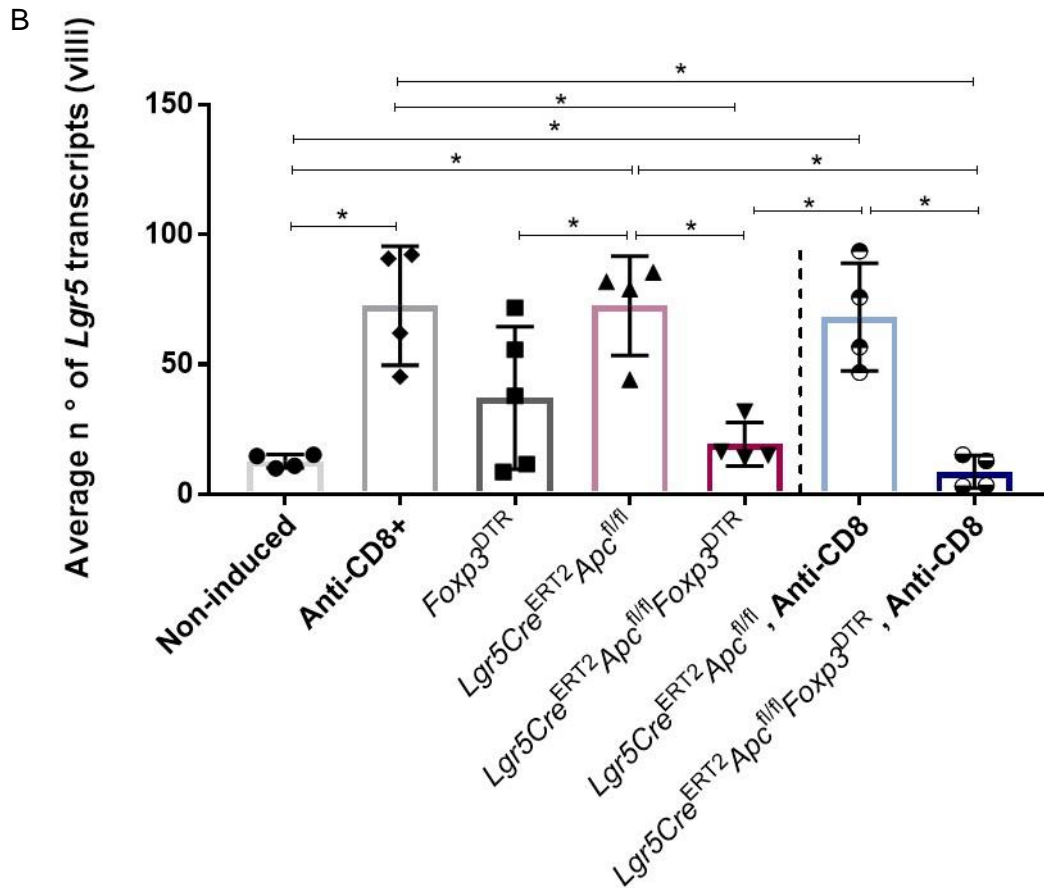
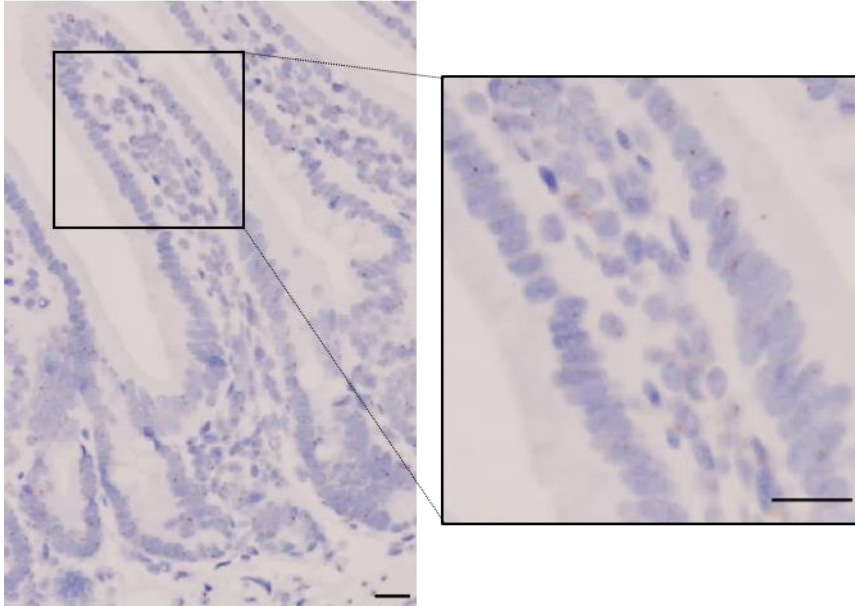


Figure 6.5 *Lgr5* expression analysis in the small intestinal villi following CD8+ T-cells depletion.

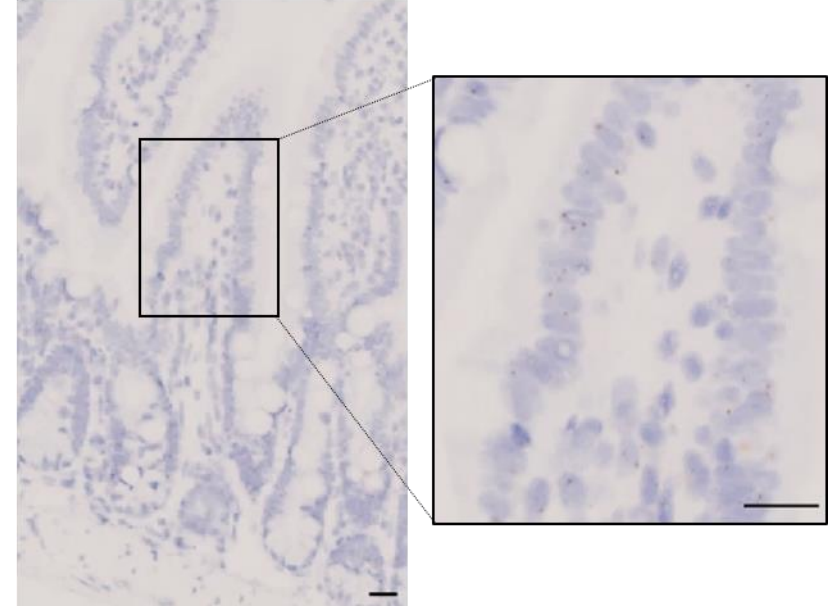
(A) Representative images of *Lgr5* (brown) RNAscope staining in the small intestine. (B) Depletion of CD8+ T-cells alone, and in *Apc* deleted mice, significantly increased the number of *Lgr5* transcripts in the villi. Data represent a single experiment,  $n \geq 4$  mice per group. Data for the non-induced, *Foxp3<sup>DTR</sup>*, *Lgr5Cre<sup>ERT2</sup>Apc<sup>fl/fl</sup>* and *Lgr5Cre<sup>ERT2</sup>Apc<sup>fl/fl</sup>Foxp3<sup>DTR</sup>* groups are repeated in figure 6.4. (\*) P value < 0.05, two-tailed Mann Whitney U test. Error bars represent Standard Deviation (SD). Scale bars represent 20  $\mu$ m.

A

*Lgr5Cre<sup>ERT2</sup>Apc<sup>fl/fl</sup>*, Anti-IFN $\gamma$



*Lgr5Cre<sup>ERT2</sup>Apc<sup>fl/fl</sup>Foxp3<sup>DTR</sup>*,  
Anti-IFN $\gamma$



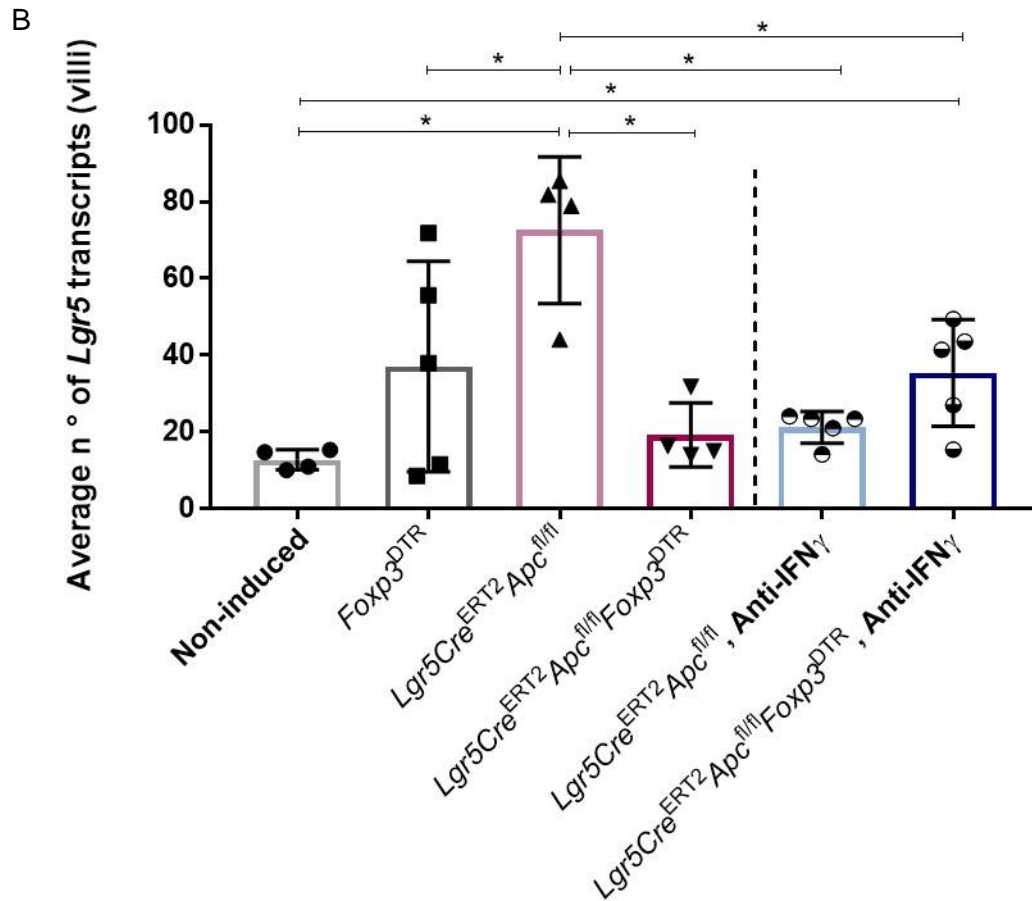


Figure 6.6 *Lgr5* expression analysis in the small intestinal villi following IFN $\gamma$  neutralisation.

(A) Representative images of *Lgr5* (brown) RNAscope staining in the small intestine. (B) IFN $\gamma$  neutralisation in *Apc* deleted mice did not alter significantly the number of *Lgr5* transcripts in the villi. IFN $\gamma$  neutralisation in *Apc* deleted/Treg depleted mice significantly increased the number of *Lgr5* transcripts in the small intestinal villi. Data represent a single experiment,  $n \geq 4$  mice per group. Data for the non-induced, *Foxp3<sup>DTR</sup>*, *Lgr5Cre<sup>ERT2</sup>Apc<sup>fl/fl</sup>* and *Lgr5Cre<sup>ERT2</sup>Apc<sup>fl/fl</sup>Foxp3<sup>DTR</sup>* groups are repeated in figures 6.4 and 6.5. (\*) P value < 0.05, two-tailed Mann Whitney U test. Error bars represent Standard Deviation (SD). Scale bars represent 20  $\mu$ m.

### 6.3 Discussion

The ISCs are essential in the maintenance of the intestinal homeostasis (Peterson and Artis 2014), where they give rise to the progenitors that, later differentiate to specific intra-epithelial cells (Munoz *et al.* 2012; Tetteh *et al.* 2016). It is well established that canonical signal pathways, such as Wnt and Notch are essential in the ISCs dynamics (Tian *et al.* 2015), however it is less known how immune cells and the adjacent ISCs interact.

I have previously demonstrated that depletion of T-cells has a direct effect in the number of aberrant crypts and I hypothesised that these immune cells had a direct effect in the ISCs homeostasis. Here, the number of *Lgr5* transcripts was quantified in the small intestines of non-induced, *Apc* deleted, T-cells depleted and IFN $\gamma$  neutralized mice.

The expression of *Lgr5*, in normal intestinal homeostasis, is restricted to the bottom of the crypts in both small and large intestines and it is lost upon cell differentiation (Barker *et al.* 2007; Barker *et al.* 2013). As expected, *Apc* deletion significantly increased the number of *Lgr5* transcripts in the small intestinal crypts and villi. Other studies have shown an increased expression of *Lgr5* in CRC cells relative to normal adjacent tissue (Fan *et al.* 2010; Wu *et al.* 2012; Baker *et al.* 2015; Wang *et al.* 2015b; Morgan *et al.* 2018).

So far, the interactions between immune cells and the ISCs were not fully studied, and this is reflected by the lack of literature in this field. Previous studies have suggested a role for the immune cells in tissue homeostasis of the intestine by showing that tissue-resident innate immune cells such as macrophages and type 3 innate lymphoid cells (ILC3s) rescue ISCs and promote their regeneration (Lindemans *et al.* 2015; Saha *et al.* 2016). Treg cells have been associated to tissue regeneration within muscles, lungs and the central nervous system (Burzyn *et al.* 2013; Arpaia *et al.* 2015; Dombrowski *et al.* 2017). Recently, Biton and colleagues have shown that CD4<sup>+</sup> T-helper (Th) cells communicate with ISCs and affect their differentiation (Biton *et al.* 2017). The authors used single-cell RNA-sequencing of intestinal epithelial cells in order to identify possible mechanisms for interactions between ISCs and immune cells (Biton *et al.* 2017). They have shown that MHC class II (MHC II) is enriched in subsets of *Lgr5* ISCs that are highly proliferative and that knockout of MHC II in the intestinal epithelial cells would promote the expansion of the ISCs pool (Biton *et al.* 2017). Moreover, the authors have shown that mice lacking T-cells had also expanded ISCs pools and that specific Treg cells depletion *in vivo* caused a reduction in the ISCs numbers (Biton *et al.* 2017). Contrary to this work, I have shown that Treg cells depleted mice had a trend for an increased

number of *Lgr5* transcripts in both crypts and villi suggesting an alteration in the homeostasis of *Lgr5* in the absence of Treg cells. Depletion of CD4+ T-cells in *Apc* deleted mice significantly decreased the number of *Lgr5* transcripts the crypts and had no significant changes in the villi. It is possible that, in the context of cancer, depletion of the immune cells will have a different effect when compared to T-cells depleted WT mice.

CD8+ T-cells depletion alone did not alter the number of *Lgr5* transcripts in the crypts, but resulted in a re-distribution from the bottom of the crypt to other parts. CD8+ depletion resulted in a significantly increased in the villi, suggesting again that depletion of immune cells have a direct impact in the ISCs. On the other hand, CD8+ T-cells depletion in *Apc* deleted mice had a trend for an increased number of *Lgr5* transcripts in crypts, but significantly increased in the villi. IFN $\gamma$  neutralisation significantly decreased the number of *Lgr5* transcripts in the crypts of *Apc* deleted mice and increased in the villi of *Apc* deleted/Treg cells depleted, suggesting one more time an interaction between the immune system and regulation of ISCs.

The quantification of the number of transcripts does not explain itself the reduction of aberrant crypts following the depletion of Treg cells, CD4+ and CD8+ T-cells. An important study would be quantifying the localization of the stem cells in the crypts in the different experimental groups. Alteration in the position of the stem cells could mean that they would not function as they usually do and that, following induction with tamoxifen, less stem cells would be transformed, being a possible reason for the reduced number of aberrant crypts following T-cells depletion. Barker and colleagues have demonstrated that only the cells located in the bottom of the crypt can initiate tumours (Barker *et al.* 2009). The presence of more transcripts does not exactly mean more *Lgr5* stem cells as it is possible that the homeostasis is interrupted and that these cells do not function anymore as normal ISCs. To verify the capacity of the ISCs, crypt and villus cells from the T-cell depleted mice could be isolated and their stemness evaluated by their capacity of developing organoids.

In summary, it was shown that depletion of T-cells and IFN $\gamma$  neutralisation affected the number and distribution of *Lgr5* transcripts, suggesting that there is a crosstalk between the immune system and the ISCs and that it must be further analysed.

## 7 General Discussion/Conclusion

Foxp3<sup>+</sup> Tregs are enriched in mouse (Akeus *et al.* 2014) and human tumours (Clarke *et al.* 2006; Betts *et al.* 2012; Syed Khaja *et al.* 2017), however it is still unclear whether these cells limit or promote the anti-tumour immune responses. Most of the studies were done in patients with advanced disease. There is a need to understand the role of these cells in the early stages of tumourigenesis.

The first aim of this project was to understand how Tregs were affected in the early stages of intestinal cancer. Using the *Lgr5Cre<sup>ERT2</sup>Apc<sup>fl/fl</sup>Foxp3<sup>DTR</sup>* mouse model it was possible to delete the *Apc* gene in the Lgr5 ISCs mimicking an early event of the intestinal tumourigenesis initiation. It was hypothesised that the number and frequency of Tregs would increase 15 days following *Apc* deletion. It was shown for the first time, in this model, that Tregs accumulate in both small and large intestines, but also spleen and MLN indicating that the suppressive immune response is also enhanced in the distant sites. As previously discussed in chapter 3, the mechanism responsible for the accumulation of Tregs upon ISCs *Apc* deletion is still not clarified. Possibly there is a disruption of the epithelial barrier, promoting infiltration of bacteria and, as a consequence, activation of the immune system leading to the attraction of Tregs to the lesions sites. Another possibility is that ISCs can function as non-conventional antigen-presenting cells, attracting and activating Tregs (Figure 7.1).

Little changes were detected in other immune markers following *Apc* deletion. One possible reason for this observation was that at this early time point where the analysis was performed, large scale changes in the immune activation were not detectable. Another possible explanation is that as the analysis was performed using the whole small and large intestines potentially local changes were masked.

The second aim was to investigate whether Tregs play a pro- or anti-tumoral role in the *Lgr5Cre<sup>ERT2</sup>Apc<sup>fl/fl</sup>Foxp3<sup>DTR</sup>* mouse model. Depletion of Tregs have been previously reported as having a beneficial effect in both mouse models (Chaput *et al.* 2007; Goudin *et al.* 2016) and cancer patients. This was tested in few clinical trials in patients with metastatic disease (Dannull *et al.* 2005), including patients with inoperable metastatic CRC (Scurr *et al.* 2017a; Scurr *et al.* 2017b), where it was observed an unleashed immune response and, as a consequence, an improved survival outcome.

It was hypothesised that Treg depletion would enhance the anti-tumour immune responses and limit tumour initiation and progression. As expected, Treg depletion in

*Apc* deleted mice resulted in a decreased tumour burden in the mice intestines, particularly in the large intestine.

The reduced tumour burden following Treg depletion was also supported by the reduced gene expression of Wnt and ISC markers, considering that their high expression is associated with tumour progression (2012; Polakis 2012). Treg depletion also resulted in an increase frequency of CD8+ producing Granzyme B and IFN $\gamma$  cells. These cells have been demonstrated to participate in the anti-tumour immune responses, suggesting that they play an important role since the early stages of tumourigenesis. Taken together, these data suggest that Tregs play key role in the early stages of tumour initiation.

Controversial data about the role of Tregs can be attributed to various reasons. In the case where cancer development is inflammation-driven Tregs may limit cancer growth by suppressing inflammation (Erdman 2010). Another explanation is that the populations of Tregs that were analysed may be heterogeneous in terms of their functional state and/or stability, possibly affecting whether they would promote or limit tumour progression.

It is possible that by giving to the *Lgr5Cre<sup>ERT2</sup>Apc<sup>fl/fl</sup>Foxp3<sup>DTR</sup>* mice dextran sodium sulphate (DSS) to induce chronic inflammation, possibly Tregs would play a key role but in the anti-tumoral immune responses. It has also been suggested a beneficial effect of a high fibre diet in the prevention of CRC (Burkitt 1971). A high fibre diet is known to have anti-inflammatory properties (Kunzmann *et al.* 2015). This is due to an increase in the metabolite butyrate produced as a consequence of fibre fermentation by the microbiota present in the large intestine (Cushing *et al.* 2015). Studies have shown that butyrate promotes differentiation of naïve CD4+ cells into Tregs, limiting inflammatory challenges (Zeng and Chi 2015).

Considering that the data in this project suggested that Tregs play a key role in the early stages of intestinal cancer by limiting the anti-tumour immune responses, the next aim was the identification of immune cell populations and cytokines that were possibly responsible for the anti-tumour immune responses following Tregs depletion. Previous data from this project showed increased frequency of CD4+ and CD8+ cells following Treg depletion in the early stages of intestinal cancer. The same was observed with the cytokine IFN $\gamma$ . Infiltration of tumours with high numbers of lymphocytes has been associated with a better prognosis and improved survival in CRC cancer patients (Galon *et al.* 2006; Mei *et al.* 2014; Braha *et al.* 2016) and in other cancer types (Al-Shibli *et al.* 2008; Dieu-Nosjean *et al.* 2008; Menegaz *et al.* 2008).

To analyse the role of T-cells and IFN $\gamma$  in the early stages of intestinal cancer, mice were injected with monoclonal antibodies to selectively deplete separately CD4 $^{+}$  and CD8 $^{+}$  cells and neutralise IFN $\gamma$ . Depletion of CD4 $^{+}$  cells, in *Apc* deleted mice, resulted in a decreased number of aberrant crypts in the first 5 cm of the small intestine. Further studies are needed to analyse the role of the different T-cell subsets involved in the early tumourigenesis. Depletion of Th1 or Th17 cells, or neutralisation of the cytokines secreted by these cells, would give new insights about the role of different CD4 $^{+}$  cell subpopulations, clarifying how which one could be targeted to stop tumour progression.

The previous findings that suggested an important role of CD8 $^{+}$  cells in the anti-tumour immune responses in the early stages of intestinal cancer were, surprisingly, contradicted by the reduction of the number of aberrant crypts in the first 5 cm of *Apc* deleted/CD8 $^{+}$  cells depleted mice. The reduction in the tumour burden was associated with a decreased gene expression of the Wnt markers. It was also shown a decreased gene expression of the ISCs markers *Lgr5* and *Ascl2*, possibly indicating a reduction in the ISC pool and, as a consequence, a reduction in the number of *Apc* deficient ISC, resulting in a decreased number of aberrant crypts. Considering that in this project CD8 $^{+}$  cells were depleted prior *Apc* deletion, there is the possibility that the stem cell pool was altered, resulting in a lower number of aberrant crypts, and not as a direct consequence of CD8 $^{+}$  cell depletion. RNAscope analysis showed an increased number of *Lgr5* transcripts in the villi when comparing to non-induced mice. Depletion of CD8 $^{+}$  cells in *Apc* deleted mice resulted in a re-distribution of the *Lgr5* transcripts from the bottom to the other areas of the crypt. Interestingly it was demonstrated an increased number of transcripts in the villi, suggesting an alteration in the homeostasis of the ISCs. This can, possibly explain the reduced number of lesions following CD8 $^{+}$  cell depletion in *Apc* deleted mice. It has been shown that stem cells are located in the bottom of the crypts and only these cells can initiate tumours (Barker *et al.* 2009). Barker and colleagues have shown that *Apc* deletion in the non-stem cell compartment led to the production of small lesions that were retained within the intestinal epithelium, however these lesions did not form tumours (Barker *et al.* 2009).

A recent study published by Biton and colleagues gave new insights into the effect of adaptive immune cells on ISCs fate (Biton *et al.* 2018). The authors showed that intestinal organoids supplemented with Tregs or their suppressive cytokine IL-10 had an expansion in the ISC pool. On the other side, organoids supplemented with T-helper subsets showed lower numbers of ISCs associated with increased cell differentiation (Biton *et al.* 2018). Next, the authors analysed the effect of MHC-II deficiency *in vivo*. Mice deficient in MHC-II, compared to control mice, had an increased proportion of ISCs

and reduced numbers of CD4+ T-cells in the intestines (Biton *et al.* 2018). These data suggests that MHC-II expression is essential for the support of ISCs. Similar to these results, mice deficient in T-cells had an increased expansion of ISCs, indicating again that T-cell interactions are essential for the ISCs differentiation. Finally, the authors showed that Treg depletion in *Foxp3<sup>DTR</sup>* mice resulted in aberrant ISC differentiations and reduction of the ISC pool. Treg depleted mice, as expected had an increased frequency of Th cells that may contribute for ICs differentiation (Biton *et al.* 2018). Altogether, these data provide new insights into the response of Lgr5+ ISCs to pro- and anti-inflammatory signals and how important these interactions are to maintain a balance between stem cell renewal and differentiation.

Further studies are needed to test the hypothesis that the different distribution of the *Lgr5* transcripts resulted in a reduced stemness and that, as a consequence, less stem cells would be recombined, giving origin to a reduced number of aberrant crypts. A way to test this would be by the isolation of cells from the crypt and villus to examine stemness. Another was the induction of *Apc* deletion by gavage so only villi cells would recombine, testing whether the population of cells expressing *Lgr5* in the villi could form tumours (Barker *et al.* 2009).

Another surprising result was the fact that IFN $\gamma$  neutralisation did not have an impact in the tumour burden as it has been demonstrated that this cytokine plays a key role in the anti-tumour immune responses in the early stages of intestinal cancer (Wang *et al.* 2015a). It is therefore important to mention that IFN $\gamma$  neutralisation was not validated by any other method such as IHC or flow cytometry, being possible that neutralisation was not successfully achieved. Importantly, the analysis of the groups where T-cell were depleted and IFN $\gamma$  was neutralised, to access tumour burden, were only done performed in the first 5 cm of the small intestine. A more complete analysis would include the quantification of the aberrant crypts in serial sections of the whole small and large intestines, possibly giving new insights about the role of IFN $\gamma$  in the early stages of intestinal cancer.

In conclusion, it was shown that Tregs are increased 15 days following *Apc* deletion. Depletion of Tregs significantly decrease the tumour burden, particularly in the large intestine, suggesting a key role of Tregs in the early stages of intestinal cancer (Figure 7.1). It is important, however, to analyse the role of Tregs in different disease contexts as they are a possible target for prevention of CRC impeding its progression to a more aggressive disease.

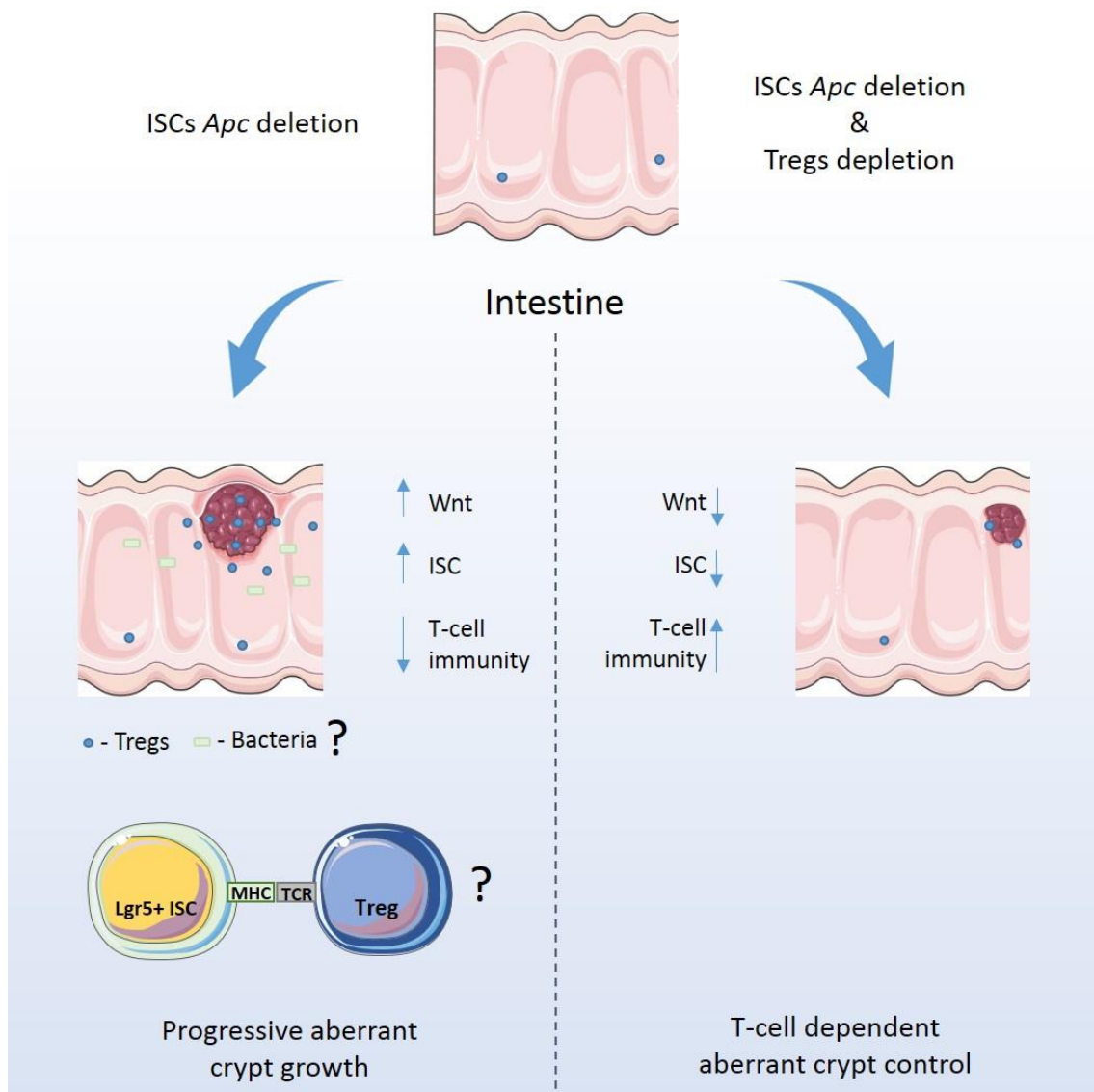


Figure 7.1 Representative model of the effects of Treg depletion in *Apc* deleted mice.

*Apc* deletion leads to the increased expression of Wnt and ISCs markers. *Apc* deleted mice have an increased number of Tregs that are responsible for the suppression of the anti-tumour immune response. Two mechanisms are proposed to explain the increased infiltration of Tregs. It is possible that the intestinal epithelial barrier is disrupted, leading to the infiltration of bacteria and activation of the immune system. Another possible mechanism is that ISCs can function as antigen-presenting cells, being able to interact and activate Tregs. Following Treg depletion, in *Apc* deleted mice, there is a reduction of Wnt and ISCs markers, and a reduction of the tumour burden, particularly in the mice's large intestine.

## 8 References

(2012). Comprehensive molecular characterization of human colon and rectal cancer. *Nature* **487**(7407):330-337.

Akeus, P., Langenes, V., Kristensen, J., von Mentzer, A., Sparwasser, T., Raghavan, S. and Quiding-Jarbrink, M. (2015). Treg-cell depletion promotes chemokine production and accumulation of CXCR3(+) conventional T cells in intestinal tumors. *Eur J Immunol* **45**(6):1654-1666.

Akeus, P., Langenes, V., von Mentzer, A., Yrlid, U., Sjolting, A., Saksena, P., . . . Quiding-Jarbrink, M. (2014). Altered chemokine production and accumulation of regulatory T cells in intestinal adenomas of APC(Min/+) mice. *Cancer Immunol Immunother* **63**(8):807-819.

Al-Shibli, K. I., Donnem, T., Al-Saad, S., Persson, M., Bremnes, R. M. and Busund, L. T. (2008). Prognostic effect of epithelial and stromal lymphocyte infiltration in non-small cell lung cancer. *Clin Cancer Res* **14**(16):5220-5227.

Alvaro, T., Lejeune, M., Salvado, M. T., Bosch, R., Garcia, J. F., Jaen, J., . . . Piris, M. A. (2005). Outcome in Hodgkin's lymphoma can be predicted from the presence of accompanying cytotoxic and regulatory T cells. *Clin Cancer Res* **11**(4):1467-1473.

Antony, P. A., Piccirillo, C. A., Akpınarli, A., Finkelstein, S. E., Speiss, P. J., Surman, D. R., . . . Restifo, N. P. (2005). CD8+ T cell immunity against a tumor/self-antigen is augmented by CD4+ T helper cells and hindered by naturally occurring T regulatory cells. *J Immunol* **174**(5):2591-2601.

Arpaia, N., Green, J. A., Molledo, B., Arvey, A., Hemmers, S., Yuan, S., . . . Rudensky, A. Y. (2015). A Distinct Function of Regulatory T Cells in Tissue Protection. *Cell* **162**(5):1078-1089.

Baker, A. M., Graham, T. A., Elia, G., Wright, N. A. and Rodriguez-Justo, M. (2015). Characterization of LGR5 stem cells in colorectal adenomas and carcinomas. *Sci Rep* **5**.

Balkwill, F. and Coussens, L. M. (2004). Cancer: an inflammatory link. In: *Nature*. Vol. 431. England, pp. 405-406.

Barker, N. (2014). Adult intestinal stem cells: critical drivers of epithelial homeostasis and regeneration. *Nat Rev Mol Cell Biol* **15**(1):19-33.

Barker, N., Ridgway, R. A., van Es, J. H., van de Wetering, M., Begthel, H., van den Born, M., . . . Clevers, H. (2009). Crypt stem cells as the cells-of-origin of intestinal cancer. *Nature* **457**(7229):608-611.

Barker, N., Tan, S. and Clevers, H. (2013). Lgr proteins in epithelial stem cell biology. *Development* **140**(12):2484-2494.

Barker, N., van de Wetering, M. and Clevers, H. (2008). The intestinal stem cell. *Genes Dev* **22**(14):1856-1864.

Barker, N., van Es, J. H., Kuipers, J., Kujala, P., van den Born, M., Cozijnsen, M., . . . Clevers, H. (2007). Identification of stem cells in small intestine and colon by marker gene Lgr5. *Nature* **449**(7165):1003-1007.

Bates, G. J., Fox, S. B., Han, C., Leek, R. D., Garcia, J. F., Harris, A. L. and Banham, A. H. (2006). Quantification of regulatory T cells enables the identification of high-risk breast cancer patients and those at risk of late relapse. *J Clin Oncol* **24**(34):5373-5380.

Batlle, E. and Clevers, H. (2017). Cancer stem cells revisited. *Nat Med* **23**(10):1124-1134.

Batlle, E., Henderson, J. T., Begthel, H., van den Born, M. M., Sancho, E., Huls, G., . . . Clevers, H. (2002). Beta-catenin and TCF mediate cell positioning in the intestinal epithelium by controlling the expression of EphB/ephrinB. *Cell* **111**(2):251-263.

Beck, P. L., Rosenberg, I. M., Xavier, R. J., Koh, T., Wong, J. F. and Podolsky, D. K. (2003). Transforming Growth Factor- $\beta$  Mediates Intestinal Healing and Susceptibility to Injury in Vitro and in Vivo Through Epithelial Cells. In: *Am J Pathol*. Vol. 162. pp. 597-608.

Bennett, C. L., Christie, J., Ramsdell, F., Brunkow, M. E., Ferguson, P. J., Whitesell, L., . . . Ochs, H. D. (2001). The immune dysregulation, polyendocrinopathy, enteropathy, X-linked syndrome (IPEX) is caused by mutations of FOXP3. *Nat Genet* **27**(1):20-21.

Betts, G., Jones, E., Junaid, S., El-Shanawany, T., Scurr, M., Mizen, P., . . . Godkin, A. (2012). Suppression of tumour-specific CD4(+) T cells by regulatory T cells is associated with progression of human colorectal cancer. *Gut* **61**(8):1163-1171.

Bevins, C. L. and Salzman, N. H. (2011). Paneth cells, antimicrobial peptides and maintenance of intestinal homeostasis. *Nat Rev Microbiol* **9**(5):356-368.

Biton, M., Haber, A., Beyaz, S., Rogel, N., Smillie, C., Shekhar, K., . . . Xavier, R. J. (2017). T helper cells modulate intestinal stem cell renewal and differentiation. *bioRxiv*.

Biton, M., Haber, A. L., Rogel, N., Burgin, G., Beyaz, S., Schnell, A., . . . Xavier, R. J. (2018). T Helper Cell Cytokines Modulate Intestinal Stem Cell Renewal and Differentiation. *Cell* **175**(5):1307-1320.e1322.

Bondurant, K. L., Lundgreen, A., Herrick, J. S., Kadlubar, S., Wolff, R. K. and Slattery, M. L. (2013). Interleukin genes and associations with colon and rectal cancer risk and overall survival. *Int J Cancer* **132**(4):905-915.

Bonnet, D. and Dick, J. E. (1997). Human acute myeloid leukemia is organized as a hierarchy that originates from a primitive hematopoietic cell. *Nat Med* **3**(7):730-737.

Boutin, A. T., Liao, W. T., Wang, M., Hwang, S. S., Karpinets, T. V., Cheung, H., . . . DePinho, R. A. (2017). Oncogenic Kras drives invasion and maintains metastases in colorectal cancer. *Genes Dev* **31**(4):370-382.

Braha, M., Chikman, B., Habler, L., Shapira, Z., Vasyanovich, S., Tolstov, G., . . . Lavy, R. (2016). Lymphocytic Infiltration as a Prognostic Factor in Patients With Colon Cancer. *Int J Surg Pathol* **24**(1):16-23.

Brenchley, J. M. and Douek, D. C. (2012). Microbial translocation across the GI tract. *Annu Rev Immunol* **30**:149-173.

Brenner, H., Kloor, M. and Pox, C. P. (2014). Colorectal cancer. *Lancet* **383**(9927):1490-1502.

Brunkow, M. E., Jeffery, E. W., Hjerrild, K. A., Paepfer, B., Clark, L. B., Yasayko, S. A., . . . Ramsdell, F. (2001). Disruption of a new forkhead/winged-helix protein, scurf, results in the fatal lymphoproliferative disorder of the scurfy mouse. *Nat Genet* **27**(1):68-73.

Buczacki, S. J., Zecchini, H. I., Nicholson, A. M., Russell, R., Vermeulen, L., Kemp, R. and Winton, D. J. (2013). Intestinal label-retaining cells are secretory precursors expressing Lgr5. *Nature* **495**(7439):65-69.

Buller, N. V., Rosekrans, S. L., Westerlund, J. and van den Brink, G. R. (2012). Hedgehog signaling and maintenance of homeostasis in the intestinal epithelium. *Physiology (Bethesda)* **27**(3):148-155.

Burkitt, D. P. (1971). Possible relationships between bowel cancer and dietary habits. *Proc R Soc Med* **64**(9):964-965.

Burnet, M. (1957). Cancer; a biological approach. I. The processes of control. *Br Med J* **1**(5022):779-786.

Burzyn, D., Kuswanto, W., Kolodin, D., Shadrach, J. L., Cerletti, M., Jang, Y., . . . Mathis, D. (2013). A special population of regulatory T cells potentiates muscle repair. *Cell* **155**(6):1282-1295.

Cancer Research UK. Available at: <http://www.cancerresearchuk.org/2-about-cancer> [Accessed: April].

Carmon, K. S., Gong, X., Lin, Q., Thomas, A. and Liu, Q. (2011). R-spondins function as ligands of the orphan receptors LGR4 and LGR5 to regulate Wnt/beta-catenin signaling. *Proc Natl Acad Sci U S A* **108**(28):11452-11457.

Carulli, A. J., Samuelson, L. C. and Schnell, S. (2014). Unraveling intestinal stem cell behavior with models of crypt dynamics. *Integr Biol (Camb)* **6**(3):243-257.

Chae, W. J. and Bothwell, A. L. (2015). Spontaneous Intestinal Tumorigenesis in Apc (Min+) Mice Requires Altered T Cell Development with IL-17A. *J Immunol Res* **2015**:860106.

Chaput, N., Darrasse-Jeze, G., Bergot, A. S., Cordier, C., Ngo-Abdalla, S., Klatzmann, D. and Azogui, O. (2007). Regulatory T cells prevent CD8 T cell maturation by inhibiting CD4 Th cells at tumor sites. *J Immunol* **179**(8):4969-4978.

- Chen, Y. L., Chang, M. C., Chen, C. A., Lin, H. W., Cheng, W. F. and Chien, C. L. (2012). Depletion of regulatory T lymphocytes reverses the imbalance between pro- and anti-tumor immunities via enhancing antigen-specific T cell immune responses. *PLoS One* **7**(10):e47190.
- Chen, Z., Laurence, A. and O'Shea, J. J. (2007). Signal transduction pathways and transcriptional regulation in the control of Th17 differentiation. *Semin Immunol* **19**(6):400-408.
- Clarke, S. L., Betts, G. J., Plant, A., Wright, K. L., El-Shanawany, T. M., Harrop, R., . . . Godkin, A. J. (2006). CD4+CD25+FOXP3+ regulatory T cells suppress anti-tumor immune responses in patients with colorectal cancer. *PLoS One* **1**:e129.
- Clevers, H. (2006). Wnt/beta-catenin signaling in development and disease. *Cell* **127**(3):469-480.
- Clevers, H., Loh, K. M. and Nusse, R. (2014). Stem cell signaling. An integral program for tissue renewal and regeneration: Wnt signaling and stem cell control. *Science* **346**(6205):1248012.
- Colbeck, E. J., Jones, E., Hindley, J. P., Smart, K., Schulz, R., Browne, M., . . . Gallimore, A. (2017). Treg Depletion Licenses T Cell-Driven HEV Neogenesis and Promotes Tumor Destruction. *Cancer Immunol Res* **5**(11):1005-1015.
- Corthay, A. (2009). How do regulatory T cells work? *Scand J Immunol* **70**(4):326-336.
- Creamer, B. (1967). The turnover of the epithelium of the small intestine. *Br Med Bull* **23**(3):226-230.
- Curiel, T. J., Coukos, G., Zou, L., Alvarez, X., Cheng, P., Mottram, P., . . . Zou, W. (2004). Specific recruitment of regulatory T cells in ovarian carcinoma fosters immune privilege and predicts reduced survival. *Nat Med* **10**(9):942-949.
- Cushing, K., Alvarado, D. M. and Ciorba, M. A. (2015). Butyrate and Mucosal Inflammation: New Scientific Evidence Supports Clinical Observation. *Clin Transl Gastroenterol* **6**(8):e108-.
- Dalerba, P., Dylla, S. J., Park, I. K., Liu, R., Wang, X., Cho, R. W., . . . Clarke, M. F. (2007). Phenotypic characterization of human colorectal cancer stem cells. *Proc Natl Acad Sci U S A* **104**(24):10158-10163.

Dannull, J., Su, Z., Rizzieri, D., Yang, B. K., Coleman, D., Yancey, D., . . . Vieweg, J. (2005). Enhancement of vaccine-mediated antitumor immunity in cancer patients after depletion of regulatory T cells. *J Clin Invest* **115**(12):3623-3633.

Davidson, W. F., Giese, T. and Fredrickson, T. N. (1998). Spontaneous development of plasmacytoid tumors in mice with defective Fas-Fas ligand interactions. *J Exp Med* **187**(11):1825-1838.

de Lau, W., Barker, N., Low, T. Y., Koo, B. K., Li, V. S., Teunissen, H., . . . Clevers, H. (2011). Lgr5 homologues associate with Wnt receptors and mediate R-spondin signalling. *Nature* **476**(7360):293-297.

Deschoolmeester, V., Baay, M., Lardon, F., Pauwels, P. and Peeters, M. (2011). Immune Cells in Colorectal Cancer: Prognostic Relevance and Role of MSI. *Cancer Microenviron* **4**(3):377-392.

Di Franco, S., Turdo, A., Todaro, M. and Stassi, G. (2017). Role of Type I and II Interferons in Colorectal Cancer and Melanoma. *Front Immunol* **8**.

Diederichsen, A. C., Hjelmborg, J., Christensen, P. B., Zeuthen, J. and Fenger, C. (2003). Prognostic value of the CD4+/CD8+ ratio of tumour infiltrating lymphocytes in colorectal cancer and HLA-DR expression on tumour cells. *Cancer Immunol Immunother* **52**(7):423-428.

Dieu-Nosjean, M. C., Antoine, M., Danel, C., Heudes, D., Wislez, M., Poulot, V., . . . Cadranel, J. (2008). Long-term survival for patients with non-small-cell lung cancer with intratumoral lymphoid structures. *J Clin Oncol* **26**(27):4410-4417.

Dombrowski, Y., O'Hagan, T., Dittmer, M., Penalva, R., Mayoral, S. R., Bankhead, P., . . . Fitzgerald, D. C. (2017). Regulatory T cells promote myelin regeneration in the central nervous system. *Nat Neurosci* **20**(5):674-680.

Drake, R. L., Vogl, A. W. and Mitchell, A. W. M. (2005). *Gray's anatomy for students*. Third ed. Philadelphia: Elsevier/Churchill Livingstone.

- Duhen, T., Geiger, R., Jarrossay, D., Lanzavecchia, A. and Sallusto, F. (2009). Production of interleukin 22 but not interleukin 17 by a subset of human skin-homing memory T cells. *Nat Immunol* **10**(8):857-863.
- Dunn, G. P., Koebel, C. M. and Schreiber, R. D. (2006). Interferons, immunity and cancer immunoediting. *Nat Rev Immunol* **6**(11):836-848.
- Dunn, G. P., Old, L. J. and Schreiber, R. D. (2004). The three Es of cancer immunoediting. *Annu Rev Immunol* **22**:329-360.
- Engelstoft, M. S., Egerod, K. L., Holst, B. and Schwartz, T. W. (2008). A gut feeling for obesity: 7TM sensors on enteroendocrine cells. *Cell Metab* **8**(6):447-449.
- Erdman, S. E. (2010). Unifying roles for regulatory T cells and inflammation in cancer. *126*(7):1651-1665.
- Erdman, S. E., Sohn, J. J., Rao, V. P., Nambiar, P. R., Ge, Z., Fox, J. G. and Schauer, D. B. (2005). CD4+CD25+ regulatory lymphocytes induce regression of intestinal tumors in ApcMin/+ mice. *Cancer Res* **65**(10):3998-4004.
- Fan, X. S., Wu, H. Y., Yu, H. P., Zhou, Q., Zhang, Y. F. and Huang, Q. (2010). Expression of Lgr5 in human colorectal carcinogenesis and its potential correlation with beta-catenin. *Int J Colorectal Dis* **25**(5):583-590.
- Fearon, E. R. and Vogelstein, B. (1990). A genetic model for colorectal tumorigenesis. *Cell* **61**(5):759-767.
- Fevr, T., Robine, S., Louvard, D. and Huelsken, J. (2007). Wnt/beta-catenin is essential for intestinal homeostasis and maintenance of intestinal stem cells. *Mol Cell Biol* **27**(21):7551-7559.
- Fontenot, J. D., Gavin, M. A. and Rudensky, A. Y. (2003). Foxp3 programs the development and function of CD4+CD25+ regulatory T cells. *Nat Immunol* **4**(4):330-336.
- Fox, J. G., Barthold, S., Davisson, M., Newcomer, C. E., Quimby, F. W. and Smith, A. (2006). *The Mouse in Biomedical Research: Normative Biology, Husbandry, and Models*. Second ed. Elsevier Science.

Fukunaga, A., Miyamoto, M., Cho, Y., Murakami, S., Kawarada, Y., Oshikiri, T., . . . Katoh, H. (2004). CD8+ tumor-infiltrating lymphocytes together with CD4+ tumor-infiltrating lymphocytes and dendritic cells improve the prognosis of patients with pancreatic adenocarcinoma. *Pancreas* **28**(1):e26-31.

Gallimore, A. and Godkin, A. (2008). Regulatory T cells and tumour immunity - observations in mice and men. *Immunology* **123**(2):157-163.

Galon, J., Costes, A., Sanchez-Cabo, F., Kirilovsky, A., Mlecnik, B., Lagorce-Pages, C., . . . Pages, F. (2006). Type, density, and location of immune cells within human colorectal tumors predict clinical outcome. *Science* **313**(5795):1960-1964.

Garcia, M. I., Ghiani, M., Lefort, A., Libert, F., Strollo, S. and Vassart, G. (2009). LGR5 deficiency deregulates Wnt signaling and leads to precocious Paneth cell differentiation in the fetal intestine. *Dev Biol* **331**(1):58-67.

Gerbe, F., van Es, J. H., Makrini, L., Brulin, B., Mellitzer, G., Robine, S., . . . Jay, P. (2011). Distinct ATOH1 and Neurog3 requirements define tuft cells as a new secretory cell type in the intestinal epithelium. *J Cell Biol* **192**(5):767-780.

Giuliani, A., Caporale, A., Corona, M., Ricciardulli, T., Di Bari, M., Demoro, M., . . . Angelico, F. (2006). Large size, villous content and distal location are associated with severe dysplasia in colorectal adenomas. *Anticancer Res* **26**(5b):3717-3722.

Glinka, A., Dolde, C., Kirsch, N., Huang, Y. L., Kazanskaya, O., Ingelfinger, D., . . . Niehrs, C. (2011). LGR4 and LGR5 are R-spondin receptors mediating Wnt/beta-catenin and Wnt/PCP signalling. *EMBO Rep* **12**(10):1055-1061.

Godfrey, V. L., Wilkinson, J. E., Rinchik, E. M. and Russell, L. B. (1991). Fatal lymphoreticular disease in the scurfy (sf) mouse requires T cells that mature in a sf thymic environment: potential model for thymic education. *Proc Natl Acad Sci U S A* **88**(13):5528-5532.

Goldszmid, R. S. and Trinchieri, G. (2012). The price of immunity. *Nat Immunol* **13**(10):932-938.

Goudin, N., Chappert, P., Megret, J., Gross, D. A., Rocha, B. and Azogui, O. (2016). Depletion of Regulatory T Cells Induces High Numbers of Dendritic Cells and Unmasks a Subset of Anti-Tumour CD8+CD11c+ PD-1<sup>lo</sup> Effector T Cells. *PLoS One* **11**(6):e0157822.

Gregorieff, A., Pinto, D., Begthel, H., Destree, O., Kielman, M. and Clevers, H. (2005). Expression pattern of Wnt signaling components in the adult intestine. *Gastroenterology* **129**(2):626-638.

Grivennikov, S. I., Greten, F. R. and Karin, M. (2010). Immunity, inflammation, and cancer. *Cell* **140**(6):883-899.

Groden, J., Thliveris, A., Samowitz, W., Carlson, M., Gelbert, L., Albertsen, H., . . . et al. (1991). Identification and characterization of the familial adenomatous polyposis coli gene. *Cell* **66**(3):589-600.

Gryfe, R., Swallow, C., Bapat, B., Redston, M., Gallinger, S. and Couture, J. (1997). Molecular biology of colorectal cancer. *Curr Probl Cancer* **21**(5):233-300.

Hadjimichael, C., Chanoumidou, K., Papadopoulou, N., Arampatzi, P., Papamatheakis, J. and Kretsovali, A. (2015). Common stemness regulators of embryonic and cancer stem cells. *World J Stem Cells* **7**(9):1150-1184.

Hadrup, S., Donia, M. and Thor Straten, P. (2013). Effector CD4 and CD8 T cells and their role in the tumor microenvironment. *Cancer Microenviron* **6**(2):123-133.

Hamanishi, J., Mandai, M., Iwasaki, M., Okazaki, T., Tanaka, Y., Yamaguchi, K., . . . Fujii, S. (2007). Programmed cell death 1 ligand 1 and tumor-infiltrating CD8+ T lymphocytes are prognostic factors of human ovarian cancer. *Proc Natl Acad Sci U S A* **104**(9):3360-3365.

Hanahan, D. and Weinberg, R. A. (2011). Hallmarks of cancer: the next generation. *Cell* **144**(5):646-674.

Harty, J. T. and Bevan, M. J. (1999). Responses of CD8(+) T cells to intracellular bacteria. *Curr Opin Immunol* **11**(1):89-93.

Hessman, C. J., Bubbers, E. J., Billingsley, K. G., Herzig, D. O. and Wong, M. H. (2012). Loss of expression of the cancer stem cell marker aldehyde dehydrogenase 1 correlates with advanced-stage colorectal cancer. *Am J Surg* **203**(5):649-653.

Hindley, J. P., Jones, E., Smart, K., Bridgeman, H., Lauder, S. N., Ondondo, B., . . . Gallimore, A. M. (2012). T-cell trafficking facilitated by high endothelial venules is required for tumor control after regulatory T-cell depletion. *Cancer Res* **72**(21):5473-5482.

Horvath, C. M. (2004). The Jak-STAT pathway stimulated by interferon gamma. *Sci STKE* **2004**(260):tr8.

Hoves, S., Trapani, J. A. and Voskoboinik, I. (2010). The battlefield of perforin/granzyme cell death pathways. *J Leukoc Biol* **87**(2):237-243.

Ihara, S., Hirata, Y. and Koike, K. (2017). TGF-beta in inflammatory bowel disease: a key regulator of immune cells, epithelium, and the intestinal microbiota. *J Gastroenterol* **52**(7):777-787.

Ingold Heppner, B., Loibl, S. and Denkert, C. (2016). Tumor-Infiltrating Lymphocytes: A Promising Biomarker in Breast Cancer. In: *Breast Care (Basel)*. Vol. 11. Wilhelmstrasse 20A, P.O. Box · Postfach · Case postale, D–79095, Freiburg, Germany · Deutschland · Allemagne, Phone: +49 761 45 20 70, Fax: +49 761 4 52 07 14, information@karger.de, pp. 96-100.

Jaks, V., Barker, N., Kasper, M., van Es, J. H., Snippert, H. J., Clevers, H. and Toftgard, R. (2008). Lgr5 marks cycling, yet long-lived, hair follicle stem cells. *Nat Genet* **40**(11):1291-1299.

Jakubowska, K., Kisielewski, W., Kańczuga-Koda, L., Koda, M. and Famulski, W. (2017). Stromal and intraepithelial tumor-infiltrating lymphocytes in colorectal carcinoma. In: *Oncol Lett*. Vol. 14. pp. 6421-6432.

James, F. R., Jiminez-Linan, M., Alsop, J., Mack, M., Song, H., Brenton, J. D., . . . Ali, H. R. (2017). Association between tumour infiltrating lymphocytes, histotype and clinical outcome in epithelial ovarian cancer. In: *BMC Cancer*. Vol. 17. London.

Jones, E., Dahm-Vicker, M., Simon, A. K., Green, A., Powrie, F., Cerundolo, V. and Gallimore, A. (2002). Depletion of CD25+ regulatory cells results in suppression of melanoma growth and induction of autoreactivity in mice. *Cancer Immun* **2**:1.

Kadur Lakshminarasimha Murthy, P., Srinivasan, T., Bochter, M. S., Xi, R., Varanko, A. K., Tung, K. L., . . . Shen, X. (2018). Radical and lunatic fringes modulate notch ligands to support mammalian intestinal homeostasis. *Elife* **7**.

Kaplan, M. H., Hufford, M. M. and Olson, M. R. (2015). The development and in vivo function of T helper 9 cells. *Nat Rev Immunol* **15**(5):295-307.

Katlinski, K. V., Gui, J., Katlinskaya, Y. V., Ortiz, A., Chakraborty, R., Bhattacharya, S., . . . Fuchs, S. Y. (2017). Inactivation of Interferon Receptor Promotes the Establishment of Immune Privileged Tumor Microenvironment. *Cancer Cell* **31**(2):194-207.

Kim, J. M., Rasmussen, J. P. and Rudensky, A. Y. (2007). Regulatory T cells prevent catastrophic autoimmunity throughout the lifespan of mice. *Nat Immunol* **8**(2):191-197.

Kinzler, K. W. and Vogelstein, B. (1996). Lessons from hereditary colorectal cancer. *Cell* **87**(2):159-170.

Klages, K., Mayer, C. T., Lahl, K., Loddenkemper, C., Teng, M. W., Ngiow, S. F., . . . Sparwasser, T. (2010). Selective depletion of Foxp3+ regulatory T cells improves effective therapeutic vaccination against established melanoma. *Cancer Res* **70**(20):7788-7799.

Koch, M., Beckhove, P., Op den Winkel, J., Autenrieth, D., Wagner, P., Nummer, D., . . . Weitz, J. (2006). Tumor infiltrating T lymphocytes in colorectal cancer: Tumor-selective activation and cytotoxic activity in situ. *Ann Surg* **244**(6):986-992; discussion 992-983.

Koch, S. (2017). Extrinsic control of Wnt signaling in the intestine. *Differentiation* **97**:1-8.

Kohn, A. D. and Moon, R. T. (2005). Wnt and calcium signaling: beta-catenin-independent pathways. *Cell Calcium* **38**(3-4):439-446.

Kontani, K., Sawai, S., Hanaoka, J., Tezuka, N., Inoue, S. and Fujino, S. (2001). Involvement of granzyme B and perforin in suppressing nodal metastasis of cancer cells in breast and lung cancers. *Eur J Surg Oncol* **27**(2):180-186.

- Kosmidis, C., Sapalidis, K., Koletsa, T., Kosmidou, M., Efthimiadis, C., Anthimidis, G., . . . Kesisoglou, I. (2018). Interferon-gamma and Colorectal Cancer: an up-to date. *J Cancer* **9**(2):232-238.
- Kotredes, K. P. and Gamero, A. M. (2013). Interferons as inducers of apoptosis in malignant cells. *J Interferon Cytokine Res* **33**(4):162-170.
- Krausova, M. and Korinek, V. (2014). Wnt signaling in adult intestinal stem cells and cancer. *Cell Signal* **26**(3):570-579.
- Kumar, K. K., Burgess, A. W. and Gulbis, J. M. (2014). Structure and function of LGR5: an enigmatic G-protein coupled receptor marking stem cells. *Protein Sci* **23**(5):551-565.
- Kunzmann, A. T., Coleman, H. G., Huang, W. Y., Kitahara, C. M., Cantwell, M. M. and Berndt, S. I. (2015). Dietary fiber intake and risk of colorectal cancer and incident and recurrent adenoma in the Prostate, Lung, Colorectal, and Ovarian Cancer Screening Trial. In: *Am J Clin Nutr*. Vol. 102. pp. 881-890.
- Ladoire, S., Martin, F. and Ghiringhelli, F. (2011). Prognostic role of FOXP3+ regulatory T cells infiltrating human carcinomas: the paradox of colorectal cancer. *Cancer Immunol Immunother* **60**(7):909-918.
- Lahl, K., Loddenkemper, C., Drouin, C., Freyer, J., Arnason, J., Eberl, G., . . . Sparwasser, T. (2007). Selective depletion of Foxp3+ regulatory T cells induces a scurfy-like disease. *J Exp Med* **204**(1):57-63.
- Leng, Z., Xia, Q., Chen, J., Li, Y., Xu, J., Zhao, E., . . . Dong, J. (2018). Lgr5+CD44+EpCAM+ Strictly Defines Cancer Stem Cells in Human Colorectal Cancer. *Cell Physiol Biochem* **46**(2):860-872.
- Li, S. K. H. and Martin, A. (2016). Mismatch Repair and Colon Cancer: Mechanisms and Therapies Explored. *Trends Mol Med* **22**(4):274-289.
- Li, X. L., Zhou, J., Chen, Z. R. and Chng, W. J. (2015). p53 mutations in colorectal cancer-molecular pathogenesis and pharmacological reactivation. *World J Gastroenterol* **21**(1):84-93.

Lindemans, C. A., Calafiore, M., Mertelsmann, A. M., O'Connor, M. H., Dudakov, J. A., Jenq, R. R., . . . Hanash, A. M. (2015). Interleukin-22 promotes intestinal-stem-cell-mediated epithelial regeneration. *Nature* **528**(7583):560-564.

Ling, K. L., Pratap, S. E., Bates, G. J., Singh, B., Mortensen, N. J., George, B. D., . . . Cerundolo, V. (2007). Increased frequency of regulatory T cells in peripheral blood and tumour infiltrating lymphocytes in colorectal cancer patients. *Cancer Immun* **7**:7.

Liu, F., Hu, X., Zimmerman, M., Waller, J. L., Wu, P., Hayes-Jordan, A., . . . Liu, K. (2011). TNFalpha cooperates with IFN-gamma to repress Bcl-xL expression to sensitize metastatic colon carcinoma cells to TRAIL-mediated apoptosis. *PLoS One* **6**(1):e16241.

Liu, S., Lachapelle, J., Leung, S., Gao, D., Foulkes, W. D. and Nielsen, T. O. (2012). CD8+ lymphocyte infiltration is an independent favorable prognostic indicator in basal-like breast cancer. *Breast Cancer Res* **14**(2):R48.

Liu, S., Yu, X., Wang, Q., Liu, Z., Xiao, Q., Hou, P., . . . Chen, S. (2017). Specific Expression of Interferon-gamma Induced by Synergistic Activation Mediator-Derived Systems Activates Innate Immunity and Inhibits Tumorigenesis. *J Microbiol Biotechnol* **27**(10):1855-1866.

Liu, Z., Huang, Q., Liu, G., Dang, L., Chu, D., Tao, K. and Wang, W. (2014). Presence of FOXP3(+)Treg cells is correlated with colorectal cancer progression. *Int J Clin Exp Med* **7**(7):1781-1785.

Lopez-Garcia, C., Klein, A. M., Simons, B. D. and Winton, D. J. (2010). Intestinal stem cell replacement follows a pattern of neutral drift. *Science* **330**(6005):822-825.

Maeda, K., Hazama, S., Tokuno, K., Kan, S., Maeda, Y., Watanabe, Y., . . . Oka, M. (2011). Impact of chemotherapy for colorectal cancer on regulatory T-cells and tumor immunity. *Anticancer Res* **31**(12):4569-4574.

Maloy, K. J. and Powrie, F. (2001). Regulatory T cells in the control of immune pathology. *Nat Immunol* **2**(9):816-822.

Mantovani, A., Allavena, P., Sica, A. and Balkwill, F. (2008). Cancer-related inflammation. *Nature* **454**(7203):436-444.

Markowitz, S. D. and Bertagnolli, M. M. (2009). Molecular origins of cancer: Molecular basis of colorectal cancer. *N Engl J Med* **361**(25):2449-2460.

Matsuoka, J., Yashiro, M., Sakurai, K., Kubo, N., Tanaka, H., Muguruma, K., . . . Hirakawa, K. (2012). Role of the stemness factors sox2, oct3/4, and nanog in gastric carcinoma. *J Surg Res* **174**(1):130-135.

Mazzoni, S. M. and Fearon, E. R. (2014). AXIN1 and AXIN2 variants in gastrointestinal cancers. *Cancer Lett* **355**(1):1-8.

Mei, Z., Liu, Y., Liu, C., Cui, A., Liang, Z., Wang, G., . . . Li, C. (2014). Tumour-infiltrating inflammation and prognosis in colorectal cancer: systematic review and meta-analysis. *Br J Cancer* **110**(6):1595-1605.

Menegaz, R. A., Michelin, M. A., Etchebehere, R. M., Fernandes, P. C. and Murta, E. F. (2008). Peri- and intratumoral T and B lymphocytic infiltration in breast cancer. *Eur J Gynaecol Oncol* **29**(4):321-326.

Mihm, M. C. and Mulé, J. J. (2015). Reflections on the Histopathology of Tumor-infiltrating Lymphocytes in Melanoma and the Host Immune Response. *Cancer Immunol Res* **3**(8):827-835.

Mirams, G. R., Fletcher, A. G., Maini, P. K. and Byrne, H. M. (2012). A theoretical investigation of the effect of proliferation and adhesion on monoclonal conversion in the colonic crypt. *J Theor Biol* **312**:143-156.

Mlecnik, B., Tosolini, M., Kirilovsky, A., Berger, A., Bindea, G., Meatchi, T., . . . Galon, J. (2011). Histopathologic-based prognostic factors of colorectal cancers are associated with the state of the local immune reaction. *J Clin Oncol* **29**(6):610-618.

Moran, G. W., Leslie, F. C., Levison, S. E., Worthington, J. and McLaughlin, J. T. (2008). Enteroendocrine cells: neglected players in gastrointestinal disorders? *Therap Adv Gastroenterol* **1**(1):51-60.

Morgan, R. G., Mortensson, E. and Williams, A. C. (2018). Targeting LGR5 in Colorectal Cancer: therapeutic gold or too plastic? *Br J Cancer* **118**(11):1410-1418.

Morin, P. J., Sparks, A. B., Korinek, V., Barker, N., Clevers, H., Vogelstein, B. and Kinzler, K. W. (1997). Activation of beta-catenin-Tcf signaling in colon cancer by mutations in beta-catenin or APC. *Science* **275**(5307):1787-1790.

Moser, A. R., Pitot, H. C. and Dove, W. F. (1990). A dominant mutation that predisposes to multiple intestinal neoplasia in the mouse. *Science* **247**(4940):322-324.

Mosmann, T. R., Cherwinski, H., Bond, M. W., Giedlin, M. A. and Coffman, R. L. (1986). Two types of murine helper T cell clone. I. Definition according to profiles of lymphokine activities and secreted proteins. *J Immunol* **136**(7):2348-2357.

Mowat, A. M. and Agace, W. W. (2014). Regional specialization within the intestinal immune system. *Nat Rev Immunol* **14**(10):667-685.

Munoz, J., Stange, D. E., Schepers, A. G., van de Wetering, M., Koo, B. K., Itzkovitz, S., . . . Clevers, H. (2012). The Lgr5 intestinal stem cell signature: robust expression of proposed quiescent '+4' cell markers. *Embo j* **31**(14):3079-3091.

Murugaiyan, G. and Saha, B. (2009). Protumor vs antitumor functions of IL-17. *J Immunol* **183**(7):4169-4175.

Neumann, J., Bahr, F., Horst, D., Kriegl, L., Engel, J., Luque, R. M., . . . Jung, A. (2011). SOX2 expression correlates with lymph-node metastases and distant spread in right-sided colon cancer. *BMC Cancer* **11**:518.

Ni, L. and Lu, J. (2018). Interferon gamma in cancer immunotherapy. *Cancer Med* **7**(9):4509-4516.

Nishikawa, H. and Sakaguchi, S. (2010). Regulatory T cells in tumor immunity. *Int J Cancer* **127**(4):759-767.

Noah, T. K. and Shroyer, N. F. (2013). Notch in the intestine: regulation of homeostasis and pathogenesis. *Annu Rev Physiol* **75**:263-288.

O'Brien, C. A., Pollett, A., Gallinger, S. and Dick, J. E. (2007). A human colon cancer cell capable of initiating tumour growth in immunodeficient mice. *Nature* **445**(7123):106-110.

Onizuka, S., Tawara, I., Shimizu, J., Sakaguchi, S., Fujita, T. and Nakayama, E. (1999). Tumor rejection by in vivo administration of anti-CD25 (interleukin-2 receptor alpha) monoclonal antibody. *Cancer Res* **59**(13):3128-3133.

Pages, F., Berger, A., Camus, M., Sanchez-Cabo, F., Costes, A., Molidor, R., . . . Galon, J. (2005). Effector memory T cells, early metastasis, and survival in colorectal cancer. *N Engl J Med* **353**(25):2654-2666.

Pages, F., Kirilovsky, A., Mlecnik, B., Asslaber, M., Tosolini, M., Bindea, G., . . . Galon, J. (2009). In situ cytotoxic and memory T cells predict outcome in patients with early-stage colorectal cancer. *J Clin Oncol* **27**(35):5944-5951.

Parham, P. (2015a). *The immune system*. 4th ed. New York: Garland Science, pp. 8,9.

Parham, P. (2015b). *The immune system*. 4th ed. New York: Garland Science, pp. 10-12.

Parham, P. (2015c). *The immune system*. 4th ed. New York: Garland Science.

Parham, P. (2015d). *The immune system*. New York: Garland Science. pp. 113-145.

Perrone, G., Ruffini, P. A., Catalano, V., Spino, C., Santini, D., Mureto, P., . . . Graziano, F. (2008). Intratumoural FOXP3-positive regulatory T cells are associated with adverse prognosis in radically resected gastric cancer. In: *Eur J Cancer*. Vol. 44. England, pp. 1875-1882.

Peterson, L. W. and Artis, D. (2014). Intestinal epithelial cells: regulators of barrier function and immune homeostasis. *Nat Rev Immunol* **14**(3):141-153.

Pino, M. S. and Chung, D. C. (2010). The chromosomal instability pathway in colon cancer. *Gastroenterology* **138**(6):2059-2072.

Polakis, P. (2012). Wnt signaling in cancer. *Cold Spring Harb Perspect Biol* **4**(5).

Poliakov, A., Cotrina, M. and Wilkinson, D. G. (2004). Diverse roles of eph receptors and ephrins in the regulation of cell migration and tissue assembly. *Dev Cell* **7**(4):465-480.

Potten, C. S. and Loeffler, M. (1990). Stem cells: attributes, cycles, spirals, pitfalls and uncertainties. Lessons for and from the crypt. *Development* **110**(4):1001-1020.

Potten, C. S., Owen, G. and Booth, D. (2002). Intestinal stem cells protect their genome by selective segregation of template DNA strands. *J Cell Sci* **115**(Pt 11):2381-2388.

Prizment, A. E., Vierkant, R. A., Smyrk, T. C., Tillmans, L. S., Nelson, H. H., Lynch, C. F., . . . Limburg, P. J. (2017). Cytotoxic T Cells and Granzyme B Associated with Improved Colorectal Cancer Survival in a Prospective Cohort of Older Women. *Cancer Epidemiol Biomarkers Prev* **26**(4):622-631.

Quezada, S. A., Peggs, K. S., Simpson, T. R. and Allison, J. P. (2011). Shifting the equilibrium in cancer immunoediting: from tumor tolerance to eradication. *Immunol Rev* **241**(1):104-118.

Radziewicz, H., Uebelhoer, L., Bengsch, B. and Grakoui, A. (2007). Memory CD8+ T cell differentiation in viral infection: a cell for all seasons. *World J Gastroenterol* **13**(36):4848-4857.

Rassouli, F. B., Matin, M. M. and Saeinasab, M. (2016). Cancer stem cells in human digestive tract malignancies. *Tumour Biol* **37**(1):7-21.

Ricci-Vitiani, L., Fabrizi, E., Palio, E. and De Maria, R. (2009). Colon cancer stem cells. *J Mol Med (Berl)* **87**(11):1097-1104.

Ricci-Vitiani, L., Lombardi, D. G., Pilozzi, E., Biffoni, M., Todaro, M., Peschle, C. and De Maria, R. (2007). Identification and expansion of human colon-cancer-initiating cells. *Nature* **445**(7123):111-115.

Ritsma, L., Ellenbroek, S. I. J., Zomer, A., Snippert, H. J., de Sauvage, F. J., Simons, B. D., . . . van Rheenen, J. (2014). Intestinal crypt homeostasis revealed at single-stem-cell level by in vivo live imaging. *Nature* **507**(7492):362-365.

Ropponen, K. M., Eskelinen, M. J., Lipponen, P. K., Alhava, E. and Kosma, V. M. (1997). Prognostic value of tumour-infiltrating lymphocytes (TILs) in colorectal cancer. *J Pathol* **182**(3):318-324.

Rowan, A. J., Lamlum, H., Ilyas, M., Wheeler, J., Straub, J., Papadopoulou, A., . . . Tomlinson, I. P. (2000). APC mutations in sporadic colorectal tumors: A mutational "hotspot" and interdependence of the "two hits". *Proc Natl Acad Sci U S A* **97**(7):3352-3357.

Ruffell, B., DeNardo, D. G., Affara, N. I. and Coussens, L. M. (2010). Lymphocytes in cancer development: polarization towards pro-tumor immunity. *Cytokine Growth Factor Rev* **21**(1):3-10.

Sabat, R., Ouyang, W. and Wolk, K. (2014). Therapeutic opportunities of the IL-22-IL-22R1 system. *Nat Rev Drug Discov* **13**(1):21-38.

Saha, S., Aranda, E., Hayakawa, Y., Bhanja, P., Atay, S., Brodin, N. P., . . . Pollard, J. W. (2016). Macrophage-derived extracellular vesicle-packaged WNTs rescue intestinal stem cells and enhance survival after radiation injury. *Nat Commun* **7**:13096.

Sakaguchi, S., Sakaguchi, N., Asano, M., Itoh, M. and Toda, M. (1995). Immunologic self-tolerance maintained by activated T cells expressing IL-2 receptor alpha-chains (CD25). Breakdown of a single mechanism of self-tolerance causes various autoimmune diseases. *J Immunol* **155**(3):1151-1164.

Salama, P., Phillips, M., Grieu, F., Morris, M., Zeps, N., Joseph, D., . . . Iacopetta, B. (2009). Tumor-infiltrating FOXP3+ T regulatory cells show strong prognostic significance in colorectal cancer. *J Clin Oncol* **27**(2):186-192.

Salama, P., Phillips, M., Platell, C. and Iacopetta, B. (2011). Low expression of Granzyme B in colorectal cancer is associated with signs of early metastatic invasion. *Histopathology* **59**(2):207-215.

Sansom, O. J., Reed, K. R., Hayes, A. J., Ireland, H., Brinkmann, H., Newton, I. P., . . . Winton, D. J. (2004). Loss of Apc in vivo immediately perturbs Wnt signaling, differentiation, and migration. *Genes Dev* **18**(12):1385-1390.

Sato, E., Olson, S. H., Ahn, J., Bundy, B., Nishikawa, H., Qian, F., . . . Odunsi, K. (2005). Intraepithelial CD8+ tumor-infiltrating lymphocytes and a high CD8+/regulatory T cell ratio are associated with favorable prognosis in ovarian cancer. *Proc Natl Acad Sci U S A* **102**(51):18538-18543.

Sato, T., van Es, J. H., Snippert, H. J., Stange, D. E., Vries, R. G., van den Born, M., . . . Clevers, H. (2011). Paneth cells constitute the niche for Lgr5 stem cells in intestinal crypts. *Nature* **469**(7330):415-418.

Sauer, B. (1998). Inducible gene targeting in mice using the Cre/lox system. *Methods* **14**(4):381-392.

Schmidt, A., Oberle, N. and Krammer, P. H. (2012). Molecular mechanisms of treg-mediated T cell suppression. *Front Immunol* **3**:51.

Schneider, K., Marbaix, E., Bouzin, C., Hamoir, M., Mahy, P., Bol, V. and Gregoire, V. (2018). Immune cell infiltration in head and neck squamous cell carcinoma and patient outcome: a retrospective study. *Acta Oncol* **57**(9):1165-1172.

Schoenborn, J. R. and Wilson, C. B. (2007). Regulation of interferon-gamma during innate and adaptive immune responses. *Adv Immunol* **96**:41-101.

Schofield, R. (1978). The relationship between the spleen colony-forming cell and the haemopoietic stem cell. *Blood Cells* **4**(1-2):7-25.

Schonhoff, S. E., Giel-Moloney, M. and Leiter, A. B. (2004). Minireview: Development and differentiation of gut endocrine cells. *Endocrinology* **145**(6):2639-2644.

Schreiber, R. D., Old, L. J. and Smyth, M. J. (2011). Cancer immunoediting: integrating immunity's roles in cancer suppression and promotion. *Science* **331**(6024):1565-1570.

Scurr, M. (2013). Escalating regulation of 5T4-specific IFN- $\gamma$ (+) CD4(+) T cells distinguishes colorectal cancer patients from healthy controls and provides a target for in vivo therapy. **1**(6).

Scurr, M., Gallimore, A. and Godkin, A. (2012). T cell subsets and colorectal cancer: discerning the good from the bad. *Cell Immunol* **279**(1):21-24.

Scurr, M., Pembroke, T., Bloom, A., Roberts, D., Thomson, A., Smart, K., . . . Godkin, A. (2017a). Low-Dose Cyclophosphamide Induces Antitumor T-Cell Responses, which Associate with Survival in Metastatic Colorectal Cancer. *Clin Cancer Res* **23**(22):6771-6780.

Scurr, M., Pembroke, T., Bloom, A., Roberts, D., Thomson, A., Smart, K., . . . Godkin, A. (2017b). Effect of Modified Vaccinia Ankara-5T4 and Low-Dose Cyclophosphamide on Antitumor Immunity in Metastatic Colorectal Cancer: A Randomized Clinical Trial. *JAMA Oncol* **3**(10):e172579.

Shabaneh, T. B., Molodtsov, A. K., Steinberg, S. M., Zhang, P., Torres, G. M., Mohamed, G. A., . . . Turk, M. J. (2018). Oncogenic BRAF(V600E) Governs Regulatory T-cell Recruitment during Melanoma Tumorigenesis. *Cancer Res* **78**(17):5038-5049.

Shahriyari, L. and Komarova, N. L. (2013). Symmetric vs. asymmetric stem cell divisions: an adaptation against cancer? *PLoS One* **8**(10):e76195.

Shankaran, V., Ikeda, H., Bruce, A. T., White, J. M., Swanson, P. E., Old, L. J. and Schreiber, R. D. (2001). IFN $\gamma$  and lymphocytes prevent primary tumour development and shape tumour immunogenicity. *Nature* **410**(6832):1107-1111.

Sheridan, B. S. and Lefrançois, L. (2010). Intraepithelial Lymphocytes: To Serve and Protect. *Curr Gastroenterol Rep* **12**(6):513-521.

Shevach, E. M. (2009). Mechanisms of foxp3<sup>+</sup> T regulatory cell-mediated suppression. *Immunity* **30**(5):636-645.

Shibutani, M., Maeda, K., Nagahara, H., Fukuoka, T., Nakao, S., Matsutani, S., . . . Ohira, M. (2017). The Prognostic Significance of the Tumor-infiltrating Programmed Cell Death-1(+) to CD8(+) Lymphocyte Ratio in Patients with Colorectal Cancer. *Anticancer Res* **37**(8):4165-4172.

Shimizu, J., Yamazaki, S. and Sakaguchi, S. (1999). Induction of tumor immunity by removing CD25<sup>+</sup>CD4<sup>+</sup> T cells: a common basis between tumor immunity and autoimmunity. *J Immunol* **163**(10):5211-5218.

Shimokawa, M., Ohta, Y., Nishikori, S., Matano, M., Takano, A., Fujii, M., . . . Sato, T. (2017). Visualization and targeting of LGR5(+) human colon cancer stem cells. *Nature* **545**(7653):187-192.

Shmelkov, S. V., Butler, J. M., Hooper, A. T., Hormigo, A., Kushner, J., Milde, T., . . . Rafii, S. (2008). CD133 expression is not restricted to stem cells, and both CD133+ and CD133- metastatic colon cancer cells initiate tumors. *J Clin Invest* **118**(6):2111-2120.

Sinicrope, F. A., Rego, R. L., Ansell, S. M., Knutson, K. L., Foster, N. R. and Sargent, D. J. (2009). Intraepithelial effector (CD3+)/regulatory (FoxP3+) T-cell ratio predicts a clinical outcome of human colon carcinoma. *Gastroenterology* **137**(4):1270-1279.

Slattery, M. L., Lundgreen, A., Bondurant, K. L. and Wolff, R. K. (2011). Interferon-signaling pathway: associations with colon and rectal cancer risk and subsequent survival. *Carcinogenesis* **32**(11):1660-1667.

Smith, G. H. (2005). Label-retaining epithelial cells in mouse mammary gland divide asymmetrically and retain their template DNA strands. *Development* **132**(4):681-687.

Snippert, H. J., van der Flier, L. G., Sato, T., van Es, J. H., van den Born, M., Kroon-Veenboer, C., . . . Clevers, H. (2010). Intestinal crypt homeostasis results from neutral competition between symmetrically dividing Lgr5 stem cells. *Cell* **143**(1):134-144.

Song, X. and Qian, Y. (2013). IL-17 family cytokines mediated signaling in the pathogenesis of inflammatory diseases. *Cell Signal* **25**(12):2335-2347.

Stutman, O. (1974). Tumor development after 3-methylcholanthrene in immunologically deficient athymic-nude mice. *Science* **183**(4124):534-536.

Sun, X., Liu, S., Wang, D., Zhang, Y., Li, W., Guo, Y., . . . Suo, J. (2017). Colorectal cancer cells suppress CD4+ T cells immunity through canonical Wnt signaling. In: *Oncotarget*. Vol. 8. pp. 15168-15181.

Syed Khaja, A. S., Toor, S. M., El Salhat, H., Ali, B. R. and Elkord, E. (2017). Intratumoral FoxP3(+)Helios(+) Regulatory T Cells Upregulating Immunosuppressive Molecules Are Expanded in Human Colorectal Cancer. *Front Immunol* **8**:619.

Szabo, S. J., Kim, S. T., Costa, G. L., Zhang, X., Fathman, C. G. and Glimcher, L. H. (2000). A novel transcription factor, T-bet, directs Th1 lineage commitment. *Cell* **100**(6):655-669.

Szabo, S. J., Sullivan, B. M., Peng, S. L. and Glimcher, L. H. (2003). Molecular mechanisms regulating Th1 immune responses. *Annu Rev Immunol* **21**:713-758.

Takahashi, K. and Yamanaka, S. (2006). Induction of pluripotent stem cells from mouse embryonic and adult fibroblast cultures by defined factors. *Cell* **126**(4):663-676.

Takahashi, T., Tagami, T., Yamazaki, S., Uede, T., Shimizu, J., Sakaguchi, N., . . . Sakaguchi, S. (2000). Immunologic self-tolerance maintained by CD25(+)CD4(+) regulatory T cells constitutively expressing cytotoxic T lymphocyte-associated antigen 4. *J Exp Med* **192**(2):303-310.

Talebi, A., Kianersi, K. and Beiraghdar, M. (2015). Comparison of gene expression of SOX2 and OCT4 in normal tissue, polyps, and colon adenocarcinoma using immunohistochemical staining. *Adv Biomed Res* **4**:234.

Teng, M. W., Ngiow, S. F., von Scheidt, B., McLaughlin, N., Sparwasser, T. and Smyth, M. J. (2010). Conditional regulatory T-cell depletion releases adaptive immunity preventing carcinogenesis and suppressing established tumor growth. *Cancer Res* **70**(20):7800-7809.

Tetteh, P. W., Basak, O., Farin, H. F., Wiebrands, K., Kretschmar, K., Begthel, H., . . . Clevers, H. (2016). Replacement of Lost Lgr5-Positive Stem Cells through Plasticity of Their Enterocyte-Lineage Daughters. *Cell Stem Cell* **18**(2):203-213.

Thalheim, T., Buske, P., Przybilla, J., Rother, K., Loeffler, M. and Galle, J. (2016). Stem cell competition in the gut: insights from multi-scale computational modelling. *J R Soc Interface* **13**(121).

Tian, H., Biehs, B., Chiu, C., Siebel, C. W., Wu, Y., Costa, M., . . . Klein, O. D. (2015). Opposing activities of Notch and Wnt signaling regulate intestinal stem cells and gut homeostasis. *Cell Rep* **11**(1):33-42.

Tosolini, M., Kirilovsky, A., Mlecnik, B., Fredriksen, T., Mauger, S., Bindea, G., . . . Galon, J. (2011). Clinical impact of different classes of infiltrating T cytotoxic and helper cells (Th1, th2, treg, th17) in patients with colorectal cancer. *Cancer Res* **71**(4):1263-1271.

Trapani, J. A. and Smyth, M. J. (2002). Functional significance of the perforin/granzyme cell death pathway. *Nat Rev Immunol* **2**(10):735-747.

Trejo, C. L., Luna, G., Dravis, C., Spike, B. T. and Wahl, G. M. (2017). Lgr5 is a marker for fetal mammary stem cells, but is not essential for stem cell activity or tumorigenesis. *NPJ Breast Cancer* **3**:16.

Trifari, S., Kaplan, C. D., Tran, E. H., Crellin, N. K. and Spits, H. (2009). Identification of a human helper T cell population that has abundant production of interleukin 22 and is distinct from T(H)-17, T(H)1 and T(H)2 cells. *Nat Immunol* **10**(8):864-871.

Tripathi, S. K. and Lahesmaa, R. (2014). Transcriptional and epigenetic regulation of T-helper lineage specification. *Immunol Rev* **261**(1):62-83.

Turk, M. J., Guevara-Patino, J. A., Rizzuto, G. A., Engelhorn, M. E., Sakaguchi, S. and Houghton, A. N. (2004). Concomitant tumor immunity to a poorly immunogenic melanoma is prevented by regulatory T cells. *J Exp Med* **200**(6):771-782.

van den Broek, M. E., Kagi, D., Ossendorp, F., Toes, R., Vamvakas, S., Lutz, W. K., . . . Hengartner, H. (1996). Decreased tumor surveillance in perforin-deficient mice. *J Exp Med* **184**(5):1781-1790.

van Oijen, M., Bins, A., Elias, S., Sein, J., Weder, P., de Gast, G., . . . Haanen, J. (2004). On the role of melanoma-specific CD8+ T-cell immunity in disease progression of advanced-stage melanoma patients. *Clin Cancer Res* **10**(14):4754-4760.

Vlad, C., Kubelac, P., Fetica, B., Vlad, D., Irimie, A. and Achimas-Cadariu, P. (2015). The prognostic value of FOXP3+ T regulatory cells in colorectal cancer. *J buon* **20**(1):114-119.

Wahab, S. M. R., Islam, F., Gopalan, V. and Lam, A. K. (2017). The Identifications and Clinical Implications of Cancer Stem Cells in Colorectal Cancer. *Clin Colorectal Cancer* **16**(2):93-102.

Wang, K., Kim, M. K., Di Caro, G., Wong, J., Shalpour, S., Wan, J., . . . Karin, M. (2014). Interleukin-17 receptor a signaling in transformed enterocytes promotes early colorectal tumorigenesis. *Immunity* **41**(6):1052-1063.

Wang, L., Wang, Y., Song, Z., Chu, J. and Qu, X. (2015a). Deficiency of interferon-gamma or its receptor promotes colorectal cancer development. *J Interferon Cytokine Res* **35**(4):273-280.

Wang, Y., Jiang, C. Q. and Fan, L. F. (2015b). Correlation of Musashi-1, Lgr5, and pEGFR expressions in human small intestinal adenocarcinomas. *Tumour Biol* **36**(8):6075-6082.

Waring, P. and Mullbacher, A. (1999). Cell death induced by the Fas/Fas ligand pathway and its role in pathology. *Immunol Cell Biol* **77**(4):312-317.

Whiteman, D. C. and Wilson, L. F. (2016). The fractions of cancer attributable to modifiable factors: A global review. *Cancer Epidemiol* **44**:203-221.

Whiteside, T. L. (2012). What are regulatory T cells (Treg) regulating in cancer and why? *Semin Cancer Biol* **22**(4):327-334.

Williams, P. L., Warwick, R., Dyson, M. and Bannister, L. H. (1989). *Gray's anatomy*. 37th ed.

Wing, J. B., Ise, W., Kurosaki, T. and Sakaguchi, S. (2014). Regulatory T cells control antigen-specific expansion of Tfh cell number and humoral immune responses via the coreceptor CTLA-4. *Immunity* **41**(6):1013-1025.

Wolf, A. M., Wolf, D., Steurer, M., Gastl, G., Gunsilius, E. and Grubeck-Loebenstien, B. (2003). Increase of regulatory T cells in the peripheral blood of cancer patients. *Clin Cancer Res* **9**(2):606-612.

Wright, N. A. and Alison, M. R. (1984). *The Biology of Epithelial Cell Populations*  
Clarendon Press : Oxford.

Wu, X. S., Xi, H. Q. and Chen, L. (2012). Lgr5 is a potential marker of colorectal carcinoma stem cells that correlates with patient survival. In: *World J Surg Oncol*. Vol. 10. p. 244.

Yang, L. and Karin, M. (2014). Roles of tumor suppressors in regulating tumor-associated inflammation. *Cell Death Differ* **21**(11):1677-1686.

Yang, L., Liu, H., Zhang, L., Hu, J., Chen, H., Wang, L., . . . Qi, Y. (2016). Effect of IL-17 in the development of colon cancer in mice. In: *Oncol Lett*. Vol. 12. pp. 4929-4936.

Zallen, J. A. (2007). Planar polarity and tissue morphogenesis. *Cell* **129**(6):1051-1063.

- Zeng, H. and Chi, H. (2015). Metabolic control of regulatory T cell development and function. *Trends Immunol* **36**(1):3-12.
- Zhang, L. and Shay, J. W. (2017). Multiple Roles of APC and its Therapeutic Implications in Colorectal Cancer. *J Natl Cancer Inst* **109**(8).
- Zheng, W. and Flavell, R. A. (1997). The transcription factor GATA-3 is necessary and sufficient for Th2 cytokine gene expression in CD4 T cells. *Cell* **89**(4):587-596.
- Zhou, Y., Xia, L., Wang, H., Oyang, L., Su, M., Liu, Q., . . . Cao, D. (2018). Cancer stem cells in progression of colorectal cancer. *Oncotarget* **9**(70):33403-33415.
- Zhu, J. and Paul, W. E. (2010). Peripheral CD4+ T-cell differentiation regulated by networks of cytokines and transcription factors. *Immunol Rev* **238**(1):247-262.
- Ziai, J., Gilbert, H. N., Foreman, O., Eastham-Anderson, J., Chu, F., Huseni, M. and Kim, J. M. (2018). CD8+ T cell infiltration in breast and colon cancer: A histologic and statistical analysis. *PLoS One* **13**(1):e0190158.
- Zou, W. (2006). Regulatory T cells, tumour immunity and immunotherapy. *Nat Rev Immunol* **6**(4):295-307.

## 9 Supplementary Material

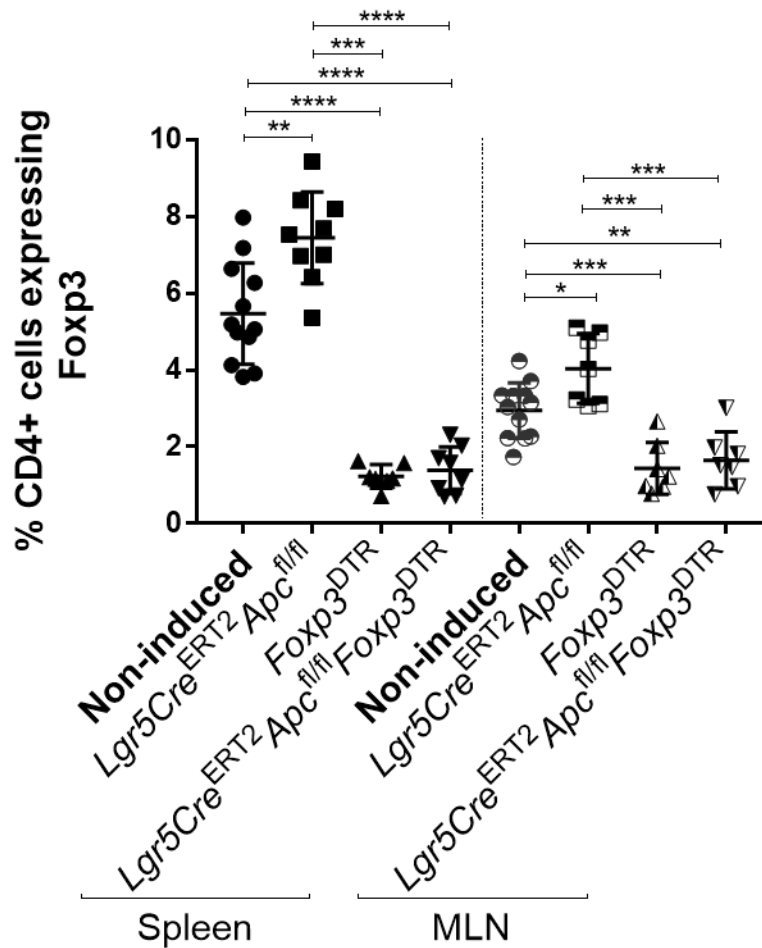


Figure S 9.1 Frequency of CD4+ cells expressing Foxp3 in the spleen and MLN.

The frequency of CD4+ cells expressing Foxp3 increased after *Apc* deletion in both spleen and MLN. The treatment with diphtheria toxin (DTR) resulted in a significantly decreased frequency of the Foxp3 marker as expected in both spleen and MLN. Data represent a single experiment,  $n \geq 7$  mice per group. (\*) P value  $< 0.05$ , (\*\*) P value  $\leq 0.01$ , (\*\*\*) P value  $\leq 0.001$ , two-tailed Mann Whitney U test.

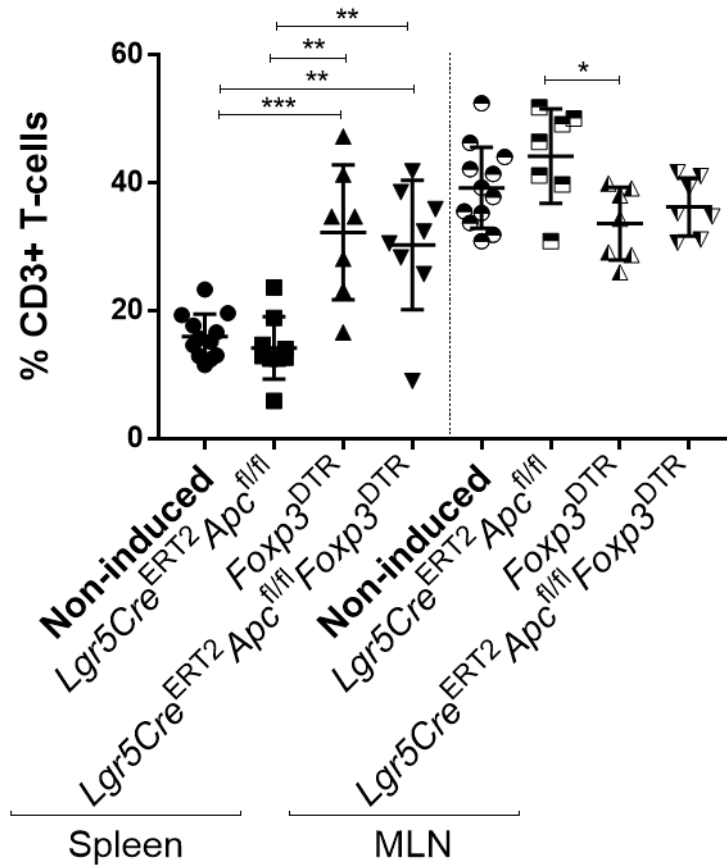


Figure S 9.2 Frequency of CD3+ T-cells in the spleen and MLN.

*Apc* deletion did not alter the frequency of CD3+ cells in the spleen. The frequency of CD3+ cells increased with Treg depletion alone and in *Apc* deleted/Treg depleted mice. The frequency of CD3+ cells was decreased in the MLN following Treg depletion when comparing to *Apc* deletion alone. There was a trend for a decreased frequency of CD3+ cells when Tregs were depleted together with *Apc* deletion although was is not significant. Data represent a single experiment,  $n \geq 7$  mice per group. (\*) P value < 0.05, (\*\*) P value  $\leq 0.01$ , (\*\*\*) P value  $\leq 0.001$ , two-tailed Mann Whitney U test.

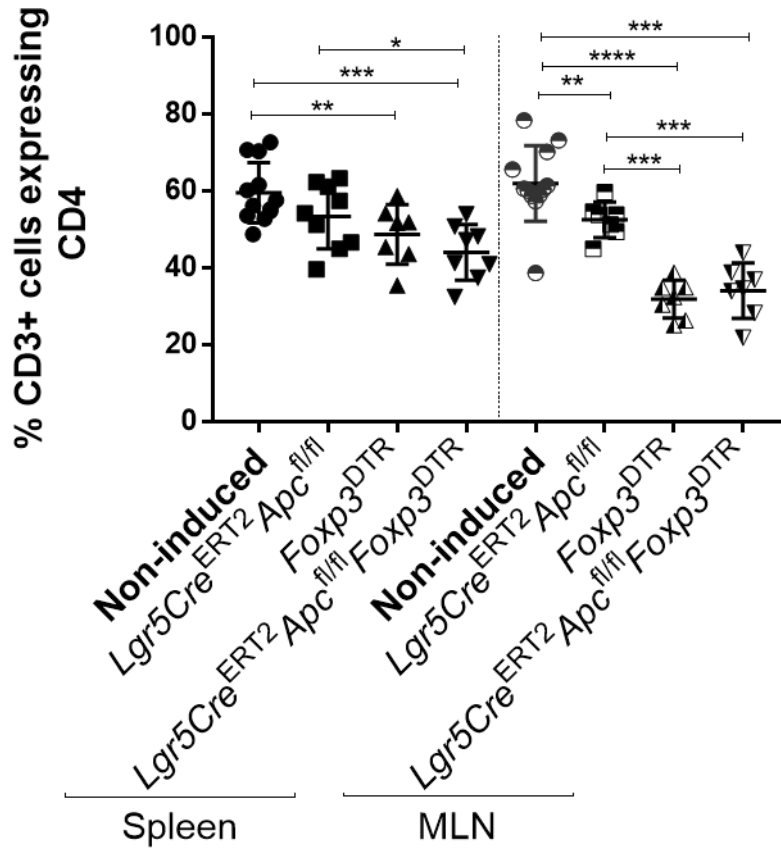


Figure S 9.3 Frequency of CD3+ cells expressing CD4 in the spleen and MLN.

The frequency of CD4+ cells was significantly with in Treg depleted and *Apc* deleted/Treg depleted mice. There was a trend for a decreased frequency of CD4+ cells following *Apc* deletion. In the MLN the frequency of CD4+ cells was significantly decreased with *Apc* deletion, Treg depletion and both treatments together. Data represent a single experiment,  $n \geq 7$  mice per group. (\*) P value < 0.05, (\*\*) P value  $\leq 0.01$ , (\*\*\*) P value  $\leq 0.001$ , (\*\*\*\*) P value  $\leq 0.0001$ , two-tailed Mann Whitney U test.

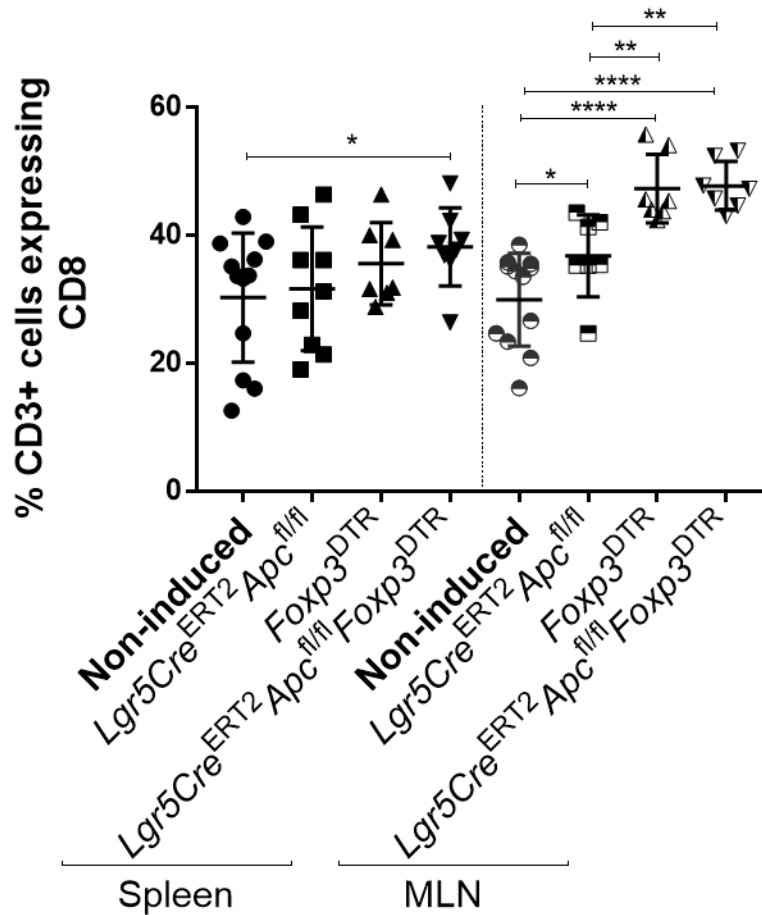


Figure S 9.4 Frequency of CD3+ cells expressing CD8 in the spleen and MLN.

The frequency of CD8+ cells, in the spleen, was increased in *Apc* deleted/Treg depleted mice. The frequency of CD8+ cells was significantly increased with *Apc* deletion, Treg depletion and both treatments together in the MLN. Data represent a single experiment,  $n \geq 7$  mice per group. (\*) P value  $< 0.05$ , (\*\*) P value  $\leq 0.01$ , (\*\*\*) P value  $\leq 0.001$ , (\*\*\*\*) P value  $\leq 0.0001$ , two-tailed Mann Whitney U test.

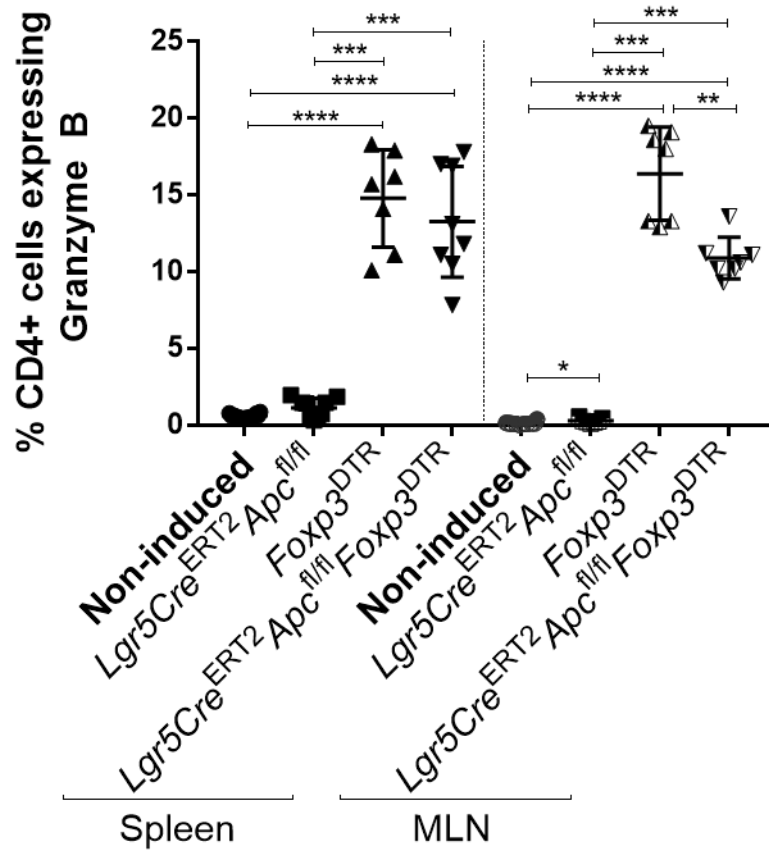


Figure S 9.5 Frequency of CD4+ expressing Granzyme B in the spleen and MLN.

The frequency of CD4+ expressing Granzyme B was not changed after *Apc* deletion. Treg depletion alone and together with *Apc* deletion resulted in a significantly increased expression of Granzyme B. The frequency of Granzyme was significantly increased in the MLN with *Apc* deletion, Treg depletion and both treatments together. Data represent a single experiment,  $n \geq 7$  mice per group. (\*) P value < 0.05, (\*\*) P value  $\leq 0.01$ , (\*\*\*) P value  $\leq 0.001$ , (\*\*\*\*) P value  $\leq 0.0001$ , two-tailed Mann Whitney U test.

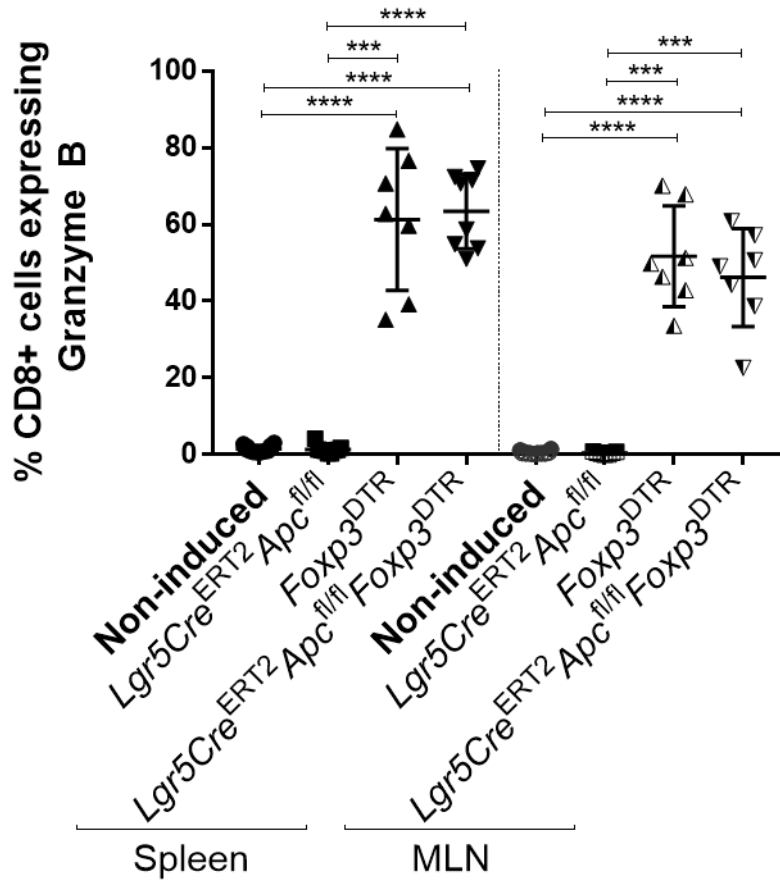


Figure S 9.6 Frequency of CD8+ cells expressing Granzyme B in the spleen and MLN.

The frequency of CD8+ cells expressing Granzyme B is significantly increased with Tregs depletion alone and *Apc* deleted/Treg depleted mice in both spleen and MLN. Data represent a single experiment,  $n \geq 7$  mice per group. (\*\*\*) P value  $\leq 0.001$ , (\*\*\*\*) P value  $\leq 0.0001$ , two-tailed Mann Whitney U test.

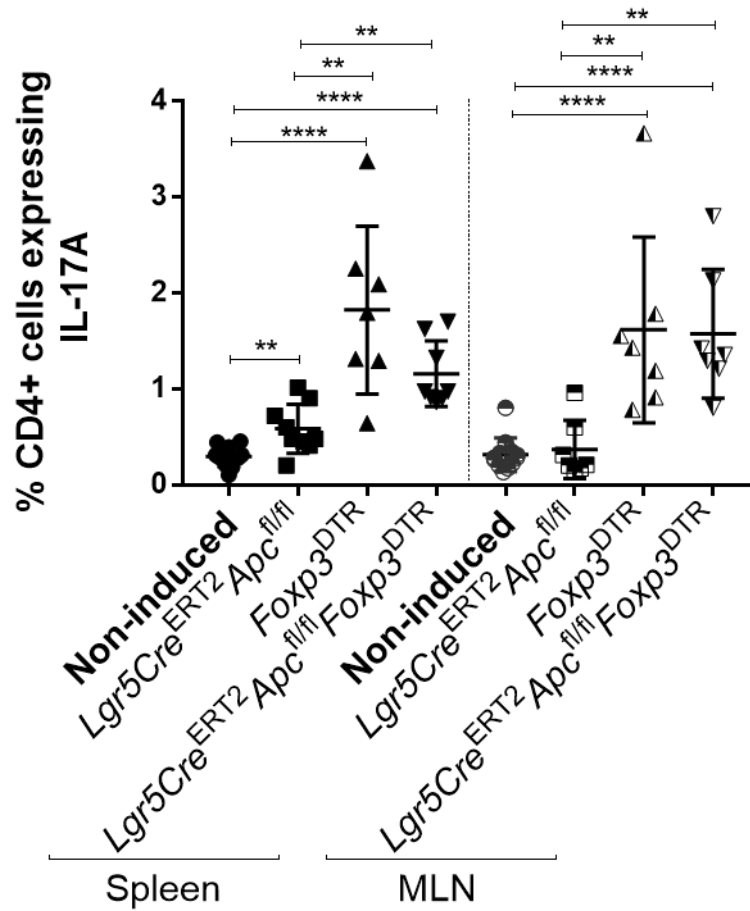


Figure S 9.7 Frequency of CD4+ cells expressing IL-17A in the spleen and MLN.

The frequency of CD4+ cells expressing IL-17A was significantly increased in the spleen with *Apc* deletion, Treg depletion and both treatments together. In the MLN the frequency of CD4+ expressing IL-17A was increased with Treg depletion alone and *Apc* deletion with Treg depletion together. Data represent a single experiment,  $n \geq 7$  mice per group. (\*\*) P value  $\leq 0.01$ , (\*\*\*) P value  $\leq 0.001$ , (\*\*\*\*) P value  $\leq 0.0001$ , two-tailed Mann Whitney U test.

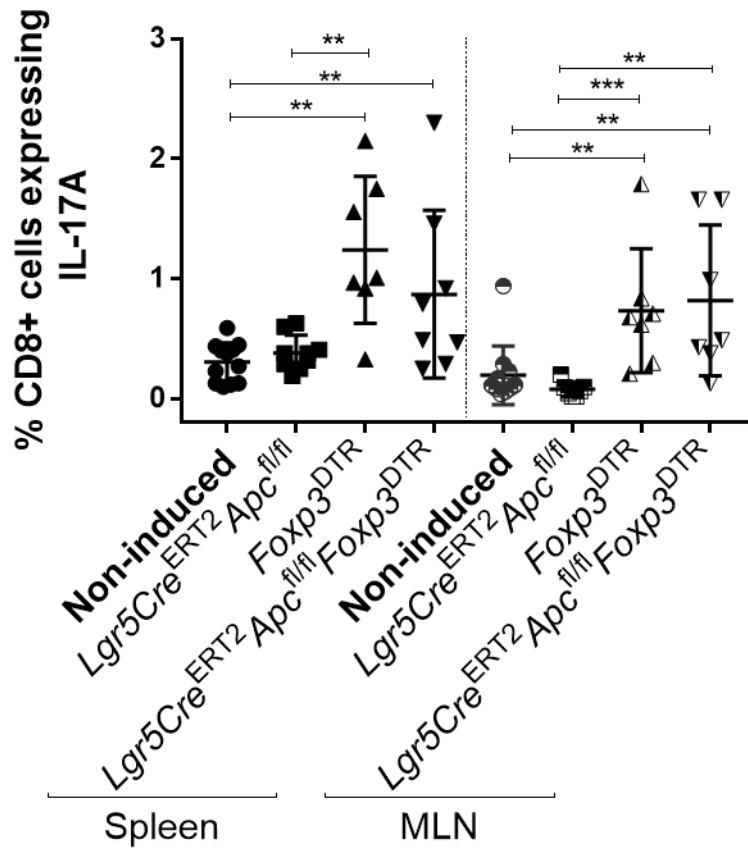


Figure S 9.8 Frequency of CD8+ cells expressing IL-17A in the spleen and MLN.

The frequency of CD8+ cells expressing IL-17A was significantly increased with Treg depletion alone and *Apc* deletion/Treg depletion in both spleen and MLN. Data represent a single experiment,  $n \geq 7$  mice per group. (\*\*) P value  $\leq 0.01$ , (\*\*\*) P value  $\leq 0.001$ , two-tailed Mann Whitney U test.

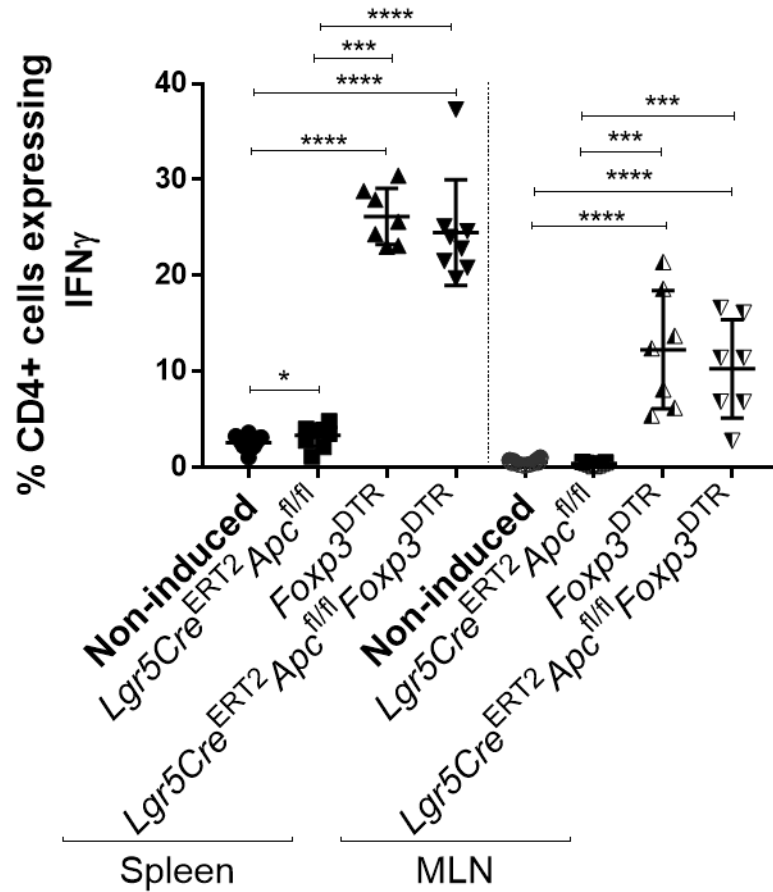


Figure S 9.9 Frequency of CD4+ cells expressing IFN $\gamma$  in the spleen and MLN.

The frequency of CD4+ cells expressing IFN $\gamma$  was significantly increased in the spleen with *Apc* deletion, Treg depletion and *Apc* deletion/Treg depletion. In the MLN the frequency of CD4+ cells expressing IFN $\gamma$  was significantly increased with Treg depletion alone and *Apc* deletion/Treg depletion. Data represent a single experiment,  $n \geq 7$  mice per group. (\*) P value < 0.05, (\*\*\*) P value  $\leq$  0.001, (\*\*\*\*) P value  $\leq$  0.0001, two-tailed Mann Whitney U test.

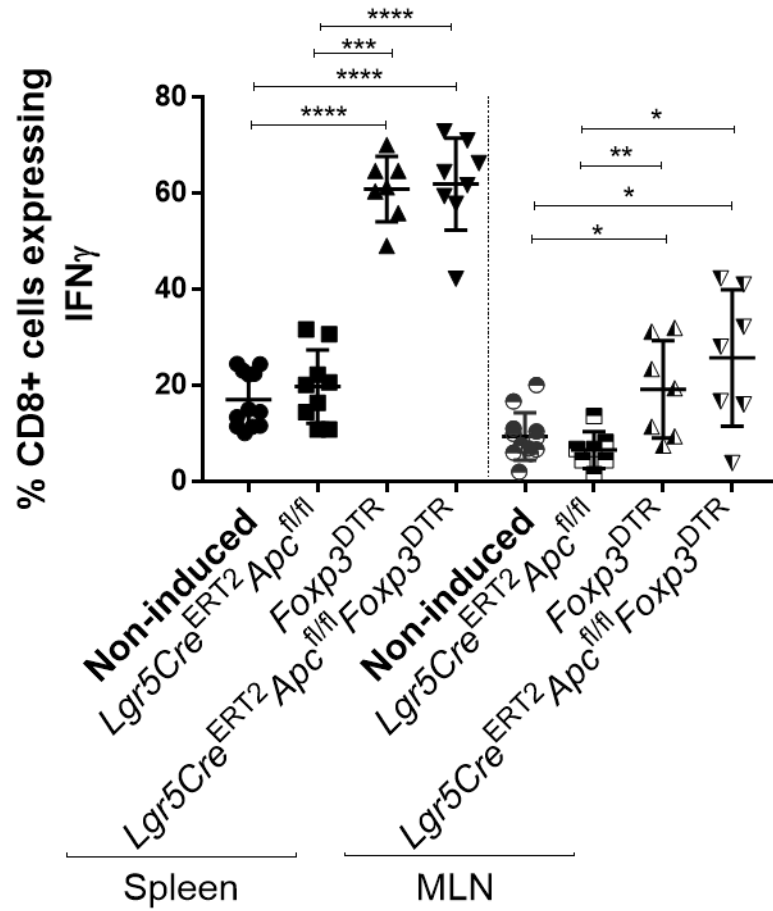


Figure S 9.10 Frequency of CD8+ cells expressing IFN $\gamma$  in the spleen and MLN.

The frequency of CD8+ cells expressing IFN $\gamma$  was significantly increased with Treg depletion alone and *Apc* deletion/Treg depletion in both spleen and MLN. Data represent a single experiment,  $n \geq 6$  mice per group. (\*\*) P value  $\leq 0.01$ , (\*\*\*) P value  $\leq 0.001$ , two-tailed Mann Whitney U test.